Exploration of ER stress and associated complications in the genesis of hyperglycemia induced cardiomyopathy and possible amelioration with chlorogenic acid

By

Preetha Rani M R
10BB15A39023

A thesis submitted to the
Academy of Scientific & Innovative Research
for the award of the degree of

DOCTOR OF PHILOSOPHY
in
SCIENCE

Under the supervision of
Prof. (Dr) K G Raghu

CSIR-National Institute for Interdisciplinary Science and
Technology (NIIST), Thiruvananthapuram, Kerala - 695019, India

Academy of Scientific and Innovative Research
AcSIR Headquarters, CSIR-HRDC campus, Sector 19,
Kamla Nehru Nagar, Ghaziabad, U.P. – 201 002, India

June 2021

CERTIFICATE

This is to certify that the work incorporated in this Ph.D. thesis entitled, "Exploration of ER stress and associated complications in the genesis of hyperglycemia induced cardiomyopathy and possible amelioration with chlorogenic acid", submitted by _Preetha Rani M R_ to the Academy of Scientific and Innovative Research (AcSIR) in fulfillment of the requirements for the award of the Degree of _Doctor of Philosophy in Biological Sciences_, embodies original research work carried out by the student. We, further certify that this work has not been submitted to any other University or Institution in part or full for the award of any degree or diploma. Research material(s) obtained from other source(s) and used in this research work has/have been duly acknowledged in the thesis. Image(s), illustration(s), figure(s), table(s) etc., used in the thesis from other source(s), have also been duly cited and acknowledged.
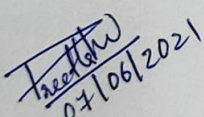
Preetha Rani M R

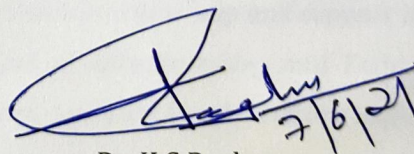07/06/2021

Dr. K.G. Raghu

07/06/2021

ii
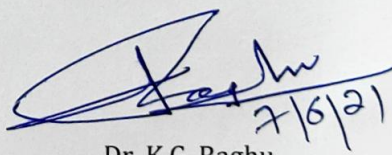
STATEMENTS OF ACADEMIC INTEGRITY

I Preetha Rani M R, a Ph.D. student of the Academy of Scientific and Innovative Research (AcSIR) with Registration No. 10BB15A39023 hereby undertake that, the thesis entitled "Exploration of ER stress and associated complications in the genesis of hyperglycemia induced cardiomyopathy and possible amelioration with chlorogenic acid" has been prepared by me and that the document reports original work carried out by me and is free of any plagiarism in compliance with the UGC Regulations on *"Promotion of Academic Integrity and Prevention of Plagiarism in Higher Educational Institutions (2018)"* and the CSIR Guidelines for *"Ethics in Research and in Governance (2020)".*

07/06/2021
Thiruvananthapuram

It is hereby certified that the work done by the student, under my/our supervision, is plagiarism-free in accordance with the UGC Regulations on *"Promotion of Academic Integrity and Prevention of Plagiarism in Higher Educational Institutions (2018)"* and the CSIR Guidelines for *"Ethics in Research and in Governance (2020)".*

Dr. K.G.Raghu
07/06/2021
Thiruvananthapuram

iii

ACKNOWLEDGEMENTS

TABLE OF CONTENTS

Chapter 2 : Materials and Methods

Chapter 3: Hyperglycemia induced alterations in redox status in H9c2 cells and possible amelioration with chlorogenic acid

Chapter 4: Cross talk between hyperglycemia and ER and effect of chlorogenic acid:

an *in vitro* study

LIST OF FIGURES

LIST OF TABLES

ABBREVIATIONS

AGE	:	Advanced glycated end products
ANP	:	Atrial natriuretic peptide
ATF4	:	Activating transcription factor 6
ATF6	:	Activating transcription factor 4
BNP	:	B-type natriuretic peptide
BSA	:	Bovine serum albumin
CA	:	Chlorogenic acid
Ca^{2+}	:	Calcium
$[Ca^{2+}]i$	:	Intracellular calcium
CHOP	:	C/EBP-homologous protein
CK-MB	:	Creatine phosphokinase-MB
$CoCl_2$	:	Cobalt chloride
CRP	:	C-reactive protein
CVDs	:	Cardiovascular diseases
DAPI	:	4', 6 diamidino-2-phenylindole
DCFH DA	:	2′, 7′ dichlorodihydrofluorescein diacetate
DCM	:	Diabetic cardiomyopathy
DMEM	:	Dulbecco's modified eagle's medium
DMSO	:	Dimethyl sulfoxide
EDTA	:	Ethylene diamene tetraacetic acid
ER	:	Endoplasmic reticulum
ERK	:	Extracellular signal-regulated kinase 1/2

ERO1α	:	ER oxidoreductin 1 α
FAM134B	:	Reticulophagy regulator 1
FBS	:	Fetal bovine serum
GAPDH	:	Glyceraldehyde 3-phosphate dehydrogenase
GPx	:	Glutathione peroxidase
GRP78	:	Glucose-regulated protein
GSH	:	Reduced glutathione
HFABP	:	Heart-type fatty acid binding protein
IRE1	:	Inositol-requiring enzyme 1
LDH	:	Lactate dehydrogenase
MDA	:	Malondialdehyde
mPTP	:	Mitochondrial permeability transition pore
MTT	:	3-(4,5-dimethylthiazol-2-yl)-2,5-diphenyl tetrazolium bromide
NCX1	:	Sodium-calcium exchanger
NOX	:	Nicotinamide adenine dinucleotide phosphate oxidase
PBS	:	Phosphate buffered saline
pCAMKII	:	Phosho calcium/calmodulin-activated protein kinaseII
PDI	:	Protein disulfide isomerase
pEIF2 α	:	Phospho eukaryotic translation initiation factor 2 α
PERK	:	Protein Kinase R-like ER Kinase
pIRE1α	:	Phosphorylated IRE1α
pJNK	:	c-Jun N-terminal kinases
PKC	:	Protein kinase C :
pPERK	:	Phospho PERK

pRYR2	:	Phospho RYR2
PVDF	:	Polyvinylidene di fluoride
qRT PCR	:	Quantitative real time polymerase chain reaction
RIPA	:	Radio immunoprecipitation assay
ROS	:	Reactive oxygen species
RNS	:	Reactive nitrogen species
RTN3	:	Reticulon-3
RYR2	:	Ryanodine receptor 2
SDS	:	Sodium dodecyl sulphate
SERCA2a	:	Sarcoplasmic/endoplasmic reticulum Ca^{2+} ATPase 2a
SGOT	:	Serum glutamic oxaloacetic transaminase
STZ	:	Streptozotocin
TRAF2	:	TNF receptor-associated factor 2
Tris HCL	:	Tris hydroxymethyl aminomethane hydrochloride
UPR	:	Unfolded protein responses
XBP1	:	X-box binding protein 1

Introduction

1.1. General introduction on diabetes mellitus

Diabetes mellitus (DM) is thought to be one of the hoariest diseases known to humans. It is becoming more common in every country regardless of income level. It is a metabolic condition marked by an increase in blood glucose levels that necessitates close monitoring and management. Insulin is produced by pancreatic beta cells, which aids in the utilization of glucose into cells for energy and is involved in a number of other functions. DM is caused by a lack of insulin production or insulin sensitivity. It is of many types; however the most common types are Type1 and Type2. Type 1 diabetes (T1DM) is characterised by an inability to produce insulin as a result of T cell mediated autoimmunity that destroys pancreatic beta cells (Gharravi et al., 2018). On the other hand Type 2 diabetes (T2DM) is marked by insulin resistance and decrease in insulin production. T1DM has a shorter life expectancy than T2DM owing to a higher risk for cardiovascular diseases (CVDs) and acute metabolic disorders (Wise, 2016). According to recent data, 629 million people will be affected by diabetes by 2049 (English and Lenters-Westra, 2018). Its rising prevalence is expected to have a greater social and economic effect as a result of disease related complications (Urrutia, 2021). Nonetheless, when risk factors are addressed and early diagnosis and care are provided, long term complications can be avoided.

The global epidemics of diabetes and CVDs are also on the rise. They are also one of the leading causes of morbidity and mortality worldwide, affecting people in low and middle income countries the most. Globalization, rapid unplanned urbanization, and increasingly sedentary life styles hasten their negative consequences. Diabetes is at a higher risk of having severe health issues. High blood glucose levels overtime can lead serious disease of the heart and blood vessels as well as the eyes, kidneys, nerves and teeth (Khalil, 2017; Papatheodorou et al., 2016; Ahmad, 2016). In addition, people with diabetes are more likely to have infections. At the same time diabetes complications can be prevented or controlled by keeping the levels of blood glucose, blood pressure and cholesterol levels as close to normal as possible. As compared to people who do not

have diabetes, diabetics have a higher risk of cardiovascular disease. The risk of cardiovascular disease rise with age.

1.2. Cardiovascular diseases and prevalence

Cardiovascular diseases are the leading cause of the death worldwide, claiming the lives of an estimated 17.9 million people per year (WHO, 2020). Coronary heart disease, rheumatic heart disease, and other heart and blood vessel diseases are all classified as CVDs. Heart attacks and strokes account about four out of every five CVD fatalities, with one third of these deaths occurring prematurely in people under 70 years of age. The burden of CVDs in India is one of the highest in the world (Prabhakaran et al., 2018). According to the Global Burden of Disease, nearly a quarter (24.8 %) of all deaths in survey, self-reported CVD in those aged 45-59 years ranges from 14 % in Odisha and Chattisgarh, 15 % in Dadra and Nagar Haveli and 34 % in Chandigarh, Jammu and Kashmir, and Haryana. In the next age group (60+ years), states like Jammu and Kashmir (51 %), Chandigarh (55 %), Kerala (57 %), Goa (60 %) and a majority of people were diagnosed with CVD. On the other hand the prevalence was comparitively low in Nagaland (16 %), Chattisgarh (21 %) and Uttar Pradesh (22 %).
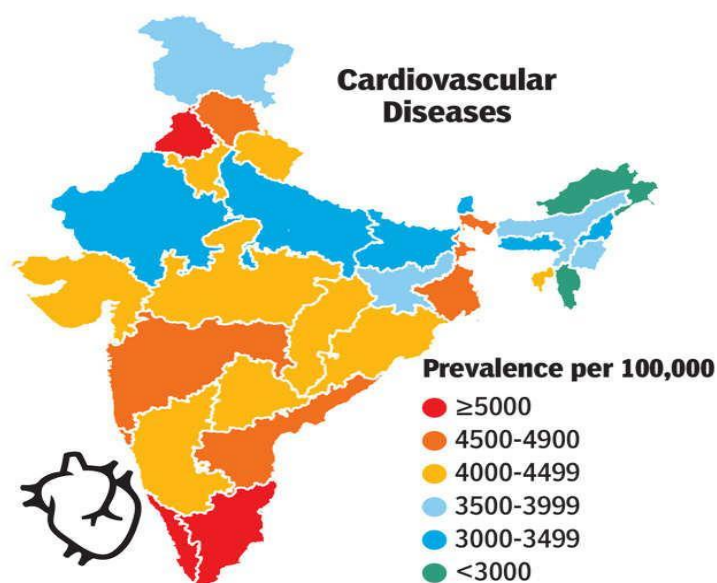
Times of India, 2018

Figure.1.1. Prevalence of cardiovascular diseases in India

1.3. Cardiovascular diseases and diabetes

Cardiovascular disease is a common complication of diabetes that accounts for 80 % of the mortality rate in diabetes (Amos et al., 1997). Coronary artery disease is the most common cause of increased morbidity and mortality in people with diabetes and atherosclerosis of the coronary arteries is the primary pathogenic mechanism. The majority of myocardial defects (left ventricular (LV) hypertrophy and reduced contractility) seen in diabetes can be attributed to coronary artery diseases and hypertension. Postmortem, experimental and observational studies, on the other hand, show that diabetes causes a particular cardiomyopathy, which may lead to myocardial deterioration even though there is no coronary artery atheroma (Fisher et al., 1986). This is also supported by the fact that diabetic patients, regardless of the seriousness of coronary artery disease, have a higher risk of heart failure than non-diabetic subjects (Bagdasa et al., 2009). For the first time in medical history, a description of four patients with diabetes and heart failure but no arterial hypertension or coronary artery disease was reported in 1972. Anatomical dissection of their hearts showed LV hypertrophy and fibrosis, but no signs of coronary artery atheroma or any substrate pathology (Rubler et al., 1972). The disease was deliberated as self regulating and was named "diabetic cardiomyopathy" (DCM).

In contrast to non-diabetic subjects, epidemiological evidence has shown that macrovascular complications such as coronary artery disease, peripheral vascular disease, and stroke are more frequent among diabetic patients. And when all other cardiovascular risk factors are taken into account, this holds true for both T1DM and T2DM (Zimmet et al., 2001). Diabetes patients of both sexes are twice as likely to develop coronary artery disease, according to the Framingham study. Furthermore, death from coronary artery disease is three times more likely in diabetics than in non-diabetic subjects of the same age and gender. Diabetic patient is not only at a higher risk of developing coronary heart disease, but he is much more likely to have a poor diagnosis (Leon and Maddox, 2015). Moreover, according to some reports, strong glycemic regulation is linked to a higher rate of survival after an acute myocardial infarction (Norhammar et al., 2002). Heart failure is a major complication of DCM, which is more common in diabetics and complicates acute myocardial infarction more often than in the non-diabetic population (Voulgari, 2010). In summary, diabetics have

2-3 times the risk of CVDs and have a higher mortality rate than their aged and sex matched counter parts.

1.4. Diabetic cardiomyopathy (DCM)

Diabetic cardiomyopathy (DCM) is a form of cardiovascular disease characterised by myocardial dilation with hypertrophy in diabetic patients as well as shrink in the left ventricles systolic and diastolic function and it occurs regardless of the presence of ischemic heart disease or hypertension. The pathological alterations in the myocardial interstitium, such as the development of advanced glycated end products (AGEs), weakened compliance and ischemia dominate the early stages of DCM. Anatomically, the myocardial cells and small coronary vessels retain their morphology. These changes result in a decrease in myocardial contractility (Factor et al., 1980). As the disease progresses, interstitial and perivascular fibrosis, myocardial hypertrophy, larger thickening of the capillary basement and the growth of microaneurysms in small capillary all contribute to LV hypertrophy. This final observation may be the pathophysiological connection between diabetes microvascular and macrovascular complications (Factor et al., 1981). LV hypertrophy and myocardial dilatation characterise DCM, resulting in LV diastolic and systolic dysfunction. Diabetic fibrosis, inflammation, ischemia, and the presence of microvascular complications are all linked to these. The presence of ischemic heart disease or hypertension does not affect DCM. Metabolic anomalies (hyperglycemia, insulin resistance, hyperlipidemia and deficiency of insulin) are critical in the pathogenesis of DCM, as they activate maladaptive stimuli that cause myocardial fibrosis and collagen formation (Boudina and Abel, 2010). Metabolic disorders cause myocardial fibrosis and/or hypertrophy, either directly or indirectly. Impaired calcium cycling, myocardial insulin tolerance, enhanced lipid absorption, glucotoxicity, and activation of the renin-angiotensin aldosterone system (RAAS) have all been linked to these negative changes in cardiomyopathy (Bugger and Abel, 2009). Furthermore, in diabetes, cardiac free fatty acid uptake and use increase, resulting in decreased glucose oxidation, increased lipotoxicity, and apoptosis (Peterson et al., 2004). From cardiac hypertrophy to fibrosis, contractile dysfunction, and left ventricular failure, reactive oxygen species (ROS) play a role in the progression of heart failure (Regan et al., 1977). Typical changes in membrane and contractile function occur days after diabetic development, while morphological changes and heart dysfunction

take months to years. Chronic changes in late-stage diabetes, on the other hand, are thought to be the product of acute cardiac responses to rapidly rising glucose levels in the early stages.

1.4.1. Molecular mechanisms of DCM

DCM has a multifactorial pathogenesis. Autonomic instability, metabolic disturbances, defects in ion homeostasis, structural protein changes, and interstitial fibrosis have all been proposed as hypotheses. Sustained hyperglycemia may also increase the glycation of interstitial proteins such as collagen which cause myocardial stiffness and contractility problems. Impaired calcium homeostasis, stimulation of the renin-angiotensin pathway, amplified oxidative stress, mitochondrial dysfunction and changed substrate metabolism, are all factors that contribute to decreased myocardial contractility in diabetes mellitus.
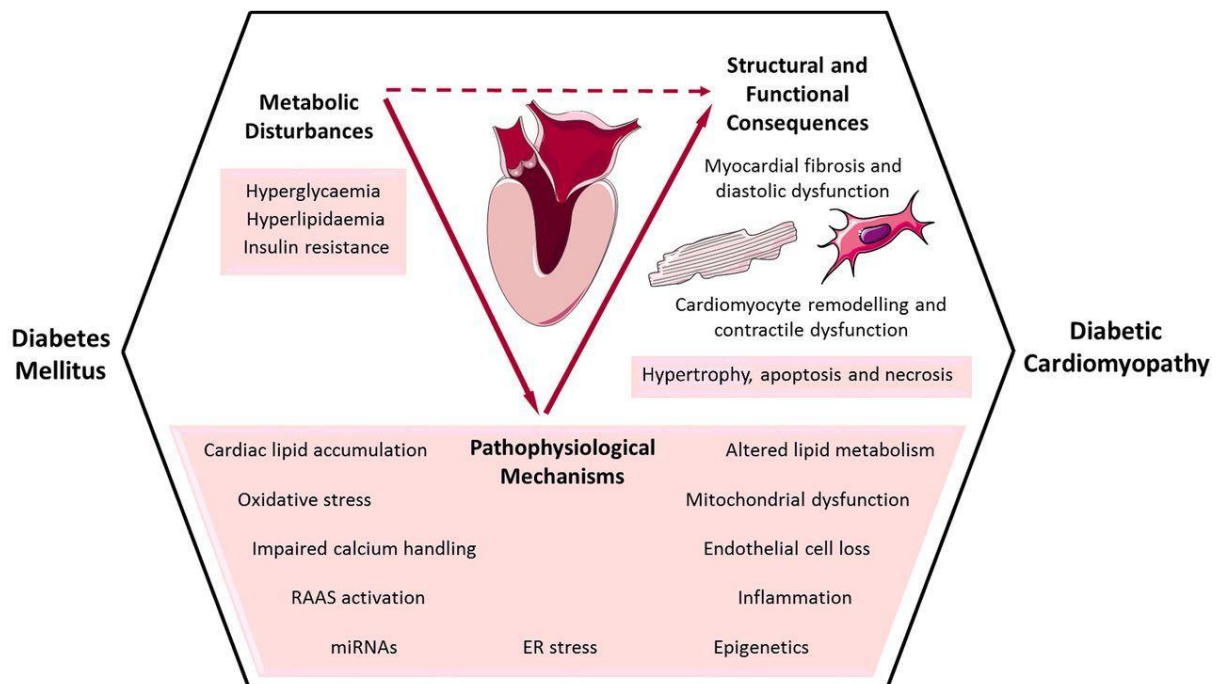
Tate et al., Clinical Science, 2017

Figure.1.2. Pathophysiological mechanisms of diabetic cardiomyopathy

1.4.2. Role of ROS and oxidative stress in DCM

ROS refers to both free radicals like superoxide ($O_2\bullet$) and hydroxyl ($OH\bullet$) as well as non-radical species like hydrogen peroxide. Earlier ROS generation was believed to be a type of pathological cellular stress, but at present scientists considered that ROS degradation and generation are physiological, homeostatic processes of many cells (Valko et al., 2007; Kayama et al., 2015). Several reports have observed prolonged oxidative stress in diabetic state, which is believed to be associated with the oxidation of additional substrates (fatty acids and glucose) found in the hyperglycemic condition (Nourooz et al., 1997) as well as mitochondrial dysfunction linked to insulin resistance (Petersen et al., 2004). The majority of ROS produced by cells under physiological conditions comes from mitochondria. Although increased mitochondrial ROS generation has been observed in various tissues only a few studies have specifically measured mitochondrial ROS production in diabetic heart. Evidence also exists for increased production of ROS from non-mitochondrial sources such as increased activity of lipoxygenase (LOX), xanthine oxidase (XO), nicotinamide adenine dinucleotide phosphate oxidase (NADPH oxidase), uncoupling of nitric oxide synthase (NOS), the interface of advanced glycation end-products (AGE) with the receptor for AGE (RAGE) and activation of protein kinase C (PKC) (Kayama et al., 2015). The development of superoxide by the mitochondrial respiratory chain as well as the oxidative stress results in reduction of myocardial contractility and eventually leads to myocyte fibrosis (Aragno et al., 2006). ROS and oxidative stress can destroy cellular DNA and speed up apoptosis in cardiomyocytes. Poly ADP ribose polymerase (PARP), a DNA reparative enzyme, is activated by DNA damage caused by oxidative stress (Du et al., 2003). PARP induces hyperglycemia-induced cellular injury by diverting metabolism of glucose from its typical glycolytic pathway (glyceraldehyde phosphate dehydrogenase inhibition) to another biochemical pathway that results in the formation of several mediators. Although there is some evidence for increased ROS development in diabetes mellitus, the impact of diabetes on antioxidant defences in the heart is debatable. Thus, glutathione peroxidase, copper/zinc superoxide dismutase, and catalase activities/expression levels were either increased or decreased (Boudina and Abel, 2007). Increased ROS development was linked to increased apoptosis in *ob/ob* and *db/db* hearts, as shown by increased *in situ* nick end-labeling (TUNEL) staining and caspase 3 activation (Barouch et al., 2003). Increased ROS-mediated cell death could induce irregular

cardiac remodelling, which could eventually lead to the morphological and functional defects associated with DCM (Kwon et al., 2003). Increased ROS development can cause cardiac dysfunction through a variety of mechanisms, in addition to cellular injury. For example ROS generation has been proposed to strengthen hyperglycemia-induced PKC activation, generation of AGE products, and enhanced glucose flux through aldose reductase pathways (Tang et al., 2012). This may play a role in the development of heart problems in people with diabetes. Increased ROS can also lead to mitochondrial uncoupling, which may compromise myocardial energetics in diabetic patients. As a result, strategies that either minimise ROS or enhance myocardial antioxidant defence mechanisms may be therapeutically effective in improving myocardial function in diabetics.

1.4.3. Intracellular lipid accumulation and DCM

Lipids will accumulate if fatty acid oxidation does not keep up with uptake, resulting in lipotoxicity (Cheng et al., 2004; Chiu et al., 2005). Studies reported that a large accumulation of lipid in heart failure patients cardiac myocytes (Sharma et al., 2004). This was most noticeable in diabetic patients, to a lesser degree in obese patients, and not at all in non-obese, non-diabetic patients, as one might expect. This means that, while lipid accumulation does not play a role in many cases of heart failure, it may be a significant factor in obese or diabetic patients. Lipid accumulation can either inhibit or encourage myocyte metabolism and contractility. Changes in myocardial substrate and energy metabolism have been identified as a key contributor in the progression of DCM (Taegtmeyer, 2002). Despite the fact that fatty acid usage in diabetic hearts has increased, it is probable that fatty acid absorption in the heart exceeds oxidation rates, resulting in lipid accumulation in the myocardium, which may encourage lipotoxicity (Szczepaniak et al., 2003). The substrate switching that characterises the diabetic heart is caused by a number of mechanisms. Increased fatty acid transmission, decreased insulin signaling, and activation of transcriptional pathways such as the peroxisome proliferator–activated receptor α (PPARα)/PGC-1 signaling network that control myocardial substrate use (Boudina and Abel, 2007). Some studies have suggested that in a mouse model of repetitive ischemia reperfusion, PPARα activation increases lipotoxicity (Dewald et al., 2005). Furthermore, cardiac-specific overexpression of PPAR α receptors worsens diabetes-induced

cardiomyopathy, while whole-body knockout of PPAR α reduces DCM induction. These findings show that cardiac lipid equilibrium is delicately controlled and easily disrupted, as in diabetes (Finck et al., 2003).

1.4.4. NADPH oxidase (NOX) in DCM

NOX are a group of membrane-bound enzymes that are the main causes of ROS in the cardiovascular system (Griendling et al., 2000). They use NADPH as an electron donor to catalyse the reduction of molecular oxygen to O_2. Indeed, NADPH oxidases tend to be the only enzymes discussed so far whose primary role appears to be the synthesis of ROS. Nox has a catalytic unit that forms a heterodimer with p22phox, a lower molecular weight subunit, and four cytosolic regulatory subunits, p40phox, p47phox, p67phox, as well as the small GTP-binding protein Rac1(Lambeth, 2004). There are different types of NOX. NOX expression patterns vary among cardiovascular cells, with some cell types expressing multiple isoforms. Despite the fact that NOX1 is greatly expressed in cultured vascular smooth muscle, it is not found in endothelial cells or cardiomyocytes (Lambeth, 2004). Cardiomyocytes, endothelial cells and fibroblasts all have high levels of NOX2 (Byrne et al., 2003; Li and Shah, 2004; Liu et al., 2004). Endothelial cells, cardiomyocytes, and fibroblasts all express NOX4, which tends to be the most commonly expressed isoform (Murdoch et al., 2006). In a failing heart, NOX activity rises (Heymes et al., 2003). Indeed, the failing myocardium of patients with ischemic cardiomyopathy or dilated cardiomyopathy is characterised by increased Rac1 activity and upregulation of NOX-mediated ROS release. Moreover surprisingly, the ROS provided by NOX will encourage the production of more ROS from other sources. ROS produced by NADPH oxidase have been shown to cause xanthine oxidase activation (McNally et al., 2003). As a result, NADPH oxidases could be crucial even in situations where other enzymes are contributing to oxidative stress.

1.4.5. Advanced glycated end products and DCM

Non enzymatic reactions of glucose or other saccharide derivatives with proteins or lipids give rise to advanced glycated end products (AGEs), which are heterogeneous molecules (Semba et al., 2010). Most symptoms of T1DM and T2DM have been linked to elevated levels of circulating glucose. Due to increased glucose supply, the formation of AGEs is accelerated in the presence of chronic hyperglycemia. Early hyperglycemia is

thought to result in a proportional rise in AGE formation and oxidative stress. In the absence of hyperglycemia, mitochondrial respiratory chain proteins turn into glycated, and causes mitochondrial DNA damage, resulting in a self-perpetuating cycle of AGE formation and oxidative stress (Testa et al., 2017). AGE accumulation in the diabetic heart may result in irreversible glycosylation of structural proteins, such as Ca^{2+} channels, and increased myocardial stiffness. Even so, AGE-induced extracellular matrix cross-linking in connective tissue facilitates myocardial fibrosis and impairs passive relaxation (Jia et al., 2016). An imbalance between AGEs (endogenous development and exogenous consumption) and the successful mechanism of the AGE detoxification system as their excretion from kidneys occurs when there is an overproduction of AGEs (Vlassara et al., 2008). AGE progression leads to metabolic burden (both hyperglycemia and hyperlipidemia), inflammation, and oxidative stress (Del and Basta, 2012). AGE accumulation effects cause endoplasmic reticulum (ER) stress and tempt apoptosis or trigger NF-κB through signaling cascade. In a variety of cell types, AGEs can bind to a variety of extracellular and intracellular proteins. AGE receptors on the cell surface can be divided into two groups based on the downstream effects of AGE binding and activation. Endocytosis, breakdown and elimination of AGEs from the circulation as well as those that activate a pro-inflammatory cellular response (Lu et al., 2004; Rodriguez et al., 2016; Vlassara and Striker, 2011). AGER1, the prototypical member of the first class, also inhibits the development of ROS and cellular defence mechanisms. AGER1 expression is upregulated in response to acute AGE exposure, but is suppressed in response to chronic oxidative stress and elevated extracellular AGE levels, which is consistent with the finding of lower AGER1 levels in diabetes and chronic inflammatory disease patients (Vlassara and Uribarri, 2014). The receptor for advanced glycation end products, RAGE, is the most significant in terms of diabetic complications. RAGE activation stimulates NADPH oxidase and other intracellular signaling pathways (Goldin et al., 2006). This receptor binds to a wide range of ligands, including AGEs, and the resulting RAGE activation stimulates NADPH oxidase and other intracellular signaling pathways such as the extracellular signal-regulated kinases 1 and 2 (ERK1/2), mitogen-activated protein kinases (MAPKs), p21[ras], p38 and Janus kinase 1(JNK) (Cai et al., 2016). AGEs cause disease *via* three main molecular mechanisms: extracellular protein modification, intracellular protein modification, and signaling cascade activation through binding to cell surface RAGE. All three mechanisms could play a role in the

onset and progression of CVDs. RAGE receptors are located in cardiomyocytes and are the significant component of cardiac ischemia reperfusion injury. Furthermore, transgenic overexpression of RAGE in the heart results in features similar to those seen in rodent models of DCM, such as decreased intracellular calcium transients and Ca^{2+} peak prolongation (Petrova et al., 2002). The development of therapeutic agents aimed at lowering circulating AGE concentrations and inhibiting RAGE activation could help to treat DM complications and coronary artery diseases (Hudson et al., 2003).

1.4.6. PKC signaling pathway during DCM

In DCM, PKC signaling pathways are triggered in response to hyperglycemia and insulin resistance. In humans, 15 PKC isoforms have been identified so far. Based on second messenger signaling and activation mode, these isoforms can be classified into three subfamilies. It has been suggested that PKC and isoforms are involved in the development of diabetic cardiac hypertrophy (Lei et al., 2013; Li et al., 2014). PKC activation is aided by oxidative stress, inflammation, and increased renin-angiotensin-aldosterone system (RAAS) activity. By stimulating the production of extracellular matrix, controlling the calcium ion metabolism of myocardial cells, activating Ang II, and inducing ROS and inflammatory factor, PKC can cause damage to myocardial tissue and blood vessels. Some of the more common cardiovascular symptoms of DCM include left ventricular hypertrophy, myocardial and cardiovascular fibrosis, and impaired LV function. These improvements, on the other hand, have been seen in animal models and in the LV myocardium of study subjects with PKC overexpression. Adenosine monophosphate-activated protein kinase has also been linked to the negative effects of PKC (Liu et al., 2014). PKCα is the most common subtype found in the hearts of mice, humans, and rabbits, while PKC β and PKC γ are measurable but expressed at much lower levels (Hambleton et al., 2006). PKC-α is the least studied of the myocardial PKC isoforms, despite the fact that it is the most highly expressed. Unlike PKC-ε and PKC-δ, it is not controlled in acute myocardial ischemia, and unlike PKC-β, it is not regulated in diabetes. PKC α activation or increased expression has been linked to hypertrophy, dilated cardiomyopathy, ischemic injury, and mitogen stimulation (Dorn and Force, 2005). PKC β expression was also found to be higher after a myocardial infarction (Simonis et al., 2007; Bowling et al., 1999). Increased activation of traditional PKC isoforms, including PKC-α has also been linked to human heart failure (Bowling et al.,

1999). As a result, PKC-α meets a key requirement for being a therapeutic target: its expression and activity are elevated in heart disease.

1.4.7. ER stress and UPR pathway

The ER, one of the largest organelles in eukaryotic cells, was discovered by Porter et al in 1945. The ER is in charge of protein synthesis and folding for the majority of secreted and membrane proteins, which account for about 35 % of all protein (Palade, 1956). Protein translocation, calcium homeostasis, lipid and steroid biosynthesis all take place in the ER (Kant et al., 2014). Possible factors, such as myocardial ischemia, diabetes, hypertension, and heart failure, may disturb this environment, triggering misfolded proteins to accumulate (Glembotski, 2007). Signaling pathways are stimulated when the ER homeostasis is disrupted by the accumulation of unfolded/misfolded protein, activating an adaptive response recognized as the unfolded protein response (UPR). The UPR targets to refurbish ER homeostasis by lowering protein loads in the ER *via* translational reduction, enhancing the transcription of chaperones and further proteins involved in protein folding and maturation, and inducing misfolded protein deprivation through the ER-associated degradation (ERAD) complex (Schroder, 2008). If it doesn't function, ER triggers the death signaling pathways (Walter and Ron, 2011). In normal conditions the ER transmembrane proteins ATF6α (activated transcription factor 6α), PERK (dsRNA activated protein kinase like ER kinase) and IRE1α (inositol requiring kinase 1α) are bound with the ER chaperone, glucose regulated protein 78 (GRP78) to remain them inactive (Lee, 2005). GRP78 dissociates from these three sensors to initiate their function when unfolded proteins accumulate in the ER. The triggered UPR then controls downstream effectors to increase ER chaperone folding and handling performance, reduce ER workload by attenuating translation, and remove unnecessary proteins by inducing ERAD (Bertolotti et al., 2000).

IRE1α is the oldest ER transmembrane protein with an ER-luminal domain, sensor domain recognizing unfolded peptides, kinase and endoribonuclease (RNase) domain on its cytosolic portion (Wang et al., 1998). IRE1α and IRE1β are two isoforms of IRE1. IRE1α is expressed all over the body, while IRE1β is only found in the stomach (Cao and Kaufman, 2012). After being released from Bip/GRP78, it is triggered by

homodimerization and autophosphorylation. Xbox binding protein 1 (XBP1) mRNA is cleaved by activated IRE1 to twitch translation of transcriptionally active spliced XBP1 (sXBP1). Active sXBP1 binds to a range of UPR target gene promoters to upregulate a variety of ER stress response elements in order to renovate ER homoeostasis and encourage cytoprotection.

PERK, like IRE1α, is a protein kinase that dimerizes and autophosphorylates after dissociating from GRP78. Activated PERK phosphorylates Ser51 on the eukaryotic initiation factor 2 (eIF2α) to prevent the formation of translational initiation complexes, resulting in protein translation being inhibited (Bertolotti et al., 2000). By reducing protein synthesis, this transient translational arrest aids in the recovery of ER homoeostasis. Meanwhile, phosphorylation of eIF2α causes the mRNA encoding activating transcription factor 4 (ATF4) to be translated, lowering the amount of unfolded proteins in the ER by activating various UPR genes.

ATF6α is a 90 kDa ER transmembrane protein under normal conditions but when stimulated, it transfers from the ER to the Golgi, where it is cleaved by site1 and site2 protease. The 50KDa fragment of cleaved ATF6α translocate from the cytosol to the nucleus, where it joins up with several bZip transcription factors and ERSE to induce transcription of several UPR-linked genes, including XBP1, CHOP, and GRP78 (Haze et al., 1999). Moreover, ATF6α has an isoform known as ATF6β. ATF6β is not needed for ER chaperone transcriptional induction and may even inhibit ATF6α activity (Thuerauf et al., 2004). During chronic ER stress, ATF6β has been shown to play a pro-survival role (Odisho et al., 2015). If adaptive mechanisms fail to restore ER homeostasis, the UPR will shift from a pro-adaptive to a pro-apoptotic state.

1.4.8. ER stress induced apoptosis

The detrimental apoptotic response occurs when the UPR fails to restore ER homeostasis. While all UPR sensor proteins are tangled in ER stress-induced apoptosis, it is unclear how the cell decides to commit suicide in response to excessive ER stress. IRE1α activates apoptosis by activating JNK and p38 *via* TRAF2 and ASK1 mechanisms in response to prolonged ER stress. Both p38 and JNK can activate the proapoptotic protein Bax by phosphorylating it. The interaction of IRE1α and TRAF2 has also been linked to stimulation of caspase12 (Saleh et al., 2006; Nakagawa et al., 2000). Caspases-

12 activation in ER-stressed cells is thought to be caused by a number of processes. Caspase-12 can be directly cleaved and triggered by m-Calpain, a cysteine protease activated by disrupted calcium homeostasis in ER-stressed cells (Nakagawa and Yuan, 2000). Caspase-7 can cleave and activate caspase-12 when it is translocated from the cytosol to the ER surface in stressed cells (Rao and Hermel, 2001). TRAF2 proteins can be recruited by ER stress-activated IRE1α and PERK, resulting in caspase-12 clustering at ER membranes (Yoneda et al., 2001). As caspase-12 is activated, it moves from the ER to the cytosol, where it cleaves procaspase-9 and activates caspase-3, the downstream effector caspases, albeit without amplification in the mitochondria (Morishima et al., 2002). As a result, caspase-12-mediated apoptosis was identified as a distinct ER apoptosis pathway independent of mitochondrial or death receptor activation. The diabetic heart showed increased expression of cleaved caspase-12 as an indication of ER stress-related apoptosis (Li et al., 2007).

CHOP/GADD153, a member of the C/EBP family of b-ZIP transcription factors that heighten apoptosis is another apoptotic pathway activated by ER stress. The ATF6α and PERK pathways regulate this. CHOP can induce apoptosis by inhibiting the expression of the antiapoptotic protein Bcl2 (McCullough et al., 2001). Furthermore, CHOP regulates the transcription of many genes that encode proapoptotic proteins such as, ER oxidoreductase 1α (ERO1 α), GADD34, carbonic anhydrase VI and death receptor 5 among others (Malhotra and Kaufman, 2007). CHOP activates GADD34, causing eIF2 to dephosphorylate, reversing translational attenuation (Novoa et al., 2001). The activation of ERO1α by CHOP promotes apoptosis by hyperoxidizing the ER and activating IP3 receptors, both of which promote apoptosis (Li et al., 2009). Furthermore, new evidence suggests that CHOP can interact with ATF4 to boost protein synthesis, resulting in ATP depletion, oxidative stress, and cell death (Han et al., 2013).
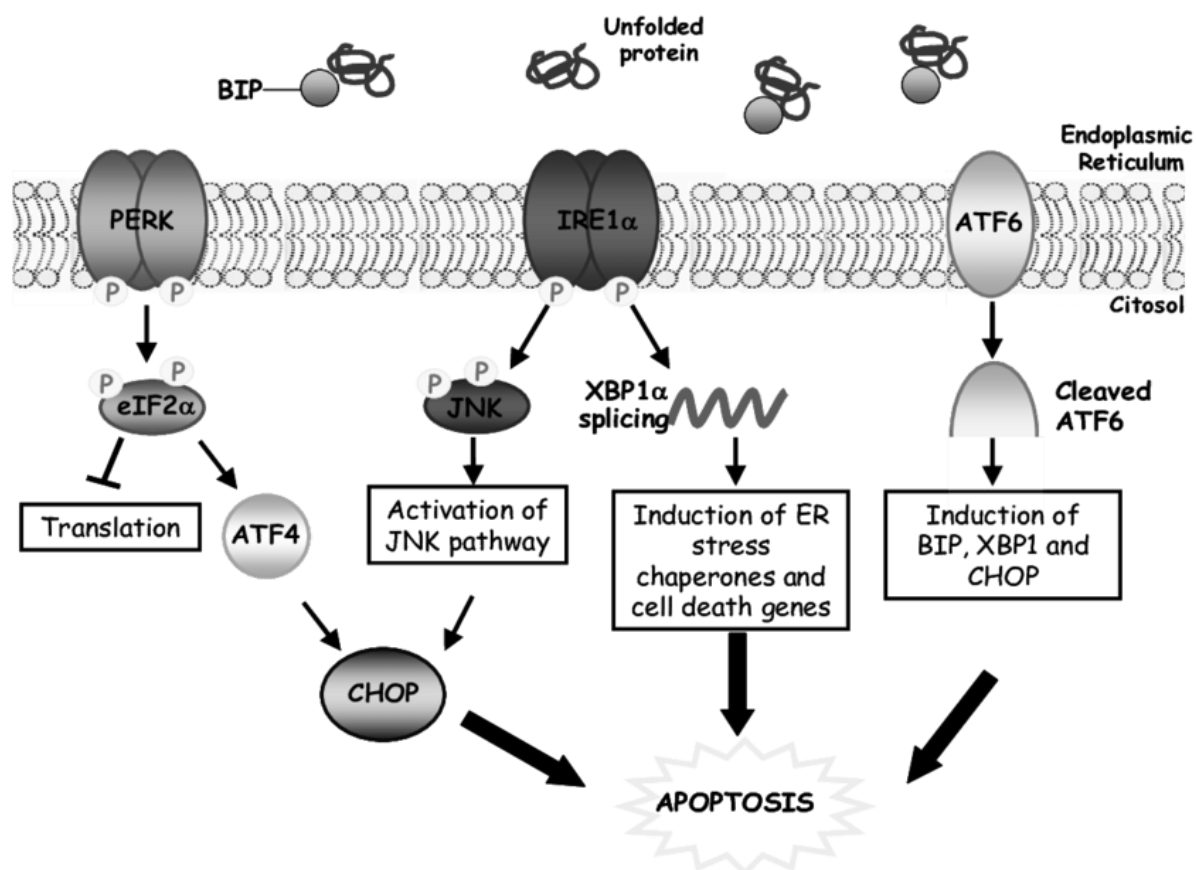
Fazio et al., Current Pharmaceutical Biotechnology, 2012

Figure 1.3.Unfolded protein response-mediated ER stress pathways

1.4.9. ER stress in heart

Numerous studies have related ER homeostasis disturbance to the pathophysiology of a variety of diseases, including heart disease. However, the precise role of ER stress signaling in the heart has yet to be determined, and whether ER stress signaling is detrimental or protective in the heart remains an open question (Belmadani, and Matrougui, 2019). Studies have shown that in a STZ-induced type 1 diabetic rat model, there is experimental evidence for the role of ER stress in cardiac apoptosis (Li et al., 2007). In diabetic hearts, both protein and mRNA levels of GRP78 and caspase-12 were upregulated as compared to normal hearts. Since apoptosis is essential in DCM (Cai et al., 2006), these findings indicated that ER stress was induced in diabetic hearts and ER stress-associated apoptosis played a role in DCM pathogenesis. Besides multiple low doses of STZ induces upregulation of many ERSR proteins, including PERK- and

ATF6-mediated pathways was found in diabetic hearts of mice (Lee and Harris, 2012). In a rat model of T2DM, TUDCA inhibiting ER stress normalises GRP78, GRP94, and mitochondrial GSK-3β, resulting in a major reduction in DCM (Miki et al., 2009). It is now widely recognised that, in addition to hyperglycemia, the diabetic heart is subjected to a slew of other factors that can trigger ER stress, including increased oxidative stress, hypoxia, homocysteine, lipid deposition, and secretory protein synthesis (Beer et al., 2005).

1.4.10. Calcium homeostasis and DCM

As an intracellular calcium (Ca^{2+}) warehouse, the ER not only sets up cytosolic Ca^{2+} signals, but also assembles and folds newly synthesised proteins, among other things. Many diseases have an upstream occurrence that involves changes in ER homeostasis, such as significant Ca^{2+} depletion. On the one hand, ineffective release of activator Ca^{2+} can result in the loss of vital cell functions. Loss of luminal Ca^{2+}, on the other hand, induces ER stress and stimulates an unfolded protein response, which can either restore normal ER function or result in cell death, depending on the period and severity of the stress (Mekahli et al., 2011). Cardiovascular contractility is largely regulated by intracellular Ca^{2+}. The release of Ca^{2+} through Ca^{2+} release channels (ryanodine receptors) of the sarcoplasmic reticulum (SR) is triggered by Ca^{2+} influx induced by activation of voltage-dependent L-type Ca^{2+} channels on membrane depolarization in the cardiomyocyte. Ca^{2+} then diffuses through the cytosolic space to contractile proteins, where it binds to troponin C, and releasing troponin I-induced inhibition. The Ca^{2+} activates the sliding of thin and thick filaments, that effect in cardiac strength and/or contraction, by binding to troponin C (Boudina and Abel, 2007). Activation of the SR Ca^{2+} pump (SERCA2a), the sarcolemmal Na-Ca^{2+} exchanger, and the sarcolemmal Ca^{2+} ATPase restore Ca^{2+} to diastolic levels (Endoh, 2006). Calcium and other ion homeostasis in diabetic cardiomyocytes have long been known to be disrupted (Cessario et al., 2006). Reduced activity of ATPases, decreased capacity of the SR to take up calcium, and reduced activities of other exchangers such as Na-Ca^{2+} and the sarcolemmal Ca^{2+} ATPase are all mechanisms by which disrupted calcium homeostasis affects cardiac function in diabetes (Zhao et al., 2006). Ca^{2+} efflux in the cardiomyocyte was decreased, SR Ca^{2+} load was depressed, ryanodine receptor expression was reduced, and Ca^{2+} efflux *via* the Na- Ca^{2+} exchanger was increased in the

db/db mouse model of T2DM (Pereira et al., 2006). In addition, in T1DM, reduced cardiac expression of SERCA2a or the Na- Ca^{2+} exchanger has been observed (Hattori et al., 2000). CaMKII, a calcium/calmodulin based protein kinase II was discovered to be activated by ER released calcium and to serve as a unifying link between ER stress and mitochondrial apoptosis in a recent study (Ozcan and Tabas, 2010). CaMKII was triggered in response to oxidative stress to mediate ER stress-induced cardiac dysfunction and apoptosis (Roe and Ren, 2013). Fortunately, a study found that reduced Ca^{2+} sensitivity in skinned fibres obtained from diabetic patients at the time of coronary artery bypass surgery resulted in depressed myofilament activity (Sen et al., 2000). Nevertheless, further research is needed to understand the mechanisms underlying the altered calcium handling in DCM patients.
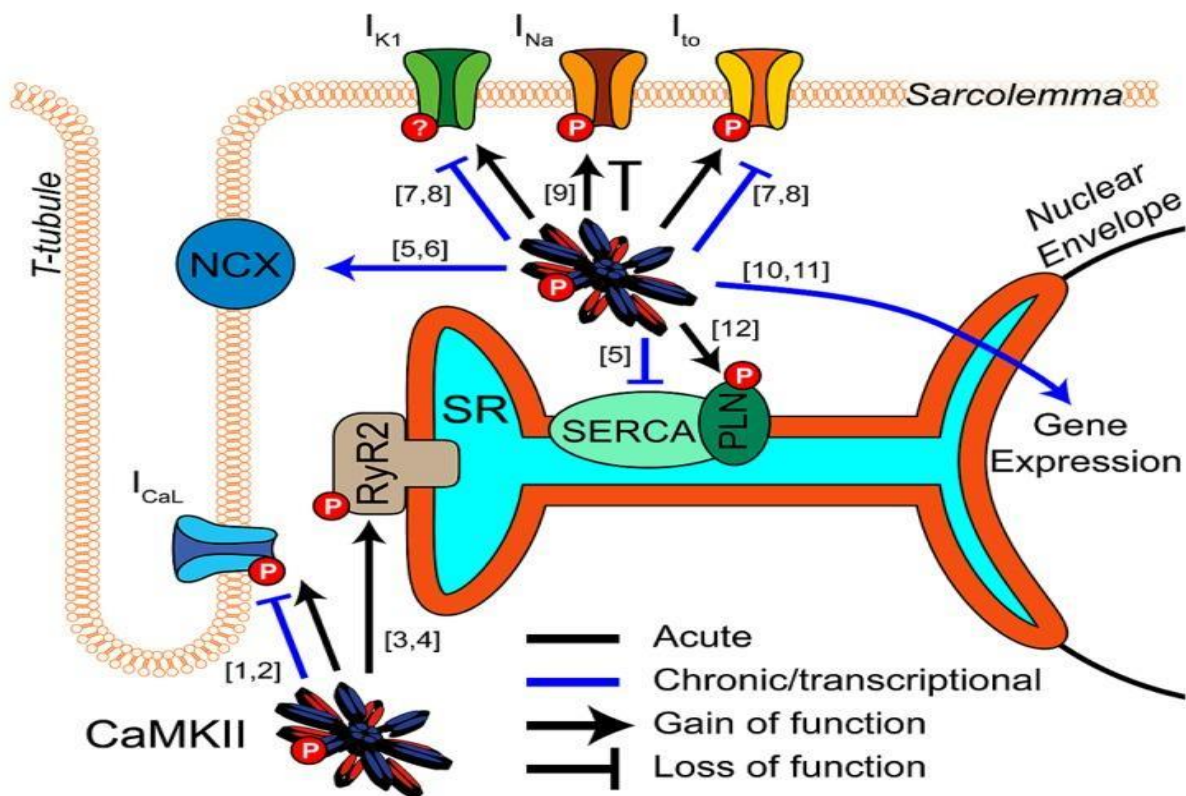
Vincent et al., Frontiers in pharmacology, 2014

Figure.1.4. CaMKII regulation of cardiomyocyte electrophysiology and Ca^{2+} handling

1.4.11. ER and mitochondria interaction during DCM

The ER and mitochondria have been observed to interact extensively in recent years, and this interaction is needed for safe cardiac function (Murley and Nunnari, 2016). Mitochondria are spatially and functionally organised in close touch with the ER, which aids mitochondrial uptake of Ca^{2+} released from the ER by IP3Rs, supplying the mitochondria with Ca^{2+} that is needed for ATP production (Rizzuto et al., 1993). ER Ca^{2+} leak and enhanced ER–mitochondrial coupling promotes mitochondrial respiration and bioenergetics in the early stages of ER stress (Bravo et al., 2011). Mitofusin 2 (Mfn2), an important physical tether between the ER and mitochondria, facilitates Ca^{2+} signaling between the two organelles (Chen et al., 2012). Numerous proteins, such as, PTPIP51, VAPB GRP75, BAP31, Pdzd8, FIS1, and VDAC1 are essential for tethering and interactions between the ER and mitochondria, such as Ca^{2+} exchange, lipid trafficking, apoptosis, autophagy, and mitochondrial fission and fusion (Gordaliza et al., 2019).

Autophagy, an essential cellular pathway that is triggered as a pro-survival pathway under physiological ER stress, is one significant interaction between the ER and mitochondria (Wei et al., 2008). The UPR arm IRE1α stimulates JNK and phosphorylates Bcl-2, causing Bcl-2 to dissociate from the autophagy-related protein Beclin-1, which is found in both the ER and the mitochondria. ER stress has been shown to be induced by mitochondria that are defective and/or impaired (Celardo et al., 2016). Furthermore, the significance of ER–mitochondrial interactions in the autophagic process stems from the idea that disrupting ER–mitochondrial contacts impairs autophagosome development (Hailey et al., 2010). These results suggest that interactions between the ER and mitochondria are critical for autophagy activation, which allows damaged proteins and organelles to be eliminated, resulting in healthy heart function. The functional and balanced interactions between the ER and mitochondria, along with Ca^{2+} handling, contractile function, autophagy, and apoptosis, lead to cardiomyocyte homeostasis and cardiac contractile function.

1.4.12. Role of ER-phagy in DCM

Autophagy is a cellular response to provocation in which damaged proteins are transferred to cytolysosomes and degraded (Xie et al., 2013). "Selective autophagy" has

been identified based on the selective degradation of substrates and can play an important role in cell homeostasis (Green and Levine, 2014). One of the type of selective autophagy is ER autophagy (reticulophagy/ ER-phagy), which is a major degradation mechanism that keeps the ER in a constant state (Cebollero et al., 2012). It's unclear how to detect ER-phagy, and the regulatory mechanism that controls it is unknown. Autophagosomes enclose ER fragments and fuse with lysosomes to degrade the internal material containing the ER in macro-ER-phagy (Leonibus et al., 2019). Lysosomal membranes invaginate and 'pinch off' portions of the ER into the lysosomal lumen in micro-ER-phagy (Wilkinson, 2019).

ER component turnover through autophagy was first revealed as a back-up mechanism for ineffective ERAD pathway of proteasomal degradation of ER proteins (Fujita et al., 2007). However, by identifying receptors required for delivering ER fragments to the lysosome through a traditional autophagy pathway, new insights into the mechanisms underlying ER-phagy have only recently been gained (Dikic, 2018). FAM134B, SEC62, RTN3, CCPG1, ATL3, and TEX264 are six mammalian ER-resident proteins that have been identified as selective ER-phagy receptors (Hübner and Dikic, 2020). ER-phagy receptors have been linked to a variety of human diseases. Most of the research related to ER-phagy receptors was studied in infectious and neurodegenerative diseases, aging and cancer (Dikic and Elazar, 2018). It's less obvious how ER-phagy affects neuronal homeostasis and neurodegenerative diseases. Moreover, ER-phagy has been linked to cancer development and progression through FAM134B and SEC62 (Islam et al., 2017). Furthermore there is no report from the role of ER-phagy in the heart. Therefore, it's important to look at their molecular pathways to see if there's an evolving stimulus for therapeutic approaches.
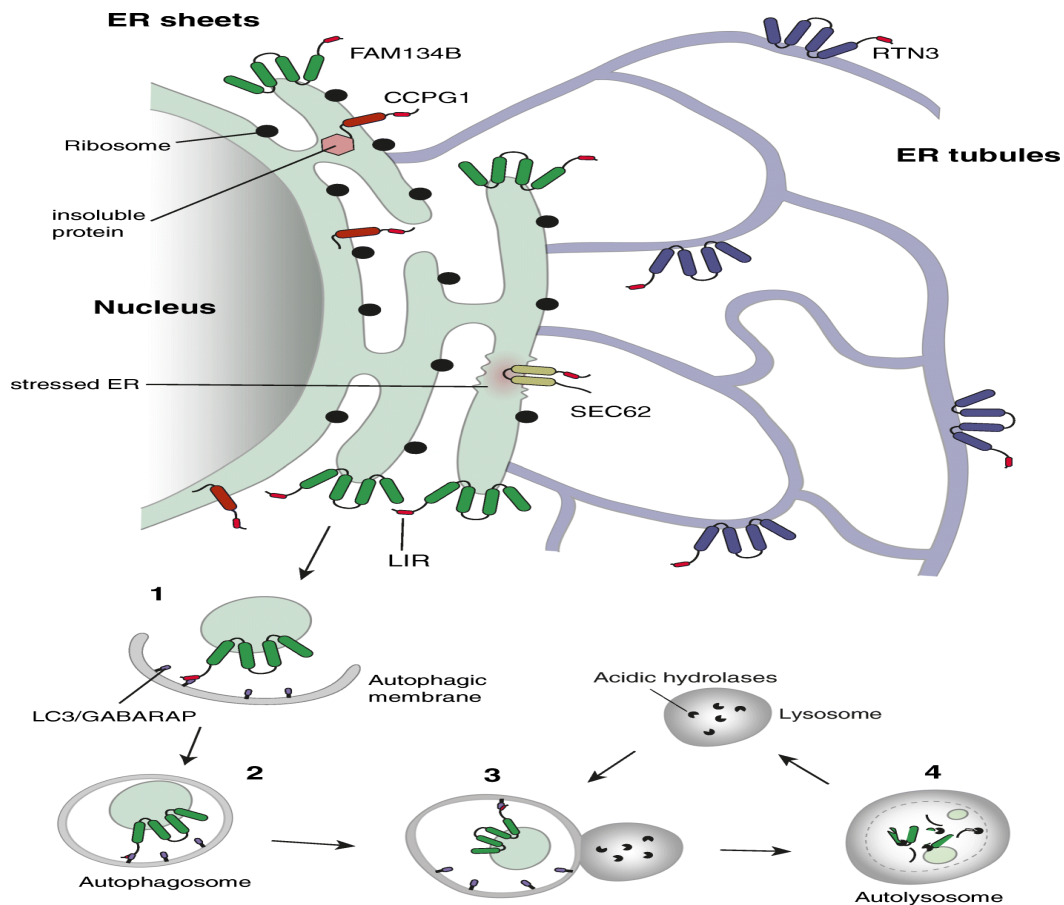
Figure.1.5. ER-phagy is mediated by ER-phagy receptors localized to distinct subdomains of the ER.

1.4.13. ER stress as a therapeutic target

ER stress and UPR are highly activated in atherosclerosis, ischemic disorders, diabetes, and heart failure, according to recent cardiovascular research (Amen et al., 2019). Therapies that target the ER stress pathways have shown to be effective in the treatment of CVDs. There are two major methods to targeting the UPR for CVDs treatment. To cope with stress, the first solution involves triggering components of the UPR's adaptive pathway. The second strategy is to inhibit the components of UPR's proapoptotic pathways. While targeting the components of the UPR as a potential therapy for cardiovascular diseases appears promising, understanding of the subject is limited (Minamino et al., 2010). ATF6α, IRE1α, spliced XBP1, PERK, eIF2α, and the proteasome, which are all potential components of the UPR and ERAD, may be good targets for therapeutic design. Chemical chaperones are small molecules that function in

the same way as the endogenous molecular chaperone machinery to stabilise misfolded proteins, help them fold properly, and reduce ER stress. Tauroursodeoxycholic (TUDCA) and 4-phenylbutyric acid (PBA) are two chemical chaperones that have been widely used in various diseases associated with ER stress. Cardiomyoblast death was reduced when ER stress was inhibited with TUDCA and PBA (Younce et al., 2010). In a rat myocardial infarction model, it was discovered that salubrinal, an eIF2α phosphatase inhibitor, increases GRP78 expression and appears to defend against ER stress induced apoptosis in cardiomyocyte apoptosis (Li et al., 2015). The statin atorvastatin, which is used to prevent CVDs, was shown to reduce the expression of caspase 12 and CHOP, as well as cardiomyocyte apoptosis, in a post-myocardial infarction model (Song et al., 2011). CHOP expression and phosphorylation were also reduced after treatment with SP600125, a JNK inhibitor that prevents CHOP upregulation in cardiomyocytes during cyclic stretching (Cheng et al., 2009). Angiotensin AT1 receptor antagonists (telmisartan and olmesartan) also reduce apoptosis and cardiac hypertrophy by inhibiting ER stress-induced apoptosis (Sukumaran et al., 2011). Furthermore, calcitriol and paricalcitol, which are Vitamin D receptor agonists, were found to protect mice from MI/R injury by inhibiting CHOP and caspase 12 expressions (Yao et al., 2015). Regrettably, the mechanisms by which signaling transitions from cell survival to cell death remain unknown. As a result, we don't know when to activate or suppress ER stress sensor proteins for treatment purposes. Changing UPR activation or reducing ER tension are still promising therapeutic targets, despite these limitations, which mean that it is still early for future therapeutic use.

1.5. Current therapeutic strategy

DCM can be responsible for a large proportion of idiopathic heart failure diagnoses in T2DM patients, as well as contributing to a poor prognosis for heart failure after myocardial ischemia. Currently, clinical guidelines are focused on managing the underlying diabetes and reducing the risk factors linked to CVD progression. Glycemic regulation has been shown to increase LV diastolic function in T2DM patients in several studies. Cardiovascular disease, on the other hand, can occur in diabetic patients who are well-treated, demonstrating the need for effective therapeutic strategies for this population (Tate et al., 2017). Currently, DCM clinical techniques are also focused on drug therapy. Controlling blood sugar is important for effectively reducing diabetes-

related cardiovascular morbidity. Disease care necessitates a healthy diet and daily exercise. According to clinical trials, using antihyperglycemic agents to regulate blood glucose in diabetic patients with early stages of myocardial dysfunction will effectively postpone the development of cardiomyopathy (Baigent et al., 2008). Metformin can significantly minimise the mortality rate in diabetic patients, according to studies (Cosmi and Cosmi, 2010). Surprisingly, many medications currently on the market will enhance heart health in addition to controlling glycemia (von Lewinski et al., 2017). Other than these clinical/epidemiological trials, there is little information available about the mechanisms by which these drugs achieve their pleiotropic effects.

Some studies found that the ability of GLP-1 receptor (especially common in β cells, where they're responsible for glucose-dependent insulin secretion) agonists to reduce proven cardiovascular risk factors including, high blood pressure, obesity, hyperglycemia and a dysfunctional lipid profile explains their potential cardioprotective impact. In many animal models of ischemic heart disease, GLP-1RAs or exogenous GLP-1 infusions have been shown to minimise infarct size and improve cardiac function. (DeNicola et al., 2014). In another study, DPP-4 inhibitors reduce fibrosis and oxidative stress, preventing cardiac diastolic dysfunction in mouse models of insulin resistance and obesity (Bostick et al., 2014). Besides, empagliflozin, SGLT2 inhibitor, improves diastolic dysfunction in diabetic mouse models, according to recent studies, which were related to increase the activity of SERCA and anti-fibrotic effects (Hammoudi et al., 2017)

In recent years, significant progress has been made toward the prospect of therapeutically modulating the expression of particular cardiac genes *in vivo*. As a result, the concept of up or down regulating the voice of crucial players in the production of DCM may be close to being a reality. Insulin resistance is caused by cardiac-specific overexpression of E3 ubiquitin ligase mitsugumin 3 enzyme, which results in proteasomal degradation of both insulin receptor and IRS-1 (Liu et al., 2015). Furthermore, transgenic mice showed an increase in fibrosis, implying that inhibiting the E3 ubiquitin ligase mitsugumin 3 may be a general therapeutic strategy for the prevention of DCM. Another molecule involved in the regulation of the IRS-1/Akt signaling pathway is forkhead box-containing protein 1, O subfamily (FoxO1). The persistent activation of FoxO1 caused by metabolic stress causes Akt signaling to be

blunted and insulin resistance to develop. In high-fat diet mice, cardiomyocyte-specific deletion of FoxO1 rescued cardiac dysfunction and maintained insulin responsiveness (Battiprolu et al., 2012). As a result, FoxO1 may be a possible therapeutic target in the future.

Meanwhile miRNA-based therapy is a multi-target therapy that regulates several pathways, making it an ideal candidate for modulating complex networks like those involved in DCM pathogenesis. The most abundant miRNA in the heart, miR-1 rises steadily from early to late stages of DCM. It inhibits the expression of anti-apoptotic and cardioprotective proteins Pim1 and Bcl-2, respectively. However, miR-133a expression, on the other hand, was significantly reduced in the hearts of STZ-induced diabetic mice. This decrease is associated to an increase in fibrotic markers including TGF, collagen and fibronectin. Overexpression of miR-133a inhibits the progression of fibrosis, indicating that this miRNA may be a therapeutic option for diabetes-induced heart fibrosis and cardiac disease. In human samples and animal models, diabetes is associated with lower expression of miR-30c and miR-181a, and overexpression of these miRNAs in cardiomyocytes subjected to elevated glucose reduced p53-induced apoptosis and hypertrophy (Raut et al., 2016). Novel clinical approaches are currently being studied in models and may be a potential new treatment choice for diabetic patients. These treatments have the ability to control common factors in DCM and heart failure, and they have a lot of promise in the cardiovascular field.

1.6. Natural compounds and DCM

Natural products have played a significant role in the treatment of various diseases including CVD and diabetic complications, by reducing oxidative stress, inflammation, and apoptosis, among other things (Hroob et al., 2019) and continue to do so. They are commonly considered to be safer, cheaper and readily available. In the pharmaceutical industry, these compounds and their derivatives have been identified as essential sources of new medicines and medicinal products. Due to their therapeutic properties such as antidiabetic, anti-oxidant, anti-inflammatory, and other biological properties, phenolic compounds, one of the most popular groups of plant secondary metabolites, may play an important role in health maintenance (Jacobo and Cisneros, 2017). According to comprehensive data, phenolic compounds provide new insights for

a novel treatment aimed at protecting or reducing a number of diseases (Mattera et al., 2017). Ephedrine comes from *Ephedra sinica*, aspirin comes from the *Salix alba* L. tree, digoxin (cardiac glycoside) comes from *Digitalis purpurea*, taxol comes from *Taxus brevifolia*, lovastatin comes from *Monascus purpureus* L., reserpine comes from *Rauvolfia serpentina*, and many other medicines come from herbal and plant sources (Harvey, 2000; Frishman et al., 2009; Cragg and Newman, 2013). Interestingly, reserpine is still an effective treatment for hypertension (Weber et al., 2014). Despite the promising future of natural products in the treatment of DCM, there are a few obstacles to overcome before using them in clinical trials. Natural products have multiple targets. Off-target effects, both positive and negative, can result as a consequence of this fact. In effect, more targeted compounds should be developed.

1.7. General introduction on chlorogenic acid (CA)

One of the most common and highly functional polyphenolic compounds in the human diet is chlorogenic acid (CA), also known as 5'O caffeoylquinic acid. Coffee beans, potato tubers, sweet potato leaves, eggplant, artichoke, sunflower seed kernels, and other foods are good sources of CA (Nabavi et al., 2017). Green coffee beans generate about 6 to 12 percent w/w total CAs, which is the highest amount of CA found in plants to date (Raskar and Bhalekar, 2019). Due to its many pharmacological effects and biological activities, such as anti-inflammatory, antioxidant, anticancer, anti-obesity, treatment of metabolic disorders, antihypertensive and gastrointestinal tract-protective actions, CA has recently received a lot of attention (Naveed et al., 2018). As a result, CA's pharmacological and toxicological evaluation has become more relevant. CA and its metabolites are safe to use and may have pharmaceutical benefits (Amano et al., 2019). However, subsequent studies have shown that a portion of the CA is consumed intact in the stomach and/or small intestine. Currently, it is estimated that approximately a third of CA is absorbed in the gastrointestinal tract and enters the bloodstream. In humans, CA has been shown to be bioavailable and differentially metabolised throughout the entire gastrointestinal tract as well as the liver and kidney (Erk et al., 2012). Various modes of action have
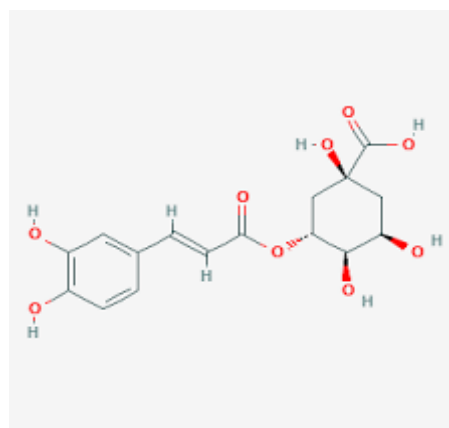
been proposed to reveal how CAs exerts their beneficial effects during metabolic syndrome. According to reports, CA's antiinflammatory effect may be due to inhibition of the ROS/NFκB signaling pathway rather than suppression of TLR4 and MyD88 (Shi et al., 2013). Another study found that CA treatment significantly reduced the expression of macrophage marker genes in adipose tissue such as Cd68, Cd11b, Cd11c and F4/80, as well as pro-inflammatory mediator genes such as MCP-1 and TNFα- in macrophages in mice fed with a high-fat diet. Besides, CA also inhibited the hepatic PPARα, which promotes fatty acid uptake into liver cells, according to the researchers. As a result, it was proposed that CA scavenge ROS produced by a high-fat diet, suppressing inflammation and thus reducing insulin resistance, fat accumulation, and body weight, while PPARα inhibition prevents liver steatosis (Shi et al., 2016). Consumption of CA has also been shown to have antihypertensive effects in the arterial vasculature by improving endothelial function and NO bioavailability. Several studies show that CA can potentially re-establish the function of lipoprotein and lipid metabolism regulatory enzymes, glycolytic as well as and gluconeogenic enzymes, in diabetic rats, resulting in greater benefits in the prevention of dyslipidemia and hyperglycemia (Bagdas et al., 2015). Although there are significant inter individual changes in its use, metabolism, and excretion in both basic and clinical research, multiple studies have shown that CA is a natural health-beneficial compound. In the current study, I found beneficial effect of CA against ER stress during hyperglycemia induced cardiac complications.

1.7. Aims and objectives

Diabetes mellitus has become an epidemic in recent years, and it is now one of the most common diseases. Individuals with diabetes are more vulnerable to cardiovascular problems and heart failure, emphasising the value of developing new therapeutic approaches. DCM refers to changes in myocardial structure and function caused by diabetes. Several molecular mechanisms have been suggested to contribute to development of DCM. Among theses the ER stress has been related to DCM. There is not much literature found on the keen molecular mechanisms that are responsible for the diabetes induced cardiac complications. Furthermore, a better understanding of the potential pathways involved in the pathophysiology of DCM is needed in order to establish novel cardioprotective strategies in the clinical arena for the prevention and amelioration of diabetes-related cardiovascular complications. Keeping this in mind the

current research aims to explore the mechanism in the alterations of H9c2 cells during hyperglycemia and diabetic rat emphasizing ER stress and associated pathways for identification of probable biochemical targets for future drug development and protective effect of CA. The objective of the present study comprises the following

- Evaluation of alterations in general biology of H9c2 cells with special emphasis on energy metabolism and redox status during hyperglycemia.

- Investigation on ER stress mainly focused on UPR pathways and ER-phagy during DCM.

- Assessment on calcium homeostasis and ER stress induced apoptosis during DCM.

- Evaluation of protective property of CA against DCM both *in vitro* and *in vivo.*

References

1. Ahmad J. The diabetic foot. *Diabetes Metab Syndr.* 2016; 10(1):48-60. doi:10.1016/j.dsx.2015.04.002.

2. Al Hroob AM, Abukhalil MH, Hussein OE, Mahmoud AM. Pathophysiological mechanisms of diabetic cardiomyopathy and the therapeutic potential of epigallocatechin-3-gallate. *Biomed Pharmacother.* 2019; 109:2155-2172. doi:10.1016/j.biopha.2018.11.086.

3. Amano Y, Honda H, Nukada Y, et al. Safety Pharmacological Evaluation of the Coffee Component, Caffeoylquinic Acid, and Its Metabolites, Using *Ex Vivo* and *In Vitro* Profiling Assays. *Pharmaceuticals (Basel).* 2019; 12 (3):110. doi:10.3390/ph12030110.

4. Amen OM, Sarker SD, Ghildyal R, Arya A. Endoplasmic Reticulum Stress Activates Unfolded Protein Response Signaling and Mediates Inflammation, Obesity, and Cardiac Dysfunction: Therapeutic and Molecular Approach. *Front Pharmacol.* 2019;10:977.10.3389/fphar.2019.00977.

5. Amos AF, McCarty DJ, Zimmet P. The rising global burden of diabetes and its complications: estimates and projections to the year 2010. *Diabet Med.* 1997;14 Suppl 5:S1-S85.

6. Aragno M, Mastrocola R, Medana C, et al. Oxidative stress-dependent impairment of cardiac-specific transcription factors in experimental diabetes. *Endocrinology*. 2006; 147(12):5967-5974. doi:10.1210/en.2006-0728.

7. Bagdas D, Etoz BC, Gul Z, et al. In vivo systemic chlorogenic acid therapy under diabetic conditions: Wound healing effects and cytotoxicity/genotoxicity profile. *Food Chem Toxicol*. 2015; 81:54-61. doi:10.1016/j.fct.2015.04.001.

8. Barouch LA, Berkowitz DE, Harrison RW, O'Donnell CP, Hare JM. Disruption of leptin signaling contributes to cardiac hypertrophy independently of body weight in mice. *Circulation*. 2003; 108 (6): 754-759. doi:10.1161/01.CIR.000 008371 6.82622.

9. Battiprolu PK, Hojayev B, Jiang N, et al. Metabolic stress-induced activation of FoxO1 triggers diabetic cardiomyopathy in mice. *J Clin Invest*. 2012;122(3):1109-1118. doi:10.1172/JCI60329.

10. Beer S, Golay S, Bardy D, et al. Increased plasma levels of N-terminal brain natriuretic peptide (NT-proBNP) in type 2 diabetic patients with vascular complications. *Diabetes Metab*. 2005; 31(6):567-573. doi:10.1016/s12623636 (07)70232-x.

11. Belmadani S, Matrougui K. Broken heart: A matter of the endoplasmic reticulum stress bad management? *World J Cardiol*. 2019; 11 (6): 159-170. doi:10.4330/wj c.v11.i6.159.

12. Bertolotti A, Zhang Y, Hendershot LM, Harding HP, Ron D. Dynamic interaction of BiP and ER stress transducers in the unfolded-protein response. *Nat Cell Biol*. 2000; 2(6):326-332. doi:10.1038/35014014.

13. Bostick B, Habibi J, Ma L, et al. Dipeptidyl peptidase inhibition prevents diastolic dysfunction and reduces myocardial fibrosis in a mouse model of Western diet induced obesity. *Metabolism*. 2014; 63 (8):1000-1011. doi:10.1016/j.metabol. 2014.04.002.

14. Boudina S, Abel ED. Diabetic cardiomyopathy revisited. *Circulation*. 2007; 115 (25):3213-3223. doi:10.1161/CIRCULATIONAHA.106.679597.

15. Boudina S, Abel ED. Diabetic cardiomyopathy, causes and effects. *Rev Endocr Metab Disord*. 2010; 11(1):31-39. doi:10.1007/s11154-010-9131-7.

16. Bowling N, Walsh RA, Song G, et al. Increased protein kinase C activity and expression of Ca2+-sensitive isoforms in the failing human heart. *Circulation*. 1999; 99 (3):384-391. doi:10.1161/01.cir.99.3.384.

17. Bravo R, Vicencio JM, Parra V, et al. Increased ER-mitochondrial coupling promotes mitochondrial respiration and bioenergetics during early phases of ER stress. *J Cell Sci*. 2011; 124 (Pt 13):2143-2152. doi:10.1242/jcs.080762.

18. Bugger H, Abel ED. Rodent models of diabetic cardiomyopathy. *Dis Model Mech*. 2009; 2 (9-10):454-66. doi: 10.1242/dmm.001941.

19. Byrne JA, Grieve DJ, Bendall JK, Li JM, Gove C, Lambeth JD, Cave AC, Shah AM. Contrasting roles of NADPH oxidase isoforms in pressure-overload versus angiotensin II-induced cardiac hypertrophy. *Circ Res*. 2003;93(9):802-5. doi: 10.1161/01.RES.0000099504.30207.F5.

20. Cai L, Wang Y, Zhou G, et al. Attenuation by metallothionein of early cardiac cell death via suppression of mitochondrial oxidative stress results in a prevention of diabetic cardiomyopathy. *J Am Coll Cardiol*. 2006;48(8):1688-1697. doi:10.1016/j.jacc.2006.07.022.

21. Cai Z, Liu N, Wang C, et al. Role of RAGE in Alzheimer's Disease. *Cell Mol Neurobiol*. 2016; 36(4):483-495. doi:10.1007/s10571-015-0233-3.

22. Cao SS, Kaufman RJ. Unfolded protein response. *Curr Biol*. 2012; 22(16):R622-R626. doi:10.1016/j.cub.2012.07.004.

23. Cebollero E, Reggiori F, Kraft C. Reticulophagy and ribophagy: regulated degradation of protein production factories. *Int J Cell Biol*. 2012; 2012:182834. doi:10.1155/2012/182834.

24. Celardo I, Costa AC, Lehmann S, et al. Mitofusin-mediated ER stress triggers neurodegeneration in pink1/parkin models of Parkinson's disease. *Cell Death Dis*. 2016; 7 (6):e2271. doi:10.1038/cddis.2016.173.

25. Cesario DA, Brar R, Shivkumar K. Alterations in ion channel physiology in diabetic cardiomyopathy. *Endocrinol Metab Clin North Am*. 2006;35(3):601-x. doi:10.1016/j.ecl.2006.05.002.

26. Chen Y, Csordás G, Jowdy C, et al. Mitofusin 2-containing mitochondrial-reticular microdomains direct rapid cardiomyocyte bioenergetic responses via interorganelle Ca(2+) crosstalk. *Circ Res*. 2012; 111(7):863-875. doi:10.1161/CIR CRESAHA.112.266585.

27. Cheng L, Ding G, Qin Q, et al. Cardiomyocyte-restricted peroxisome proliferator-activated receptor-delta deletion perturbs myocardial fatty acid oxidation and leads to cardiomyopathy. *Nat Med*. 2004; 10 (11):1245-1250. doi:10.1038/nm1116.

28. Cheng WP, Wang BW, Shyu KG. Regulation of GADD153 induced by mechanical stress in cardiomyocytes. *Eur J Clin Invest*. 2009;39 (11):960-971. doi:10.1111/j.1365-2362.2009.02193.x.

29. Chiu HC, Kovacs A, Blanton RM, et al. Transgenic expression of fatty acid transport protein 1 in the heart causes lipotoxic cardiomyopathy. *Circ Res*. 2005; 96(2):225-233. doi:10.1161/01.RES.0000154079.20681.B9.

30. Cosmi F, Cosmi D. Hypoglycemic therapy in heart disease patients with type 2 diabetes mellitus. *G Ital Cardiol (Rome)*. 2010; 11 (6):460-466.

31. Cragg GM, Newman DJ. Natural products: a continuing source of novel drug leads. *Biochim Biophys Acta*. 2013;1830 (6):3670-3695. doi:10.1016/j.bbagen.2013.02.008.

32. De Leonibus C, Cinque L, Settembre C. Emerging lysosomal pathways for quality control at the endoplasmic reticulum. *FEBS Lett*. 2019;593 (17):2319-2329. doi:10.1002/1873-3468.13571.

33. Del Turco S, Basta G. An update on advanced glycation endproducts and atherosclerosis. *Biofactors*. 2012; 38 (4):266-274. doi:10.1002/biof.1018.

34. DeNicola M, Du J, Wang Z, et al. Stimulation of glucagon-like peptide-1 receptor through exendin-4 preserves myocardial performance and prevents cardiac remodeling in infarcted myocardium. *Am J Physiol Endocrinol Metab*. 2014;307(8):E630-E643. doi:10.1152/ajpendo.00109.2014.

35. Dewald O, Sharma S, Adrogue J, et al. Downregulation of peroxisome proliferator-activated receptor-alpha gene expression in a mouse model of ischemic cardiomyopathy is dependent on reactive oxygen species and prevents lipotoxicity. *Circulation*. 2005;112 (3):407-415.

36. Di Fazio P, Ocker M, Montalbano R. New drugs, old fashioned ways: ER stress induced cell death. *Curr Pharm Biotechnol*. 2012;13(11):2228-2234. doi:10.2174/138920112802501962.

37. Dikic I, Elazar Z. Mechanism and medical implications of mammalian autophagy. *Nat Rev Mol Cell Biol*. 2018;19 (6):349-364. doi:10.1038/s41580-018-0003-4.

38. Dikic I. Open questions: why should we care about ER-phagy and ER remodelling?. *BMC Biol*. 2018;16(1):131. doi:10.1186/s12915-018-0603-7.

39. Dorn GW, Force T. Protein kinase cascades in the regulation of cardiac hypertrophy. *J Clin Invest*. 2005;115(3):527-537. doi:10.1172/JCI24178.

40. Du X, Matsumura T, Edelstein D, et al. Inhibition of GAPDH activity by poly(ADP-ribose) polymerase activates three major pathways of hyperglycemic damage in endothelial cells. *J Clin Invest*. 2003;112(7):1049-1057. doi:10.1172/JCI18127.

41. Endoh M. Signal transduction and Ca2+ signaling in intact myocardium. *J Pharmacol Sci*. 2006;100(5):525-537. doi:10.1254/jphs.cpj06009x.

42. English E, Lenters-Westra E. HbA1c method performance: The great success story of global standardization. *Crit Rev Clin Lab Sci*. 2018; 55(6):408-419. doi:10.1080/10408363.2018.1480591.

43. Erk T, Williamson G, Renouf M, et al. Dose-dependent absorption of chlorogenic acids in the small intestine assessed by coffee consumption in ileostomists. *Mol Nutr Food Res*. 2012;56(10):1488-1500. doi:10.1002/mnfr.201200222.

44. Factor SM, Bhan R, Minase T, Wolinsky H, Sonnenblick EH. Hypertensive-diabetic cardiomyopathy in the rat: an experimental model of human disease. *Am J Pathol*. 1981;102(2):219-228.

45. Factor SM, Minase T, Sonnenblick EH. Clinical and morphological features of human hypertensive-diabetic cardiomyopathy. *Am Heart J*. 1980;99(4):446-458. doi:10.1016/0002-8703(80)90379-8.

46. Finck BN, Han X, Courtois M, et al. A critical role for PPARα-mediated lipotoxicity in the pathogenesis of diabetic cardiomyopathy: modulation by dietary fat content. *Proc Natl Acad Sci U S A*. 2003; 100(3):1226-1231. doi:10.1073/pnas.0336724100.

47. Fischer VW, Barner HB, Larose LS. Pathomorphologic aspects of muscular tissue in diabetes mellitus. *Hum Pathol*. 1984; 15(12):1127-1136. doi:10.1016/s0046-8177(84)80307-x.

48. Fisher BM, Gillen G, Lindop GB, Dargie HJ, Frier BM. Cardiac function and coronary arteriography in asymptomatic type 1 (insulin-dependent) diabetic

patients: evidence for a specific diabetic heart disease. *Diabetologia*. 1986; 29(10):706-712. doi:10.1007/BF00870280.

49. Frishman WH, Beravol P, Carosella C. Alternative and complementary medicine for preventing and treating cardiovascular disease. *Dis Mon*. 2009;55(3):121-192. doi:10.1016/j.disamonth.2008.12.002.

50. Fujita E, Kouroku Y, Isoai A, et al. Two endoplasmic reticulum-associated degradation (ERAD) systems for the novel variant of the mutant dysferlin: ubiquitin/proteasome ERAD (I) and autophagy/lysosome ERAD (II). *Hum Mol Genet*. 2007; 16(6):618-629. doi:10.1093/hmg/ddm002.

51. Gharravi AM, Jafar A, Ebrahimi M, et al. Current status of stem cell therapy, scaffolds for the treatment of diabetes mellitus. *Diabetes Metab Syndr*. 2018;12(6):1133-1139. doi:10.1016/j.dsx.2018.06.021.

52. Glembotski CC. Endoplasmic reticulum stress in the heart. *Circ Res*. 2007;101(10):975-984. doi:10.1161/CIRCRESAHA.107.161273.

53. Goldin A, Beckman JA, Schmidt AM, Creager MA. Advanced glycation end products: sparking the development of diabetic vascular injury. *Circulation*. 2006;114(6):597-605. doi:10.1161/CIRCULATIONAHA.106.621854.

54. Gordaliza-Alaguero I, Cantó C, Zorzano A. Metabolic implications of organelle-mitochondria communication. *EMBO Rep*. 2019; 20(9):e47928. doi:10.15252/embr.201947928.

55. Green DR, Levine B. To be or not to be? How selective autophagy and cell death govern cell fate. *Cell*. 2014;157(1):65-75. doi:10.1016/j.cell.2014.02.049.

56. Griendling KK, Sorescu D, Ushio-Fukai M. NAD(P)H oxidase: role in cardiovascular biology and disease. *Circ Res*. 2000; 86(5):494-501. doi:10.1161/01.res.86.5.494.

57. Hailey DW, Rambold AS, Satpute-Krishnan P, et al. Mitochondria supply membranes for autophagosome biogenesis during starvation. *Cell*. 2010;141(4):656-667. doi:10.1016/j.cell.2010.04.009.

58. Hambleton M, Hahn H, Pleger ST, et al. Pharmacological- and gene therapy-based inhibition of protein kinase Calpha/beta enhances cardiac contractility and attenuates heart failure. *Circulation*. 2006; 114(6):574-582. doi:10.1161/CIRCULATIONAHA.105.592550.

59. Hammoudi N, Jeong D, Singh R, et al. Empagliflozin Improves Left Ventricular Diastolic Dysfunction in a Genetic Model of Type 2 Diabetes. *Cardiovasc Drugs Ther*. 2017;31(3):233-246. doi:10.1007/s10557-017-6734-1.

60. Han J, Back SH, Hur J, et al. ER-stress-induced transcriptional regulation increases protein synthesis leading to cell death. *Nat Cell Biol*. 2013;15(5):481-490. doi:10.1038/ncb2738.

61. Harvey A. Strategies for discovering drugs from previously unexplored natural products. *Drug Discov Today*. 2000;5(7):294-300. doi:10.1016/s1359-6446 (00) 01511-7.

62. Hattori Y, Matsuda N, Kimura J, et al. Diminished function and expression of the cardiac Na+-Ca2+ exchanger in diabetic rats: implication in Ca2+ overload. *J Physiol*. 2000;527 Pt 1(Pt 1):85-94. doi:10.1111/j.1469-7793.2000.00085.x.

63. Haze K, Yoshida H, Yanagi H, Yura T, Mori K. Mammalian transcription factor ATF6 is synthesized as a transmembrane protein and activated by proteolysis in response to endoplasmic reticulum stress. *Mol Biol Cell*. 1999;10(11):3787-3799. doi:10.1091/mbc.10.11.3787.

64. Heymes C, Bendall JK, Ratajczak P, et al. Increased myocardial NADPH oxidase activity in human heart failure. *J Am Coll Cardiol*. 2003;41(12):2164-2171. doi:10.1016/s0735-1097(03)00471-6.

65. Hübner CA, Dikic I. ER-phagy and human diseases. *Cell Death Differ*. 2020;27(3):833-842. doi:10.1038/s41418-019-0444-0.

66. Hudson BI, Bucciarelli LG, Wendt T, et al. Blockade of receptor for advanced glycation endproducts: a new target for therapeutic intervention in diabetic complications and inflammatory disorders. *Arch Biochem Biophys*. 2003;419(1):80-88. doi:10.1016/j.abb.2003.08.030.

67. Islam F, Gopalan V, Wahab R, Smith RA, Qiao B, Lam AK. Stage dependent expression and tumor suppressive function of FAM134B (JK1) in colon cancer. *Mol Carcinog*. 2017;56(1):238-249. doi:10.1002/mc.22488.

68. Jacobo-Velázquez DA, Cisneros-Zevallos L. Recent Advances in Plant Phenolics. *Molecules*. 2017;22(8):1249. doi:10.3390/molecules22081249.

69. Jia G, DeMarco VG, Sowers JR. Insulin resistance and hyperinsulinaemia in diabetic cardiomyopathy. *Nat Rev Endocrinol*. 2016; 12(3):144-153. doi:10.1038/nrendo.2015.216.

70. Kayama Y, Raaz U, Jagger A, et al. Diabetic Cardiovascular Disease Induced by Oxidative Stress. *Int J Mol Sci.* 2015;16 (10):25234-25263. doi:10.3390/ijms161025234.

71. Khalil H. Diabetes microvascular complications-A clinical update. *Diabetes Metab Syndr.* 2017;11 Suppl 1:S133-S139. doi:10.1016/j.dsx.2016.12.022.

72. Kwon SH, Pimentel DR, Remondino A, Sawyer DB, Colucci WS. H(2)O(2) regulates cardiac myocyte phenotype via concentration-dependent activation of distinct kinase pathways. *J Mol Cell Cardiol.* 2003;35(6):615-621. doi:10.1016/s0022-2828(03)00084-1.

73. Lambeth JD. NOX enzymes and the biology of reactive oxygen. *Nat Rev Immunol.* 2004;4(3):181-189. doi:10.1038/nri1312.

74. Lee AS. The ER chaperone and signaling regulator GRP78/BiP as a monitor of endoplasmic reticulum stress. *Methods.* 2005;35(4):373-381.doi:10.1016/j.ymeth.2004.10.010.

75. Lee KU, Harris RA. Mitochondria and endoplasmic reticulum in diabetes and its complications. *Exp Diabetes Res.* 2012; 2012:985075. doi:10.1155/20 12/98 507 5.

76. Lei S, Li H, Xu J, et al. Hyperglycemia-induced protein kinase C β2 activation induces diastolic cardiac dysfunction in diabetic rats by impairing caveolin-3 expression and Akt/eNOS signaling. *Diabetes.* 2013; 62 (7):2318-2328. doi:10.2337/db12-1391.

77. Leon BM, Maddox TM. Diabetes and cardiovascular disease: Epidemiology, biological mechanisms, treatment recommendations and future research. *World J Diabetes.* 2015;6(13):1246-1258. doi:10.4239/wjd.v6.i13.1246.

78. Li JM, Shah AM. Endothelial cell superoxide generation: regulation and relevance for cardiovascular pathophysiology. *Am J Physiol Regul Integr Comp Physiol.* 2004;287(5):R1014-R1030. doi:10.1152/ajpregu.00124.2004.

79. Li RJ, He KL, Li X, Wang LL, Liu CL, He YY. Salubrinal protects cardiomyocytes against apoptosis in a rat myocardial infarction model via suppressing the dephosphorylation of eukaryotic translation initiation factor 2α. *Mol Med Rep.* 2015;12(1):1043-1049. doi:10.3892/mmr.2015.3508.

80. Li SY, Gilbert SA, Li Q, Ren J. Aldehyde dehydrogenase-2 (ALDH2) ameliorates chronic alcohol ingestion-induced myocardial insulin resistance and

endoplasmic reticulum stress. *J Mol Cell Cardiol*. 2009; 47(2):247-255. doi:10.1016/j.yjmc c.2009.03.017.

81. Li Z, Abdullah CS, Jin ZQ. Inhibition of PKC-θ preserves cardiac function and reduces fibrosis in streptozotocin-induced diabetic cardiomyopathy. *Br J Pharmacol*. 2014;171(11):2913-2924. doi:10.1111/bph.12621.

82. Li Z, Zhang T, Dai H, et al. Involvement of endoplasmic reticulum stress in myocardial apoptosis of streptozocin-induced diabetic rats. *J Clin Biochem Nutr*. 2007; 41(1):58-67. doi:10.3164/jcbn.2007008.

83. Liu F, Song R, Feng Y, et al. Upregulation of MG53 induces diabetic cardiomyopathy through transcriptional activation of peroxisome proliferation-activated receptor α. *Circulation*. 2015; 131(9):795-804. doi:10.1161/CIRCUL ATIONAHA.114.012285.

84. Liu J, Ormsby A, Oja-Tebbe N, Pagano PJ. Gene transfer of NAD(P)H oxidase inhibitor to the vascular adventitia attenuates medial smooth muscle hypertrophy. *Circ Res*. 2004; 95 (6):587-594. doi:10.1161/01.RES.0000 142317.8 8591.e6.

85. Liu Q, Wang S, Cai L. Diabetic cardiomyopathy and its mechanisms: Role of oxidative stress and damage. *J Diabetes Investig*. 2014;5(6):623-634. doi:10.111 1/jdi.12250.

86. Lu C, He JC, Cai W, Liu H, Zhu L, Vlassara H. Advanced glycation endproduct (AGE) receptor 1 is a negative regulator of the inflammatory response to AGE in mesangial cells. *Proc Natl Acad Sci U S A*. 2004;101(32):11767-11772. doi:10.1 073/pnas.0401588101.

87. Malhotra JD, Kaufman RJ. Endoplasmic reticulum stress and oxidative stress: a vicious cycle or a double-edged sword?. *Antioxid Redox Signal*. 2007;9(12):2277-2293. doi:10.1089/ars.2007.1782.

88. Mattera R, Benvenuto M, Giganti MG, et al. Effects of Polyphenols on Oxidative Stress-Mediated Injury in Cardiomyocytes. *Nutrients*. 2017;9(5):523. doi:10.339 0/nu9050523.

89. McCullough KD, Martindale JL, Klotz LO, Aw TY, Holbrook NJ. Gadd153 sensitizes cells to endoplasmic reticulum stress by down-regulating Bcl2 and perturbing the cellular redox state. *Mol Cell Biol*. 2001;21(4):1249-1259. doi:10.112 8/MCB.21.4.1249-1259.2001.

90. McNally JS, Davis ME, Giddens DP, et al. Role of xanthine oxidoreductase and NAD(P)H oxidase in endothelial superoxide production in response to oscillatory shear stress. *Am J Physiol Heart Circ Physiol*. 2003;285(6):H2290-7. doi: 10.1152/ajpheart.00515.2003.

91. Mekahli D, Bultynck G, Parys JB, De Smedt H, Missiaen L. Endoplasmic-reticulum calcium depletion and disease. *Cold Spring Harb Perspect Biol*. 2011;3(6):a004317. doi:10.1101/cshperspect.a004317.

92. Miki T, Miura T, Hotta H, et al. Endoplasmic reticulum stress in diabetic hearts abolishes erythropoietin-induced myocardial protection by impairment of phospho-glycogen synthase kinase-3beta-mediated suppression of mitochondrial permeability transition. *Diabetes*. 2009;58(12):2863-2872. doi:10.2337/db09-0158.

93. Minamino T, Komuro I, Kitakaze M. Endoplasmic reticulum stress as a therapeutic target in cardiovascular disease. *Circ Res*. 2010;107(9):1071-1082. doi:10.1161/CIRCRESAHA.110.227819.

94. Morishima N, Nakanishi K, Takenouchi H, Shibata T, Yasuhiko Y. An endoplasmic reticulum stress-specific caspase cascade in apoptosis. Cytochrome c-independent activation of caspase-9 by caspase-12. *J Biol Chem*. 2002;277(37):34287-34294. doi:10.1074/jbc.M204973200.

95. Murdoch CE, Zhang M, Cave AC, Shah AM. NADPH oxidase-dependent redox signaling in cardiac hypertrophy, remodelling and failure. *Cardiovasc Res*. 2006;71(2):208-215. doi:10.1016/j.cardiores.2006.03.016.

96. Murley A, Nunnari J. The Emerging Network of Mitochondria-Organelle Contacts. *Mol Cell*. 2016;61(5):648-653. doi:10.1016/j.molcel.2016.01.031.

97. Nabavi SF, Tejada S, Setzer WN, et al. Chlorogenic Acid and Mental Diseases: From Chemistry to Medicine. *Curr Neuropharmacol*. 2017;15(4):471-479. doi:10.2174/1570159X14666160325120625.

98. Nakagawa T, Yuan J. Cross-talk between two cysteine protease families. Activation of caspase-12 by calpain in apoptosis. *J Cell Biol*. 2000;150 (4):887-894. doi:10.1083/jcb.150.4.887.

99. Nakagawa T, Zhu H, Morishima N, et al. Caspase-12 mediates endoplasmic-reticulum-specific apoptosis and cytotoxicity by amyloid-beta. *Nature*. 2000;403 (6765):98-103. doi:10.1038/47513.

100. Naveed M, Hejazi V, Abbas M, et al. Chlorogenic acid (CGA): A pharmacological review and call for further research. *Biomed Pharmacother*. 2018;97:67-74. doi:10.1016/j.biopha.2017.10.064.

101. Norhammar A, Tenerz A, Nilsson G, et al. Glucose metabolism in patients with acute myocardial infarction and no previous diagnosis of diabetes mellitus: a prospective study. *Lancet*. 2002;359(9324):2140-2144. doi:10.1016/S0140-6736(02)09089-X.

102. Nourooz-Zadeh J, Rahimi A, Tajaddini-Sarmadi J, et al. Relationships between plasma measures of oxidative stress and metabolic control in NIDDM. *Diabetologia*. 1997;40(6):647-653. doi:10.1007/s001250050729.

103. Novoa I, Zeng H, Harding HP, Ron D. Feedback inhibition of the unfolded protein response by GADD34-mediated dephosphorylation of eIF2alpha. J Cell Biol. 2001;153(5):1011-1022. doi:10.1083/jcb.153.5.1011.

104. Odisho T, Zhang L, Volchuk A. ATF6β regulates the Wfs1 gene and has a cell survival role in the ER stress response in pancreatic β-cells. *Exp Cell Res*. 2015;330(1):111-122. doi:10.1016/j.yexcr.2014.10.007.

105. Ozcan L, Tabas I. Pivotal role of calcium/calmodulin-dependent protein kinase II in ER stress-induced apoptosis. *Cell Cycle*. 2010;9(2):223-224. doi:10.4161/cc.9.2.10596.

106. Palade GE. The endoplasmic reticulum. *J Biophys Biochem Cytol*. 1956;2(4 Suppl):85-98. doi:10.1083/jcb.2.4.85.

107. Papatheodorou K, Papanas N, Banach M, Papazoglou D, Edmonds M. Complications of Diabetes 2016. *J Diabetes Res*. 2016;2016:6989453. doi:10.1155/2016/6989453.

108. Pereira L, Matthes J, Schuster I, et al. Mechanisms of (Ca2+)i transient decrease in cardiomyopathy of db/db type 2 diabetic mice. *Diabetes*. 2006;55(3):608-615. doi:10.2337/diabetes.55.03.06.db05-1284.

109. Petersen KF, Dufour S, Befroy D, Garcia R, Shulman GI. Impaired mitochondrial activity in the insulin-resistant offspring of patients with type 2 diabetes. *N Engl J Med*. 2004;350(7):664-671. doi:10.1056/NEJMoa031314.

110. Peterson LR, Herrero P, Schechtman KB, et al. Effect of obesity and insulin resistance on myocardial substrate metabolism and efficiency in young

women. *Circulation*. 2004; 109 (18): 2191-2196. doi:10.1161/01. CIR.0000127 959.28627.F8.

111. Petrova R, Yamamoto Y, Muraki K, et al. Advanced glycation endproduct-induced calcium handling impairment in mouse cardiac myocytes. *J Mol Cell Cardiol*. 2002;34(10):1425-1431. doi:10.1006/jmcc.2002.2084.

112. Porter KR, Claude A, Fullam EF. A study of tissue culture cells by electron microscopy : methods and preliminary observations. *J Exp Med*. 1945;81(3):233-246. doi:10.1084/jem.81.3.233.

113. Prabhakaran D, Singh K, Roth GA, Banerjee A, Pagidipati NJ, Huffman MD. Cardiovascular Diseases in India Compared With the United States. *J Am Coll Cardiol*. 2018; 72(1):79-95. doi:10.1016/j.jacc.2018.04.042.

114. Rao RV, Hermel E, Castro-Obregon S, et al. Coupling endoplasmic reticulum stress to the cell death program. Mechanism of caspase activation. *J Biol Chem*. 2001;276(36):33869-33874. doi:10.1074/jbc.M102225200.

115. Raskar V, Bhalekar MR. Formulation of coffee bean extract (Chlorogenic Acid) solid lipid nanoparticles for lymphatic uptake on oral administration. *J. drug* deliv. ther. 2019. *9*(4), 477-484. doi.org/10.22270/jddt.v 9i4.3201.

116. Raut SK, Singh GB, Rastogi B, et al. miR-30c and miR-181a synergistically modulate p53-p21 pathway in diabetes induced cardiac hypertrophy. *Mol Cell Biochem*. 2016; 417(1-2):191-203. doi:10.1007/s11010-016-2729-7.

117. Regan TJ, Lyons MM, Ahmed SS, et al. Evidence for cardiomyopathy in familial diabetes mellitus. *J Clin Invest*. 1977; 60(4):884-899. doi:10.1172/JCI10 8843.

118. Rizzuto R, Brini M, Murgia M, Pozzan T. Microdomains with high Ca2+ close to IP3-sensitive channels that are sensed by neighboring mitochondria. *Science*. 1993; 262(5134):744-747. doi:10.1126/science.8235595.

119. Roe ND, Ren J. Oxidative activation of Ca(2+)/calmodulin-activated kinase II mediates ER stress-induced cardiac dysfunction and apoptosis. *Am J Physiol Heart Circ Physiol*. 2013;304(6):H828-H839. doi:10.1152/ajpheart.00752.2012.

120. Rubler S, Dlugash J, Yuceoglu YZ, Kumral T, Branwood AW, Grishman A. New type of cardiomyopathy associated with diabetic glomerulosclerosis. *Am J Cardiol*. 1972;30(6):595-602. doi:10.1016/0002-9149(72)90595-4.

121. Saleh M, Mathison JC, Wolinski MK, et al. Enhanced bacterial clearance and sepsis resistance in caspase-12-deficient mice. *Nature*. 2006;440 (7087):1064-1068. doi:10.1038/nature04656.

122. Schröder M. *Cell Mol Life Sci*. 2008;65(6):862-894. doi:10.1007/s00018-007-7383-5.

123. Semba RD, Nicklett EJ, Ferrucci L. Does accumulation of advanced glycation end products contribute to the aging phenotype?. *J Gerontol A Biol Sci Med Sci*. 2010;65(9):963-975. doi:10.1093/gerona/glq074.

124. Sen L, Cui G, Fonarow GC, Laks H. Differences in mechanisms of SR dysfunction in ischemic vs. idiopathic dilated cardiomyopathy. *Am J Physiol Heart Circ Physiol*. 2000;279(2):H709-H718. doi:10.1152/ajpheart.2000.279.2.H709.

125. Sharma S, Adrogue JV, Golfman L, et al. Intramyocardial lipid accumulation in the failing human heart resembles the lipotoxic rat heart. *FASEB J*. 2004;18 (14): 1692-1700. doi:10.1096/fj.04-2263com.

126. Shi H, Dong L, Jiang J, et al. Chlorogenic acid reduces liver inflammation and fibrosis through inhibition of toll-like receptor 4 signaling pathway. *Toxicology*. 2013; 303:107-114. doi:10.1016/j.tox.2012.10.025.

127. Shi H, Shi A, Dong L, et al. Chlorogenic acid protects against liver fibrosis in vivo and in vitro through inhibition of oxidative stress. *Clin Nutr*. 2016;35 (6):1366-1373. doi:10.1016/j.clnu.2016.03.002.

128. Simonis G, Briem, SK, Schoen SP, et al. Protein kinase C in the human heart: differential regulation of the isoforms in aortic stenosis or dilated cardiomyopathy. *Mol. Cell. Biochem*. 2007. 305(1), 103-111. doi: 10.1007 /s11010-007-9533-3.

129. Song XJ, Yang CY, Liu B, et al. Atorvastatin inhibits myocardial cell apoptosis in a rat model with post-myocardial infarction heart failure by downregulating ER stress response. *Int J Med Sci*. 2011;8(7):564-572. doi:10.715 0/ijms.8.564.

130. Sukumaran V, Watanabe K, Veeraveedu PT, et al. Olmesartan, an AT1 antagonist, attenuates oxidative stress, endoplasmic reticulum stress and cardiac inflammatory mediators in rats with heart failure induced by experimental autoimmune myocarditis. *Int J Biol Sci*. 2011;7 (2):154-167. doi:10.7150/ijb s.7.154.

131. Szczepaniak LS, Dobbins RL, Metzger GJ, et al. Myocardial triglycerides and systolic function in humans: in vivo evaluation by localized proton spectroscopy and cardiac imaging. *Magn Reson Med*. 2003; 49 (3):417-423. doi:10.1002/mrm.10372.

132. Taegtmeyer H. Switching metabolic genes to build a better heart. *Circulation*. 2002; 106(16):2043-2045. doi:10.1161/01.cir.0000036760.4 2319.3f.

133. Tang WH, Martin KA, Hwa J. Aldose reductase, oxidative stress, and diabetic mellitus. *Front Pharmacol*. 2012; 3:87. doi:10.3389/fphar.2012.00087.

134. Tate M, Grieve DJ, Ritchie RH. Are targeted therapies for diabetic cardiomyopathy on the horizon? *Clin Sci (Lond)*. 2017; 131 (10):897-915. doi: 10.1042/CS20160491.

135. Testa R, Bonfigli AR, Prattichizzo F, La Sala L, De Nigris V, Ceriello A. The "Metabolic Memory" Theory and the Early Treatment of Hyperglycemia in Prevention of Diabetic Complications. *Nutrients*. 2017;9(5):437. doi:10.339 0/nu9050437.

136. Thuerauf DJ, Morrison L, Glembotski CC. Opposing roles for ATF6alpha and ATF6beta in endoplasmic reticulum stress response gene induction. *J Biol Chem*. 2004;279(20):21078-21084. doi:10.1074/jbc.M400713200.

137. Urrutia I, Martín-Nieto A, Martínez R, et al. Incidence of diabetes mellitus and associated risk factors in the adult population of the Basque country, Spain. *Sci Rep*. 2021;11(1):3016. doi:10.1038/s41598-021-82548-y.

138. Valko M, Leibfritz D, Moncol J, Cronin MT, Mazur M, Telser J. Free radicals and antioxidants in normal physiological functions and human disease. *Int J Biochem Cell Biol*. 2007;39(1):44-84. doi:10.1016/j.biocel.2006.07.001.

139. van der Kant R, Neefjes J. Small regulators, major consequences - Ca^{2+} and cholesterol at the endosome-ER interface. *J Cell Sci*. 2014; 127(Pt 5):929-938. doi:10.1242/jcs.137539.

140. Villegas-Rodríguez ME, Uribarri J, Solorio-Meza SE, et al. The AGE-RAGE Axis and Its Relationship to Markers of Cardiovascular Disease in Newly Diagnosed Diabetic Patients. *PLoS One*. 2016;11(7):e0159175. doi:10.1371/ journal.pone. 0159175.

141. Vincent KP, McCulloch AD, Edwards AG. Toward a hierarchy of mechanisms in CaMKII-mediated arrhythmia. Front Pharmacol. 2014;5:110. doi:10.3389/fphar. 2014.00110.

142. Vlassara H, Uribarri J. Advanced glycation end products (AGE) and diabetes: cause, effect, or both?. *Curr. Diabetes Rep.* 2014. 14(1), 1-10. doi: 10.1007/s1189 2-013-0453-1.

143. Vlassara H, Striker GE. AGE restriction in diabetes mellitus: a paradigm shift. *Nat Rev Endocrinol*. 2011;7(9):526-539. doi:10.1038/nrendo.2011.74.

144. Vlassara H, Uribarri J, Cai W, Striker G. Advanced glycation end product homeostasis: exogenous oxidants and innate defenses. *Ann N Y Acad Sci*. 2008;1126:46-52. doi:10.1196/annals.1433.055.

145. von Lewinski D, Kolesnik E, Wallner M, Resl M, Sourij H. New Antihyperglycemic Drugs and Heart Failure: Synopsis of Basic and Clinical Data. *Biomed Res Int*. 2017;2017:1253425. doi:10.1155/2017/1253425.Voulgari C, Papadogiannis D, Tentolouris N. Diabetic cardiomyopathy: from the pathophysiology of the cardiac myocytes to current diagnosis and management strategies. *Vasc Health Risk Manag*. 2010;6:883-903. doi:10.2147/VHRM.S11681.

146. Walter P, Ron D. The unfolded protein response: from stress pathway to homeostatic regulation. *Science.* 2011;334(6059):1081-1086. doi:10.1126/scien ce.1209038.

147. Wang XZ, Harding HP, Zhang Y, Jolicoeur EM, Kuroda M, Ron D. Cloning of mammalian Ire1 reveals diversity in the ER stress responses. *EMBO J*. 1998;17(19):5708-5717. doi:10.1093/emboj/17.19.5708.

148. Weber MA, Schiffrin EL, White WB, et al. Clinical practice guidelines for the management of hypertension in the community a statement by the American Society of Hypertension and the International Society of Hypertension. *J Hypertens*. 2014;32(1):3-15. doi:10.1097/HJH.0000000000000065.

149. Wei Y, Sinha S, Levine B. Dual role of JNK1-mediated phosphorylation of Bcl-2 in autophagy and apoptosis regulation. *Autophagy*. 2008;4(7):949-951. doi:10.416 1/auto.6788.

150. Wilkinson S. ER-phagy: shaping up and destressing the endoplasmic reticulum. *FEBS J*. 2019;286(14):2645-2663. doi:10.1111/febs.14932.

151. Wise J. Type 1 diabetes is still linked to lower life expectancy. *BMJ*. 2016; 353:i1988. doi:10.1136/bmj.i1988.

152. Xie F, Li L, Chen L. Autophagy, a new target for disease treatment. *Sci China Life Sci*. 2013;56(9):856-860. doi:10.1007/s11427-013-4530-0.

153. Yao T, Ying X, Zhao Y, et al. Vitamin D receptor activation protects against myocardial reperfusion injury through inhibition of apoptosis and modulation of autophagy. *Antioxid Redox Signal*. 2015; 22(8):633-650. doi:10.1089/ars. 2014.5887.

154. Yoneda T, Imaizumi K, Oono K, et al. Activation of caspase-12, an endoplasmic reticulum (ER) resident caspase, through tumor necrosis factor receptor-associated factor 2-dependent mechanism in response to the ER stress. *J Biol Chem*. 2001;276 (17):13935-13940. doi:10.1074/jbc.M010677200.

155. Younce CW, Wang K, Kolattukudy PE. Hyperglycaemia-induced cardiomyocyte death is mediated via MCP-1 production and induction of a novel zinc-finger protein MCPIP. *Cardiovasc Res*. 2010; 87(4):665-674. doi:10.109 3/cvr/cvq102.

156. Zhao XY, Hu SJ, Li J, Mou Y, Chen BP, Xia Q. Decreased cardiac sarcoplasmic reticulum Ca2+ -ATPase activity contributes to cardiac dysfunction in streptozotocin-induced diabetic rats. *J Physiol Biochem*. 2006; 62(1):1-8. doi:10.1007/BF03165800.

157. Zimmet P, Alberti KG, Shaw J. Global and societal implications of the diabetes epidemic. *Nature*. 2001; 414(6865):782-787. doi:10.1038/414782a.

Materials and Methods

2.1. Materials

2.1.1. Chemicals and reagents

Chlorogenic acid (99 % purity) was from Natural Remedies Pvt Ltd (Bangalore, India). D-glucose, metformin, streptozotocin, sodium citrate, citric acid, fructose, cholesterol, salt mixture, vitamin mixture, casein, paraformaldehyde, triton X 100, cobalt chloride and halothane were bought from Sisco Research Laboratories (SRL), Pvt Ltd., Mumbai, Maharashtra, India. Dulbecco's modified eagle's medium (DMEM), penicillin-streptomycin antibiotics, trypsin ethylenediaminetetraacetate (EDTA) and fetal bovine serum (FBS) were from Gibco (USA). Thapsigargin, phenyl butyric acid (PBA), dimethyl sulfoxide (DMSO), 3-(4,5-dimethyl-thiazol-2-yl)-2,5-diphenyl tetrazolium bromide (MTT), calcein AM, protease inhibitor cocktail, 4,6 diamidoino -2- phenylindole (DAPI), RIPA buffer, tween 20, and 2, 7-dichlorodihydrofluorescein diacetate (DCFH-DA) were from Sigma Aldrich (St Louis, MO, USA). Okamet 500 (metformin hydrochloride tablets) and normal saline (NS) were purchased from Cipla, Ltd., Mumbai, India. Lard was purchased from MP Biomedicals India Pvt Ltd., Mumbai, India. Endoplasmic reticulum red fluorescent protein (ER RFP) was from Invitrogen, USA. Standard rat feed was purchased from Feed mill unit, Kerala Veterinary and Animal Sciences University (KVASU), Mannuthy, Thrissur. Isoflurane (Forane, 250 mL solution) was bought from D. Vijay Pharma Pt. Ltd., Mumbai, India. Capillary blood collection tubes (BD SurePrep™) and serum tubes (BD Vacutainer® Plus) were purchased from Becton, Dickinson and Company, Franklin Lakes, NJ, US. Calnexin, TRAF2 and fetuin A antibodies were from Abcam (USA). PERK, GRP78, ATF6, caspase12, pJNK, PDI, BNP, SOD1, SOD2, ERK1/2, pERK1/2 were from Santa Cruz, USA. I purchased ATF4, PKCα, CHOP, pEIF2α, ERO1α, SERCA2a, pCaMKII, NCX1 and troponin from Cell Signaling Technology, USA. RTN3, SEC62, FAM134B were from My Biosource, USA and copeptin, RYR2, pRYR2, pIRE1α, pPERK antibodies from Immunotag ,Geno Technology Inc., USA. All other chemicals and reagents were of analytical grade.

2.1.2. Assay kits

Superoxide dismutase and caspase 3 activity kits were from Biovision, USA. Protein carbonyl, total antioxidant, GSH, GPx, aconitase, Ca^{2+} assay kit were from Cayman Ann Arbor, USA. TBARS estimation kit was from Himedia, India. LDH cytotoxicity detection kit was bought from Clontech Laboratories, Inc. USA. Cell based advanced glycated end products (AGE) competitive ELISA kit was bought from Cell Biolabs, Inc, USA. Atrial natriuretic peptide (ANP) ELISA kit was from Elabscience, USA. PKC kinase activity kit was bought from Enzo Lifesciences, USA. ER transcription factor profiling plate array was bought from Signosis, USA. Nuclear extraction kit was from Abcam, USA. BCA protein assay kit was bought from Pierce, USA. Primers for PCR were from Hysel India Pvt Ltd, New Delhi, India. Superscript III 1st strand synthesis system kit was from Life technologies, Bangalore, India. Serum parameters were estimated using kits from Agappe Diagnostics, Kerala, India. Estimation of insulin, ANP and Hb1Ac ELISA kits were from ImmunoTag, Geno Technology Inc., USA.

2.1.3. Cell culture

H9c2 cardiomyoblasts were bought from American Type Culture Collection (ATCC), USA. The cells were grown in DMEM supplemented with 10 % FBS (fetal bovine serum), 100 U penicillin/mL and 100 µg streptomycin/mL, and incubated at 5 % CO2 at 37 °C. Before the experiments, cells were passaged routinely and subcultured to 70 % confluence.

2.2. Methods

In vitro experiments

2.2.1. MTT assay

The MTT assay is a colorimetric method for determining metabolic activity in cells. It is based on the ability of NADPH-dependent cellular oxidoreductase enzymes to reduce the tetrazolium dye MTT to its insoluble formazan, which has a purple hue. The insoluble formazan crystals were dissolved in DMSO and the coloured solution was then examined using a multimode spectrophotometer. Briefly, cells were seeded in a 96 well paltes. After respective treatment, 100 µL of MTT solution (5 mg/mL) was poured to each well and incubated at 37 °C for 4 h. The formazan crystals formed was thus dissolved in DMSO. The plates were read in a microplate reader (Biotek Synergy 4, US) at 570 nm after 20 min and the percentage of cell viability was measured (Wilson, 2000).

2.2.2. Lactate dehydrogenase (LDH) release

Release of LDH into the medium by cells from all experimental groups was measured using LDH cytotoxicity assay kit. LDH is a cytoplasmic enzyme that is found in the majority of cells. LDH is released from cells and into the surrounding cell-culture supernatant when the cell cytoplasmic membranes are damaged (or ruptured). The measurement of LDH in cell culture supernatant assesses cell death levels. With this assay, LDH present in the surrounding cell-culture medium takes part in a coupled reaction that converts yellow tetrazolium salt (INT) into a red formazan product. Briefly, 100 µL of medium was collected from cultured cells and was added with 100 µL of LDH reaction solution containing NAD^+, lactic acid, INT and diaphorase. The mixture was then incubated with gentle shaking for 30 min at room temperature, and the absorbance was read at 490 nm.

2.2.3. Detection of intracellular reactive oxygen species (ROS)

Intracellular ROS levels were determined using 2'7' dichloro dihydro fluroscein diacetate (DCFH-DA) as probe (Choi et al., 2008). DCFH-DA is cleaved intracellular by nonspecific esterase and turns to high fluorescence upon oxidation by ROS. After respective treatments, cells were washed with phosphate buffer saline (PBS, pH 7.4) and then incubated with DCFH-DA (20 µM) for 20 min at 37 °C in a humidified atmosphere of 5 % CO_2. After incubation, cells were washed with phosphate buffer (pH 7.4). Fluorescence imaging was done (Ex. 488 nm; Em. 525 nm) to visualize the ROS generation using a spinning disk imaging system (BD™ pathway Bioimager system,BD Biosciences).

2.2.4. Oil red O staining

Oil red O staining is used to stain neutral lipids (triglycerides and diacylglycerols) as well as cholesterol esters, but it won't stick to biological membranes. The theory of this technique is based on the oil red O's low solubility in the solvent, which is further reduced by diluting the oil red O in water before use. Briefly cells were washed twice with PBS before fixation with 10 % formalin for 1 h and subsequently rinsed with distilled water. The cells were stained for 2 h by absolute immersion in oil red O stain and then rinsed with distilled water. By keeping the stained cells at a temperature of about 32 °C, the excess water has been evaporated. 1 mL of isopropyl alcohol was applied to assess the lipid content, and the extracted dye was immediately removed by gentle pipetting. OD was measured at 510 nm on a microplate reader (Ramirez et al., 1992).

2.2.5. Estimation of protein carbonyl content

Protein carbonyl content was determined using assay kit. Briefly, after respective treatments, cells were collected and homogenized on ice in 1-2 mL of cold buffer (50 mM phosphate buffer, pH 6.7 containing 1 mM EDTA). The supernatants were collected after centrifugation at 10,000 x g for 15 min at 4 °C. 200 μL of the samples were transferred to 2 mL plastic tubes (supernatant). The sample and control tubes were loaded with 800 μL of 2.5 M HCl. All tubes were held for 1 h in the dark. 1 mL of 20 % TCA was added and vortexed. The samples were centrifuged at 10,000 x g for 10 min at 4 °C and the supernatant was extracted. 1 mL of 60 % TCA was resuspended from the pellet. It was then incubated for 5 min on ice and then centrifuged at 10,000 x g for 10 min at 4 °C. The supernatant was extracted, and 1 mL of (1:1) ethyl acetate/ethanol mixture was resuspended from the pellet. It was then well vortexed and centrifuged for 10,000 g at 4 ° C for 10 min. Again it was centrifuged at 10,000×g for 10 min at 4 °C to remove any leftover debris. 220 μL of supernatant was taken, and the absorbance was read at 370 nm using a multimode plate reader.

2.2.6. Estimation of thiobarbituric acid reactive substances (TBARS)

Lipid peroxidation was estimated using TBARS assay kit. TBARS are formed as a byproduct of lipid peroxidation (i.e. as degradation products of fats) which can be detected by the TBARS assay using thiobarbituric acid as a reagent. Briefly, after respective treatments, the cells were collected along with culture medium and sonicated for 5 seconds. 100 μL of the standard and sample were added to tubes containing 100 μL of sodium dodecyl sulfate (SDS) and 4 mL of coloring reagent. Then tubes were boiled for 1 h and were placed in an ice bath for 10 min to stop the reaction. After that, it was centrifuged for 10 min at 1,600 × g at 4 °C and incubated at room temperature for 30 min. Finally 150 μL of samples were taken and absorbance was read at 530 nm in a plate reader.

2.2.7. Preparation of cell lysate for antioxidant enzyme activities

The harvested cells were homogenised with 20 mM of Tris HCL buffer (pH 7.5) containing 0.2% Triton X 100 and 0.5 mM PMSF and sonicated for 30 seconds on ice. Total cell lysates were centrifuged at 3000 rpm at 4 °C for 15 min and supernatants were utilised for subsequent assays.

2.2.8. Activity of superoxide dismutase (SOD)

The total SOD activity (cytosolic and mitochondrial components) was evaluated as per instructions of a commercially available kit. The assay relies on the use of WST-1 (2-(4-iodophenyl)-3-(4-nitrophenyl)-5-(2,4-disulfo-phenyl)-2H-tetrazolium, monosodium salt) highly water-soluble tetrazolium salt, which produces a water-soluble formazan dye by reducing it with a superoxide anion. 20 μl of sample solution was added to each sample and blank 2 well, while 20 μl of H$_2$O was added to each Blank 1 and Blank 3 well. After that each well received 200 μl of WST working Solution. 20 μl of dilution buffer was added to each Blank 2 and Blank 3 well. Each sample and Blank 1 well received 20 μl of enzyme working solution, which was thoroughly mixed. Finally plates were incubated for 20 min at 37 °C. The absorbance was read at 450 nm.

$$\text{SOD activity} = \frac{(A_{Blank1} - A_{Blank3}) - (A_{sample} - A_{Blank2})}{(A_{Blank1} - A_{Blank3})} \times 100$$

2.2.9. Glutathione peroxidase (GPx) activity

GPx activity was assayed spectrophotometrically using assay kit, which is based on reducing the oxidized glutathione coupled to the oxidation of NADPH. The disappearance of NADPH was determined. Briefly after trypsinization cells were collected by centrifugation (2000 × g) for 10 min at 4 °C. The cell pellets were homogenized in cold buffer (1 mM DTT, 5 mM EDTA and 50 mM tris-HCl, pH 7.5) and centrifuged (10,000 × g) for 15 min at 4°C. The supernatant obtained was used for the assay. 100 μL of assay buffer, 50 μL of a co-substrate mixture and 20 μL of supernatant (samples) were added to the subsequent wells. Then 20 μL of cumene hydroperoxide was added to all wells for initiating the reaction. The absorbance was measured at 340 nm.

2.2.10. Total antioxidant activity

This assay was based on the ability of antioxidants present in the sample to inhibit the oxidation of 2,2'-azino-bis (3-ethylbenzothiazoline-6-sulphonic acid (ABTS*) to reduced ABTS**+ by metmyoglobin. The amount of ABTS**+ produced was monitored by measuring the absorbance at 405 nm. For performing the assay, cells were collected by centrifugation (2000 × g) for 10 min at 4 °C. The pellets were subjected to sonication and centrifuged at 10,000 × g for 15 min at 4 °C. 10 μL of metmyoglobin and 150 μL of chromogen were added to 10 μL of the sample. The reaction was initiated by adding

hydrogen peroxide. The wells were incubated for 5 min at room temperature, and then absorbance was measured.

2.2.11. Estimation of glutathione (GSH)

The GSH assay kit utilizes an optimized enzymatic recycling method, using glutathione reductase for the quantification of GSH. The cell pellets were homogenized in 2 mL of cold buffer and were centrifuged at 10,000×g for 15 min at 4 °C. After that the supernatant was deproteinized and 50 µL of standard and sample were added to the designated wells and covered with the plate cover. The assay cocktail mixture contains MES buffer, reconstituted cofactor mixture, reconstituted enzyme mixture, water and reconstituted DTNB. 150 µL of assay cocktail mixture was added to each well containing sample and standard and incubated in the dark on a shaker for 30 min and the absorbance was measured at 407 nm.

2.2.12. Activity of NADPH oxidase

NADPH oxidase activity was measured, as previously described, by SOD inhibitable cytochrome C (Qin et al., 2006). In the 96 well culture plates, H9c2 cell lysates were distributed. Cytochrome C (500 µM) and NADPH (100 µM) were added in the presence or absence of SOD (200 UmL) and incubated at room temperature for 30 min. The absorbance of cytochrome C was calculated using a microplate reader set to 550 nm. Activity of NADPH oxidase was calculated from the difference between absorbance with or without SOD and is expressed as nanomoles per milligram protein.

2.2.13. Activity of aconitase

Activity of aconitase was measured using assay kit as per manufactures instructions. Cells were washed with cold PBS after the respective treatments (pH 7.4). Fresh PBS was then applied and the cells were centrifuged at 800 x g for 10 min at 4 ᵒC. The supernatant was then discarded and the cell pellet was resuspended in a 1 mL homogenization buffer. The cell suspension was sonicated for 5 seconds and the cell suspension was centrifuged at 20000 x g for 10 min at 4 ᵒC. This resultant supernatant was mixed with 50 µL of assay buffer, 50 µL of NADP⁺ reagent, 50 µL of aconitase substrate solution and incubated for 15 min at 37 ᵒC. The absorbance was taken once in every min at 400 nm for 10 min.

2.2.14. Quantification of advanced glycated end (AGE) products

The content of AGE protein adducts was determined by enzyme immunoassay kit. Samples and standard of 50 µL were added to the wells of the AGE conjugate coated plate

and incubated at room temperature for 10 min on an orbital shaker. To that 50 μL of the diluted anti-AGE antibody was added to each well, incubated at room temperature for 1 h. It was washed with 250 μL of 1X wash buffer. 100 μL of the diluted secondary antibody-HRP conjugate was added to all wells and incubated for 1 h at room temperature. 100 μL of substrate solution was added to each well and incubated at room temperature for 2-20 min. The enzyme reaction was terminated by adding 100 μL of stop solution. The color development was measured at 450 nm.

2.2.15. Activity of protein kinase C (PKC)

PKC activity was determined spectrophotometrically by the ELISA method. In this assay, the substrate was readily phosphorylated by PKC which is precoated on the wells. Samples were added to these wells followed by addition of ATP to initiate the reaction. The plate was incubated for 90 min, and a phosphospecific substrate antibody was added to the wells. The phosphospecific antibody was subsequently bound by a peroxidase conjugated secondary antibody. The assay was developed with TMB and color was developed in proportion to PKC phosphotransferase activity. The color development was stopped with the acid solution, and the absorbance was measured at 450 nm.

2.2.16. Quantification of atrial natriuretic peptide (ANP)

ANP was measured using the assay kit. Briefly, the cells were trypsinized after washing with cold PBS and centrifuged for 5 min. The pellet obtained was again washed with PBS and centrifuged for 10 min. Finally the supernatants were collected. 50 μL of samples were added to each well. To this, 50 μL of biotinylated detection antibody working solution was added. Then it was incubated for 45 min at 37 °C. After decanting, 350 μL of wash buffer was added. Then it was soaked for 1 min, and the solution was aspirated. 100 μL of HRP conjugate solution was added to each well and incubated for 30 min at 37 °C. The solution was aspirated again and 90 μL of substrate reagent was added to each well and incubated for about 15 min at 37 °C. Finally 50 μL of stop solution was added, and the absorbance was measured at 450 nm.

2.2.17. Analysis of ER stress marker by imaging

For fluorescent imaging of ER, the cells were stained with 1 μM ER- RFP in serum free medium and incubated for 16 h at 37 °C, after 48 h of exposure to different treatments. The stain was washed off with PBS and cells were visualized in fluorescent microscope.

2.2.18. Cellular nuclear extracts

After respective treatment, nuclear extracts of the cells were isolated using nuclear extraction assay kit. Briefly, the cell pellet was resuspended in 100 µL of 1 x -pre extraction buffer (containing DTT and PIC at 1:1000 ratio) per 10^6 cells followed by centrifugation for 1 min at 12000 rpm. The cytoplasmic extract was separated from the nuclear pellet. The protein concentration of a nuclear extract was measured.

2.2.19. ER transcription factor (TF) activation profiling plate array

I performed a TF activation profile according to the manufacturer's (Signosis, Inc. USA) protocol. Nuclear extract was extracted with the nuclear extraction kit. Briefly, samples mixed with TF binding buffer mix (15 µL) and TF probe mix (3 µL) were incubated for 30 min at room temperature to shape a complex of TF probe-DNA. The complex of the TF probe DNA was isolated by an isolation column. The complex was denatured for 5 min at 98°C and the denatured probe hybridized at 42°C overnight with the 96 well hybridization plate. Plates were washed three times and streptavidin-HRP conjugate was incubated. The substrate solution was added to each well after incubation at room temperature for 45 min and incubated for 1 min. The luciferase activity was detected using a luminometer.

2.2.20. Estimation of Ca^{2+} content

The total Ca^{2+} content in the cell was assayed as per the manufacturer's protocol given with the assay kit. The assay utilizes an optimized o-cresolphthalein-calcium reaction in which, in the presence of Ca^{2+} that absorbs between 560 nm and 590 nm, a vivid purple complex is formed. The colour intensity is directly proportional to the Ca^{2+} concentration in the sample.

2.2.21. Evaluation of intracellular Ca^{2+} overload

Intracellular Ca^{2+} overload was detected by staining the cells with FURA 2AM. When added to cells, Fura-2AM crosses cell membranes and once inside the cell, the acetoxymethyl groups are removed by cellular esterases. Removal of the acetoxymethyl esters regenerates "Fura-2", the pentacarboxylate calcium indicator. After treatment, cells were stained with Fura-2AM (5 µM) and incubated at 37 °C for 30 min. After incubation with stain, cells were washed three times with PBS and the images were visualized using bioimager (BD™ pathway Bioimager system,BD Biosciences). The dye was excited at 340/380 nm and the emission range was 510 nm.

2.2.22. Mitochondrial permeability transition pore (mPTP)

In order to analyze mPTP, the cells were loaded with calcein-AM (0.25 mM) for 30 min in the presence of 8 mM $CoCl_2$ to quench cytosolic and nuclear calcein fluorescence for mPTP opening analysis (Javadov et al., 2006). Within the mitochondria, calcein fluorescence is then compartmentalized until mPTP opening allows the distribution of cobalt within the mitochondria, leading to the mitochondrial matrix.

2.2.23. Detection of autophagy

Cells were grown in 96 well plate for desired time. After removing the medium, 100 µL of the autophagosome detection reagent was added to each well. The cells were washed with the 100 µL of the wash buffer 3–4 times and measured the fluorescence intensity (λex = 360 nm / λem = 520 nm) using a fluorescence microscope.

2.2.24. Analysis of caspase-3 activity

The cells were resuspended in a lysis buffer and kept on ice for 10 min. The reaction buffer of 50 µL containing 10 mM dithiothreitol was added to each sample. 5 µL of 1 mM substrate (DEVD- AFC) was added and incubated at 37 ^{o}C for 90 min. Then the samples were read on a multimode plate reader (Synergy, USA) at 400 nm excitation and 505 nm emission wavelengths.

2.2.25. Immunofluorescence

Cells were seeded and the following days, cells were treated. Prior to permeabilization in 0.25 % Triton X-100 in PBS for 15 min at room temperature with gentle agitation, cells were fixed with 1 mL of 4 % paraformaldehyde in PBS for 20 min. Cells were blocked for 1 h with 10% natural goat serum followed by incubation with primary antibodies (4 °C, overnight) and secondary antibodies (1 h, at room temperature). Primary antibodies were detected with fluorescently labelled anti-rabbit Alexa 555 (Abcam, USA). Nuclei were counterstained with DAPI (1 mg/mL in PBS) and visualized with an Olympus fluorescence microscope.

2.2.26. RNA extraction and quantitative real-time PCR

Total RNA was extracted using Trizol reagent. Total RNA (1000 ng) was used employing PrimeScript® RT reagent kit as a reverse transcription template (Takara, Japan). Gene expression quantification was detected by RT-PCR. In triplicate, both samples were analyzed. Relative amounts of mRNA were normalized by β-actin, an internal control, and a control sample and calculated by using the comparative Ct $(2-\Delta\Delta Ct)$ (cycle

threshold) method. Signals from the control group were assigned a relative value of 1.0. The primer sequences used were:

XBP1 sense	5'-ACA CGC TTG GGA ATG GAC -3'
XBP1 antisense	5'CCA TGG GAA GAT GTT CTG -3'
β-actin sense	5'-TAA AGA CCT CTA TGC CAA CAC AGT-3'
β-actin anti- sense	5'-CAC GAT GGA GGG GCC GGA CTC ATC-3'

2.2.27. Western blotting

Immunoblotting was used to analyse the expression of SOD1, SOD2, PKC α, ERK1/2, pERK1/2, Rac1,p47 phox, RAGE, AGER1, PERK, pPERK, pEIF2α, ATF6α, ATF4, IRE1α, pIRE1α , TRAF2, pJNK , ERO1α, PDI, caspase 12, calnexin, GRP78, CHOP, SEC62, FAM134B, pCaMKII, RYR2, pRYR2, NCX1,SERCA2a and β actin. Cells were seeded in a T25 flask containing 5 mL of DMEM medium and treatments were carried out. At the end of the treatments, the cells were harvested and lysed with ice-cold RIPA buffer containing a protease inhibitor cocktail and the homogenate was centrifuged at 10,000 x g for 15 min at 4 °C. Total protein in the supernatant was quantified using a BCA protein assay kit. Total protein (40 μg) from each sample was separated by 10 % SDS-PAGE at 55 V. 25 μL of experimental samples was loaded into each well. The protein in the gel was transferred into PVDF membrane using Trans-Blot Turbo™ (BioRad, USA). The membrane was blocked with BSA in tris buffered saline-Tween 20 (TBST) for 1 h at room temperature, and then incubated with the specific primary antibodies (1:1000), and actin (1:1000) in 1 % BSA in TBST with gentle agitation at 4 °C overnight. The incubation was followed by 3 times wash with TBST for 10 min in a shaker, followed by addition of HRP-conjugated secondary antibodies (1:1000) in 0.25 % BSA in TBST for 90 min at room temperature with shaking. After three washes with TBST, the membranes were developed using Clarity ™ Western ECL substrate (BioRad, USA) and the relative intensity of bands was quantified using Bio-Rad Quantity One version 4.5 software in a Bio-Rad gel documentation system.

In vivo experiments

2.2.28. Estimation of fasting blood glucose (FBG)

All rats were fasted for 16 h and FBG (blood drop was collected from tail tip prick) was measured in an Accu-Chek ® Active blood glucose meter by using glucose strips (Roche Diabetes Care India, Pvt. Ltd.).

2.2.29. Estimation of serum AGEs

The blood was centrifuged and the serum was diluted with PBS at pH 7.4 in a 1:50 ratio. The amount of AGE was measured at the excitation wavelength 350nm and emission 440 nm against PBS (Kalousova et al., 2002).

2.2.30. Estimation of glycated haemoglobin (HbA1c)

HbA1c assay was performed with kit from Immunotag, USA. The reagents were brought to room temperature and the column was prepared. The hemolysate was prepared from whole blood using reagent R1 (potassium phthalate 50 mmol/L, detergent 5 g/L) collected in heparin coated vials. 50 μL of standard was added to standard wells and 40 μL of sample was added to sample wells. 10 μL of anti HbA1c antibody was added to sample standard wells and incubated for 60 min at 37 °C after thorough mixing. After incubation, the plates were washed with a wash buffer. 50 μL of substrate solution A and B were added to each well and incubated for 10 min at 37 °C in the dark. Stop solution of 50 μL was added to each well, then the blue colour was changed into yellow immediately. The OD was measured at 450 nm within 10 min after adding the stop solution. The results were expressed in ng/mL.

2.2.31. Estimation of plasma insulin

Insulin was determined using rat insulin ELISA kit. Briefly, 40 μL of samples were applied to the wells, followed by 10 μL of anti-INS antibody. After that, 50 μL of streptavidin-HRP was applied to both the sample and standard wells. It was mixed and incubated for 1h at 37 °C. The plates were washed five times with a wash buffer. Each well received 50 μL of substrate solution A and 50 μL of substrate solution B. At 37 °C, the plates were sealed and left in the dark for another 10 min. Finally, 50 μL of stop solution were applied, and the blue colour was immediately changed to yellow. Absorbance was measured at 450 nm within 10 min after addition of stop solution.

2.2.32. Homeostatic model assessment of insulin resistance (HOMA-IR)

Fasting blood glucose and insulin values were used to calculate HOMA-IR, an index of insulin resistance (Matthews et al., 1985).

HOMA-IR= fasting blood glucose (mg/dL) × insulin (mU L)/405.

2.2.33. Heart mass index (HMI)

The hearts were weighed, and the HMI was calculated as the ratio of heart mass to body weight.

2.2.34. Serum atrial natriuretic peptide (ANP)

The serum ANP was estimated by ELISA method. In short, 50 µL of normal, blank, or serum samples were taken into the corresponding labelled wells and immediately added 50 µL of biotin-labelled antibody to the labelled wells. It was then well blended and incubated at 37 °C for 45 min, and washed with the wash buffer (3 times). 100 µL of SABC working solution (kit reagent) was applied to all the wells after the washing phase and incubated at 37 °C for 30 min. It was then washed (5 times) and added 90 µL of TMB substrate to each well and incubated for 20 min in the dark at 37 °C. 50 µL of stop solution was then applied and the absorbance at 450 nm was read. The standard ANP curves were constructed and concentrations of ANP were calculated and expressed in pg/mL.

2.2.35. Determination of triglycerides (TG)

As per the manufacturer's instructions (Agappe Diagnostics, India) the reagents were reconstituted. 1 mL of working reagent Reconstituted R2 (≥ 1100 U/L lipoprotein lipase, ≥800 U/L glycerol kinase, ≥3000 U/L glycerol-3- phosphate oxidase, 350 U/L peroxidase, 0.7 mmol/L 4-aminoantipyrine) with R1 (50 mmol/L PIPES buffer pH 7.0, 1.0 mmol/L N-ethyl-N-sulfopropyl-n-anisidine (ADPS), 15 mmol/L magnesium salt) was combined with 10 µL sample/standard and then incubated for 5 min at room temperature. In comparison to reagent blank, absorbance was measured at 546 nm. Results were expressed as mg/dL.

TG (mg/dL) = (OD of sample /OD of standard) x 200

2.2.36. Determination of total cholesterol (TC)

TC in the serum was measured using kit from Agappe Diagnostics. 1 mL of working reagent (dissolved R2 (≥ 200 U/L cholesterol esterase, ≥ 250 U/L cholesterol oxidase, ≥ 1000 U/L peroxidase, 0.5 mmol/L 4-aminoantipyrine) with R1 (50 mmol/L PIPES buffer, phenol, sodium cholate, 4- aminoantipyrine, cholesterol esterase, cholesterol oxidase, and peroxidase) was combined with 10 µL of sample/standard and incubated at room temperature for 5 min. The OD of the standard or sample against a reagent blank was observed at 505 nm. Results were expressed as mg/dL.

TC= (Absorbance of sample/ Absorbance of standard) × 200

2.2.37. Estimation of of high density lipoprotein- cholesterol (HDL –C)

HDL was measured using kit from Agappe Diagnostics. 10 µL of sample/standard was mixed with 1 mL of HDL cholesterol reagent (14 mmol/L phosphotungstate, 1.0 mmol/L magnesium chloride) and incubated for 5 min at 37 ^{0}C. Absorbance of the

standard or sample was measured at 505 nm against reagent blank. Results were expressed as mg/dL.

HDL (mg/dL) = (OD of sample /OD of standard) × calibrator concentration

2.2.38. Determination of low density lipoprotein- cholesterol (LDL- C)

LDL was measured using a kit from Agappe Diagnostics. The reagents were reconstituted as per the manufacturer's instructions. 450 μL LDL Direct R1 reagent {25 mmol/L goods buffer pH 6.8, cholesterol esterase 5 IU/L, cholesterol oxidase 5 IU/L, catalase 1000 IU/L, N-(2-hydroxy-3-sulfo-propyl)-3,5 dimethoxy aniline 0.6mmol/L(H-DAOS)} was combined with 5 μL of sample/standard and incubated for 5 min at 37 °C. To this 150 μl of Reagent 2 (cholesterol esterase, cholesterol oxidase and 4- aminoantipyrin) was added. It was then mixed and incubated for 5 min at 37 °C. Absorbance was measured at 505 nm against reagent blank. Results were expressed as mg/dL.

LDL (mg/ dL) = (OD of sample/ OD of standard) ×calibrator concentration

2.2.39. Activity of serum glutamic-oxaloacetic transaminase (SGOT)

SGOT was estimated by the kinetic determination of aspartate aminotransferase (AST) using the diagnostic kit (Agappe Diagnostics Ltd., Kerala, India) according to the kit protocols. In short, 1 mL of working reagent was combined with 100 μL of serum samples and incubated for 1 min at 37 °C. Using a multimode plate reader (Tecan Infinite M200PRO, Austria), the absorbance was then calculated at 340 nm for 3 min with a 1 min interval. The per min absorbance shift (almost OD/min) was determined, and the enzyme activities were estimated using the equation;

Enzyme activity (U/L) = (ΔOD/min) x 1745

2.2.40. Lactate dehydrogenase (LDH) activity

The serum concentration of S-LDH was estimated by the kinetic determination of pyruvate (kit reagent) to lactate conversion by LDH using the assay kit. Briefly, 1 mL of working reagent (made as to the kit instructions) was mixed with 10 μL of serum samples and incubated at 37 °C for 1 min. Then the absorbance was measured at 340 nm using a multimode plate reader (Infinite M200PRO, Tecan, Austria) for 3 min in 1 min interval. The change in absorbance per min (ΔOD/min) was calculated, and the enzyme activities were estimated using the equation;

LDH activity (U/L) = (ΔOD/min) x 16030

2.2.41. Quantification of c reactive protein (CRP)

Briefly, 200 µL of CRP ULTRA R1 (glycine buffer) was mixed with 5 µL of calibrator, sample and blank and incubated for 5 min at 37 °C. After incubation, 100 µL of CRP ultra R2 (latex suspension coated with anti CRP antibodies) was added to all wells including blank. Absorbance was measured immediately after 2 min at 570/800 nm. The delta absorbance was calculated and a standard curve was constructed from which the CRP-ultra levels of standard and samples were calculated.

2.2.42. Activity of creatine kinase – MB (CK-MB)

Briefly, 1 mL of working reagent (made as per kit instructions) was mixed with 40 µL of serum samples and incubated at 37 °C for 100 seconds. Then the absorbance was measured at 340 nm for 5 min in 1 min interval. The change in absorbance per min (ΔOD/min) was calculated, and the enzyme activities were estimated using the equation;

$$\text{CK-MB activity (U/L)} = (\Delta OD/min) \times 8254.$$

2.2.43. Superoxide dismutase (SOD) activity

Activity of SOD was measured by the method of Kakkar et al., 1984. Tissues were homogenized in 0.25M sucrose and centrifuged. The assay mixture included 0.1 mL of 186 µM PMS, 1.2 mL of sodium pyrophosphate buffer (0.052 M, pH 8.3), 0.3ml of 300 µM NBT, 0.2 mL of 780 µM NADH, properly diluted enzyme preparation and distilled water to a final volume of 3 mL. The reaction was triggered by the addition of NADH and incubated for 1 min at 30 °C. The reaction was halted by 1.0 mL of glacial acetic acid being applied and the mixture was vigorously stirred. In the mixture, 4 ml n-butanol was added and well shaken. The mixture was permitted to stand for 10 min, centrifuged, the butanol layer extracted and weighed against a butanol blank at 560 nm. An enzyme-devoid system has represented as the control. One unit activity is defined as the enzyme concentration required for inhibition of chromagen production/absorbance at 560 nm by 50 % in one min under the assay conditions. Specific activity is defined as the units per milligram protein.

2.2.44. Estimation of thiobarbituric acid reactive substances (TBARS)

Levels of TBARS were estimated by the method of Niehaus and Samuelsson, 1968. Tissue homogenate was prepared in 0.1M Tris-HCl buffer. 1mL of the homogenate was combined with 2 mL of the TCA-TBA-HCl reagent and thoroughly mixed. The tubes were boiled for 15 min and the precipitate was extracted by centrifugation after cooling for 10 min at 1000 x g. The absorbance of the samples was read against a blank at 535 nm

(without tissue homogenate). The findings are expressed as tissue μmoles/g and determined from the coefficient of extinction of MDA.

2.2.45. Immunoblot analysis

Heart tissue homogenate was lysed. Concentration of protein was quantified by the BCA method. Equal amounts of protein (40 μg) from each sample were separated by SDS–PAGE and transferred onto a nitrocellulose membrane (Millipore Corporation, USA). Then the membrane was blocked by 5 % BSA in Tris-buffered saline containing 0.05 % (v/v) Tween-20 (TBS-T) for 1 h at RT. Then, the membranes were incubated overnight at 37 ºC ith the primary antibodies (BNP, copeptin , HFABP, troponin, fetuin A, GRP78, calnexin, PERK, ATF6, IRE1α, CHOP). The membranes were washed with TBST and incubated with the appropriate secondary HRP-conjugated antibodies at a 1:2000 dilution. Following 30 min wash, the membranes were visualized by enhanced chemiluminescence. The band intensity was measured and quantified.

2.2.46. Tissue collection and histology

After sacrifice, the hearts were taken out and cut into pieces with a sharp razor and immediately fixed in 10 % neutral buffered formalin solution. Tissues were then dehydrated in graded ethanol series, cleared in xylene and embedded in paraffin wax. 5 μm thick sections were prepared using a microtome and stained with hematoxylin and eosin (H&E) and van Geison stain. Stained tissues were dehydrated with 70 % alcohol, followed by 90 % ethanol, placed in two changes of 100 % ethanol for 3 min each, and cleaned with two changes of xylene (3 min each). Slides were examined under Nikon Eclipse TS 100 inverted microscope for the examination of collagen deposition and photomicrographs were taken at original magnification of 40X.

2.2.47. Statistical analysis

Data were reported as mean ± standard error of mean (SEM). Data were subjected to one-way variance analysis (ANOVA) and Duncan's multiple range tests using SPSS for windows, standard version 7.5.1, measured the significance of variations between means and the significance accepted at $p \leq 0.05$.

References

1. Choi SW, Benzie IF, Ma SW, Strain JJ, Hannigan BM. Acute hyperglycemia and oxidative stress: direct cause and effect?. *Free Radic Biol Med*. 2008;44(7):1217-1231. doi:10.1016/j.freeradbiomed.2007.12.005.

2. Javadov S, Baetz D, Rajapurohitam V, Zeidan A, Kirshenbaum LA, Karmazyn M. Antihypertrophic effect of Na+/H+ exchanger isoform 1 inhibition is mediated by reduced mitogen-activated protein kinase activation secondary to improved mitochondrial integrity and decreased generation of mitochondrial-derived reactive oxygen species. *J Pharmacol Exp Ther*. 2006;317(3):1036-1043. doi:10.1124/jpet. 105.100107.

3. Kakkar P, Das B, Viswanathan PN. A modified spectrophotometric assay of superoxide dismutase. *Indian J Biochem Biophys*. 1984;21(2):130-132

4. Kalousová M, Skrha J, Zima T. Advanced glycation end-products and advanced oxidation protein products in patients with diabetes mellitus. *Physiol Res*. 2002;51(6):597-604.

5. Matthews DR, Hosker JP, Rudenski AS, Naylor BA, Treacher DF, Turner RC. Homeostasis model assessment: insulin resistance and beta-cell function from fasting plasma glucose and insulin concentrations in man. *Diabetologia*. 1985;28(7):412-419. doi:10.1007/BF00280883.

6. Niehaus WG Jr, Samuelsson B. Formation of malonaldehyde from phospholipid arachidonate during microsomal lipid peroxidation. *Eur J Biochem*. 1968;6 (1):126-130. doi:10.1111/j.1432-1033.1968.tb00428.x.

7. Qin F, Patel R, Yan C, Liu W. NADPH oxidase is involved in angiotensin II-induced apoptosis in H9C2 cardiac muscle cells: effects of apocynin. *Free Radic Biol Med*. 2006;40(2):236-246. doi:10.1016/j.freeradbiomed.2005.08.010.

8. Ramírez-Zacarías JL, Castro-Muñozledo F, Kuri-Harcuch W. Quantitation of adipose conversion and triglycerides by staining intracytoplasmic lipids with Oil red O. *Histochemistry*. 1992;97(6):493-497. doi:10.1007/BF00316069.

9. Wilson AP. Cytotoxicity and viability assays. *Animal cell culture: a practical approach*. Oxford University Press, New York. 2000: *3*, 175 - 219.

Hyperglycemia induced alterations in redox status in H9c2 cells and possible amelioration with chlorogenic acid

3.1. Introduction

The prevalence of diabetes is growing worldwide. Diabetes can lead to complications of multiorgan dysfunction and increase the chance of dying prematurely. But over 60 % of deaths in diabetic patients are because of CVD and associated problems (Leon and Maddox, 2015). Diabetes can affect cardiac tissue even if no other cardiovascular risk factors are present. DCM makes up structural and functional abnormalities of the myocardium without coronary artery disease or hypertension (Aneja et al., 2008). Hyperglycemia, insulin resistance and impaired cardiac insulin metabolic signaling are all significant clinical anomalies that play an important role in the development of DCM (Jia et al., 2016). Relationships between glucose levels and CVD are remarkably inconsistent (Qi and Qi, 2012). Hyperglycemia has been considered as a major contributor of DCM. This may be due to the instigation of classical oxidative stress pathways like polyol, hexosamine, AGEs and protein kinase C. Increased development of mitochondrial ROS, non-enzymatic protein glycation and glucose autoxidation result from these pathways resulting in cardiac injury. Currently, treatment regimens for diabetes related cardiovascular disease depend on traditional therapies that emphasize glycemic regulation, lipid reduction and oxidative stress reduction.

Oxidative stress results when the rate of oxidant production exceeds the rate of oxidant scavenging. Enhanced glucose flux both enriches oxidant production and impairs antioxidant defenses through multiple interacting pathways (Turan and Dhalla, 2014). Recent research has shown that oxidative harm caused by ROS or RNS derived from hyperglycemia plays a key role in diabetic injury throughout multiple organs (Liu et al., 2014). Increased ROS production can lower the antioxidant ability of the diabetic myocardium, resulting in oxidative stress and myocardial harm.

Increased ROS or RNS production from non-mitochondrial sources such as activation of NOX and modulating the mitochondrial electron chain to produce superoxide (Steinberg et al., 2000). This may be caused by increased free fatty acid concentrations in

the heart because of a lack of insulin mediated glucose metabolism. Superoxide is formed by activated NOX, which can then combine with NO to form highly reactive and damaging peroxynitrite species. NOXs have been identified as a main contributing factor in this condition (Olukman et al., 2010).

The development of AGEs because of non-enzymatic glycation and oxidation of proteins and lipids is a significant consequence of high glucose induced cell injury. AGEs can interact to the receptor for advanced glycation end products on cardiac cell membranes, which promotes pro-inflammatory and pro-fibrotic signaling and raises oxidative stress mediators (Candido et al., 2003; Haidara et al., 2006; Yamagishi et al., 2012).

Another mechanism by which hyperglycemia has negative cardiovascular effects is activation of the PKC signaling pathway. PKC activation by hyperglycemia promotes the expression of connective tissue growth factor which leads to fibrosis (Way et al., 2002). In addition, PKC has received special attention in the pathogenesis of cardiomyopathy due to its important role in the intracellular signaling pathway for regulating cellular growth, cardiac myocyte development and inotropic function (Meier and King, 2000). Studies have also shown that PKCα, the major isozyme, has also been demonstrated to be a crucial modulator of cardiomyocyte hypertrophy development via ERK1/2-dependent signaling pathway (Hahn et al., 2003). However, studies have reported regarding the connection between ROS and ERK1/2 activation (Xu et al., 2016).

There are very few studies done on the functional hazards of AGE, PKCα, ERK and weakened antioxidant defense systems during hyperglycemia. Based on this, efforts are focussed to understand precisely the contribution of these pathways in the genesis of DCM *in vitro* model.

Recently much attention has been given to bioactives from medicinal plants in search of therapeutics against hyperglycemic cardiomyopathy. There are ample examples of the natural product derived cardiovascular therapeutics such as reserpine, diltiazem etc (Suroowan and Mahomoodally, 2015). Affordability, minimum adverse effects and tolerability to prolonged use necessities for better therapeutics to the general public. In this scenario chlorogenic acid (CA), a natural chemical compound which is the ester of caffeic acid and (−)quinic acid and abundant in our daily beverage coffee (Farah and

Donangelo, 2006) and common fruits (Clifford, 1999; Gonthier et al., 2003, Mahmood et al., 2012) is an ideal choice. It is also a blood pressure lowering agent (Watanabe, 2006). In addition, it has many biological properties, including antibacterial, antioxidant, and anticarcinogenic activities (Kasai et al., 2000; Kono et al., 1997). It plays a major role in glucose and lipid metabolism (Meng et al., 2013). Furthermore, (Reshma et al., 2015) there are reports on cardioprotective properties of the extract containing CA. So I was planning to investigate the beneficial properties of CA against hyperglycemia induced alterations in H9c2 cells.

The present chapter deals with the alterations in H9c2 cells during hyperglycemia emphasizing the oxidative stress, glycation, and PKC α ERK axis for identification of probable biochemical targets and protective effect of CA.

3.2. Methods employed

3.2.1. Induction of hyperglycemia

Hyperglycemia was induced by treating H9c2 cells with 33 mM glucose for 48 h. In order to rule out the effect of changes in osmolarity, mannitol was used for some experiments. After 48 h control and treated cells were subjected to various assays. The experimental group consists of

- C- control (5.5 mM glucose)
- HG- high glucose (33 mM glucose)
- Met- high glucose + metformin (1 mM)
- CA1- high glucose + CA (10 μM)
- CA2- high glucose + CA (30 μM)
- Mnt- 5.5 mM glucose + mannitol (27.5 mM)

After respective treatments, cells were analyzed for following various parameters. Details of procedures are given in chapter 2.

- ✔ Evaluation of cell viability (refer 2.2.1)
- ✔ Determination of LDH Leakage (refer 2.2.2)
- ✔ Detection of intracellular ROS (refer 2.2.3)
- ✔ Intracellular lipid accumulation (refer 2.2.4)

✔   Estimation of protein carbonyl content & TBARS (refer 2.2.5 & 2.2.6)

✔   Activity of SOD (refer 2.2.8)

✔   GPx activity & GSH determination (refer 2.2.9 & 2.2.11)

✔   Total antioxidant assay (refer 2.2.10)

✔   Activity of NADPH oxidase (refer 2.2.12)

✔   Studies on AGE (refer 2.2.14)

✔   Activity of PKC (refer 2.2.15)

✔   Quantification of ANP (refer 2.2.16)

3.3. Results

3.3.1. Cytoprotective effect of CA

In order to select an ideal concentration of CA, cell viability was checked with 10 µM, 30 µM, 50 µM and 75 µM of the same. Then I selected 10 µM and 30 µM based on viability results (Figure.3.1a).

3.3.2. Effect of CA on HG induced cell death

Incubation of H9c2 cells with 33 mM glucose (HG) for 48 h caused significant cell death (1.32 fold; $p \leq 0.05$; Figures.3.1b & c). Interestingly, CA of 10 µM and 30 µM concentrations or metformin (1 mM) significantly ($p \leq 0.05$) improved (1.2, 1.27 and 1.18 fold respectively) cell viability compared to HG group (Figures.3.1b & c). In order to rule out the effect of changes in osmolarity, mannitol was used. No significant changes were found in the mannitol group as compared to the HG group.
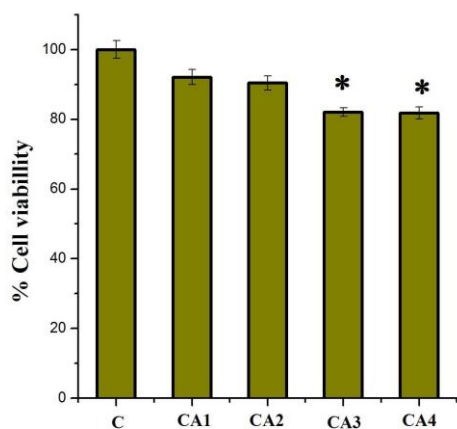
a   **b**
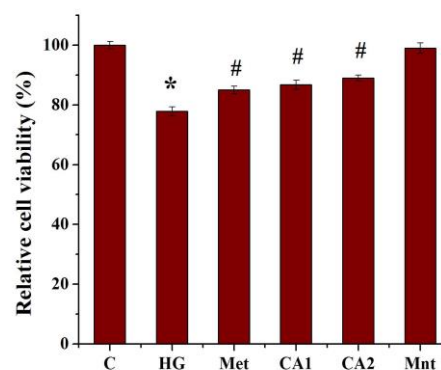
c
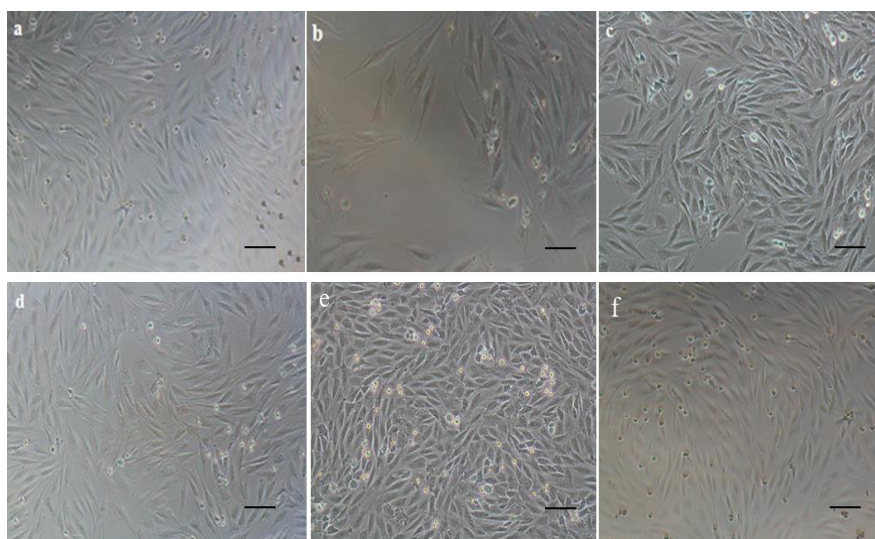
Figure.3.1.   MTT assay. a) H9c2 cells were treated with different concentrations of chlorogenic acid (10 µM, 30 µM, 50 µM, 75 µM). C- Control (5.5 mM glucose), CA1- Control + chlorogenic acid (10 µM), CA2 - Control + chlorogenic acid(30 µM), CA3- Control + chlorogenic acid (50 µM), CA4 - Control + chlorogenic acid (75 µM). **b) Cell death in H9c2 cells after treatment with 33 mM glucose (high glucose).** C- Control (5.5 mM glucose), HG-High glucose treated group (33 mM glucose), Met – High glucose treated cells + metformin (1 mM), CA1 – High glucose treated cells + chlorogenic acid (10 µM), CA2 - High glucose treated cells + chlorogenic acid (30 µM), Mnt - High glucose treated cells + mannitol (27.5 mM). **c) Representative microscopic images**. (a) Control, (b) high glucose treated group, (c) HG + metformin, (d) HG + chlorogenic acid (10 µM), (e) HG + chlorogenic acid (30 µM), (f) HG + mannitol (27.5 mM). Scale bar corresponds to 50 µm. Values are expressed as mean ± SEM where n = 6. * p ≤ 0.05 significantly different from the control group. # p ≤ 0.05 significantly different from the HG treated group.

3.3.3. Lactate dehydrogenase (LDH) release

LDH release to the medium is a significant marker of cardiac cell injury. There was a significant increase of LDH release in HG (4.27 fold) compared to control while with CA, LDH release was reduced by 1.5 and 2.33 fold (p ≤0.05) for 10 µM and 30 µM respectively compared to HG treated cells, indicating the cytoprotective potential of CA (Figure.3.2). Metformin also reduced the release of LDH by 2.82 fold (p ≤ 0.05) compared to HG cells (Figure.3.2).
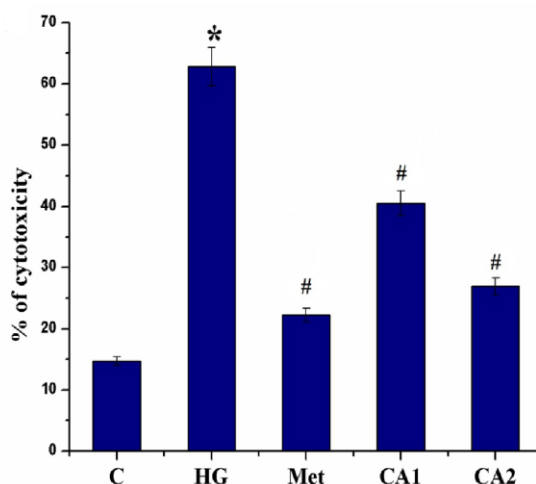
Figure.3.2. Lactate dehydrogenase release. C- Control (5.5 mM glucose), HG-High glucose treated group (33 mM glucose), Met – High glucose treated cells + metformin (1 mM), CA1 – High glucose treated cells + chlorogenic acid (10 μM), CA2 - High glucose treated cells + chlorogenic acid (30 μM). Values are expressed as mean ± SEM where n = 6. * $p \leq 0.05$ significantly different from the control group. # $p \leq 0.05$ significantly different from the HG treated group.

3.3.4. Intracellular ROS generation during hyperglycemia

To check the effect of hyperglycemia on redox status, the amount of ROS was quantified using DCFDA. There was a significant increase ($p \leq 0.05$) in the ROS levels during hyperglycemia (3.5 fold; Figures.3.3a & b). ROS was found reduced upon treatment with different concentrations of CA (1.4 and 1.9 for 10 μM and 30 μM) in a dose-dependent manner compared to HG and 2.05 fold for metformin respectively ($p \leq 0.05$; Figures.3.3a & b).
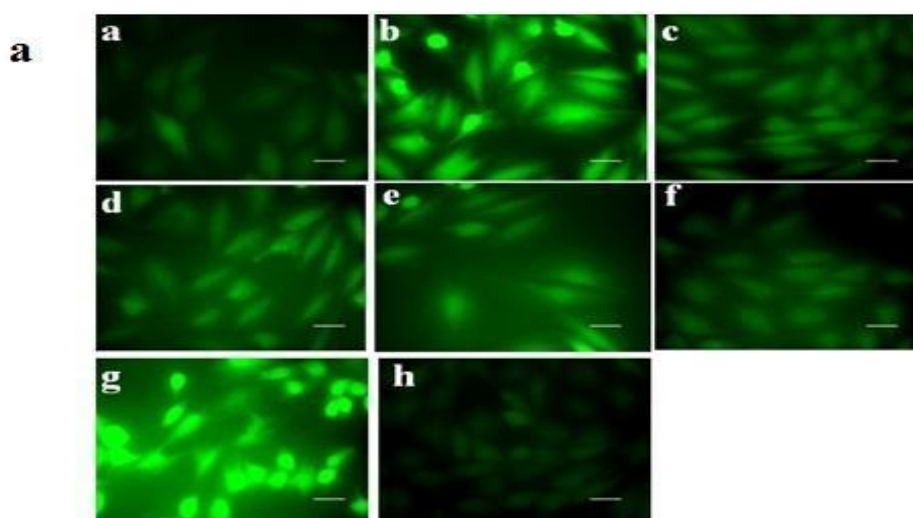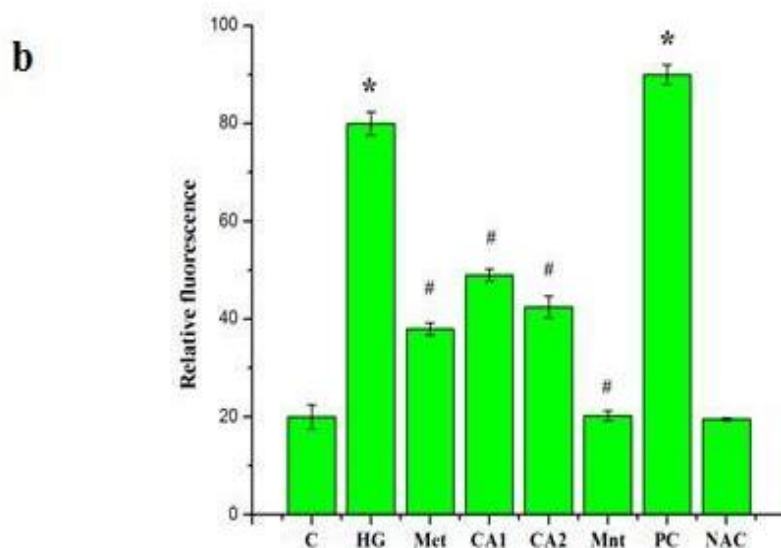
Figure.3.3. Intracellular reactive oxygen species generation determined using DCFDA. a) Reactive oxygen species generation in various groups. (a) Control, (b) high glucose treated group , (c) HG + metformin, (d) HG + chlorogenic acid (10 µM), (e) HG + chlorogenic acid (30 µM), (f) Mnt- HG + mannitol, (g) Control + H_2O_2, (h) Control + 1 mM n acetyl cysteine. Scale bar corresponds to 100 µm. b). **Relative fluorescent intensity of the fluorescent images**. C- Control (5.5 mM glucose), HG-High glucose treated group (33 mM glucose), Met – High glucose treated cells + metformin (1 mM), CA1 – High glucose treated cells + chlorogenic acid (10 µM), CA2 - High glucose treated cells + chlorogenic acid (30 µM), Mnt- Control + mannitol (27.5 mM), PC -Control + 300 µM H_2O_2, NAC-Control + 1 mM N acetyl cysteine. Values are expressed as mean ± SEM where n =6. * p ≤ 0.05 significantly different from the control group. # p ≤ 0.05 significantly different from the HG treated group.

3.3.5. Lipid droplet formation during hyperglycemia

Oil red O staining shows that there was a significant increase in the formation of lipid droplets in the HG group (2.06 fold, Figure.3.4a) compared to the control group. CA of both concentrations (1.21 and 1.33 fold for 10 µM and 30 µM) found to reduce the lipid droplet formation (Figures.3.4a & b). Metformin also decreases the lipid droplet accumulation by 1.47 fold (Figure.3.4b).

a

b
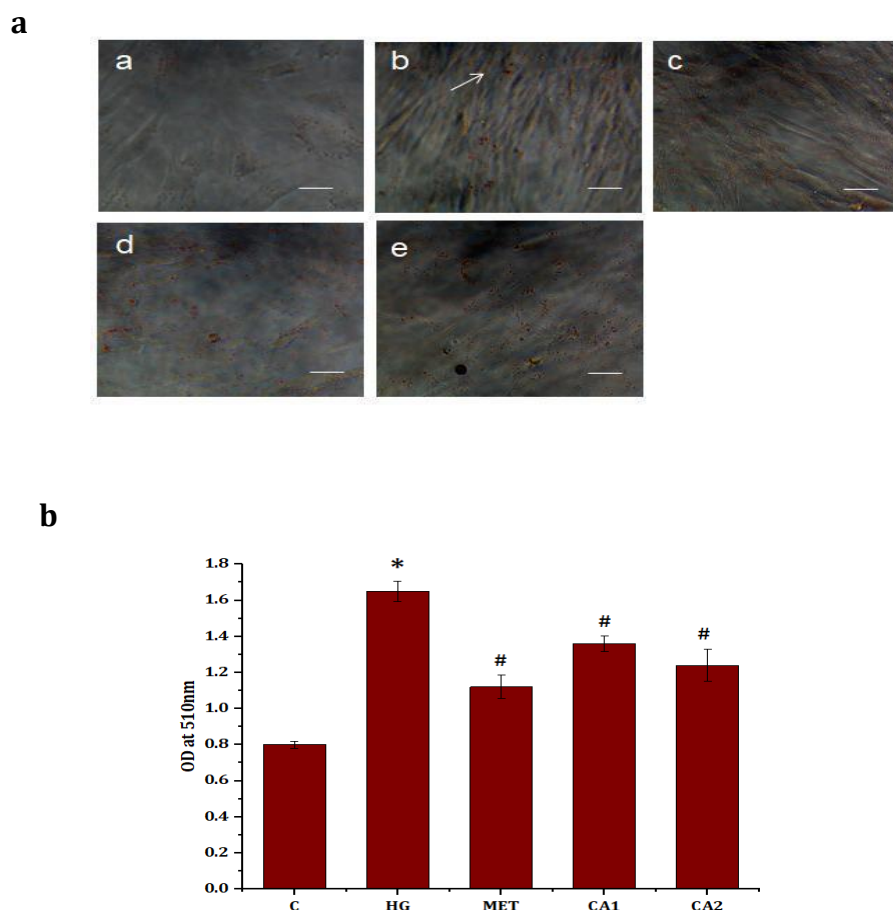
Figure.3.4. Analysis of lipid droplet formation using oil red O staining. a) Lipid droplet generation in various groups. (a) Control (5.5 mM), (b) high glucose treated group (33 mM), (c) HG + metformin (1 mM), (d) HG + chlorogenic acid (10 μM), (e) HG + chlorogenic acid (30 μM). Scale bar corresponds to 100 μm. **b) Quantification of lipid by oil red O staining.** C-control (5.5 mM glucose), HG-High glucose treated group (33 mM glucose), Met – High glucose treated cells + metformin (1 mM), CA1 – High glucose treated cells + chlorogenic acid (10 μM), CA2 - High glucose treated cells + chlorogenic acid (30 μM). Values are expressed as mean ± SEM where n = 6. * $p \leq$ 0.05 significantly different from the control group. # $p \leq$ 0.05 significantly different from HG treated group.

3.3.6. Lipid peroxidation during hyperglycemia

HG treatment increased lipid peroxidation by 2.5 fold compared to control ($p \leq$ 0.05; Figure.3.5a). Treatment with CA significantly decreased lipid peroxidation by 1.38 and 2.17 fold for 10 μM and 30 μM of CA respectively compared to HG indicating protection against oxidative stress during hyperglycemia. Metformin treatment also reduced lipid peroxidation significantly by 1.6 fold ($p \leq$ 0.05; Figure.3.5a) compared to HG.

3.3.7. Protein oxidation in HG treated cardiomyocytes

Oxidative stress is associated with protein oxidation and the concentration of protein carbonyls was also significantly higher (5.3 fold; $p \leq 0.05$) with HG. CA co-treatment significantly reduced the concentration of protein carbonyls by 1.45 fold and 1.56 fold for 10 µM and 30 µM when compared to HG. Metformin treatment also decreased protein carbonyl level significantly ($p \leq 0.05$; 1.6 fold; Figure.3.5b).

a   **b**
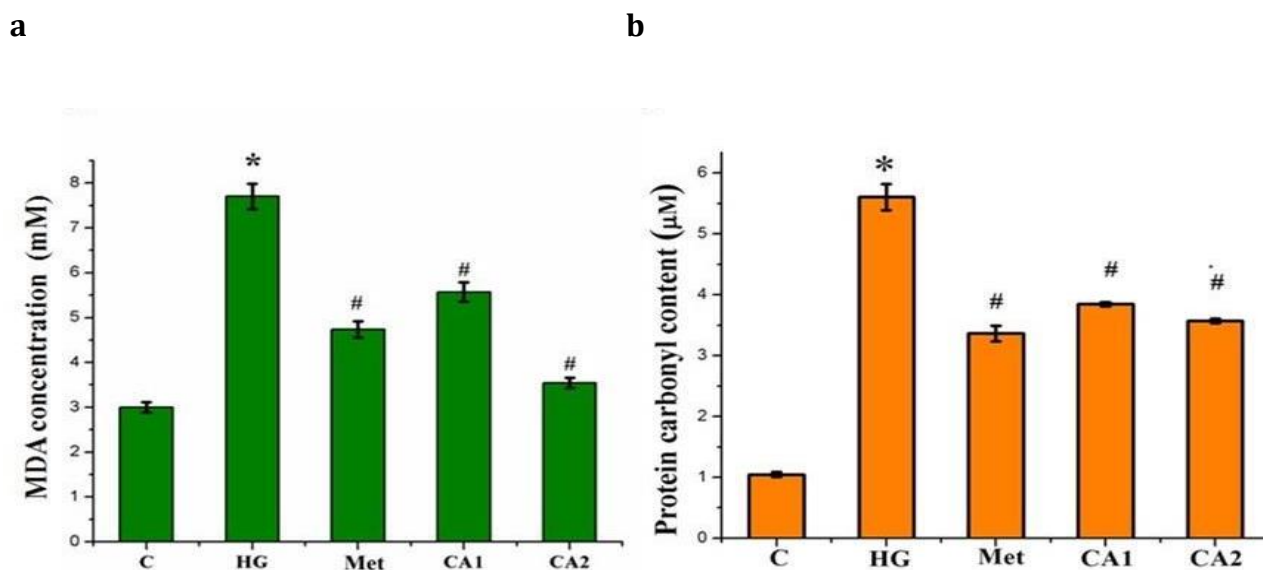
Figure.3.5. Determination of oxidative stress. a) Level of malondialdehyde generation in different groups. b) Estimation of protein carbonyl content. C- Control (5.5 mM glucose), HG- High glucose treated group(33 mM glucose), Met – High glucose treated cells + metformin (1 mM), CA1 – High glucose treated cells + chlorogenic acid (10 µM), CA2 - High glucose treated cells + chlorogenic acid (30 µM). Values are expressed as mean ± SEM where n = 6. * $p \leq 0.05$ significantly different from the control group. # $p \leq 0.05$ significantly different from HG treated group.

3.3.8. Effect of hyperglycemia on endogenous antioxidant system

3.3.8.1. Activity of SOD

Alteration in innate antioxidant status of the cell during hyperglycemia was studied. Activity of SOD was significantly ($p \leq 0.05$) reduced by 1.3 fold during hyperglycemia (Figure.3.6a). CA co-treatment improved SOD activity in a significant manner. 10 µM and 30 µM of CA caused 1.3 and 1.4 fold increase of SOD activity. SOD1 (CuZnSOD) and SOD2 (MnSOD) protein expression analyzed by western blot also showed significant reduction ($p \leq 0.05$) in HG treated cells when compared with control (1.14 and

5.5 fold for SOD1 and SOD2 respectively). CA or metformin resumed the protein levels of SOD1 (1.15, 1.33 and 1.06 for 10 µM and 30 µM of CA and metformin respectively; p ≤ 0.05; Figure.3.6b) and SOD2 (4.21, 4.9 and 3.38 for 10 µM and 30 µM of CA and metformin respectively; p ≤ 0.05; Figure.3 6c) in a significant manner.

a   **b**

c
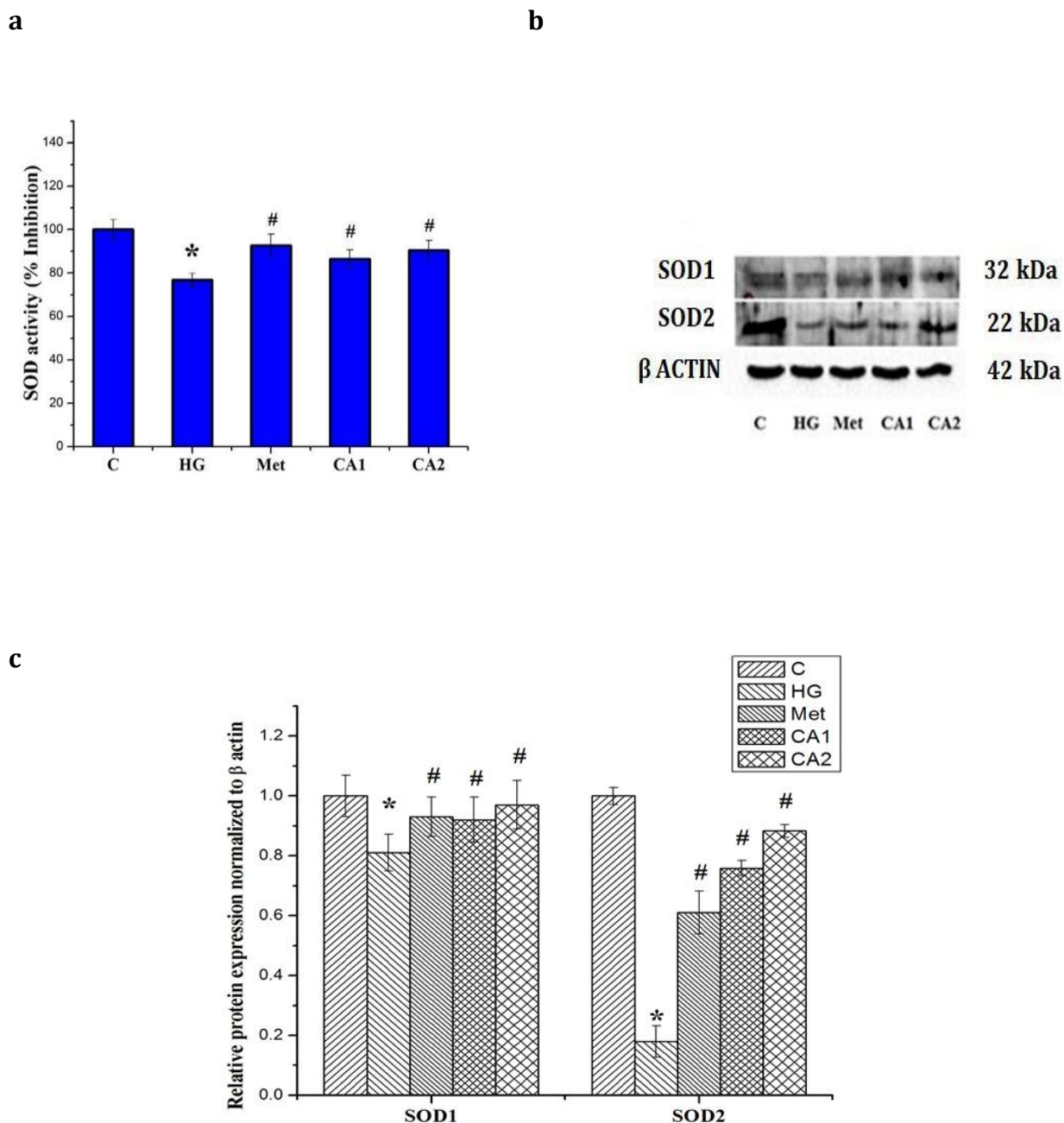
Figure. 3.6 (a) Activity of superoxide dismutase during hyperglycemia (b) Immunoblot analysis of SOD1 and SOD2 (c) Densitometric analysis of SOD1 and SOD2 with respect to β-actin. C- Control (5.5 mM glucose), HG-High glucose treated group (33 mM glucose), Met – High glucose treated cells + metformin (1 mM), CA1 – High glucose treated cells + chlorogenic acid (10

µM), CA2 - High glucose treated cells + chlorogenic acid (30 µM). Values are expressed as mean ± SEM where n = 6. * p ≤ 0.05 significantly different from the control group. # p ≤ 0.05 significantly different from the HG treated group.

3.3.8.2. Activity of GPx and determination of GSH

Activities of GPx were significantly reduced by 1.79 fold (p ≤ 0.05; Figure.3.7b) during hyperglycemia. CA (1.8 and 1.92 fold for 10 µM and 30 µM of CA respectively) restored the activity of GPx during hyperglycemia (Figure.3.7a). I also estimated GSH during hyperglycemia. In HG treated cells, there was significant depletion of GSH (8.27 fold) compared to control while treatment with CA prevented the reduction of GSH significantly relative to HG treated cells (5.9 and 6.8 for 10 µM and 30 µM of CA; p ≤ 0.05; Figure.3.7b). Metformin also improved GSH significantly (7.52 fold; p ≤ 0.05).

a   **b**
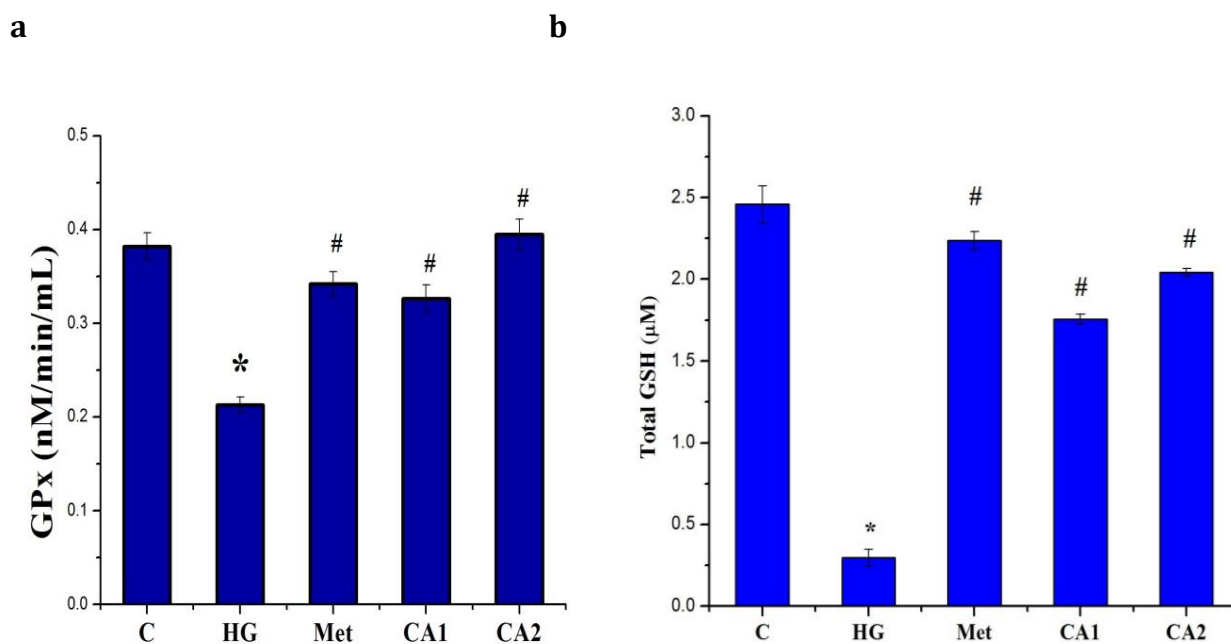
Figure.3.7. High glucose reduced intracellular redox scavenger system. a) Glutathione peroxidase (GPx) activity. b) Determination of total glutathione (GSH) levels C- Control (5.5 mM glucose), HG-High glucose treated group (33 mM glucose), Met – High glucose treated cells + metformin (1 mM), CA1 – High glucose treated cells + chlorogenic acid (10 µM), CA2 - High glucose treated cells + chlorogenic acid (30 µM). Values are expressed as mean ± SEM where n = 6. * p ≤ 0.05 significantly different from the control group. # p ≤ 0.05 significantly different from the HG treated group.

3.3.9. Total antioxidant capacity

There was significant ($p \leq 0.05$) reduction in antioxidant capacity in HG treated cells (1.3 fold) compared to control while CA significantly improved total antioxidant capacity (1.04 and 1.32 for 10 µM and 30 µM of CA; $p \leq 0.05$; Figure 3.8).
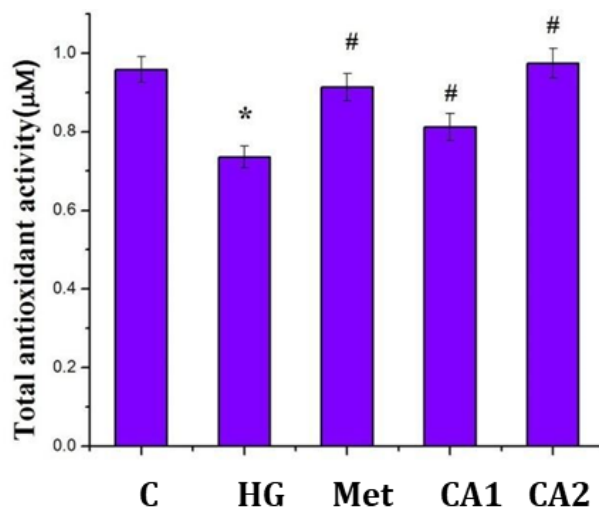
Figure.3.8. Total antioxidant activity during hyperglycemia. C- Control (5.5 mM glucose), HG- High glucose treated group (33 mM glucose), Met – High glucose treated cells + metformin (1 mM), CA1 – High glucose treated cells + chlorogenic acid (10 µM), CA2 - High glucose treated cells + chlorogenic acid (30 µM). Values are expressed as mean ± SEM where n = 6. * $p \leq 0.05$ significantly different from the control group. # $p \leq 0.05$ significantly different from the HG treated group.

3.3.10. Analysis of NADPH oxidase during high glucose

There was a significant increase in the activity of NADPH oxidase (2.09 fold; $p \leq 0.05$; Figure.3.9a) in the HG treated H9c2 cells with respect to control cells. In addition, I also analysed its subunits, Rac1 and p47 phox. p47 phox (1.42 fold) and Rac1 (1.39 fold) were also found to increase in the HG treated H9c2 cells (Figure.3.9b). While treatment with CA of both concentrations (1.9 fold and 1.57 fold for 10 µM and 30 µM of CA) reduced the activity of NADPH oxidase by decreasing the expression of Rac1 (3.4 and 1.2 fold for 10 µM and 30 µM of CA) as well as p47 phox (1.61 and 1.13 fold 10 µM and 30 µM of CA) respectively (Figure.3.9c). Metformin is also found to ameliorate the NADPH oxidase activity.

a

b

c
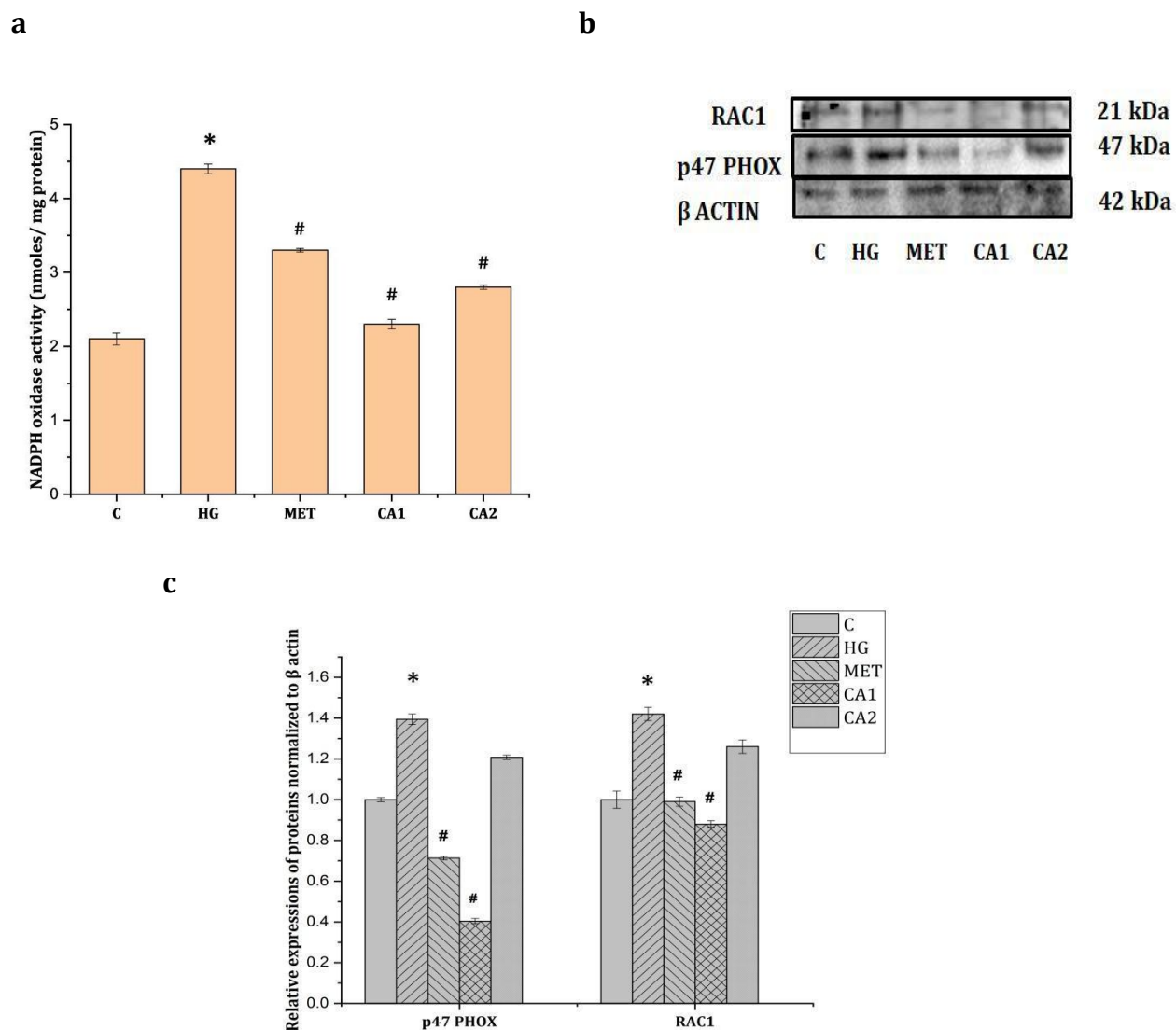
Figure. 3.9. High glucose enhanced NADPH oxidase activity. a) Activity of NADPH oxidase (b) Immunoblot analysis of Rac1 and P47 phox (c) Densitometric analysis of Rac1 and p47 phox with respect to β-actin. C- Control (5.5 mM glucose), HG-High glucose treated group (33 mM glucose), Met – High glucose treated cells + metformin (1 mM), CA1 –High glucose treated cells + chlorogenic acid (10 µM), CA2 - High glucose treated cells + chlorogenic acid (30 µM). Values are expressed as mean ± SEM where n = 6. * $p \leq 0.05$ significantly different from the control group. # $p \leq 0.05$ significantly different from the HG treated group.

3.3.11. Production of AGEs during hyperglycemia

During hyperglycemia, there were elevated levels of AGE products (2.18 fold increase compared to control; $p \leq 0.05$). While CA at 10 µM and 30 µM decreased the level of AGE by 1.34 and 1.54 fold ($p \leq 0.05$) respectively compared to HG (Figure.3.10a). In addition, expression of RAGE (1.49 fold) was also found to increase in the HG group

compared to the control group. Also during hyperglycemia AGER1 level was found to decrease by 1.81 fold. Treatment with CA was found to improve the expression of RAGE (1.49 and 1.71 fold for 10µM and 30 µM of CA respectively; Figures.3.10b & c) as well as AGER1 (1.9 and 2.46 fold for 10µM and 30 µM of CA) respectively. Metformin also decreased the AGE content by 1.8 fold with respect to HG.

a

b

c
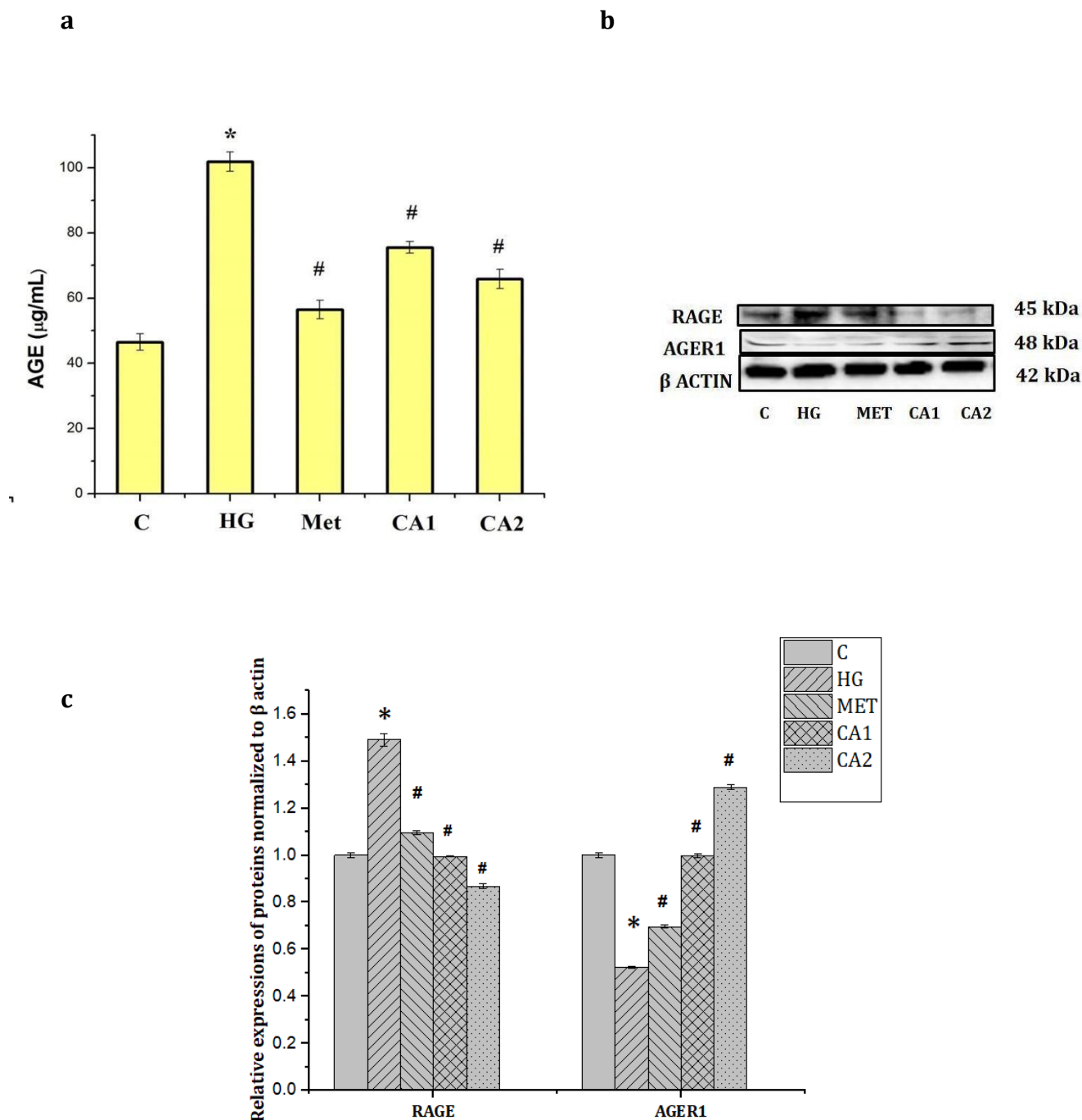
Figure.3.10. High glucose enhanced advanced glycated end products. a) Estimation of AGE content. b) Immunoblot analysis of RAGE and AGER1. c) Densitometric analysis of RAGE &

AGER1 with respect to β-actin. C- Control (5.5 mM glucose), HG-High glucose treated group (33 mM glucose), Met – High glucose treated cells + metformin (1 mM), CA1 –High glucose treated cells + chlorogenic acid (10 µM), CA2 - High glucose treated cells + chlorogenic acid (30 µM). Values are expressed as mean ± SEM where n = 6. * p ≤ 0.05 significantly different from the control group. # p ≤ 0.05 significantly different from HG treated group

3.3.12. Activity of PKC during hyperglycemia

HG treated cells showed an enhanced activity of PKC by 2.6 fold (p ≤0.05; Figure.3.11) compared to control whereas CA ameliorated the activity of PKC significantly (1.99 and 2.16 fold for 10 µM and 30 µM CA; p ≤0.05; Figure.3.11) compared to HG treated cells. Metformin also reduced the activity of PKC by 2.33 fold as compared to hyperglycemia group (Figure.3.11).
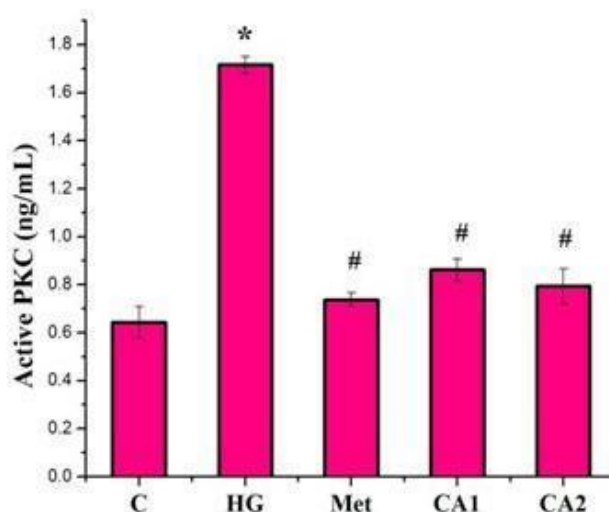
Figure 3. 11. PKC Activity; C- Control (5.5 mM glucose), HG-High glucose treated group (33 mM glucose), Met – High glucose treated cells + metformin (1 mM), CA1 – High glucose treated cells + chlorogenic acid (10 µM), CA2 - High glucose treated cells + chlorogenic acid (30 µM), Mnt- Control + mannitol (27.5 mM). Values are expressed as mean ± SEM where n = 6. * p ≤ 0.05 significantly different from the control group. # p ≤ 0.05 significantly different from the HG treated group.

3.3.13. PKC α and phosphorylation of ERK1/2

Western blot analysis of PKC α showed the expression of PKC α isoform in the lysate was increased by 1.74 fold (Figure.3.12a) in the hyperglycemic groups compared with the control groups. CA treatment had a mitigatory effect and showed decreased

levels of PKC α compared to HG cells in a significant manner (1.46 and 1.48 for 10 µM and 30 µM of CA respectively compared to hyperglycemia group, p ≤0.05; Figures.3.12a & b). The activation state of ERK1/2 was evaluated in different groups using the ratio of phosphorylated ERK1/2 to total ERK1/2. In HG treated cells, phosphorylated ERK1/2 to total ERK1/2 ratio was increased by 1.94 fold compared with those in control group (p ≤0.05), whereas treatment with CA resulted in normalized activation states of pERK1/2 compared with HG treated groups (1.577 and 1.45 for 10 µM and 30 µM of CA compared to hyperglycemia group, p ≤ 0.05; Figures.3.12a & c). Metformin resumed the protein levels in a significant manner relative to HG treated cells (1.37 for PKC α and 1.19 for pERK1/2 /ERK1/2, p ≤ 0.05, Figures.3.12a & c)

a

b

c
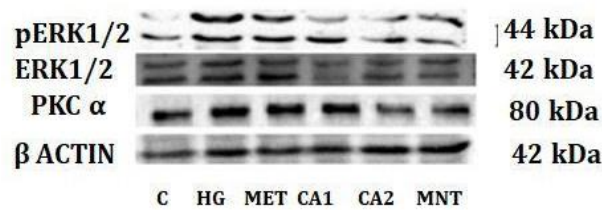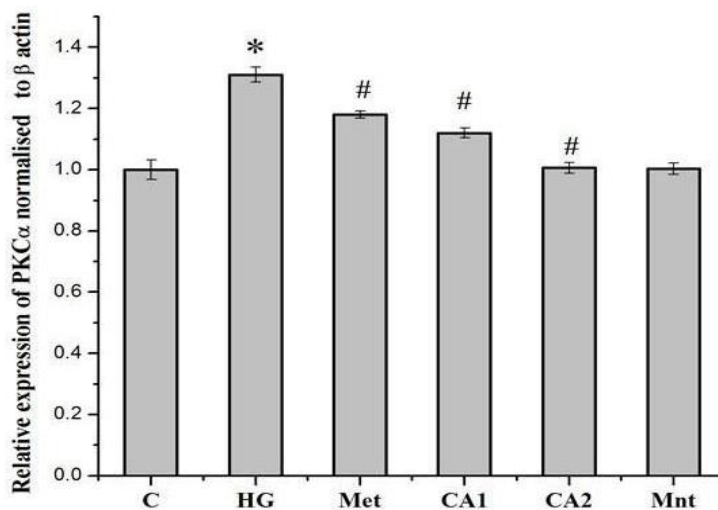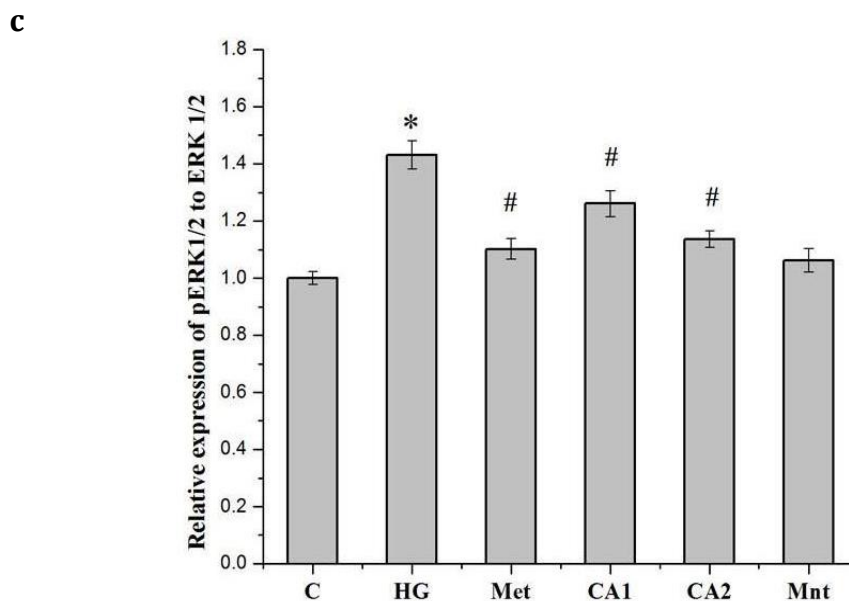
Figure 3.12. PKC ERK activation during hyperglycemia. a)Immunoblot analysis of PKC α, ERK1/2, pERK1/2; b) Densitometric analysis of protein expression of PKC α with respect to β-actin c) Densitometric analysis of relative expression of pERK1/2 to ERK1/2. C- Control (5.5 mM glucose), HG-High glucose treated group (33 mM glucose), Met – High glucose treated cells + metformin (1 mM), CA1 – High glucose treated cells + chlorogenic acid (10 μM), CA2- High glucose treated cells + chlorogenic acid (30 μM), Mnt- Control + mannitol (27.5 mM). Values are expressed as mean ± SEM where n = 6. * p ≤ 0.05 significantly different from the control group. # p ≤ 0.05 significantly different from the HG treated group.

3.3.14. Detection of ANP

There was a significant increase (p ≤ 0.05) in ANP levels in HG group (3.49 fold; Figure.3.13). Co -treatment with CA at 10 μM and 30 μM reduced ANP levels significantly (p ≤ 0.05) by 2.14 fold and 2.35 fold respectively compared to HG. Treatment with metformin also significantly (p ≤ 0.05) reduced ANP levels by 2.53 fold compared to HG (Figure.3.13).
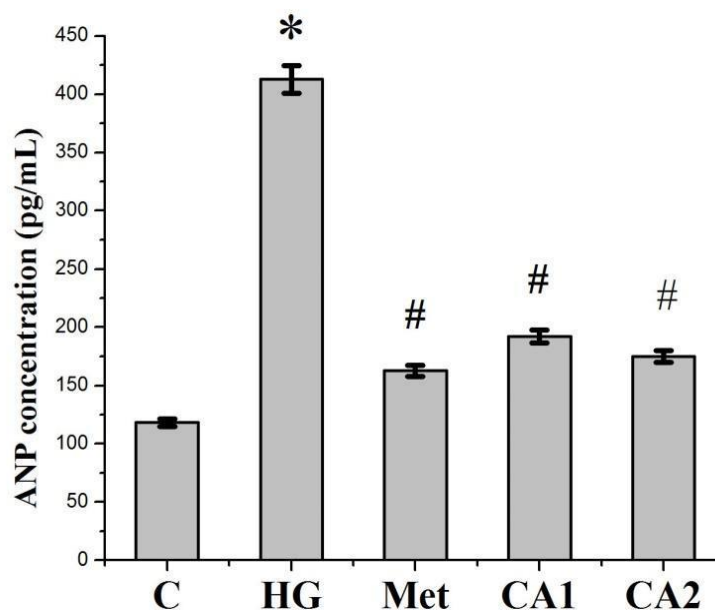
Figure 3.13. Quantification of ANP during hyperglycemia. C- Control (5.5 mM glucose), HG-High glucose treated group (33 mM glucose), Met – High glucose treated cells + metformin (1 mM), CA1 – High glucose treated cells + chlorogenic acid (10 μM), CA2 - High glucose treated cells + chlorogenic acid (30 μM). Values are expressed as mean ± SEM where n = 6. * $p ≤ 0.05$ significantly different from the control group. # $p ≤ 0.05$ significantly different from the HG treated group.

3.4. Discussion

Diabetes mellitus is causing a public health issue that needs to be tackled at multiple levels. For the prevention and management of associated comorbidities such as neuropathy, nephropathy and CVD is of paramount importance. CVD remains the prominent cause of mortality and morbidity with diabetes (Global reports, 2016). The role of hyperglycemic oxidative stress in the development of DCM is a fact and is under extensive investigation for prevention and management of diabetic CVD (Kaneto et al., 2010; Tsutsui et al., 2011). H9c2 cell line is my *in vitro* model which mimics almost all electrical and biochemical features of adult cardiac myocytes (Kuznetsov et al., 2015). Many effective interventions through antioxidant of both natural and synthetic origin are recommended for attenuating oxidative stress associated cardiac complications (Hill, 2008), but it is still an unmet need. So this is a burning health issue and needs to be researched from various corners for better therapeutic outcome due to the involvement of

pleiotropic pathways in the genesis of oxidative stress in the cardiovascular system (Mapanga and Essop, 2016). The emerging importance of AGE in cardiac health during diabetes has attracted the attention of basic scientists and cardiologists recently (Baye et al., 2017). The exact role of AGE in inducing cardiac dysfunction has not been studied yet in detail for therapeutic intervention. In the present investigation, studies were conducted in an integrated way with the special emphasis on innate antioxidant status, glycation, signaling pathways like PKC and ERK and to reveal their cumulative contribution to cardiac injury.

The initial observation revealed the surplus generation of ROS with hyperglycemia. Mitochondria, xanthine oxidase, uncoupled nitric oxide synthases and infiltrating inflammatory cells are all possible sources of ROS (Cave et al., 2005). Regardless of the existence of several ROS sources, NADPH oxidases which are mainly involved in redox signaling are a major source of ROS. The NADPH oxidase complex consists of a membrane bound cytochrome b558 which consists of two subunits of p22 phox and gp91 phox and four cytosolic subunit comprising p47phox, p67phox and rac1 (Baboir, 1999). Chronic NADPH oxidase activation is mainly by two mechanisms: 1) increase in oxidase subunit expression and 2) post translational modifications and regulatory subunit translocation (Griendling, 2000, Baboir, 1999). Interestingly in the present study I found an increased NADPH oxidase activity due to the increased overexpression of subuit Rac1 and p47 phox during hyperglycemia. CA was found to reduce the expression.

In order to identify the various factors associated with ROS in evoking cardiac pathology detailed investigation was done on the innate antioxidant status of H9c2 cells. Maintenance of adequate antioxidant levels is crucial to prevent or even manage a significant number of diseases associated with stress. Total antioxidant capacity reflects as a biomarker of diseases, biochemistry, medicine, food and nutritional sciences (Kusano and Ferrari, 2008). The major enzymatic innate antioxidants include SOD and GPx. As a major antioxidant enzyme family, superoxide dismutases (SODs), including copper-zinc superoxide dismutase (SOD1,CuZnSOD) and manganese superoxide dismutase (SOD2, MnSOD) play a pivotal role in scavenging free radicals. SOD catalyzes the conversion of superoxide anion radicals produced in the body to hydrogen peroxide, thereby reducing the feasibility of interaction of superoxide anion with nitric oxide to form reactive peroxynitrite (Maritim et al., 2003). The process by which SOD converts $O_2\bullet$ to H_2O_2 is

based on the alternate oxidation and reduction of a redox active transition metal, such as copper (Cu) or manganese (Mn), in the enzyme's active site (Fukai and Ushio, 2011). Because each SOD is sectionally localised, approaches to target their site-specific expression will be crucial and might be exploited to build new SOD-dependent therapies (Zelko et al., 2002). It is worth to note that over-expression of MnSOD ultimately prevented an increase in polyol pathway flux, increased intracellular AGE formation, increased PKC activation and an increase in hexosamine pathway activity in endothelial cells (Brownlee, 2001). This reveals the significant role of SOD during stress conditions associated with DCM. This report was my inspiration to see in detail the alteration of MnSOD and CuZnSOD in H9c2 cells during hyperglycemia and my finding in H9c2 cells are in accordance with Michael Brownlee, 2001 and I found significant down regulation of protein and activity level with hyperglycemia.

GPx/GSH system is important in oxidative stress (Espinosa et al., 2015). It is located in the nucleus, mitochondria and cytoplasm. It metabolizes hydrogen peroxide to water by using reduced glutathione as a hydrogen donor (Sies, 1999; Santini et al., 1997). It is a major intracellular redox scavenger system. Other oxidative stress-detoxifying enzymes, such as GSH transferases, use GSH as a substrate (Jurkovič et al., 2008). The impact of oxidative stress is clearly visible with depletion of GSH in the present study with HG.

The accumulation of lipid droplets within cardiomyocytes induces cardiac lipotoxicity (Zhang et al., 2011). Cardiomyocytes in healthy hearts have few droplets while diabetic rats store excessive lipids (Marfella et al., 2009). Lipids are retained in cardiomyocytes as triglycerides, but they are quickly mobilized to free fatty acids. The deposition of lipid droplets tends to develop oxidative stress. In addition, some lipotoxic heart models show abnormal PKC activation as well as faulty adrenergic signaling pathways (Drosatos et al., 2009). Here I found elevated levels of lipid droplets with high glucose. CA was found to be decreasing the incidence of lipid droplets.

Lipids are reported as one of the vital targets of ROS. ROS oxidizes the lipids to generate peroxides and aldehydes. Lipid peroxidation products are tangled in the transcriptional regulation of innate antioxidant systems (Espinosa et al., 2015). Lipid peroxidation products have been observed in many inflammatory complications including

cardiovascular disorders (Ramana et al., 2013) and can serve as a marker for the risk of CVD (Trpkovic, 2015). Lipid peroxidation was found to increase with hyperglycemia. This is expected to amplify the severity of complications of oxidative stress in myoblast and contribute significantly to the pathogenesis of DCM most probably through activation of various signaling pathways like PKC α and ERK axis (Von et al., 1989).

ROS can harm proteins also. Biomolecule carbonylation is one of the utmost communal biomarkers of oxidative stress. Protein carbonyl content is actually the most general indicator and by far the most commonly used marker of protein oxidation. The use of protein carbonyl as a biomarker of oxidative stress has several advantages over testing other oxidation items due to the relative early formation and relative stability of carbonylated proteins. Protein carbonyls have a remarkable stability and a wide variety of downstream functional implications as compared to other oxidative modifications. Protein carbonyls are also positively correlated with AGEs. In the present study, there is an increased protein oxidation in response to high glucose. CA and metformin prevents the protein carbonyl formation.

AGE content has been shown to be a biomarker for the DCM (Yeboah et al., 2004) individualistic from other well-known risk factors such as hyperlipidemia, hypertension and smoking. AGEs is reported to cause serious complications on the myocardium *via* cross linking of extracellular cardiac proteins and actions mediated by AGE receptors expressed on the myocardium (Bidasee et al., 2003; Bidasee et al., 2004; Zieman and Kass, 2004). They have been linked to systolic and diastolic cardiac dysfunction in diabetics. There is now emerging evidence that glycation induces oxidative stress and vice versa (Schleicher and Friess, 2007). Physiologically sustained exposure of proteins to glucose for a long time causes them to undergo a series of non enzymatic reactions and forms AGEs. It may change the structure and function of cardiac antioxidant enzymes such that they are unable to detoxify free radicals, exacerbating oxidative stress (Maritim, 2003). I found a significant increase in AGE content in cell lysate revealing hyperglycemia induced AGE formation in H9c2 cells. This result gives an idea to explore the possibilities of development of antiglycation agents as therapeutics for hyperglycemia induced cardiac complications. In order to confirm the AGE level, I also analysed two more proteins that are involved in the accumulation and clearance of AGE products. The association of AGEs with their key cellular receptor, RAGE leads to vascular and immune cell perturbation in

diabetic conditions. Recent studies suggest that the AGE RAGE knot indorses the downstream enhancement of the enzyme NADPH oxidase and thus the development of ROS (Perrone et al., 2020). This is on par with my previous results. Furthermore when RAGEs are activated by AGEs or other ligands, several signals are transduced, including mitogen-activated protein kinases (MAPKs), extracellular signal-regulated kinases 1 and 2 (ERK), p21ras, p38, and Janus kinase (Cai et al., 2016). During hyperglycemia, there is a significant increase in the expression of RAGE. CA and metformin reduces the AGE RAGE bond. This was again confirmed by the AGER1 level. AGER1 is cell surface receptors for AGEs that have the opposite role of RAGE and are involved in the control of AGE endocytosis and clearance (He et al., 2001). Chronic diabetes and other conditions of sustained oxidative stress have been linked to lower levels of AGER1. Here also I found a reduced expression of AGER1 in response to high glucose. CA and metformin improves the expression of scavenger receptor, AGER1. All of these results suggest that during hyperglycemia, AGE production is elevated and RAGE also increases, while scavenge receptors of AGEs is downregulated perhaps resulting in AGEs accumulation. CA and metformin reverses the AGE mediated mechanism which may possibly contribute other complications.

For a better scientific basis for this idea, the details of cross talk between glycation and other pathways relevant to cardiac function are very important. So efforts were made to study alterations in PKC α -ERK axis which has strong link with AGE formation and associated complications (Bonke et al., 2008) in the myocardium. PKC represents a family of more than 11 phospholipid-dependent serine/threonine kinases that are entangled in a variety of pathways that regulate cell death, growth, and stress responsiveness (Ding et al., 2011). Some isoforms of PKC family that are particularly influenced to redox stress are incriminated in CVD (Giorgi et al., 2010). In the heart, PKC activation leads to rapid changes in contractility performance (Dorn and Rosen, 2002). During hyperglycemia, there is preferential activation of PKC α and PKC βI/2 isoforms in the heart and aorta (Inoguchi et al., 1992). I found a significant increase in activity of PKC during hyperglycemia. In addition, I also found the overexpression of isoforms of PKC, PKC α and phosphorylated ERK1/2 with hyperglycemia. Activation of PKC-ERK axis during hyperglycemia has been demonstrated by various scientific reports. There are reports to connect that oxidative stress and AGE cause overexpression of PKC (Scivittaro et al.,

2002). Based on this information and my own result there is a possibility of cross talk between oxidative stress, AGE and PKC which together contribute to cardiac dysfunction.

In order to check injuries relevant to human cardiac diagnosis, I analyzed ANP. ANP is a 28 amino acid peptide that is synthesized and released by cardiac cells during any stress for protective adaptation. It is also an important diagnostic serum marker for cardiac injury and health (Brandt et al., 1993). ANP secretion is a calcium dependent process, initiated by intracellular calcium overload (Ruskoaho et al., 1987). This cardiac peptide induces cardioprotection by modulating the mPTP opening at reperfusion (Hong et al., 2012). Currently the studies based on the correlation between ANP and ROS generation during the development of cardiovascular diseases is limited (Clark et al., 1993). During acute hyperglycemia there is a rapid increase of ANP levels in response to sodium and fluid retention (McKenna et al., 2000; Böhlen et al., 1994). With hyperglycemia, there was a significant increase in ANP for protective (physiological) adaptation in H9c2 cells revealing the genesis of cardiac stress through various pathways.

CA is one of the most abundant polyphenols found in the human diet. I am sure that the potential antioxidant activity of CA contributes significantly to its beneficial activity against hyperglycemia in H9c2 cells. It is reported to have antidiabetic activity through inhibition of glucose-6-phosphate translocase 1 and reduction of the sodium gradient-driven apical glucose transport (McCarty, 2005). These additional properties may be contributing partially to the beneficial activity of CA in this study.

From my findings, I conclude that during hyperglycemia there is an alteration in redox machinery of the cells through oxidative stress, glycation, PKC α- ERK axis and CA was beneficial to cardiac cells against hyperglycemia.

References

1. Aneja A, Tang WH, Bansilal S, Garcia MJ, Farkouh ME. Diabetic cardiomyopathy: insights into pathogenesis, diagnostic challenges, and therapeutic options. *Am J Med*. 2008;121(9):748-757. doi:10.1016/j.amjmed.2008.03.046.
2. Babior BM. NADPH oxidase: an update. *Blood*. 1999; 93(5):1464-1476.
3. Baye E, de Courten MP, Walker K, et al. Effect of dietary advanced glycation end products on inflammation and cardiovascular risks in healthy overweight adults: a

randomised crossover trial. *Sci Rep*. 2017;7(1):4123. doi:10.1038/s41598-017-04214-6.

4. Bidasee KR, Nallani K, Yu Y, et al. Chronic diabetes increases advanced glycation end products on cardiac ryanodine receptors/calcium-release channels. *Diabetes*. 2003; 52(7):1825-1836. doi:10.2337/diabetes.52.7.1825.

5. Bidasee KR, Zhang Y, Shao CH, et al. Diabetes increases formation of advanced glycation end products on Sarco (endo) plasmic reticulum Ca2+-ATPase. *Diabetes*. 2004;53 (2):463-473. doi:10.2337/diabetes.53.2.463.

6. Böhlen L, Ferrari P, Papiri M, Allemann Y, Shaw S, Wiedmann P. Atrial natriuretic factor increases in response to an acute glucose load. *J Hypertens*. 1994;12(7):803-807.

7. Brandt RR, Wright RS, Redfield MM, Burnett JC Jr. Atrial natriuretic peptide in heart failure. *J Am Coll Cardiol*. 1993;22(4 Suppl A):86A-92A. doi:10.1016/0735-1097(93)90468-g.

8. Brownlee M. Biochemistry and molecular cell biology of diabetic complications. *Nature*. 2001;414(6865):813-820. doi:10.1038/414813a.

9. Cai Z, Liu N, Wang C, et al. Role of RAGE in Alzheimer's Disease. *Cell Mol Neurobiol*. 2016;36(4):483-495. doi:10.1007/s10571-015-0233-3.

10. Candido R, Forbes JM, Thomas MC, et al. A breaker of advanced glycation end products attenuates diabetes-induced myocardial structural changes. *Circ Res*. 2003;92(7):785-792. doi:10.1161/01.RES.0000065620.39919.20.

11. Cave A, Grieve D, Johar S, Zhang M, Shah AM. NADPH oxidase-derived reactive oxygen species in cardiac pathophysiology. *Philos Trans R Soc Lond B Biol Sci*. 2005;360(1464):2327-2334. doi:10.1098/rstb.2005.1772.

12. Clark BA, Sclater A, Epstein FH, Elahi D. Effect of glucose, insulin, and hypertonicity on atrial natriuretic peptide levels in man. *Metabolism*. 1993;42(2):224-228. doi:10.1016/0026-0495(93)90040-u.

13. Clifford MN. Chlorogenic acids and other cinnamates–nature, occurrence and dietary burden. *J. Sci. Food Agric.* 1999; 79 (3):362-372. doi.org/10.1002/(SICI)1097-0010(19990301)79:3<362::AID-JSFA256>3.0.CO;2-D.

14. Ding RQ, Tsao J, Chai H, Mochly-Rosen D, Zhou W. Therapeutic potential for protein kinase C inhibitor in vascular restenosis. *J Cardiovasc Pharmacol Ther*. 2011;16(2):160-167. doi:10.1177/1074248410382106.

15. Dorn GW, Mochly-Rosen D. Intracellular transport mechanisms of signal transducers. *Annu Rev Physiol*. 2002;64:407-429. doi:10.1146/annurev.physiol.64.081501.155903.

16. Drosatos K, Bharadwaj KG, Lymperopoulos A, et al. Cardiomyocyte lipids impair β-adrenergic receptor function via PKC activation. *Am J Physiol Endocrinol Metab*. 2011;300(3):E489-E499. doi:10.1152/ajpendo.00569.2010.

17. Espinosa-Diez C, Miguel V, Mennerich D, et al. Antioxidant responses and cellular adjustments to oxidative stress. *Redox Biol*. 2015;6:183-197. doi:10.1016/j.redox. 2015.07.008.

18. Farah A, Donangelo, CM. Phenolic compounds in coffee. *Braz. J. Plant Physiol.* 2006. 18(1): 23-36. doi.org/10.1590/S1677-04202006000100003.

19. Fukai T, Ushio-Fukai M. Superoxide dismutases: role in redox signaling, vascular function, and diseases. *Antioxid Redox Signal*. 2011;15(6):1583-1606. doi:10.1089/ars. 2011.3999.

20. Giorgi C, Agnoletto C, Baldini C, et al. Redox control of protein kinase C: cell- and disease-specific aspects. *Antioxid Redox Signal*. 2010;13(7):1051-1085. doi:10.1089/ ars. 2009.2825.

21. Global Reports on Diabetes. WHO, 2016.

22. Gonthier MP, Verny MA, Besson C, Rémésy C, Scalbert A. Chlorogenic acid bioavailability largely depends on its metabolism by the gut microflora in rats. *J Nutr*. 2003;133(6):1853-1859. doi:10.1093/jn/133.6.1853.

23. Griendling KK, Sorescu D, Ushio-Fukai M. NAD(P)H oxidase: role in cardiovascular biology and disease. *Circ Res*. 2000;86(5):494-501. doi:10.1161/01.res.86.5.494

24. Hahn HS, Marreez Y, Odley A, et al. Protein kinase Calpha negatively regulates systolic and diastolic function in pathological hypertrophy. *Circ Res*. 2003;93(11):1111-1119. doi:10.1161/01.RES.0000105087.79373.17.

25. Haidara MA, Yassin HZ, Rateb M, Ammar H, Zorkani MA. Role of oxidative stress in development of cardiovascular complications in diabetes mellitus. *Curr Vasc Pharmacol*. 2006;4(3):215-227. doi:10.2174/157016106777698469.

26. He CJ, Koschinsky T, Buenting C, Vlassara H. Presence of diabetic complications in type 1 diabetic patients correlates with low expression of mononuclear cell AGE-receptor-1 and elevated serum AGE. *Mol Med*. 2001;7(3):159-168.

27. Hill MF. Emerging role for antioxidant therapy in protection against diabetic cardiac complications: experimental and clinical evidence for utilization of classic and new

antioxidants. *Curr Cardiol Rev.* 2008;4(4):259-268. doi:10.2174/15734030878 6349453.

28. Hong L, Xi J, Zhang Y, et al. Atrial natriuretic peptide prevents the mitochondrial permeability transition pore opening by inactivating glycogen synthase kinase 3β via PKG and PI3K in cardiac H9c2 cells. *Eur J Pharmacol.* 2012; 695(1-3):13-19. doi:10.1016/j.ejphar.2012.07.053.

29. Inoguchi T, Battan R, Handler E, Sportsman JR, Heath W, King GL. Preferential elevation of protein kinase C isoform beta II and diacylglycerol levels in the aorta and heart of diabetic rats: differential reversibility to glycemic control by islet cell transplantation. *Proc Natl Acad Sci U S A*. 1992; 89(22):11059-11063. doi:10.1073/pnas.89.22.11059.

30. Jia G, DeMarco VG, Sowers JR. Insulin resistance and hyperinsulinaemia in diabetic cardiomyopathy. *Nat Rev Endocrinol.* 2016; 12(3):144-153. doi:10.1038/nrendo.2015. 216.

31. Jurkovič S, Osredkar J, Marc J. Molecular impact of glutathione peroxidases in antioxidant processes. *Biochem. Med*. 2008; 18(2):162-174.

32. Kaneto H, Katakami N, Matsuhisa M, Matsuoka TA. Role of reactive oxygen species in the progression of type 2 diabetes and atherosclerosis. *Mediators Inflamm.* 2010;2010:453892. doi:10.1155/2010/453892.

33. Kasai H, Fukada S, Yamaizumi Z, Sugie S, Mori H. Action of chlorogenic acid in vegetables and fruits as an inhibitor of 8-hydroxydeoxyguanosine formation in vitro and in a rat carcinogenesis model. *Food Chem Toxicol.* 2000;38(5):467-471. doi:10.1016/s0278-6915(00)00014-4.

34. Kono Y, Kobayashi K, Tagawa S, et al. Antioxidant activity of polyphenolics in diets. Rate constants of reactions of chlorogenic acid and caffeic acid with reactive species of oxygen and nitrogen. *Biochim Biophys Acta.* 1997;1335(3):335-342. doi:10.1016/s0304-4165(96)00151-1.

35. Kusano C, Ferrari, B. Total antioxidant capacity: a biomarker in biomedical and nutritional studies*. J Mol Cell Biol.* 2008; 7(1):1-15.

36. Kuznetsov AV, Javadov S, Sickinger S, Frotschnig S, Grimm M. H9c2 and HL-1 cells demonstrate distinct features of energy metabolism, mitochondrial function and sensitivity to hypoxia-reoxygenation. *Biochim Biophys Acta.* 2015;1853(2):276-284. doi:10.1016/j.bbamcr.2014.11.015.

37. Leon BM, Maddox TM. Diabetes and cardiovascular disease: Epidemiology, biological mechanisms, treatment recommendations and future research. *World J Diabetes*. 2015;6(13):1246-1258. doi:10.4239/wjd.v6.i13.1246.

38. Liu Q, Wang S, Cai L. Diabetic cardiomyopathy and its mechanisms: Role of oxidative stress and damage. *J Diabetes Investig*. 2014;5(6):623-634. doi:10.1111/jdi.12250.

39. Mahmood T, Anwar F, Abbas M, Saari N. Effect of maturity on phenolics (phenolic acids and flavonoids) profile of strawberry cultivars and mulberry species from Pakistan. *Int J Mol Sci*. 2012;13(4):4591-4607. doi:10.3390/ijms13044591.

40. Mapanga RF, Essop MF. Damaging effects of hyperglycemia on cardiovascular function: spotlight on glucose metabolic pathways. *Am J Physiol Heart Circ Physiol*. 2016;310(2):H153-H173. doi:10.1152/ajpheart.00206.2015.

41. Marfella R, Di Filippo C, Portoghese M, et al. Myocardial lipid accumulation in patients with pressure-overloaded heart and metabolic syndrome. *J Lipid Res*. 2009;50(11):2314-2323. doi:10.1194/jlr.P900032-JLR200.

42. Maritim AC, Sanders RA, Watkins JB 3rd. Diabetes, oxidative stress, and antioxidants: a review. *J Biochem Mol Toxicol*. 2003;17(1):24-38. doi:10.1002/jbt.10058.

43. McCarty MF. A chlorogenic acid-induced increase in GLP-1 production may mediate the impact of heavy coffee consumption on diabetes risk. *Med Hypotheses*. 2005;64(4):848-853. doi:10.1016/j.mehy.2004.03.037.

44. McKenna K, Smith D, Tormey W, Thompson CJ. Acute hyperglycaemia causes elevation in plasma atrial natriuretic peptide concentrations in Type 1 diabetes mellitus. *Diabet Med*. 2000;17(7):512-517. doi:10.1046/j.1464-5491.2000.00318.x.

45. Meier M, King GL. Protein kinase C activation and its pharmacological inhibition in vascular disease. *Vasc Med*. 2000;5(3):173-185. doi:10.1177/1358836X0000500307.

46. Meng S, Cao J, Feng Q, Peng J, Hu Y. Roles of chlorogenic Acid on regulating glucose and lipids metabolism: a review. Evid Based Complement Alternat Med. 2013; 2013:801457. doi: 10.1155/2013/801457.

47. Olukman M, Orhan CE, Celenk FG, Ulker S. Apocynin restores endothelial dysfunction in streptozotocin diabetic rats through regulation of nitric oxide synthase and NADPH oxidase expressions. *J Diabetes Complications*. 2010;24(6):415-423. doi:10.1016/j.jdiacomp.2010. 02.001.

48. Perrone A, Giovino A, Benny J, Martinelli F. Advanced Glycation End Products (AGEs): Biochemistry, Signaling, Analytical Methods, and Epigenetic Effects. *Oxid Med Cell Longev*. 2020; 2020:3818196. doi:10.1155/2020/3818196.

49. Qi Q, Qi L. Lipoprotein (a) and cardiovascular disease in diabetic patients. *Clin Lipidol*. 2012;7(4):397-407. doi:10.2217/clp.12.46.

50. Ramana KV, Srivastava S, Singhal SS. Lipid Peroxidation Products in Human Health and Disease 2016. *Oxid Med Cell Longev*. 2017; 2017:2163285. doi:10.1155/ 2017/2163285.

51. Reshma PL, Lekshmi VS, Sankar V, Raghu KG. Tribulus terrestris (Linn.) Attenuates Cellular Alterations Induced by Ischemia in H9c2 Cells Via Antioxidant Potential. *Phytother Res*. 2015;29(6):933-943. doi:10.1002/ptr.5336.

52. Ruskoaho H, Lang RE, Toth M, Ganten D, Unger T. Release and regulation of atrial natriuretic peptide (ANP). *Eur Heart J*. 1987;8 Suppl B:99-109. doi:10.1093/eurheartj/8.suppl_b.99.

53. Santini SA, Marra G, Giardina B, et al. Defective plasma antioxidant defenses and enhanced susceptibility to lipid peroxidation in uncomplicated IDDM. *Diabetes*. 1997;46(11):1853-1858. doi:10.2337/diab.46.11.1853.

54. Schleicher E, Friess U. Oxidative stress, AGE, and atherosclerosis. *Kidney Int Suppl*. 2007;(106):S17-S26. doi:10.1038/sj.ki.5002382.

55. Scivittaro V, Ganz MB, Weiss MF. AGEs induce oxidative stress and activate protein kinase C-beta(II) in neonatal mesangial cells. *Am J Physiol Renal Physiol*. 2000;278(4):F676-F683. doi:10.1152/ajprenal.2000.278.4.F676.

56. Sies H. Glutathione and its role in cellular functions. *Free Radic Biol Med*. 1999;27(9-10):916-921. doi:10.1016/s0891-5849(99)00177-x.

57. Steinberg HO, Paradisi G, Hook G, Crowder K, Cronin J, Baron AD. Free fatty acid elevation impairs insulin-mediated vasodilation and nitric oxide production. *Diabetes*. 2000;49(7):1231-1238. doi:10.2337/diabetes.49.7.1231.

58. Suroowan S , Mahomoodally F. Common phyto-remedies used against cardiovascular diseases and their potential to induce adverse events in cardiovascular patients. *Clin. Phytoscience*. 2015; 1(1):1-13.

59. Thallas-Bonke V, Thorpe SR, Coughlan MT, et al. Inhibition of NADPH oxidase prevents advanced glycation end product-mediated damage in diabetic nephropathy through a

protein kinase C-alpha-dependent pathway. *Diabetes.* 2008;57(2):460-469. doi:10.2337/db07-1119.

60. Triggle CR, Ding H. Cardiovascular impact of drugs used in the treatment of diabetes. *Ther Adv Chronic Dis.* 2014;5(6):245-268. doi:10.1177/2040622314546125.

61. Trpkovic A, Resanovic I, Stanimirovic J, et al. Oxidized low-density lipoprotein as a biomarker of cardiovascular diseases. *Crit Rev Clin Lab Sci.* 2015;52(2):70-85. doi:10.3109/10408363.2014.992063.

62. Tsutsui H, Kinugawa S, Matsushima S. Oxidative stress and heart failure. *Am J Physiol Heart Circ Physiol.* 2011;301(6):H2181-H2190. doi:10.1152/ajpheart.00554.2011.

63. Turan B, Dhalla NS. Diabetic Cardiomyopathy Biochemical and Molecular Mechanisms. Advances in Biochemistry in Health and Disease. New York : Springer; 2014.

64. von Ruecker AA, Han-Jeon BG, Wild M, Bidlingmaier F. Protein kinase C involvement in lipid peroxidation and cell membrane damage induced by oxygen-based radicals in hepatocytes. *Biochem Biophys Res Commun.* 1989;163(2):836-842. doi:10.1016/0006-291x(89)92298-5.

65. Watanabe T, Arai Y, Mitsui Y, et al. The blood pressure-lowering effect and safety of chlorogenic acid from green coffee bean extract in essential hypertension. *Clin Exp Hypertens.* 2006;28(5):439-449. doi:10.1080/10641960600798655.

66. Way KJ, Isshiki K, Suzuma K, et al. Expression of connective tissue growth factor is increased in injured myocardium associated with protein kinase C beta2 activation and diabetes. *Diabetes.* 2002;51(9):2709-2718. doi:10.2337/diabetes.51.9.2709.

67. Xu Z, Sun J, Tong Q, et al. The Role of ERK1/2 in the Development of Diabetic Cardiomyopathy. *Int J Mol Sci.* 2016;17(12):2001. doi:10.3390/ijms17122001.

68. Yamagishi S, Maeda S, Matsui T, Ueda S, Fukami K, Okuda S. Role of advanced glycation end products (AGEs) and oxidative stress in vascular complications in diabetes. *Biochim Biophys Acta.* 2012; 1820(5):663-671. doi:10.1016/j.bbagen.2011.03.014.

69. Yeboah FK, Alli I, Yaylayan VA, Yasuo K, Chowdhury SF, Purisima EO. Effect of limited solid-state glycation on the conformation of lysozyme by ESI-MSMS peptide mapping and molecular modeling. *Bioconjug Chem.* 2004; 15(1):27-34. doi:10.1021/bc034083v.

70. Zelko IN, Mariani TJ, Folz RJ. Superoxide dismutase multigene family: a comparison of the CuZn-SOD (SOD1), Mn-SOD (SOD2), and EC-SOD (SOD3) gene structures, evolution, and expression. *Free Radic Biol Med.* 2002; 33(3):337-349. doi:10.1016/s0891-5849(02)00905-x.

71. Zhang L, Ussher JR, Oka T, Cadete VJ, Wagg C, Lopaschuk GD. Cardiac diacylglycerol accumulation in high fat-fed mice is associated with impaired insulin-stimulated glucose oxidation. *Cardiovasc Res*. 2011; 89(1):148-156. doi:10.1093/cvr/cvq266.

72. Zieman SJ, Kass DA. Advanced glycation endproduct crosslinking in the cardiovascular system: potential therapeutic target for cardiovascular disease. *Drugs*. 2004;64(5):459-470. doi:10.2165/00003495-200464050-00001.

Cross talk between hyperglycemia and ER and effect of chlorogenic acid: an *in vitro* study

4.1. Introduction

Diabetic cardiomyopathy finds out diabetes related changes in the structure and function of the myocardium that are independent of coronary artery diseases or hypertension. However, the causes of DCM are unclear, and the best ways to mitigate the risks are still being investigated. The molecular mechanisms underlying the pathological changes in the diabetic heart are multifactorial and complex, with oxidative stress playing a key role. From the previous chapter I found that an increased oxidative stress and free fatty acids, enhanced glycation end products and elevated PKC activity in response to HG. Studies suggesting that oxidative stress elevated free fatty acids and impaired protein clearance have all been linked to the activation of the ER response in the diabetic heart, which has been linked to autophagy and apoptotic cell death (Yang et al., 2015). For the proper maintenance of cardiac physiology and maintaining heart output in response to pathological stresses requires careful management of the protein quality control system in the myocardium. The ER is considered as a crucial organelle for the cellular protein quality control and acts as a gatekeeper for the multistep maturation of budding polypeptides into fully functional proteins. Studies on the alterations and control of protein quality mechanism in the heart in diabetic patients have provided new insights into the molecular pathogenesis of DCM and providing proof of principle confirmation that fine tuned intonation of the UPR^{ER} and autophagic event is a strategy to treat DCM and prevent heart failure in diabetic conditions.

The ER is an ostentatious membranous network in all eukaryotic cells. The chief function is to maintain many homeostatic responses that include proper folding and maturation of recently synthesized secretory and transmembrane proteins (Grootjans et al., 2006), calcium (Ca^{2+}) storage, steroid, lipid and cholesterol biosynthesis, assembly of core-asparagine-linked oligosaccharides, and biosynthesis of secreted and membrane proteins (Rao and Bredesen, 2004). Several factors can disrupt ER functions which results in the accumulation of unfolded and misfolded proteins and leads to

cellular dysfunction and pathological consequences, namely ER stress and further activates the UPR (Mohan et al., 2019). UPR has biphasic functions (Siwecka et al., 2019) such as physiological and pathological based on the magnitude of stress. During physiological stress UPR affords an adaptive tool by which cells can boost protein folding and processing abilities of the ER (Malhotra and Kaufman, 2011). But if the stress is prolonged UPR undergoes pathological stress. This is found to cause many diseases. Mainly three ER transmembrane sensors, protein kinase RNA (PKR)-like ER kinase (PERK), inositol requiring enzyme1α (IRE1α) and activating transcription factor 6α (ATF6α) sense the misfolded or unfolded proteins gathered in the ER. The acute or mild ER stress enhances survival of the cell by persuading the adaptive response, ER hormesis, which maintains cellular health (Mollereau et al., 2014). Although UPR activation intends to renovate cellular function, prolonged ER stress can trigger apoptosis, which destroys the target cells (Lee and Harris, 2012). ER stress is involved in several processes of cardiovascular diseases, such as ischemia / reperfusion (I/R) injury, cardiomyopathy, cardiac hypertrophy, heart failure, and atherosclerosis (Toth et al., 2007). Signaling pathways for surviving with ER stress may exist as a significant direction for the discovery of therapeutic targets and design of novel treatment systems.

Since the storehouse of Ca^{2+} is ER, any turbulence in the ER causes impaired cardiac cycle. Ca^{2+} ion is very much important for regulating the muscle contraction and electrical signals that determine the cardiac rhythm. That is why altered calcium homeostasis is strongly associated with the progression of heart failure (Sutanto and Heijman, 2019). Hyperglycemia can directly affect Ca^{2+} homeostasis, resulting in diastolic dysfunction (Dobrin and Lebeche, 2010).

The ER and mitochondria have a very close relationship. When mitochondria – ER contact points are studied biochemically, they are referred to as mitochondria associated membranes (MAMs). Indeed, mitochondria and ER interact actively through MAM which is crucial for controlling a number of cellular functions comprising lipid trafficking, mitochondrial dynamics, ER stress, Ca^{2+} signaling, apoptosis and macroautophagy (Gordaliza et al., 2019). As a result, it's unsurprising that ER dysfunction will lead to mitochondrial dysfunction and ER stress mediated apoptotic cell death (Takuma et al., 2005). On the other hand, several studies have shown that mitochondrial dysfunction causes ER stress.

Studies had shown that ER stress and autophagy are interconnected. Autophagy is infrequently and insistently started in response to stress to evade cell death, but the excessive induction leads to cell death. ER-phagy, a selective type of autophagy, has been involved in the response to ER stress (Bernales et al., 2007). ER-phagy plays a significant role in reshaping ER after expansion simultaneous with oxidative stress, and in the lysosomal deprivation of protein accumulates within the ER lumen (Dikic, 2018). To maintain ER homeostasis, there is always a low level of ER-phagy occurring under basal conditions. The mechanisms and regulation of ER-phagy remain intangible. So the modulation of ER stress may serve as a potential tactic to improve the ER stress mediated cardiac injury during diabetes.

Since the prevalence of diabetes and its induced complications such as DCM is increasing day by day and still this is an incurable disease, so there is an urgent need of suitable therapeutics for the management of DCM. In this scenario, CA was found effective in reducing hyperglycemia induced alterations such as oxidative stress, glyction and PKC activity. In this chapter CA was evaluated against ER stress and associated pathways such as UPR, calcium signaling, apoptosis and ER-phagy during DCM employing an in *vitro* model.

4.2. Methods employed (Please refer chapter 2 for details)

Studies carried out in this chapter includes

✔ Determination of ER stress by fluorescence imaging (refer 2.2.17)
✔ Studies on UPR pathway by immunoblot, immunofluorescence and qRT PCR (refer 2.2.25, 2.2.26 & 2.2.27)
✔ Studies on ERO1α and PDI by western blot analysis (refer 2.2.27)
✔ Determination of intracellular calcium overload by fluorescence imaging and total Ca^{2+} content (refer 2.2.20 & 2.2.21)
✔ Investigation on calcium channels by western blot (refer 2.2.27)
✔ Studies on mitochondrial dysfunction (refer conitase and mPTP; refer 2.2.13 & 2.2.22)
✔ Determination of autophagy by fluorescence imaging (refer 2.2.23)
✔ Investigation on ER-phagy by immunofluorescence and immunoblot analysis (refer 2.2.25 & 2.2.27)

✔ Studies on ER stress mediated cell death by western blot analysis (refer 2.2.27)

4.3. Results

4.3.1. Effect of HG on ER

To examine the impact of HG on ER, I performed fluorescent imaging by ER RFP. The data depicted that HG significantly increased ER stress (2 fold; Figures. 4.1a & b) While treatment with CA (1.33 and 1.42 fold for 10 μM and 30 μM of CA) and metformin (1.39 fold) reduced ER stress (Figures. 4.1a & b).

a
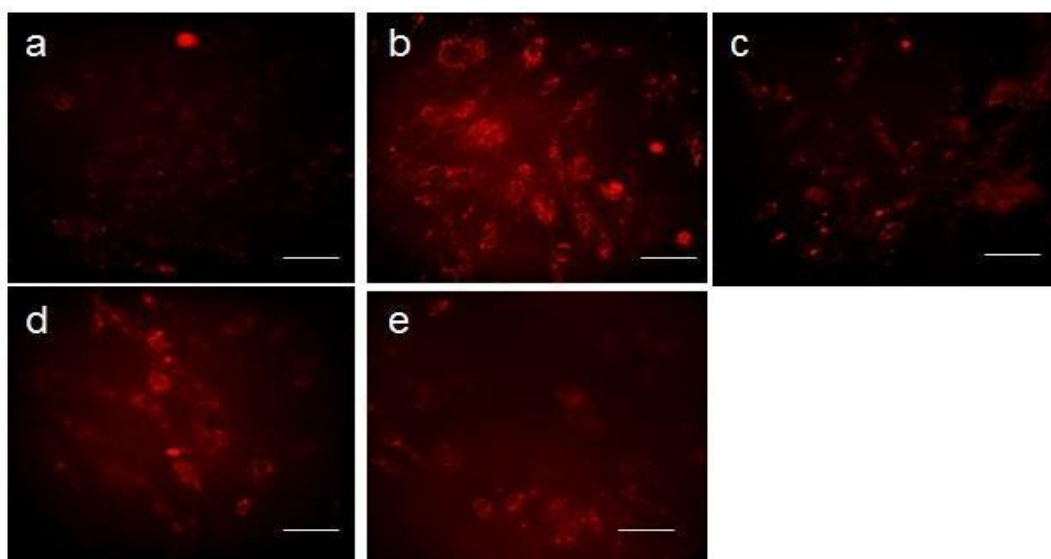
b
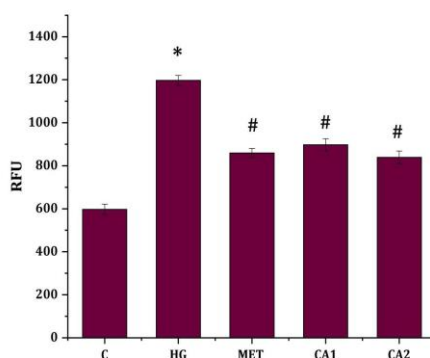
Figure.4.1. Determination of ER stress by CellLight™ ER-RFP (Calreticulin). **a) Expression of red fluorescence in various groups.** a) C- Control (5.5 mM glucose), b) HG-High glucose treated group(33 mM glucose), c) Met – High glucose treated cells + metformin (1 mM), d) CA1 –High glucose treated cells + chlorogenic acid (10 μM), e)CA2 - High glucose treated cells + chlorogenic acid (30 μM). Scale bar: 50 μm. **b) Relative fluorescent intensity of the fluorescent images.** C control (5.5 mM glucose), HG-High glucose treated group (33 mM glucose), Met – High glucose

treated cells + metformin (1 mM), CA1 – High glucose treated cells + chlorogenic acid (10 μM), CA2 - High glucose treated cells + chlorogenic acid (30 μM). Values are expressed as mean ± SEM where n = 6. * $p \leq 0.05$ significantly different from the control group. # $p \leq 0.05$ significantly different from the HG treated group.

4.3.2. Effect of HG on ER stress marker in H9c2 cells

To confirm the ER sress, I further investigated ER stress maker GRP78. The results revealed that HG exposure significantly increased the expression of GRP78 (1.74 fold; $p \leq 0.05$; Figures.4.2a & b) compared with the control group. Co-treatment with CA of 10 μM and 30 μM reduced the expression of GRP78 by 1.46 and 1.48 fold compared to HG. Metformin also reduced the GRP78 levels compared to HG groups.

a
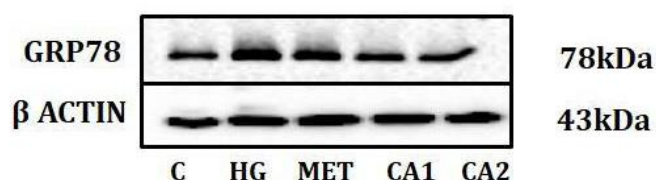
b
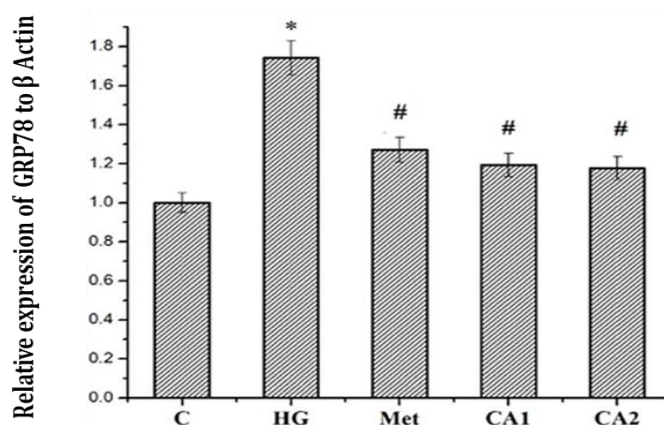
Figure.4.2. Expression of ER stress marker. a) Immunoblot analysis of GRP78. b) Densitometric analysis of protein expression of GRP78 with respect to β-actin . C control (5.5 mM glucose), HG-High glucose treated group (33 mM glucose), Met – High glucose treated cells + metformin (1 mM), CA1 – High glucose treated cells + chlorogenic acid (10 μM), CA2 - High glucose treated cells + chlorogenic acid (30 μM). Values are expressed as mean ± SEM

where n = 3. * p ≤ 0.05 significantly different from the control group. # p ≤ 0.05 significantly different from the HG treated group.

4.3.3. CA ameliorates UPR signaling pathway during hyperglycemia

To further confirm the role of HG on induction of ER stress I explored the underlying mechanism by studying the UPR signaling pathways in depth.

4.3.3.1. PERK pathway

HG treatment markedly increased the expression of PERK-mediated EIF2α phosphorylation and ATF4 (Figure.4.3a). PERK/EIF2α/ATF4 signaling is known to mediate ER stress. The activation state of PERK was evaluated in different groups using the ratio of phosphorylated PERK to PERK. In HG treated cells, phosphorylated PERK to total PERK ratio was increased by 1.94 fold compared with those in control groups (p ≤ 0.05), whereas treatment with CA resulted in normalized activation states of pPERK compared with HG treated groups (1.577 and 1.45 for 10 µM and 30 µM of CA; p ≤ 0.05;Figures.4.3a & c). HG treatment significantly upregulated the expression of pEIF2α and ATF4 by 1.48 and 2.9 fold (Figures.4.3b &d) respectively. While treatment with CA at both concentrations (10 µM and 30 µM) and metformin downregulated the expression of pEIF2α by 1.38, 2.01 and 1.34 fold and ATF4 by 1.166, 1.54 and 1.55 fold respectively.

a

b

c

d
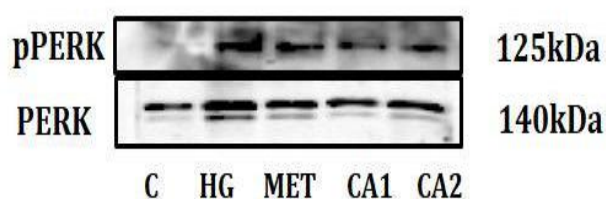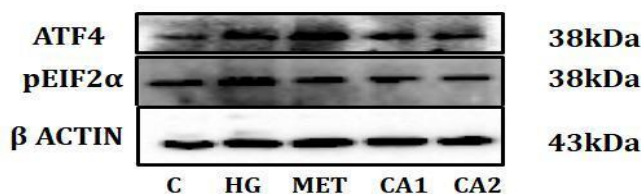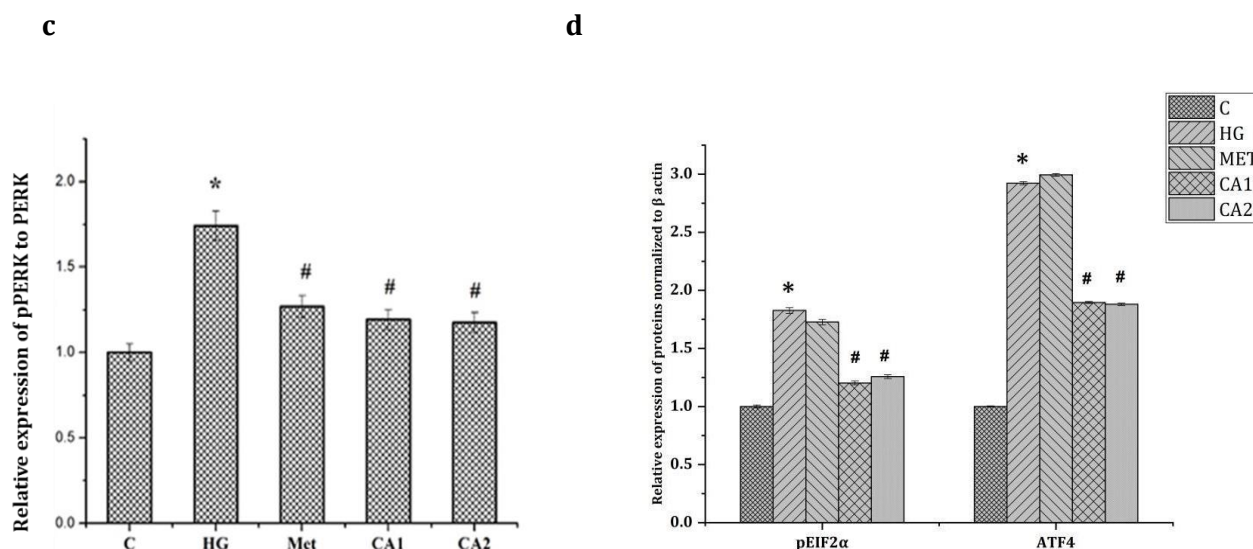
Figure.4.3. Western blot analysis of PERK pathway. a) Immunoblot of PERK and pPERK. b) Western blot of ATF4, pEIF2α, β actin. c) Densitometric analysis of relative expression of pPERK to PERK. d) Densitometric analysis of protein expressions of ATF4 and pEIF2α with respect to β-actin. C- Control (5.5 mM glucose), HG-High glucose treated group (33 mM glucose), Met – High glucose treated cells + metformin (1 mM), CA1 –High glucose treated cells + chlorogenic acid (10 µM), CA2 - High glucose treated cells + chlorogenic acid (30 µM). Values are expressed as mean ± SEM where n = 3. * p ≤ 0.05 significantly different from the control group. # p ≤ 0.05 significantly different from the HG treated group.

4.3.3.2. IRE1α pathway

In addition, I also analysed IRE1α signaling. Western blot analysis showed that in HG treated cells, phosphorylated IRE1α to total IRE1α ratio was increased by 1.29 fold compared with those in control groups (p ≤ 0.05; Figure.4.4a), whereas treatment with CA resulted in normalized activation states of pIRE1α compared with HG treated groups (1.58 and 1.24 for 10 µM and 30 µM of CA compared to HG group; p ≤ 0.05; Figures.4.4a & b). Besides, protein expression of TRAF2 (2.52 fold) and pJNK (2.27 fold) was increased after HG incubation (Figure.4.4a). Treatment with CA significantly reduced the expression of TRAF2 (1.08 and 1.76 fold for 10 µM and 30 µM of CA) and pJNK (1.32 and 1.55 fold for 10 µM and 30 µM of CA; Figures. 4.4a & c). mRNA expression of XBP1 was found to have increased significantly (2.25 fold; p ≤ 0.05; Figure 4.4d) in the HG model compared with the control group. At mRNA level, expression was down regulated

in the CA treated groups of both concentrations (1.14 and 1.38 fold). Metformin treatment down regulated IRE1 α signaling pathway (Figures.4.4a & d).

a

b

c

d
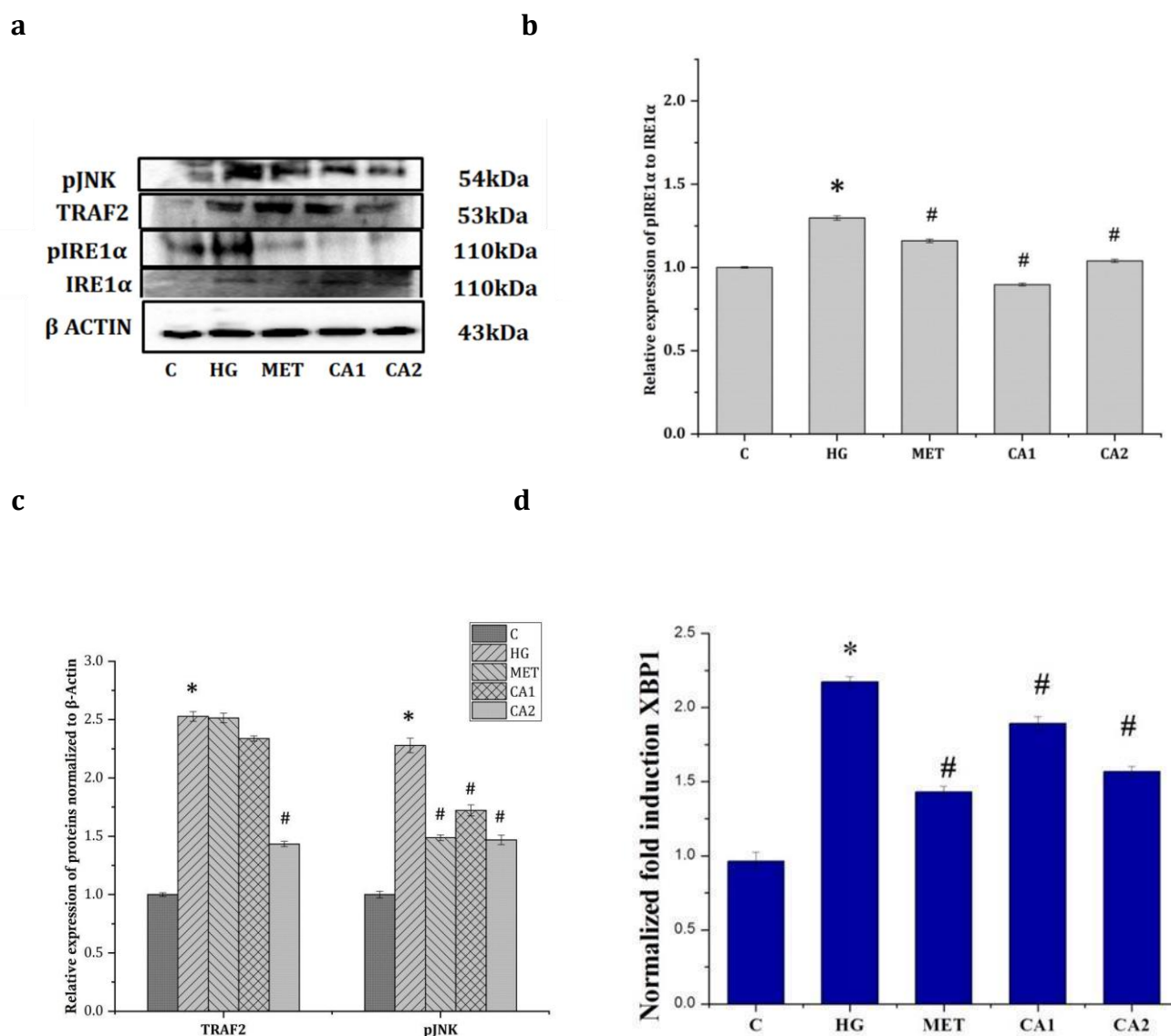
Figure.4.4. Analysis of IRE1 pathway during hyperglycemia. a) Immunoblot of IRE1α, p IRE1α , TRAF2, pJNK and β actin. b) Densitometric analysis of relative expression of pIRE1α to IRE1α. c) Densitometric analysis of protein expressions with respect to β-actin.d) Gene expression of XBP1 determined by qRT PCR analysis. β Actin was used as an internal control. C- Control (5.5 mM glucose),HG-High glucose treated group(33 mM glucose), Met – High glucose treated cells + metformin (1 mM), CA1 –High glucose treated cells + chlorogenic acid (10 µM), CA2 - High glucose treated cells + chlorogenic acid (30 µM). Values are expressed as mean ± SEM where n = 3. * $p \leq 0.05$ significantly different from the control group. # $p \leq 0.05$ significantly different from the HG treated group.

4.3.3.3. ATF6α pathway

Compared with the control group, the HG group showed enhanced ATF6α expression (2.28 fold; Figure. 4.5a). CA prevented the upregulation of ATF6α levels (2.71 and 3.54 fold; Figures.4.5a & b) compared to the HG group. Metformin also protected the H9c2 cells from HG insult by modulating the ATF6α pathway (Figures.4.5a & b). I also examined the ATF6α cytoplasmic nuclear translocation. Immunostaining showed that there was an increased translocation of ATF6α into the nucleus in HG treated H9c2 cells (Figure.4.5c). While CA and metformin treatment was found to reduce the translocation (Figure.4.5c).

a

b

c
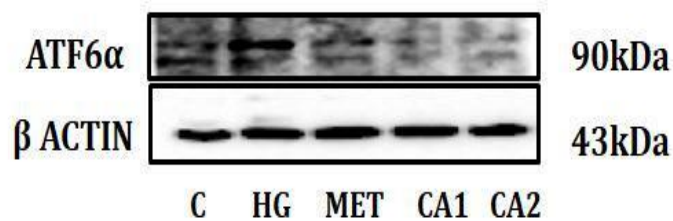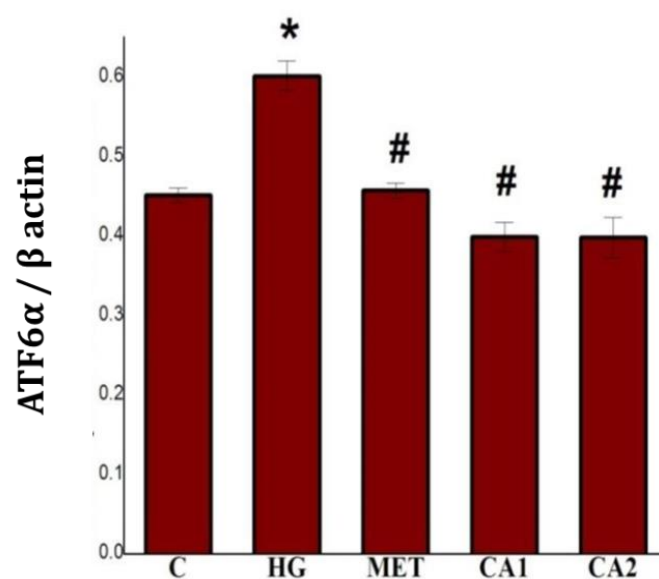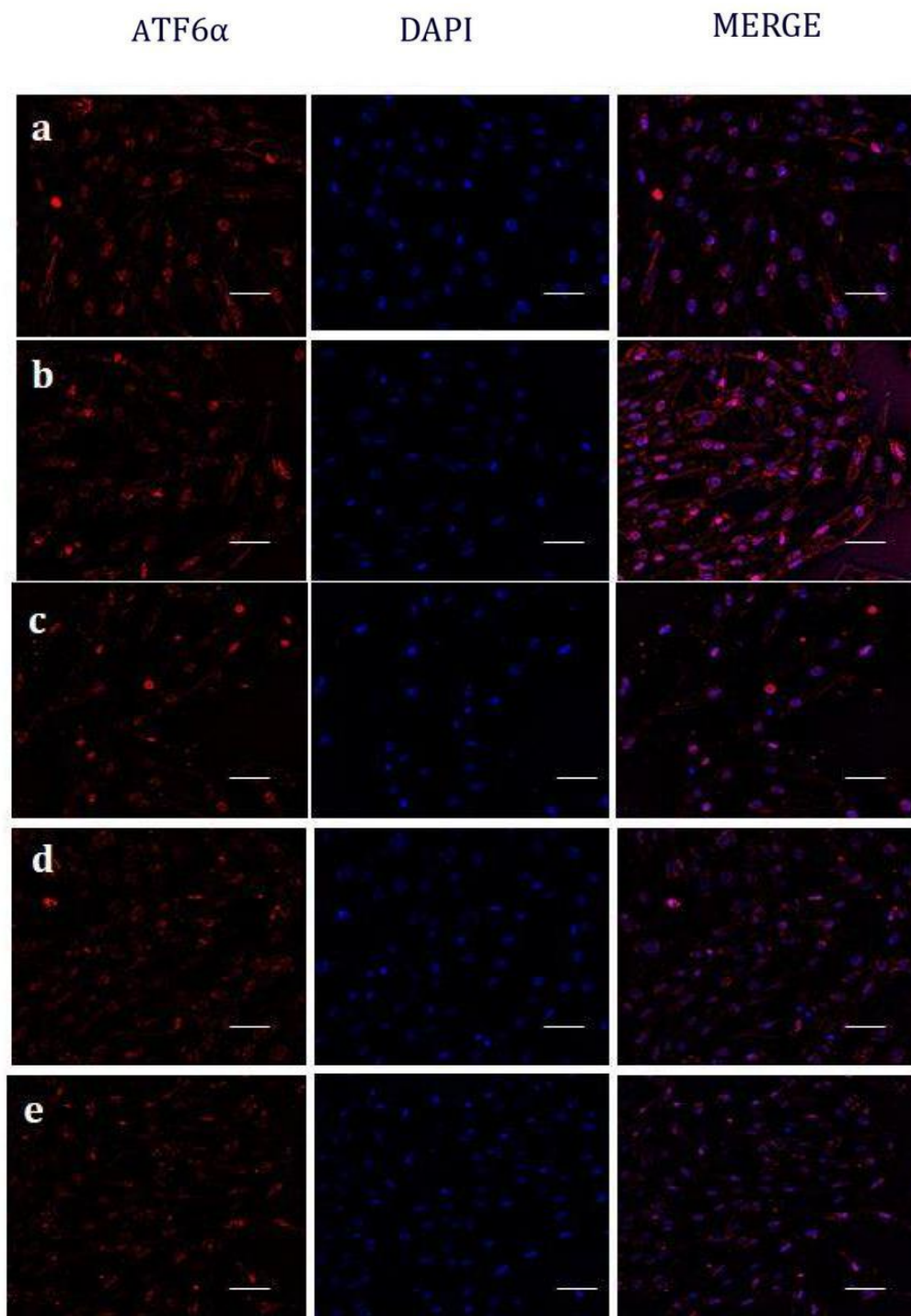
Figure.4.5. ATF6α pathway during hyperglycemia. a) Western blot analysis of ATF6α .
b) Densitometric analysis of protein expression ATF6α of with respect to β-actin. C-
Control (5.5 mM glucose), HG-High glucose treated group (33 mM glucose), Met – High glucose
treated cells + metformin (1 mM), CA1 –High glucose treated cells + chlorogenic acid (10 μM),
CA2 - High glucose treated cells + chlorogenic acid (30 μM). **c) Representative**

immunostaining images of ATF6α in H9c2 cardiomyocytes after HG (33 mM) treatment for 48 h in presence or absence of various concentrations of CA or metformin are shown. ATF6α visualised by Alexa 888 (red) and nuclei stained with DAPI (blue) with fluorescent microscope. a) C- Control (5.5 mM glucose), b) HG-High glucose treated group(33 mM glucose), c) Met – High glucose treated cells + metformin (1 mM), d) CA1 –High glucose treated cells + chlorogenic acid (10 μM), e) CA2 - High glucose treated cells + chlorogenic acid (30 μM). Scale bar corresponds to 50 μm. Values are expressed as mean ± SEM where n = 3. * p ≤ 0.05 significantly different from the control group. # p ≤ 0.05 significantly different from the HG treated group.

4.3.4. CA modulates ER stress and associated signaling pathways in H9c2 cells during hyperglycemia

To further elucidate the mechanistic actions of the CA during hyperglycemia, I evaluated the modulatory effects of CA during hyperglycemia on 16 major nuclear transcription factors using a nuclear transcription factor array. On the basis of the results, I was noted that during hyperglycemia, CA had good effects at promoting nuclear levels of transcription factors (Figure.4.6), forkhead box protein O1 (FOXO1), nuclear factor (erythroid-derived 2)-like 2 (Nrf2), SREBP1, and CBF. CA also had significant effects on UPR transcription factors mainly activating transcription factor 4 (ATF4), ATF3, GADD153, XBP1, ERR and p53. CA showed inductive effects on activator protein 1 (AP-1), interferon regulatory factors (IRF), and nuclear factor kappa-light-chain-enhancer of activated B cells (NFkB), CA promoted core binding factor/nuclear transcription factor YY1 (CBF/NFY). Collectively, the results demonstrate that CA can modulate levels of multiple nuclear transcription factors.
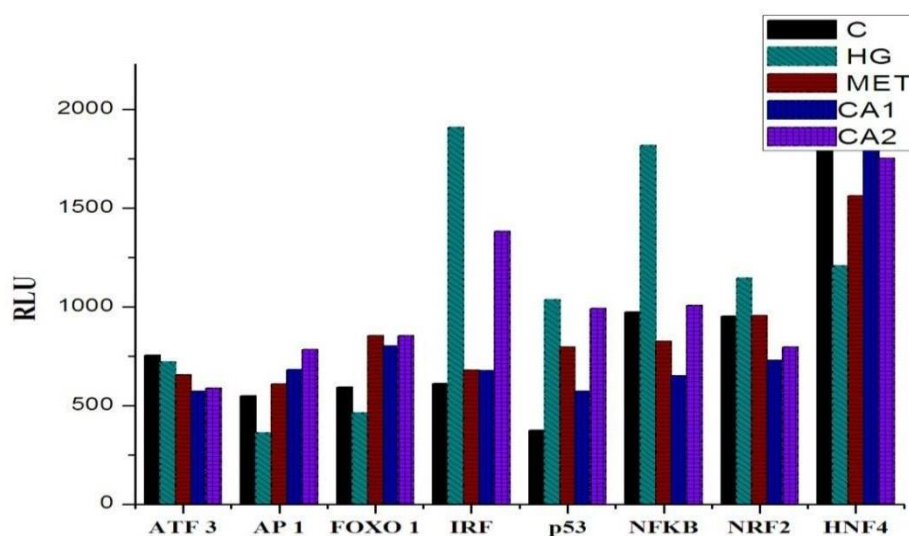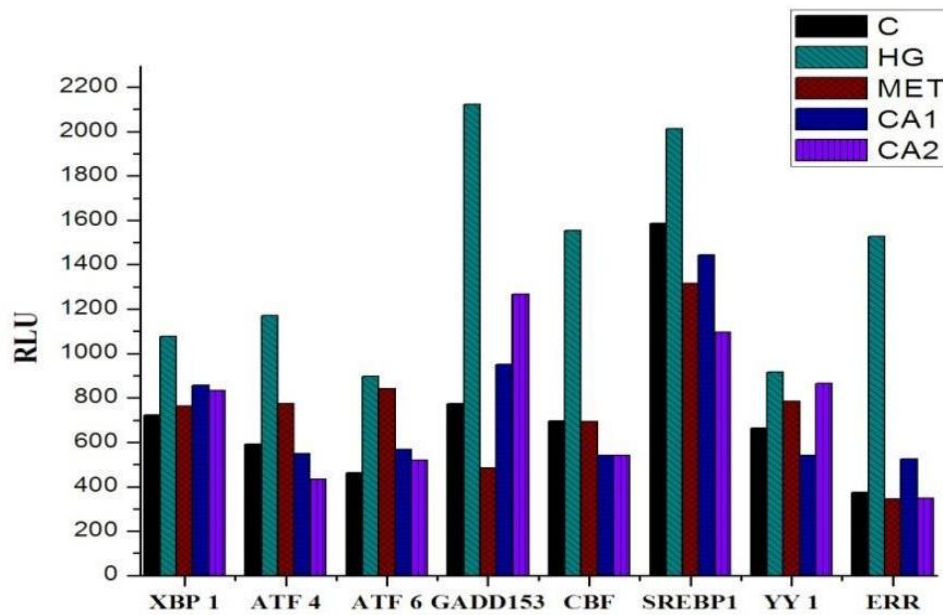
Figure.4.6. TF profiling array of ER stress during hyperglycemia. C- Control (5.5 mM glucose), HG-High glucose treated group (33 mM glucose), Met – High glucose treated cells + metformin (1 mM), CA1 – High glucose treated cells + chlorogenic acid (10 μM), CA2 - High glucose treated cells + chlorogenic acid (30 μM).

4.3.5. Effect of CA on oxidative protein folding during hyperglycemia

There was an overexpression of PDI (1.56 fold) and ERO1α (1.53 fold) in HG induced H9c2 cells compared with control groups (Figure.4.7a). CA (10 μM) and metformin prevented upregulation of ERO1α (1.15 and 1.32 fold) and PDI (1.27 and 1.17 fold) in a significant manner (Figures.4.7a & b; p ≤ 0.05).

a

b
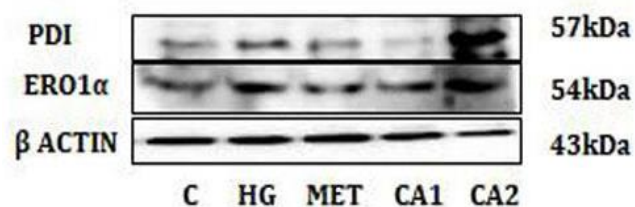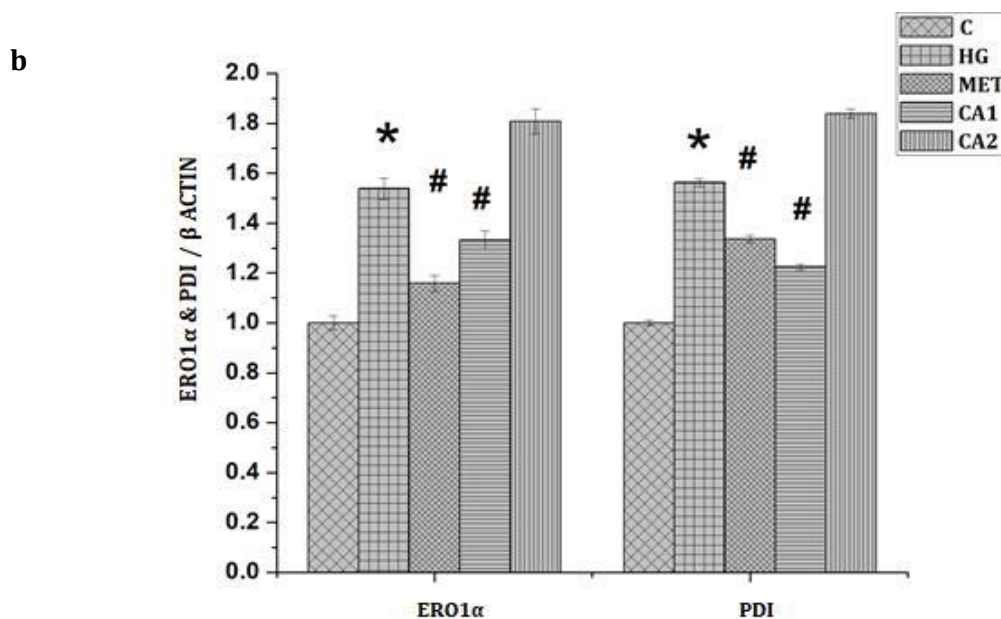
Figure. 4.7. Expression of PDI and ERO1α in HG treated H9c2 cells. a) Immunoblot analysis of PDI and ERO1α. b) Densitometric analysis PDI and ERO1α with respect to β-Actin. C-Control (5.5 mM glucose), HG-High glucose treated group (33 mM glucose), Met – High glucose treated cells + metformin (1 mM), CA1 – High glucose treated cells + chlorogenic acid (10 µM), CA2 - High glucose treated cells + chlorogenic acid (30 µM). Values are expressed as mean ± SEM where n = 3. * $p \leq 0.05$ significantly different from the control group. # $p \leq 0.05$ significantly different from HG treated group

4.3.6. Investigation on calcium homeostasis during HG induced ER stress

In order to confirm the ER stress induced Ca^{2+} dyshomeostasis, here I added two more groups' thapsigargin (ER stress activator) and PBA (ER stress inhibitor).

4.3.6.1. Intracellular Ca^{2+} overload

HG induced intracellular Ca^{2+} overload in H9c2 cells, which was manifest from increased blue fluorescence of Fura-2AM (Figure. 4.8.) compared to the control group. Co-treatment with CA reduced Ca^{2+} overload compared to that of HG treated group.
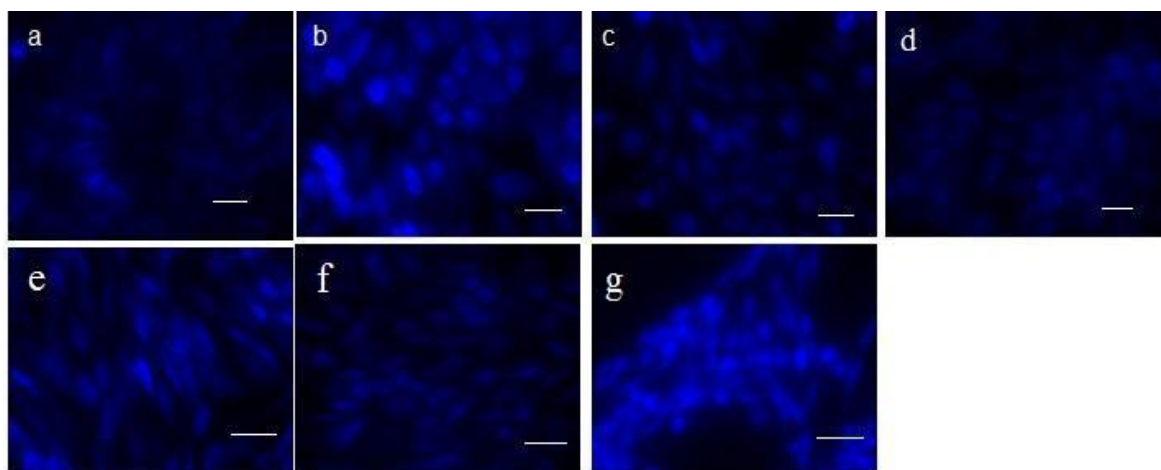
Figure.4.8. [Ca²⁺]i overload in H9c2 cells with HG, CA and metformin. Representative fluorescent microscopic images of H9c2 cells stained with Fura-2AM. C- a) C- Control (5.5 mM glucose) ,b) HG-High glucose treated group(33 mM glucose), c) Met – High glucose treated cells + metformin (1 mM), d) CA1 –High glucose treated cells + chlorogenic acid (10 µM), e) CA2 - High glucose treated cells + chlorogenic acid (30 µM), P, High glucose treated cells + phenyl butyric acid(1mM) , T, Control (5.5 mM glucose + thapsigargin (5 µM). Scale bar: 50 µm.

4.3.6.2. Total calcium content

There is no significant change in the total Ca^{2+} content in HG treated H9c2 cells compared to that of control cells. Only thapsigargin treated groups show low calcium content compared to control cells in a significant manner (Figure.4.9).
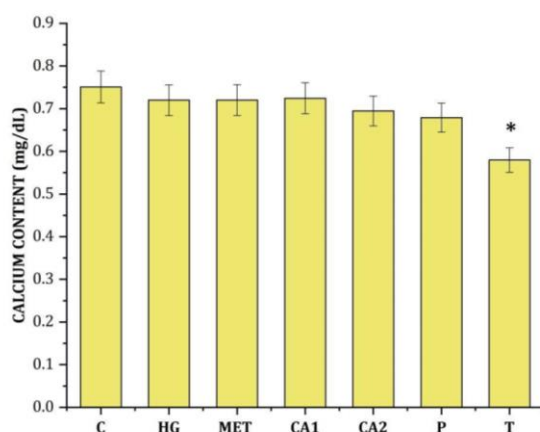
Figure.4.9. Total calcium content during HG. C- Control (5.5 mM glucose), HG-High glucose treated group(33 mM glucose), Met – High glucose treated cells + metformin (1 mM), CA1 – High glucose treated cells + chlorogenic acid (10 µM), CA2 - High glucose treated cells + chlorogenic acid (30 µM), P- High glucose treated cells + phenyl butyrate (100 µM), T - Control cells + thapsigargin (5 µM). Values are expressed as mean ± SEM where n = 3. * p ≤

0.05 significantly different from the control group. # p ≤ 0.05 significantly different from the HG treated group.

4.3.6.3. Studies on proteins related to calcium homeostasis during hyperglycemia

Alteration of various proteins from calcium homeostasis pathways (pCaMKII, RYR2, pRYR2, NCX1, SERCA2a) of the cell during hyperglycemia was studied. Expression of pCaMKII was significantly increased in HG treated cells (1.4 fold; Figure 4.10a) compared to the control group. Ratio of phosphorylated RYR2 to total RYR2 was increased by 2.15 fold in HG treated cells, compared with control groups (Figures. 4.10b & d; p ≤ 0.05), whereas treatment with CA resulted in normalized activation states of pRYR2 compared with HG treated groups (1.43 and 3.49 for 10 μM and 30 μM of CA respectively compared to hyperglycemia group; p ≤ 0.05; Figure 4.10d). NCX1 protein expressions were also increased significantly (1.4 fold; p ≤ 0.05; Figures. 4.10a & c) in HG treated cells when compared with control. CA resumed the protein level of NCX1 (1.95 and 1.22 fold for 10 μM and 30 μM of CA; p ≤ 0.05; Figure. 4.10c) in a significant manner. I also investigated the expression of SERCA2a during hyperglycemia. There was significant (p ≤ 0.05) reduction in the expression of SERCA2a in HG group (1.6 fold) compared to control while CA upregulated the expression of SERCA2a (1.44 and 1.55 fold for 10 μM and 30 μM of CA respectively, Figures.4.10a & c). Metformin also improved the expression of pCaMKII (1.4 fold), NCX1 (1.14 fold) and SERCA2a (3.83 fold) significantly (Figures.4.10a & c). PBA was found to be effective in regulating calcium homeostasis. Thapsigargin treated cells showed the similar pattern of HG treated groups in all aspects (Figures.4.10a & b).
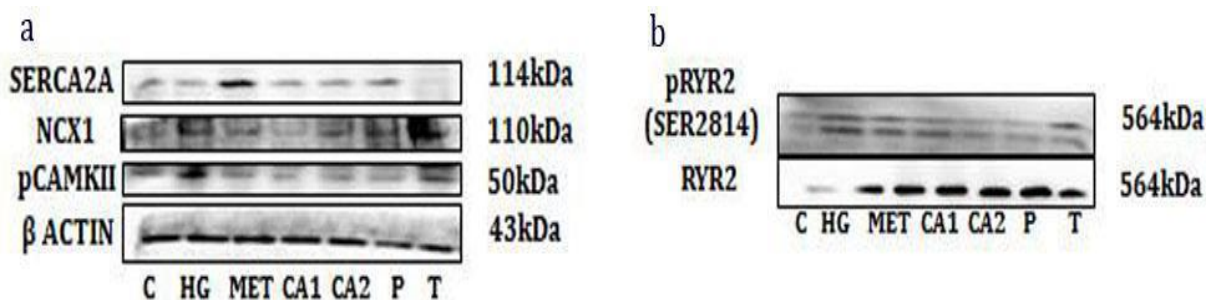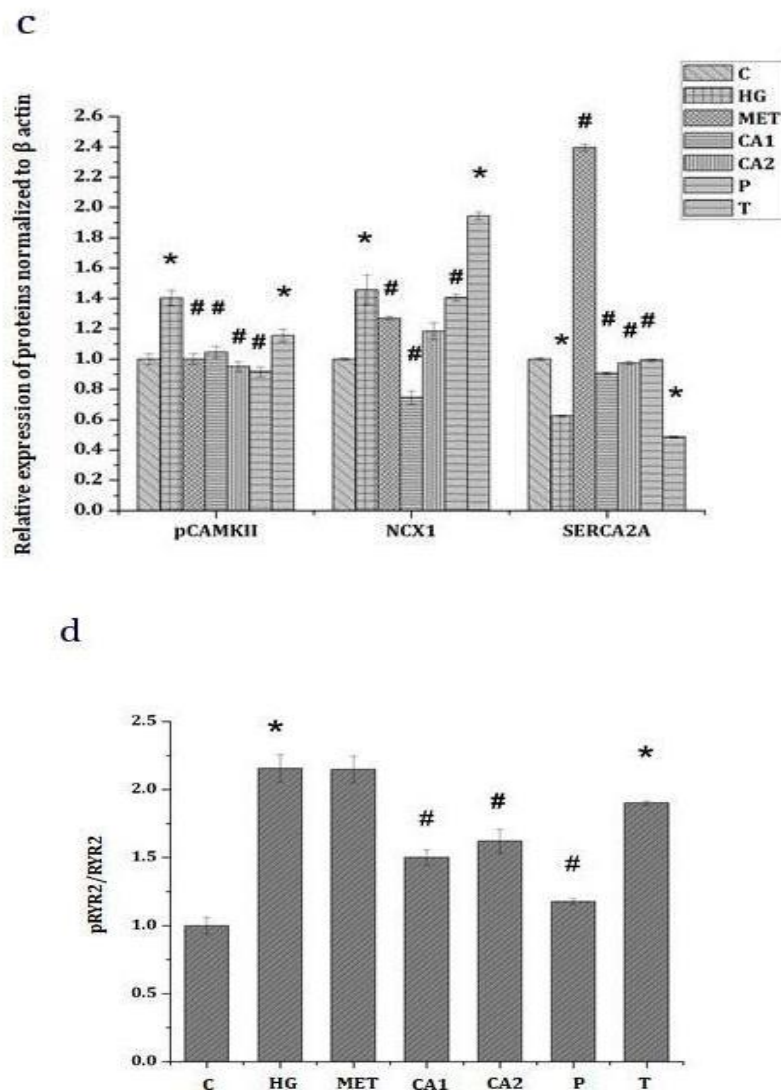
Figure. 4.10. Studies on proteins related to calcium homeostasis during HG induced ER stress. a) Representative image showing the results of immunoblotting with anti-pCaMKII, anti-NCX1, anti-SERCA2a and β-actin antibodies. b)Immunoblots for total RyR2, phosphorylated RyR2 (pRyR2 Ser-2808 in H9c2 cardiomyocytes after HG (33 mM) treatment for 48 h in presence or absence of various concentration of chlorogenic acid or metformin. (c) Densitometry values of pCaMKII, NCX1, and SERCA2a were normalized to the β-actin. (d)Quantification of pRyR2 Ser-2814 levels normalized to total RyR2 protein expression. C- Control (5.5 mM glucose), HG-High glucose treated group (33 mM glucose), Met – High glucose treated cells + metformin (1 mM), CA1 – High glucose treated cells + chlorogenic acid (10 μM), CA2 - High glucose treated cells + chlorogenic acid (30 μM), P- High glucose treated cells + phenyl butyrate (100 μM), T - Control cells + thapsigargin (5 μM). Values are expressed as mean ± SEM where n = 3. * p ≤ 0.05 significantly different from the control group. # p ≤ 0.05 significantly different from the HG treated group.

4.3.7. Effect of CA on mitochondrial dysfunction during hyperglycemia induced ER stress

4.3.7.1 Activity of aconitase during hyperglycemia

Activity of aconitase was significantly decreased (1.78 fold; Figure.4.11) in H9c2 cells on treatment with HG compared to the control group. CA at both concentrations (1.48 and 1.78 fold for 10 µM and 30 µM) showed significant efficacy in preventing HG induced alteration in the activity of aconitase. Metformin also shows considerable (1.47 fold) improvement in the aconitase activity. Thapsigargin also had reduced aconitase activity compared to the control group (Figure.4.11).
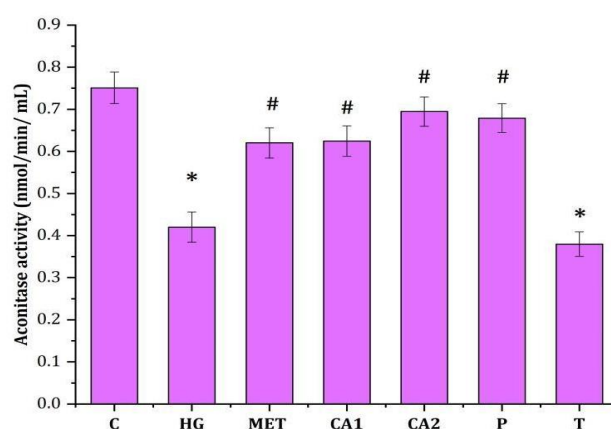
Figure. 4.11. Aconitase activity during hyperglycemia on H9c2 cells. C- Control (5.5 mM glucose), HG-High glucose treated group (33 mM glucose), Met – High glucose treated cells + metformin (1 mM), CA1 – High glucose treated cells + chlorogenic acid (10 µM), CA2 - High glucose treated cells + chlorogenic acid (30 µM), P- High glucose treated cells + phenyl butyrate (100 µM), T - Control cells + thapsigargin (5 µM). Values are expressed as mean ± SEM where n = 6. * $p \leq 0.05$ significantly different from the control group. # $p \leq 0.05$ significantly different from the HG treated group.

4.3.7.2. Effect of CA on mPTP during HG induced ER stress

Integrity of mPTP was analysed by calcein-$CoCl_2$ staining. In control cells calcein fluorescence was much sorted, corresponding to the mitochondrial space and showed punctiform fluorescence. In HG and thapsigargin treated H9c2 cells, a de-compartmentalization of calcein fluorescence was detected, indicating mPTP opening (Figure 4.12). However, CA and metformin treatment cells appeared with punctiform fluorescence. This indicated that CA was effective in retaining the mPTP.
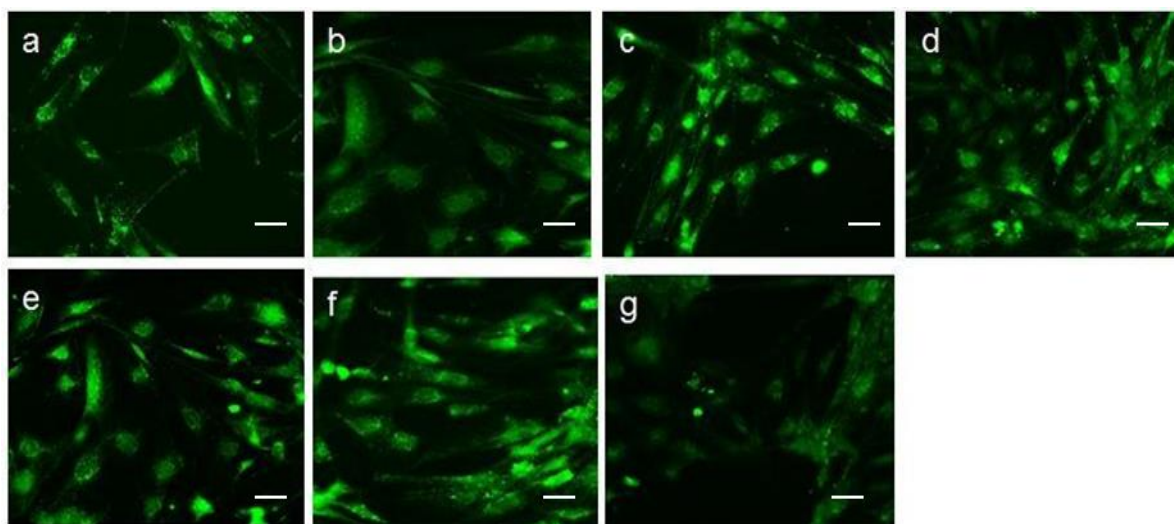
Figure 4.12. Mitochondrial permeability transition pore. Representative fluorescent microscopic images of H9c2 cells stained with calcein-CoCl₂. a) C- Control (5.5 mM glucose),b) HG-High glucose treated group(33 mM glucose), c) Met – High glucose treated cells + metformin (1 mM), d) CA1 –High glucose treated cells + chlorogenic acid (10 μM), e) CA2 - High glucose treated cells + chlorogenic acid (30 μM), P, High glucose treated cells + phenyl butyric acid(1mM) , T, Control (5.5 mM glucose + thapsigargin (5 μM). Scale bar: 50 μm.

4.3.8. Effect of HG induced ER stress mediated apoptosis in H9c2 cardiomyocytes

ER stress apoptotic markers CHOP and caspase 12 levels were also analysed by western blot. There was a significant increase in the expression of CHOP (2.06 fold) and caspase 12 (1.68 fold) in HG treated H9c2 cells compared with control cells (Figure.4.13a). Also HG exposure significantly increased the expression of calnexin (1.23 fold; $p \leq 0.05$; Figure.4.13a) compared with the control group. In addition, I found that caspase 3 activity was markedly upregulated (4.68 fold; Figure.4.13c) in HG treated H9c2 cells. Both concentrations of CA (10 μM and 30 μM) showed the significant reduction in the activity of caspase 3 ($p \leq 0.05$; Figure.4.13c) as well as the expression of CHOP, calnexin and caspase 12 in a dose dependent manner (Figures.4.13a & b; $p \leq 0.05$). Metformin was also found effective in preventing apoptosis by decreasing CHOP (1.05 fold), and caspase 3 activity (1.3 fold) but not calnexin and caspase 12 (Figures.4.13a & b).

a

b

c
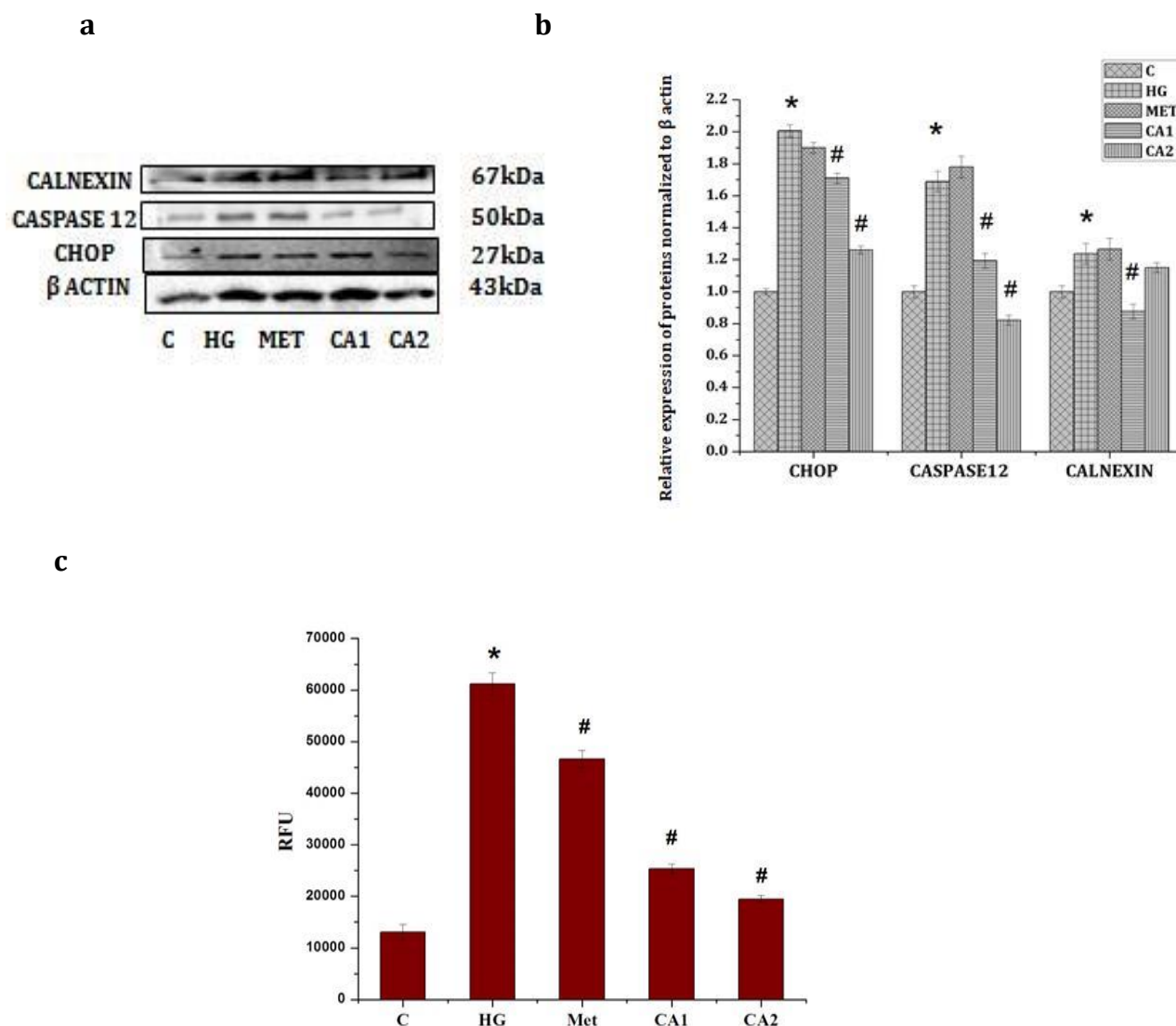
Figure 4.13 . Effect of HG on ER stress mediated apoptosis on H9c2 cells. (a) Western blot analysis of CHOP, calnexin, caspase 12, β-actin. (b) Relative expression of CHOP, calnexin, caspase 12 normalized to β-actin. c) Activity of caspase 3 during hyperglycemia. C- Control (5.5 mM glucose), HG-High glucose treated group (33 mM glucose), Met – High glucose treated cells + metformin (1 mM), CA1 – High glucose treated cells + chlorogenic acid (10 µM), CA2 - High glucose treated cells + chlorogenic acid (30 µM). Values are expressed as mean ± SEM where n = 3 for immunoblot analysis and n=6 for caspase 3 activity. * $p \leq 0.05$ significantly different from the control group. # $p \leq 0.05$ significantly different from the HG treated group.

4.3.9. Effect of HG on autophagy

Autophagosome formation was increased in HG-treated H9c2 cells (1.55 fold; $p \leq$ 0.05; Figures.4.14a & b) compared with control cells, while cotreatment of these cells

with CA of both concentrations 10 µM and 30 µM diminished the fluorescent intensity by 1.16 and 1.34 fold. (p ≤ 0.05). Metformin also reduced the autophagosome formation by 1.2 fold (Figures.4.14a & b).

a
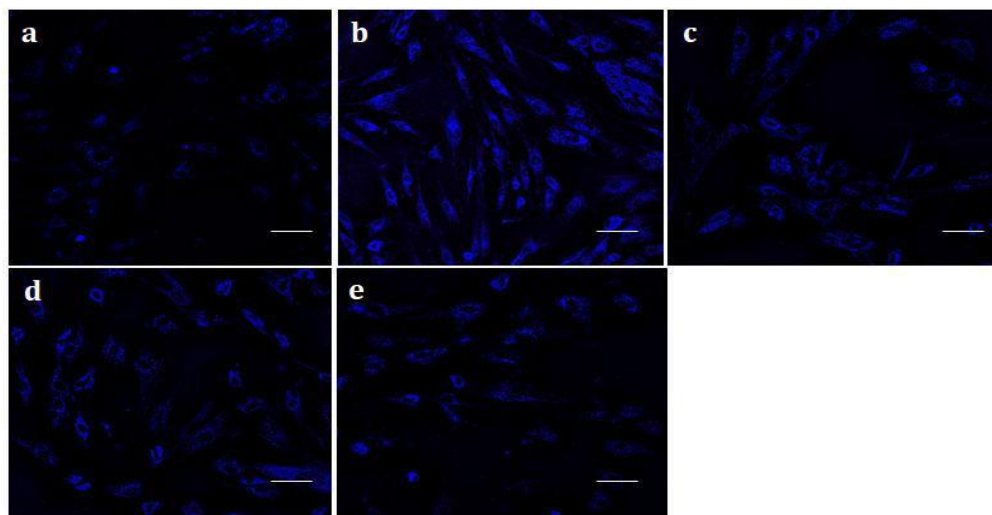
b
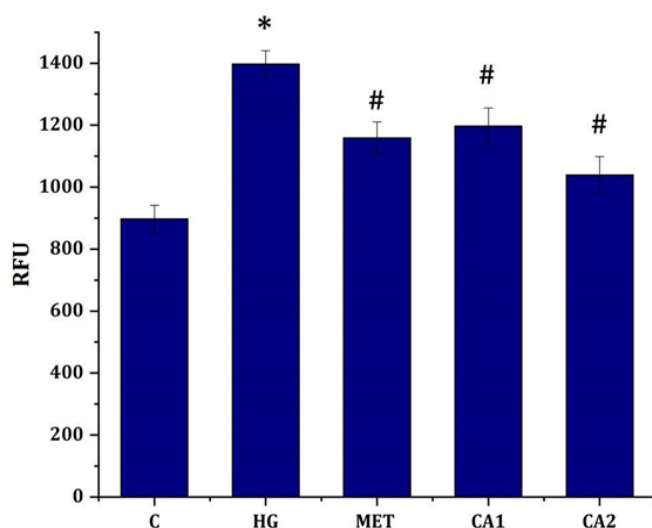
Figure. 4.14. Detection of autophagy in H9c2 cardiomyocytes after HG (33 mM) treatment for 48 h in presence or absence of various concentrations of chlorogenic acid or metformin. **a) Representative microscopic images of autophagosome formation.** (a) Control, (b) high glucose treated group, (c) HG + metformin, (d) HG + chlorogenic acid (10 µM), (e) HG + chlorogenic acid (30 µM). Scale bar corresponds to 50 µm. **b) Relative fluorescent**

intensity of the fluorescent images. C- Control (5.5 mM glucose), HG-High glucose treated group (33 mM glucose), Met – High glucose treated cells + metformin (1 mM), CA1 – High glucose treated cells + chlorogenic acid (10 µM), CA2 - High glucose treated cells + chlorogenic acid (30 µM). Values are expressed as mean ± SEM where n =6 . * p ≤ 0.05 significantly different from the control group. # p ≤ 0.05 significantly different from the HG treated group.

4.3.10. ER-phagy during hyperglycemia

I sought to investigate ER-phagy during hyperglycemia. The SEC62 was found overexpressed in HG treated cells by 1.49 fold (p ≤ 0.05; Figures. 4.15a & b) in a significant manner. Whereas FAM134B was downregulated by 2.58 fold compared to control cells. While cotreatment with CA was found to be effective in regulating the ER-phagy by decreasing the expression of SEC62 (1.20 and 1.28 for 10 µM and 30 µM of CA) and increasing the expression of FAM134B (3.36 and 3.08 fold for 10 µM and 30 µM of CA). Ialso analysed the expression of RTN3 by immunostaining. HG group shows an increased expression of RTN3 (Figure.4.15c). While CA at both concentrations reduced the expression level of RTN3. Metformin was also found effective in reverting the expression of these proteins induced by HG treatment (Figures. 4.15a & c).
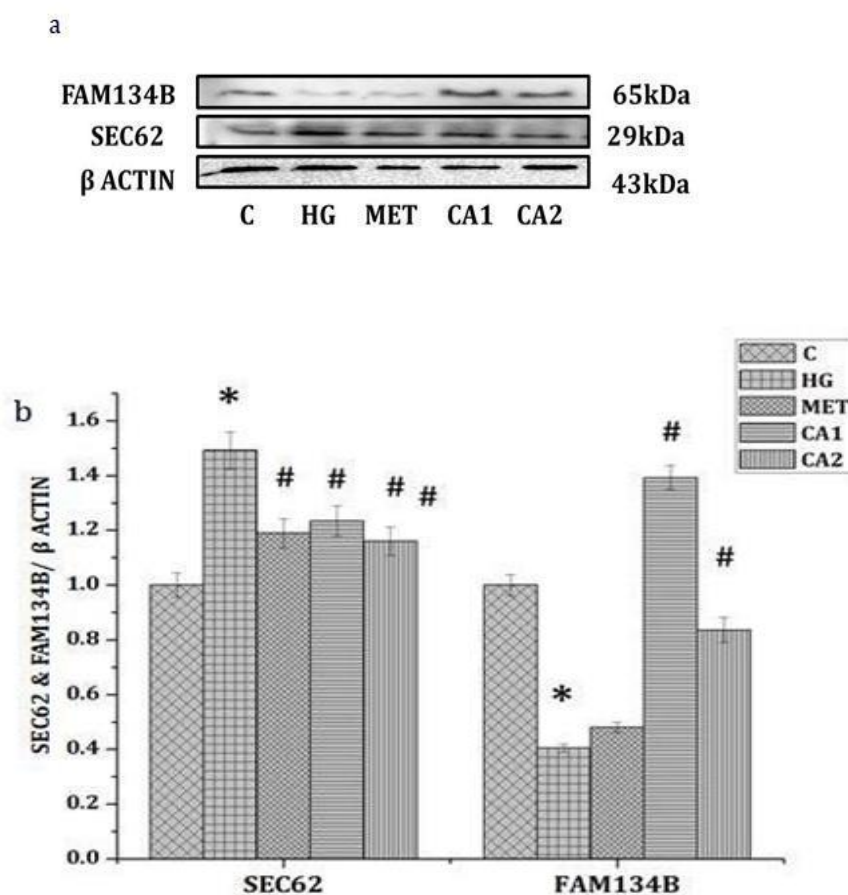
c
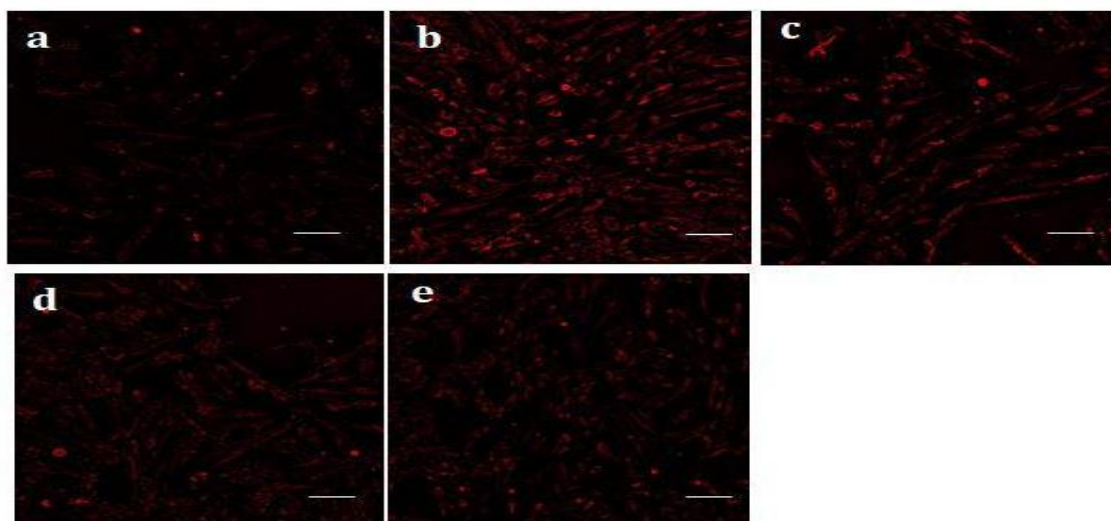
Figure.4.15.ER-phagy during hyperglycemia. a) Immunoblot analysis of SEC62 and FAM134B. b) Densitometry values of SEC62 and FAM14B were normalized to the β-actin. C- Control (5.5 mM glucose), HG-High glucose treated group (33 mM glucose), Met – High glucose treated cells + metformin (1 mM), CA1 – High glucose treated cells + chlorogenic acid (10 μM), CA2 - High glucose treated cells + chlorogenic acid (30 μM). **c) The representative fluorescent images of anti RTN3 in H9c2 cardiomyocytes after HG (33 mM) treatment for 48 h in presence or absence of various concentrations of chlorogenic acid or metformin.** (a) Control, (b) High glucose treated group , (c) HG + metformin, (d) HG + chlorogenic acid (10 μM), (e) HG + chlorogenic acid (30 μM), Scale bar corresponds to 50 μm. Values are expressed as mean ± SEM where n = 3 for western blot and n=6 for immunostaining. * $p \leq 0.05$ significantly different from the control group. # $p \leq 0.05$ significantly different from the HG treated group.

4.4. Discussion

Here further investigations on ER stress mediated pathologies in H9c2 cells treated with HG were evaluated. Earlier reports indicate that unsolved, prolonged ER stress causes severe consequences in cell longevity which may be accompanied with heart disease (Mohan et al., 2019). There are some reports pertaining to the involvement of various pathways of ER in DCM (Jia et al., 2018) but details are not available. Here Ihave conducted detailed investigations on various pathways of ER such as PERK, IRE1α, ATF6α, calcium signaling, role of ER-phagy, apoptosis in DCM. These integrated studies are essential for elucidating the various molecular mechanisms responsible for the genesis of DCM and its association with ER function. In addition,

efficacy of CA was evaluated against ER stress in an *in vitro* model. Here, with the help of molecular and biochemical evidence, I demonstrate that diabetes induces ER stress which is responsible for many pathological changes in the heart. In the previous chapter I observed the surplus generation of oxidative stress during hyperglycemia in H9c2 cells (Rani et al., 2018). There are some reports which exhibit the relation between oxidative stress and ER stress (Cao and Kaufman, 2014). So in this chapter focused on behaviour of various critical proteins involved in ER biology during hyperglycemia and their cross talk with heart function.

The ER is a subcellular organelle which is involved in proteins folding to make them functional. A variety of pathological conditions associated with ER dysfunctions leads to accumulation of unfolded proteins. This activates an evolutionary complex mechanism known as ER stress response or unfolded protein responses (UPR) (Nishitoh, 2012). Chronic ER stress induces UPR and decreases the crucial protein expressions which may be detrimental to cellular functions and even causes cell death (Amen et al., 2019). The UPR is mainly regulated by three molecules namely PERK, IRE1α, ATF6α. All these are residing in the ER membrane and play significant roles in the development of cardiovascular diseases (Mohan et al., 2019). These protein senses unfolded, aggregates and activates downstream signaling pathways.

At first I investigated whether hyperglycemia induces ER stress. This was analysed using a red fluorescent protein which binds to calreticulin sequence. Calreticulin, a Ca^{2+} binding chaperone found in the ER, is noted for its function in the protein folding and quality control. During ER stress, it is overexpressed. Besides, the induction of calreticulin enhanced autophagic flux and stimulated the development of autophagosomes (Yang et al., 2019). Here the result exhibited an increased expression of red fluorescence indicating ER stress in response to high glucose but treatment with CA showed a decreased red fluorescence suggesting that CA was found to be effective in reducing ER stress.

Furthermore, I illustrated the underlying mechanism of ER stress during hyperglycemia. In normal condition, three UPR sensors are bound to a protein, GRP78, ER stress sensor which prevents their stimulation (Shen et al., 2002). However, during ER stress, GRP78 detaches from these chaperone proteins resulting in their activation.

The significant expression of GRP78 protein over baseline expression is considered to be a marker for the presence of cellular ER stress (Ibrahim et al., 2019). Thus expression of GRP78 was found to be higher in patients having heart failure (Okada et al., 2004). Similarly results showed an increased expression of GRP78 in H9c2 cells in response to HG. CA and metformin found to effective in reducing GRP78 expression.

Next, I target the UPR pathways such as PERK, IRE1α and ATF6α pathway. PERK pathway is a well-characterized pathway of the UPR which involves the activation of PERK. This phosphorylates eukaryotic initiation factor 2 α (eIF2α). Phosphorylation of eIF2α attenuates the initiation process of translation and releases the problem of global protein synthesis on the ER (Lu et al., 2004). PERK may also engage in atherosclerosis, cardiac ischemia and arrhythmia (Szegezdi et al., 2009; Liu et al., 2014). Cumulative studies found that PERK inhibitors are beneficial to CVD. Here I observed an elevated expression of PERK during hyperglycemia in *in vitro* model. Here after my attention was on the downstream signaling of the PERK pathway. I found the activation of PERK causes the phosphorylation of eIF2α during hyperglycemia. In addition, previous studies had reported that during ER stress, ATF4 a transcriptional regulator induces the expression of other ER chaperones and various genes that are mainly involved in antioxidant activity and other cellular functions like autophagy (Iurlaro and Muñoz-Pinedo, 2016). Here I also found an increased expression of ATF4 during hyperglycemia in H9c2 cells. Moreover, increased expression of ATF4 has caused cardiomyocyte loss (Freundt et al., 2018). But treatment with CA reduced the expression of proteins involved in the PERK pathway.

I further examined the expression of another UPR pathway, IRE1α, the most evolutionarily conserved arm of the UPR. The IRE1α pathway controls chaperone induction and ER associated degradation in response to ER stress (Lee and Harris, 2012). Upon ER stress, IRE1α auto phosphorylates and activates the JNK pathway by recruiting TRAF2 (Sisinni et al., 2019). Partial inhibition of IRE1α arm plays an important role in electrical remodelling (Liu and Dudley, 2019). Also reports demonstrate that IRE1α modulation thwarts metaflammation and relieves development of atherosclerosis (Tufanli et al., 2017). Furthermore, auto phosphorylation of IRE1 activates a novel ribonuclease activity which splices and activates XBP1 mRNA (Yoshida et al., 2001). Similar to earlier reports, here also IRE1α–

TRAF2 interaction was found enhanced and led to activation of JNK at HG conditions. Over-expression of XBP1 at mRNA levels was also increased on HG treatment with cardiomyocytes. CA ameliorates IRE1α pathway.

I also analysed ATF6α, which is the third pathway of UPR. ATF6α is an ER transmembrane protein which is relocated to the Golgi complex after dissociating from GRP78 under ER stress (Shen et al., 2002). It is processed by proteases and becomes active. Once activated it translocates to the nucleus and functions as a transcription factor that controls the expression of genes or promoter for ER stress response elements such as GRP78, PDI,etc (Amen et al., 2019). Several studies have reported that ATF6α activity was increased during myocardial infarction (Toko et al., 2010). The data showed that activation of ATF6α occurs in response with hyperglycemia in HG treated H9c2 cells. From my findings it was noted that all the three UPR pathways PERK, IRE1α, and ATF6α, were activated during hyperglycemia. At the same time, CA reduces the expression of proteins involved in the three UPR pathways and thereby suppresses the UPR pathway. This may be one of the mechanisms that attenuate ER stress.

Thereafter I studied the effect of hyperglycemia on protein folding by analysing two important markers, ERO1α (endoplasmic reticulum oxireductin1 α) and PDI (protein disulfide isomerase). ERO1α and PDI are major electron flow pathways that catalyze oxidative folding of secretory proteins. During prolonged ER stress, ATF4 activates genes involved in protein synthesis, such as GADD34 and ERO1α; ERO1α, which mainly controls in the oxidation of PDI and leads to hyper-oxidation in ER (Martucciello, 2020). Here I found an overexpression of ERO1α in HG condition. There are numerous reports which showed the CVDs diseases. Moreover, diabetes causes a rise of reduced PDI in the heart, which may further lead to improper folding of the proteins (Toldo et al., 2011). In contrast my data showed that PDI was found to be overexpressed during hyperglycemia. This indicates the occurrence of hyperoxidation during hyperglycemia. This hyperoxidation in the ER causes disturbances in the storage of calcium. CA was found to decrease the expression of ERO1α and PDI and thus attenuates hyperoxidation during hyperglycemia in H9c2 cells.

I also investigated the effect of ER stress on calcium homeostasis during hyperglycemia.Calcium have significant role in the function of cardiac myocyte biology

and ER is the main organelle for the storage of calcium ions, so special attention was given to proteins relevant to Ca^{2+} homeostasis. The movement of Ca^{2+} ions in and out from the cells and organelles has to be maintained in balance for the proper functioning of cells. Cell death may occur if cells have increased concentrations of Ca^{2+} for a longer period of time (Pinton and Rizzuto, 2006). So for the proper maintenance of calcium homeostasis, there are a number of Ca^{2+} transporters, Ca^{2+} channels and exchangers. Abnormal regulation of calcium ions may impair the pumping function of the heart. Recently reports have suggested that increased ERO1α and CHOP expression induces the release of calcium ions from ER through the IP3R channel (Li et al., 2009). This causes an increase in the cytoplasmic Ca^{2+} which in turn activates CaMKII (Sano and Reed, 2013). An increased intracellular calcium overload was observed during hyperglycemia. In addition during heart failure CaMKII overactivity is found to be increased and also several studies found that CaMKII as one of the vital pro-arrhythmic factors (Swaminathan et al., 2012). I found an enhanced expression of CaMKII in response to HG. Then the activated CaMKII phosphorylates another important cardiac channel ryanodine receptor (RyR2). RyR2 is the major mediator which releases stored calcium from SR and mainly controls the Ca^{2+}-transient amplitude, which is associated with the power of systolic contraction. The cardiac ryanodine receptor is known for its active involvement in the pathogenesis of cardiac disease. An increased RyR2-mediated Ca^{2+} leak from SR have been found in heart failure patients (Bers, 2002). Here also I observed a similar pattern of enhanced expression of RYR2 in HG treated cardiomyocytes. For further investigation of study I also investigated NCX1, Na^+/Ca^{2+} exchanger1 another important key protein in the regulation of calcium homeostasis and found upregulation of the same. CaMKII-dependent RyR2 phosphorylation can activate the sarcolemmal NCX1, which extrudes Ca^{2+} from the cell and maintains calcium homeostasis in the heart (Dibb et al., 2007). Several studies reported that elevated intracellular sodium in myocytes from diabetic hearts which inturn increases NCX1-mediated Ca^{2+} influx and reduces extrusion (Doliba et al., 2000). Numerous studies suggests that sarcoplasmic reticulum Ca ATPase (SERCA2a), whose protein expression is decreased in heart failure (Salin et al., 2019). The reduced expression of SERCA2a during hyperglycemia indicates the inhibition of calcium flow from cytosol to sarcoplasmic reticulum (SR) and thereby restores the intracellular calcium content. From findings I concluded that hyperglycemia causes reduced ER Ca^{2+} load that could

arise from enhanced activity of NCX1, reduced SERCA2a function, and increased cytosolic ER Ca^{2+} leak *via* RyR2.

Regulation of Ca^{2+} signaling is a central mechanism that connects ER mitochondria interactions. Besides, redox imbalances in the ER have ramifications within the mitochondria. The current information suggest that a strong or prolonged influx of calcium ions into mitochondria may lead to the development and opening of a large high conductivity pore on the inner mitochondrial membrane called mitochondrial permeability transition pore, a channel or uniporter powered by a large electrochemical gradient and is crucial for inner mitochondrial membrane stability (Malhotra and Kaufman, 2011). The most active inducers of permeability transition are mitochondrial calcium overload and cellular redox status. Moreover, there is evidence that mPTP plays an important role in the pathogenesis of a variety of cardiac disorders. During hyperglycemia, there is an alteration in the transition pore. Perhaps, the reduced activity of aconitase supports the involvement of ER stress mediated mitochondrial damage. CA and metformin administration was found to be effective in reducing mitochondrial dysfunction.

UPR takes part in both pro-surviving as well as proapoptotic pathways and the switching from prosurvival to proapoptotic or vice versa is yet to be unravelled. Here Ialso examined the mechanism of cell death induced by ER stress with HG. I found that HG induces apoptotic cell death in association with non-stop activation of UPR in H9c2 cells. Cell death was mainly modulated by a wide range of essentials like intracellular calcium overload that regulate ER Ca^{2+} stores (Pinton et al., 2008). Calnexin, the calcium binding ER chaperone plays a vital role in Ca^{2+} regulation, phagocytosis, and cell sensitivity to apoptosis in the ER. Upregulation of calnexin has been shown to be a noble indicator of cell sensitivity to ER stress-mediated cell death (Guérin et al., 2008). Increased expression of calnexin was found in H9c2 cells treated with glucose. Also I investigated whether hyperglycemia affects the expression of CHOP, a crucial player in ER stress-mediated apoptosis. Over expression of CHOP was observed in diabetic hearts. In addition I also checked various caspase proteins. Among different caspases, caspase 12, is a very important protease and is bound to the ER membrane and is activated during ER stress (Berchtold et al., 2016). In fact, Ca^{2+} released from the ER may activate calpain, which cleaves caspase-12 during the ER stress or in response to the

mobilization of intracellular Ca^{2+} stores (Pinton et al., 2008). Activated caspase-12 acts on downstream caspases to trigger apoptosis. The level of caspase 12 as well as caspase 3 was significantly increased upon treatment with HG. CA ameliorates ER stress mediated apoptosis by reducing the expression of CHOP, caspase 12, calnexin and caspase 3 activity.

Autophagy and ER stress are mechanistically connected with the UPR, stimulating autophagy. The precise mechanism of ER stress and autophagy, however, is still unknown. The understanding of how the UPR interacts with autophagy will aid in the development of new therapies for a variety of diseases. Autophagy is assumed to be a two-edged sword in the pathogenesis of cardiac disorders, behaving either protectively or maladaptively based on the situation (Sciarretta et al., 2018). So autophagy emerges as a potential target in the sense of pharmacological relevance. Various studies have shown the significant increase of autophagosomes in the ischemic heart. Besides, the cytosolic Ca^{2+} signal regulates protein intricate in several stages of autophagosome development, which is well established (Kondratsky et al., 2013). I observed more numbers of autophagosomes in the cardiomyocyte in response to HG.

Based on this, detailed study was conducted on ER-phagy, a selective autophagy, lysosomal degradation of the ER. Deterioration of damaged / old ER by ER-phagy is very much essential for ER homeostasis (Schuck et al., 2014). ER-phagy assures the prompt and precise elimination of unsought cellular components mainly lipids and misfolded proteins and also leads to turnover of ER by procuring the autophagy machinery to the precise point of the ER (Grumati et al., 2018). ER-phagy is regulated by four receptors namely SEC62, FAM134B, RTN3 and CCPG1. SEC62 is a transmembrane protein found in the ER, a component of the translocon complex that mainly regulates the protein import in the ER especially in mammalian cells. The main role is to conciliate macro ER-phagy during cell recovery from ER stress response and furnish ER constituents to the auto lysosomal system for ER-phagy (Fumagalli et al., 2016). Here I found there is an increased expression of SEC62 during hyperglycemia. FAM134B or reticulophagy regulator1, another ER-phagy receptor is mainly found in the sheets of ER and targets for degradation. Loss of function of FAM134B is accompanied with many disorders and diseases (Bhaskara et al., 2019). During hyperglycemia I found a downregulation of FAM134B. Another ER-phagy receptor located in the ER tubules is

RTN3, which is involved in the degradation of tubules. An increase in the local concentration of RTN3 induces dissolution of ER tubules and their subsequent lysosomal degradation occurs in an autophagy-dependent manner. An increased expression of RTN3 was found in HG treated H9c2 cells. From results I observed that ER-phagy was found to be activated during HG conditions. Altered UPR response and calcium homeostasis are expected to contribute to the induction of ER-phagy. Herein I suggest that ER-phagy is involved in the DCM, which has never been reported earlier. More studies on ER-phagy are yet to be unraveled.

From overall results it demonstrated that CA is found effective in controlling ER stress by regulating UPR pathways namely PERK, IRE1α, and ATF6α. In this study, all the pharmacological activities reported above may contribute indirectly to the beneficial effects exhibited by CA. Moreover, I also found that CA not only regulates UPR pathway, but also maintains Ca^{2+} homeostasis by regulating different Ca^{2+} channels like RYR2, NCX1, SERCA2a. In addition, it also reverses ER-phagy and eventually suppresses ER stress induced apoptosis.

The salient findings of this study revealed that ER stress has a significant role in calcium homeostasis, mitochondrial function, ER-phagy regulation and apoptosis during hyperglycemia. Intriguingly CA attenuated or mitigated the ER stress, intracellular calcium anomalies, lessened mPTP opening, restored aconitase activity, reduced ER-phagy and apoptosis during hyperglycemia in H9c2 cells. Furthermore, *in vivo* study is needed for the confirmation of beneficial effects of CA against diabetes induced heart problems.

References

1. Amen OM, Sarker SD, Ghildyal R, Arya A. Endoplasmic Reticulum Stress Activates Unfolded Protein Response Signaling and Mediates Inflammation, Obesity, and Cardiac Dysfunction: Therapeutic and Molecular Approach. *Front Pharmacol*. 2019;10:977. doi:10.3389/fphar.2019.00977.

2. Berchtold LA, Prause M, Størling J, Mandrup-Poulsen T. Cytokines and Pancreatic β-Cell Apoptosis. *Adv Clin Chem*. 2016;75:99-158. doi:10.1016/bs.acc.2016.02.001.

3. Bernales S, Schuck S, Walter P. ER-phagy: selective autophagy of the endoplasmic reticulum. *Autophagy*. 2007;3(3):285-287. doi:10.4161/auto.3930.

4. Bers DM. Cardiac excitation-contraction coupling. *Nature*. 2002;415(6868):198-205. doi:10.1038/415198a.

5. Bhaskara RM, Grumati P, Garcia-Pardo J, et al. Curvature induction and membrane remodeling by FAM134B reticulon homology domain assist selective ER-phagy. *Nat Commun*. 2019;10(1):2370. doi:10.1038/s41467-019-10345-3.

6. Cao SS, Kaufman RJ. Endoplasmic reticulum stress and oxidative stress in cell fate decision and human disease. *Antioxid Redox Signal*. 2014;21(3):396-413. doi:10.1089/ars.2014.5851.

7. Dibb KM, Graham HK, Venetucci LA, Eisner DA, Trafford AW. Analysis of cellular calcium fluxes in cardiac muscle to understand calcium homeostasis in the heart. *Cell Calcium*. 2007;42(4-5):503-512. doi:10.1016/j.ceca.2007.04.002.

8. Dikic I. Open questions: why should we care about ER-phagy and ER remodelling?. *BMC Biol*. 2018;16(1):131. doi:10.1186/s12915-018-0603-7.

9. Dobrin JS, Lebeche D. Diabetic cardiomyopathy: signaling defects and therapeutic approaches. *Expert Rev Cardiovasc Ther*. 2010;8(3):373-391. doi:10.1586/erc.10.17.

10. Doliba NM, Babsky AM, Wehrli SL, Ivanics TM, Friedman MF, Osbakken MD. Metabolic control of sodium transport in streptozotocin-induced diabetic rat hearts. *Biochemistry (Mosc)*. 2000;65(4):502-508.

11. Freundt JK, Frommeyer G, Wötzel F, et al. The Transcription Factor ATF4 Promotes Expression of Cell Stress Genes and Cardiomyocyte Death in a Cellular Model of Atrial Fibrillation. *Biomed Res Int*. 2018;2018:3694362. doi:10.1155/2018/3694362.

12. Fumagalli F, Noack J, Bergmann TJ, et al. Translocon component Sec62 acts in endoplasmic reticulum turnover during stress recovery [published correction appears in Nat Cell Biol. 2016 Dec 23;19(1):76]. *Nat Cell Biol*. 2016;18(11):1173-1184. doi:10.1038/ncb3423.

13. Gordaliza-Alaguero I, Cantó C, Zorzano A. Metabolic implications of organelle-mitochondria communication. *EMBO Rep*. 2019; 20(9):e47928. doi:10.15252/embr.201947928.

14. Grootjans J, Kaser A, Kaufman RJ, Blumberg RS. The unfolded protein response in immunity and inflammation. *Nat Rev Immunol*. 2016;16(8):469-484. doi:10.1038/nri.2016.62.

15. Grumati P, Dikic I, Stolz A. ER-phagy at a glance. *J Cell Sci*. 2018;131(17):jcs217364. doi:10.1242/jcs.217364.

16. Guérin R, Arseneault G, Dumont S, Rokeach LA. Calnexin is involved in apoptosis induced by endoplasmic reticulum stress in the fission yeast. *Mol Biol Cell*. 2008;19(10):4404-4420. doi:10.1091/mbc.e08-02-0188.

17. Ibrahim IM, Abdelmalek DH, Elfiky AA. GRP78: A cell's response to stress. *Life Sci*. 2019;226:156-163. doi:10.1016/j.lfs.2019.04.022.

18. Iurlaro R, Muñoz-Pinedo C. Cell death induced by endoplasmic reticulum stress. *FEBS J*. 2016;283(14):2640-2652. doi:10.1111/febs.13598.

19. Jia G, Hill MA, Sowers JR. Diabetic Cardiomyopathy: An Update of Mechanisms Contributing to This Clinical Entity. *Circ Res*. 2018;122(4):624-638. doi:10.1161/CIRCRESAHA.117.311586.

20. Kondratskyi A, Yassine M, Kondratska K, Skryma R, Slomianny C, Prevarskaya N. Calcium-permeable ion channels in control of autophagy and cancer. *Front Physiol*. 2013;4:272. doi:10.3389/fphys.2013.00272.

21. Lee KU, Harris RA. Mitochondria and endoplasmic reticulum in diabetes and its complications. *Exp Diabetes Res*. 2012;2012:985075. doi:10.1155/2012/985075.

22. Li G, Mongillo M, Chin KT, et al. Role of ERO1-alpha-mediated stimulation of inositol 1,4,5-triphosphate receptor activity in endoplasmic reticulum stress-induced apoptosis. *J Cell Biol*. 2009;186(6):783-792. doi:10.1083/jcb.200904060.

23. Liu M, Dudley SC Jr. The role of the unfolded protein response in arrhythmias. *Channels (Austin)*. 2018;12(1):335-345. doi:10.1080/19336950.2018.1516985.

24. Liu Z, Cai H, Zhu H, et al. Protein kinase RNA-like endoplasmic reticulum kinase (PERK)/calcineurin signaling is a novel pathway regulating intracellular calcium accumulation which might be involved in ventricular arrhythmias in diabetic cardiomyopathy. *Cell Signal*. 2014;26(12):2591-2600. doi:10.1016/j.cellsig.2014.08.015.

25. Lu PD, Jousse C, Marciniak SJ, et al. Cytoprotection by pre-emptive conditional phosphorylation of translation initiation factor 2. *EMBO J*. 2004;23(1):169-179. doi:10.1038/sj.emboj.7600030.

26. Malhotra JD, Kaufman RJ. ER stress and its functional link to mitochondria: role in cell survival and death. *Cold Spring Harb Perspect Biol*. 2011;3(9):a004424. doi:10.1101/cshperspect.a004424.

27. Martucciello S, Masullo M, Cerulli A, Piacente S. Natural Products Targeting ER Stress, and the Functional Link to Mitochondria. *Int J Mol Sci*. 2020; 21(6):1905. doi:10.3390/ijms21061905.

28. Mohan S, R PRM, Brown L, Ayyappan P, G RK. Endoplasmic reticulum stress: A master regulator of metabolic syndrome. *Eur J Pharmacol*. 2019;860:172553. doi:10.1016/j.ejphar.2019.172553.

29. Mollereau B, Manié S, Napoletano F. Getting the better of ER stress. *J Cell Commun Signal*. 2014;8(4):311-321. doi:10.1007/s12079-014-0251-9.

30. Nishitoh H. CHOP is a multifunctional transcription factor in the ER stress response. *J Biochem*. 2012;151(3):217-219. doi:10.1093/jb/mvr143.

31. Okada K, Minamino T, Tsukamoto Y, et al. Prolonged endoplasmic reticulum stress in hypertrophic and failing heart after aortic constriction: possible contribution of endoplasmic reticulum stress to cardiac myocyte apoptosis. *Circulation*. 2004; 110(6):705-712.

32. Pinton P, Giorgi C, Siviero R, Zecchini E, Rizzuto R. Calcium and apoptosis: ER-mitochondria Ca2+ transfer in the control of apoptosis. *Oncogene*. 2008; 27(50):6407-6418. doi:10.1038/onc.2008.308.

33. Pinton P, Rizzuto R. Bcl-2 and Ca2+ homeostasis in the endoplasmic reticulum. *Cell Death Differ*. 2006; 13(8):1409-1418. doi:10.1038/s j.cdd.4401960.

34. Preetha Rani MR, Anupama N, Sreelekshmi M, Raghu KG. Chlorogenic acid attenuates glucotoxicity in H9c2 cells via inhibition of glycation and PKC α upregulation and safeguarding innate antioxidant status [published correction appears in Biomed Pharmacother. 2021 Jan;133:111071]. *Biomed Pharmacother*. 2018; 100:467-477. doi:10.1016/j.biopha.2018.02.027.

35. Rao RV, Bredesen DE. Misfolded proteins, endoplasmic reticulum stress and neurodegeneration. *Curr Opin Cell Biol*. 2004;16(6):653-662. doi:10.1016/ j.ceb.2004.09.012.

36. Salin Raj P, Swapna SUS, Raghu KG. High glucose induced calcium overload via impairment of SERCA/PLN pathway and mitochondrial dysfunction leads to

oxidative stress in H9c2 cells and amelioration with ferulic acid. *Fundam Clin Pharmacol*. 2019;33(4):412-425. doi:10.1111/fcp.12452.

37. Sano R, Reed JC. ER stress-induced cell death mechanisms. *Biochim Biophys Acta*. 2013;1833(12):3460-3470. doi:10.1016/j.bbamcr.2013.06.028.

38. Schuck S, Gallagher CM, Walter P. ER-phagy mediates selective degradation of endoplasmic reticulum independently of the core autophagy machinery. *J Cell Sci*. 2014;127(Pt 18):4078-4088. doi:10.1242/jcs.154716.

39. Sciarretta S, Maejima Y, Zablocki D, Sadoshima J. The Role of Autophagy in the Heart. *Annu Rev Physiol*. 2018;80:1-26. doi:10.1146/annurev-physiol-021317-121427.

40. Shen J, Chen X, Hendershot L, Prywes R. ER stress regulation of ATF6 localization by dissociation of BiP/GRP78 binding and unmasking of Golgi localization signals. *Dev Cell*. 2002;3(1):99-111. doi:10.1016/s1534-5807(02)00203-4.

41. Sisinni L, Pietrafesa M, Lepore S, et al. Endoplasmic Reticulum Stress and Unfolded Protein Response in Breast Cancer: The Balance between Apoptosis and Autophagy and Its Role in Drug Resistance. *Int J Mol Sci*. 2019;20(4):857. doi:10.3390/ijms20040857.

42. Siwecka N, Rozpędek W, Pytel D, et al. Dual role of Endoplasmic Reticulum Stress-Mediated Unfolded Protein Response Signaling Pathway in Carcinogenesis. *Int J Mol Sci*. 2019;20(18):4354. doi:10.3390/ijms20184354.

43. Sutanto H and Heijman J (2019) The Role of Calcium in the Human Heart: With Great Power Comes Great Responsibility. Front. Young Minds. 7:65. doi: 10.3389/frym.2019.00065.

44. Swaminathan PD, Purohit A, Hund TJ, Anderson ME. Calmodulin-dependent protein kinase II: linking heart failure and arrhythmias. *Circ Res*. 2012;110(12):1661-1677. doi:10.1161/CIRCRESAHA.111.243956.

45. Szegezdi E, Macdonald DC, Ní Chonghaile T, Gupta S, Samali A. Bcl-2 family on guard at the ER. *Am J Physiol Cell Physiol*. 2009;296(5):C941-C953. doi:10.1152/ajpcell.00612.2008.

46. Takuma K, Yan SS, Stern DM, Yamada K. Mitochondrial dysfunction, endoplasmic reticulum stress, and apoptosis in Alzheimer's disease. *J Pharmacol Sci*. 2005;97(3):312-316. doi:10.1254/jphs.cpj04006x.

47. Toko H, Takahashi H, Kayama Y, et al. ATF6 is important under both pathological and physiological states in the heart. *J Mol Cell Cardiol*. 2010;49(1):113-120. doi:10.1016/j.yjmcc.2010.03.020.

48. Toldo S, Boccellino M, Rinaldi B, et al. Altered oxido-reductive state in the diabetic heart: loss of cardioprotection due to protein disulfide isomerase. *Mol Med*. 2011;17(9-10):1012-1021. doi:10.2119/molmed.2011.00100.

49. Toth A, Nickson P, Mandl A, Bannister ML, Toth K, Erhardt P. Endoplasmic reticulum stress as a novel therapeutic target in heart diseases. *Cardiovasc Hematol Disord Drug Targets*. 2007;7(3):205-218. doi:10.2174/187152907781745260.

50. Tufanli O, Telkoparan Akillilar P, Acosta-Alvear D, et al. Targeting IRE1 with small molecules counteracts progression of atherosclerosis. *Proc Natl Acad Sci U S A*. 2017;114(8):E1395-E1404. doi:10.1073/pnas.1621188114.

51. Yang L, Zhao D, Ren J, Yang J. Endoplasmic reticulum stress and protein quality control in diabetic cardiomyopathy. *Biochim Biophys Acta*. 2015;1852(2):209-218. doi:10.101 6/j.bbadis.2014.05.006.

52. Yang Y, Ma F, Liu Z, et al. The ER-localized Ca^{2+}-binding protein calreticulin couples ER stress to autophagy by associating with microtubule-associated protein 1A/1B light chain 3. *J Biol Chem*. 2019;294(3):772-782. doi:10.1074/jbc.RA118.005166.

53. Yoshida H, Matsui T, Yamamoto A, Okada T, Mori K. XBP1 mRNA is induced by ATF6 and spliced by IRE1 in response to ER stress to produce a highly active transcription factor. *Cell*. 2001;107(7):881-891. doi:10.1016/s0092-8674(01)00611-0.

Investigation on ER stress during diabetic cardiomyopathy and possible amelioration with chlorogenic acid: an *in vivo* study

5.1. Introduction

ER stress and UPR in the heart are associated with DCM. To alleviate the effects of ER stress in diabetic cardiovascular complications, further clinical trials, and related pathological models are required. In the previous chapters, the role of ER stress as well as associated pathways like oxidative stress, calcium homeostasis, ER-phagy and apoptosis were elucidated and also possible protective effect of CA against hyperglycemia induced complications in H9c2 cells was seen. The results showed CA exhibits significant protection against hyperglycemia induced molecular alterations by modulating redox machinery of the cells through ameliorating oxidative stress, glycation and PKC α- ERK axis. CA also offered protection through the UPR pathway. Also, it was found to regulate calcium homeostasis by modulating CaMKII. In addition, CA treatment provided protection against ER stress induced apoptosis in H9c2 cells. CA was found to reduce the ER-phagy. In order to validate the *in vitro* results, I conducted *in vivo* experiments in rats using diet induced DCM model.

5.2. Methods

5.2.1 Experimental animal

Male wistar rats (weighing 190 - 220 g) were used for the experiment. Rats were obtained from Kerala Veterinary College, Mannuthy (Kerala, India). All procedures involving animals were conducted in strict accordance with the protocols and guidelines approved by the Animal Ethics Committee of Jubilee Mission Medical College and Research Institute (IAEC No. JMMC&RI/SARF/IAEC/RP-02/2017). Animals were housed in polypropylene cages and were kept in an environment with controlled temperature (22 ± 2°C), humidity (55-60%) and photoperiod (12:12h) of light - dark cycle and fed a standard diet supplied and given water *ad libitum*.

5.2.2. Experimental design

After two weeks of acclimatization, the rats were randomly divided into the two groups: (1) control group; (2) diabetic model group. The control group (n=12) were fed a normal rat chow throughout the experimental period and the diabetic model group (n=33) were fed with a diabetogenic diet (high fat high fructose diet) for 60 days. The composition of diet is given in Table.5. 1.

Table 5.1. Composition of diabetogenic diet

Diet component	Composition percentage (%)
Carbohydrate	46.5
Fat (Lard)	25.7
Protein	18.6
Total Calorie	4.9 kCa/g

After 60 days the rats in diabetic model group were given a single dose intraperitoneal injection of 25 mg/kg STZ in a citrate buffer (Sigma, USA); and the rats in the control group received normal saline by means of intraperitoneal injection. On day 3 after STZ injection, tail blood glucose was measured using the Accu-chek glucometer (LifeScan, USA). The animals with blood glucose (fasting) above 300 mg/dL were considered as diabetic for the present study and grouped into various experimental groups and continued in a diabetogenic diet for another 60 days. On the 121st day these diabetic animals were again divided into different groups and the experiments were continued for 60 days. The animals under these groups received test material CA - 5 &10 mg/kg bwt, and metformin (50 mg/kg bwt) through oral gavage for another 60 days. Vehicle (normal saline) was administered to the control and diabetic groups. Finally, rats were divided into seven groups and each contains 6 animals and details are given below:

Group 1- N, Control (Normal diet for 180 days)

Group 2- HFFD, high fat, high fructose diet for 180 days with a single dose of STZ

Group 3- MET, high fat, high fructose diet for 180 days with a single dose of STZ + metformin (50 mg/kg bwt from 121st day to 180th day)

Group 4- CA5, high fat, high fructose diet for 180 days with a single dose of STZ + CA5 (5 mg/kg bwt from 121st day to 180th day)

Group 5- CA10, high fat, high fructose diet for 180 days with a single dose of STZ + CA10 (10 mg/kg bwt from 121st day to 180th day)

Group 6- NCA10, Normal diet + CA (10 mg/kg bwt) (to check toxicity of CA)

Group 7- HD, High fat high fructose diet for 180 days

Duration of the entire study was 180 days (6 months). Food and water intake were determined daily; body weight was checked weekly. The fasting blood glucose was monitored weekly by tail tip prick using glucose strips. For sacrifice, rats were fasted overnight, and inhaled carbon dioxide gas. The hearts were immediately harvested and snapped frozen in liquid nitrogen for biochemical analyses and serum was separated from blood taken from cardiac puncture under isoflurane (30 % isoflurane and 70 % propylene glycol) inhalation, and stored in -80 °C for further experiments.

5. 3. Parameters studied

Studies carried out in this chapter include the following and details of procedure are given in chapter 2:

- ✓ Blood glucose, glycated haemoglobin, serum AGE levels (refer 2.2.28, 2.2.29 2.2.30)
- ✓ Insulin level and HOMA-IR (refer 2.2.31 and 2.2.32)
- ✓ Analysis of lipid profile (TG, total cholesterol, LDL, HDL, refer 2.2.35, 2.2.36, 2.2.37, 2.2.38)
- ✓ Lactate dehydrogenase, creatine kinase- isoenzyme of myocardial Specificity (CK-MB), C - reactive protein (CRP), Serum glutamate oxaloacetic Transaminase (SGOT) (refer 2.2.39, 2.2.40, 2.2.41, 2.2.42)
- ✓ HMI, SOD activity, TBARS (refer 2.2.33, 2.2.43, 2.2.44)
- ✓ Cardiac injury markers ANP, BNP, HFABP, troponin by ELISA and western blot (refer 2.2.34 and 2.2.45)
- ✓ Fetuin A and copeptin by immunoblot analysis (refer 2.2.45)
- ✓ ER stress markers by western blot analysis (refer 2.2.45)
- ✓ Histopathology of heart (refer 2.2.46)

5.4. Results

5.4.1. Induction of DCM in rats

High fat high fructose diet and low dose (25 mg/kg bwt) streptozotocin (STZ) developed classical symptoms of diabetes, including polyuria, polydipsia, and hyperglycemia. Herein the ER stress markers as well as the effect of CA on metabolic parameters relevant to diabetes induced cardiac complications have been assessed.
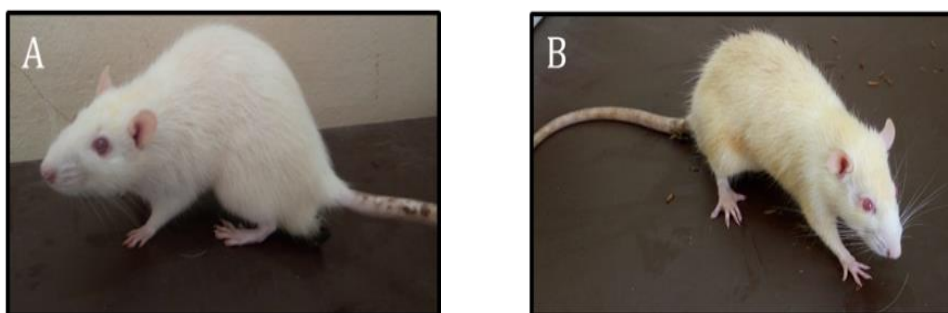
Figure.5.1. Photograph of experimental rats at the end of the experiment. A) N- Control group (Normal diet). B) HFFD- High fat and fructose diet group/ STZ

5.4.2. Effect of CA on fasting blood glucose and glycated haemoglobin

The blood glucose level of HFFD rats reached 505 mg/dL after 180 days whereas blood glucose of control rats was ranging from 80 to 90 mg/dL. Administration of CA and metformin significantly reduced blood glucose level in comparison to HFFD groups (Figure 5.2a.). HbA1c levels were significantly increased in the diabetic rats (5.61 fold) compared to the control group. However a significant improvement in HbA1c levels was observed with both doses of CA (CA5 for 3.41 and CA10 for 3.02 fold) and metformin (4.04 fold) groups compared to HFFD rats (Figure 5.2b). High fat high fructose diet alone group and toxicity group of CA (blood glucose ranges from 80 to 90 mg/dL) does not show any significant changes.

a
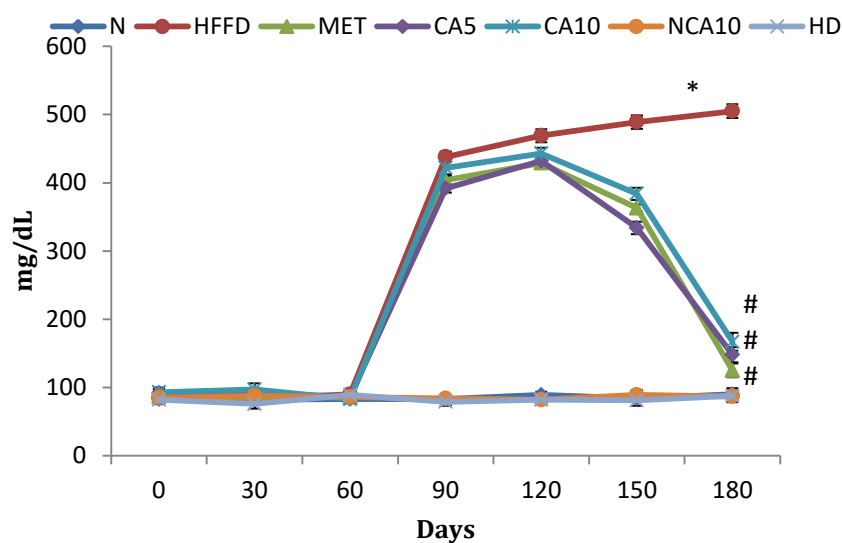
b
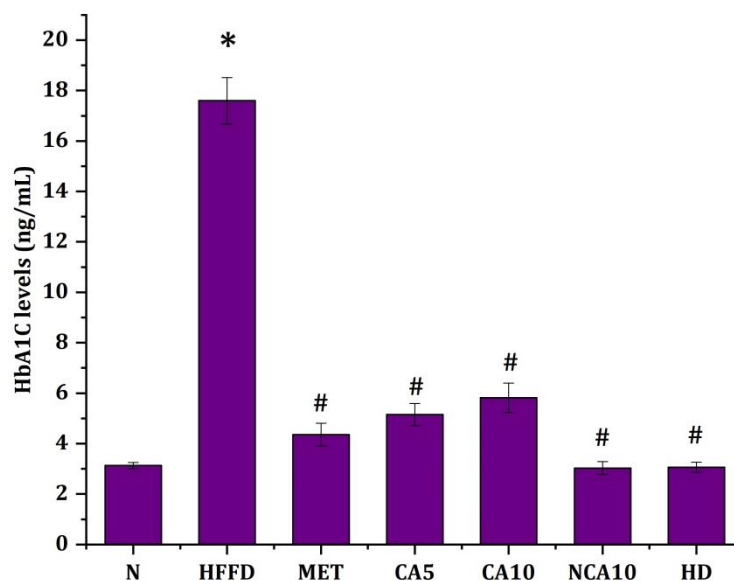
Figure.5.2. Effect of CA on glucose tolerance. a) The glycemic response curve. b) HbA1c levels. N - Control group (Normal diet); HFFD - High fat and fructose diet group/ STZ; MET - High fat and fructose diet group/ STZ with metformin 50 mg/kg bwt , CA5 - High fat and fructose diet group/ STZ with CA 5 mg/kg bwt; CA10 - High fat and fructose diet group/ STZ with CA 10 mg/kg bwt; NC10- Normal diet with CA 10 mg/kg; HD- High fat and fructose diet group . Results are expressed as mean ± SEM where n = 6. * $p \leq 0.05$ significantly different from the control group. # $p \leq 0.05$ significantly different from HFFD group.

5.4.3. Production of AGE in DCM

There was a significant increase of AGE products (1.35 fold, p ≤ 0.05) in the serum of the HFFD group compared to control rats (Figure.5.3.). While CA treatment significantly decreased the AGE levels (1.18 and 1.12 fold for CA5 and CA10 respectively) compared to HFFD (Figure.5.3.). Metformin also decreased the AGE content (1.08 fold) with respect to the HFFD group.
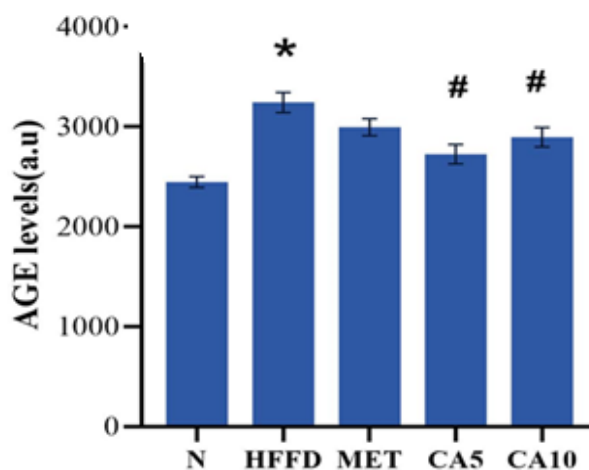
Figure.5.3. Formation of AGE in experimental animals. N - Control group (Normal diet) ; HFFD - High fat and fructose diet group/ STZ; MET - High fat and fructose diet group/ STZ with metformin 50 mg/kg bwt , CA5 - High fat and fructose diet group/ STZ with CA 5 mg/kg bwt; CA10 - High fat and fructose diet group/ STZ with CA 10 mg/kg bwt. Results are expressed as mean ± SEM where n = 6. * p ≤ 0.05 significantly different from the control group. # p ≤ 0.05 significantly different from HFFD group.

5.4.4. CA reduces insulin resistance in diabetic rats

To evaluate the severity of the diabetes, I analysed plasma insulin and insulin resistance. The plasma level of insulin in HFFD rats was increased by 2.06 fold compared to control rats (Figure 5.4a). While treatment with CA of both doses (1.26 and 1.88 fold for CA5 and CA10) and metformin (1.85 fold) improved the insulin levels compared to the HFFD groups. HOMA IR was also significantly increased in the HFFD group rats (2.71 fold; p ≤ 0.05) compared to control rats. This was significantly reduced by the administration of CA (2.688 fold for CA5 and 1.60 fold for CA10). Similarly, metformin also improved (2.17 fold) insulin resistance (Figure. 5.4b).

a

b
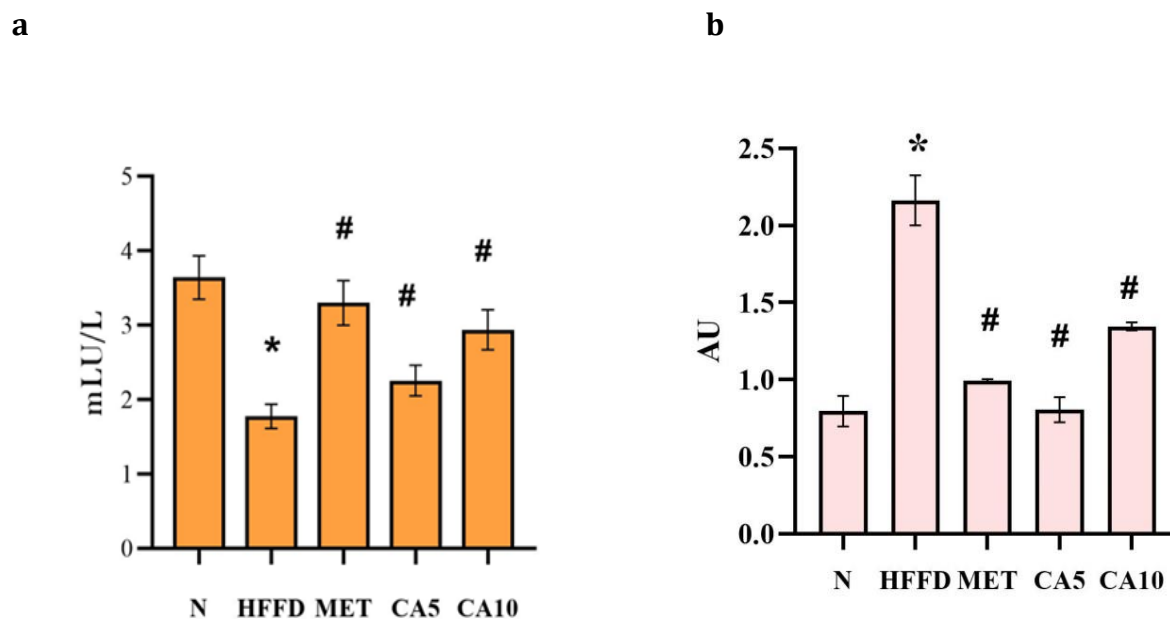
Figure. 5.4. **Effect of CA on insulin tolerance. a) Plasma insulin levels and b) HOMA IR** . N - Control group (normal diet); HFFD- High fat and fructose diet group/ STZ; MET- High fat and fructose diet group/ STZ with metformin 50 mg/kg bwt, CA5- High fat and fructose diet group/ STZ with CA 5mg/kg bwt; CA10- High fat and fructose diet group/ STZ with CA 10 mg/kg bwt. Results are expressed as mean ± SEM where n = 6. * $p \leq 0.05$ significantly different from the control group. # $p \leq 0.05$ significantly different from the HFFD group.

5.4.5. Effect of HFFD on lipid profile

HFFD diabetic rats showed significant elevation of TG (1.95 fold), TC (2.06 fold) and LDL (2.68 fold) compared to the control rats. Treatment with CA at 5 and 10 mg/kg bwt significantly prevented the increase of TG (1.14 and 2.093 fold), TC (1.58 and 1.51) and LDL (1.22 and 1.4 fold) levels. However, HDL level was found to be reduced (2.25 fold) in the HFFD rats compared to control rats. While administration of CA at both doses (1.47 and 1.43 fold for CA5 and CA10) significantly improved the HDL levels compared to HFFD rats. Metformin at a dose of 50 mg/kg bwt also significantly reversed the alterations observed in lipid profile (Table.5.2).

Parameters	Normal	HFFD	Metformin	CA5 (5 mg/kg)	CA10 (10 mg/kg)
TG (mg/dL)	82.66±3.13	161.61±6.17*	103.75±3.9#	141.42±5.4#	77.19±2.9#
TC (mg/dL)	96.07±3.6	198.31±7.5 *	163.38±6.2#	125.28± 4.7#	131.12±4.3#
LDL (mg/dL)	23.81±0.90	63.98±2.44*	32.90±1.25#	52.43±2#	45.42±1.73#
HDL (mg/dL)	72.11±2.75	31.9±1.06*	55.11±1.65#	46.90±1.79#	45.90±1.75#

Table.5.2. Lipid profile in diabetic rats. Results are expressed as mean ± SEM where n = 6. * p ≤ 0.05 significantly different from the control group. # p ≤ 0.05 significantly different from the HFFD group.

5.4.6. Analysis of biochemical parameters in the diabetic rats

The levels of LDH, CKMB, CRP and SGOT were significantly increased in the HFFD rats in comparison with normal rats. On the other hand rats treated with CA significantly reduced the activities of enzymes and level of CRP which was elevated by HFFD. (Table.5.3).

Groups	LDH (U/L)	CRP (mg/L)	CKMB (U/L)	SGOT (U/L)
Normal	51.29±1.95	1.755±0.06	19.80±1.70	9.306±0.355
HFFD	323.27±12.34*	5.311±0.2*	118.85±9.2*	44.78±1.71*
Metformin	236.70±9.03#	3.75±0.14#	92.44±9.26#	23.26±0.88#
CA5 (5 mg/kg)	239.38±9.14#	3.53±0.13#	87.49±8.93#	26.75±1.02#
CA10(10 mg/kg)	168.84±6.44#	3.75±0.14#	79.23±6.80#	23.84±0.9072#
NCA10	58.2±1.95	1.898±0.08	25.69±1.99	11.25±1.95
HD	60±3.02	1.963±0.096	28.56±4.55	12.63±1.35

Table.5.3. Effects of CA on activities of LDH, CRP, CK-MB and SGOT. Results are expressed as

mean ± SEM where n = 6. * p ≤ 0.05 significantly different from the control group. # p ≤ 0.05 significantly different from HFFD group.

5.4.7. Assessment of antioxidant status on the heart of diabetic rats

SOD activity was remarkably reduced in the heart of the diet induced diabetic model (1.59 fold) compared to the normal rats (Table.5.4), whereas treatment with CA (1.26 and 1.29 fold for CA5 and CA10 mg/kg bwt) and metformin (1.36 fold) significantly increased the activity of SOD compared to diabetic control. HFFD also caused oxidative stress in the myocardium which was evident from elevated concentration of lipid peroxidation products like MDA and the result is shown in Table.5.4. From the result it is found that the concentration of MDA was significantly raised (4.47 fold) in the HFFD group when compared to the control group. This elevated level was significantly reduced by the administration of CA (1.32 and 1.47 fold for CA5 and CA10) and metformin (1.93 fold) compared to HFFD group.

Group	SOD activity (units/mg protein)	MDA (mM/100g wet tissue)
N	5.03±0.18	0.87±0.0014
HFFD	3.29±0.22*	3.89±0.28*
MET	4.5±0.29#	2.01±0.16#
CA5	4.15±0.36#	2.94±0.56#
CA10	4.26±0.41#	2.64±0.22#
NCA10	4.98±0.23	0.97±0.05
HD	4.86±0.19	1.07±0.09

Table.5.4. Effect of CA on antioxidant status. Units - enzyme concentration required to inhibit chromagen by 50 % in 1 min. Results are expressed as mean ± SEM where n = 6. * p ≤ 0.05 significantly different from the control group. # p ≤ 0.05 significantly different from the HFFD group.

In order to rule out the toxicity of CA and the effect of high fat high fructose diet I included groups HD and NCA10. As observed by the evaluation of glucose level, glycated hemoglobin levels biochemical parameters (LDH, CRP, CKMB, SGOT), and antioxidant activities, the diet alone group and toxicity group did not show any significant changes during the experimental period. So this group is not included in the further experiments.

5.4.8. Effects of CA on heart weight/body weight ratio in diabetic rats

HW/BW ratio was found significantly (1.38 fold; p≤0.05) increased in HFFD rats compared to normal group. But the administration of CA to diabetic rats improved the body weight and heart weight, and thereby decreased HW/BW ratio (1.03 and 1.05 fold for 5 and 10 mg/kg bwt respectively, p≤0.05). Metformin improved the HW/BW ratio (Figure.5.5).
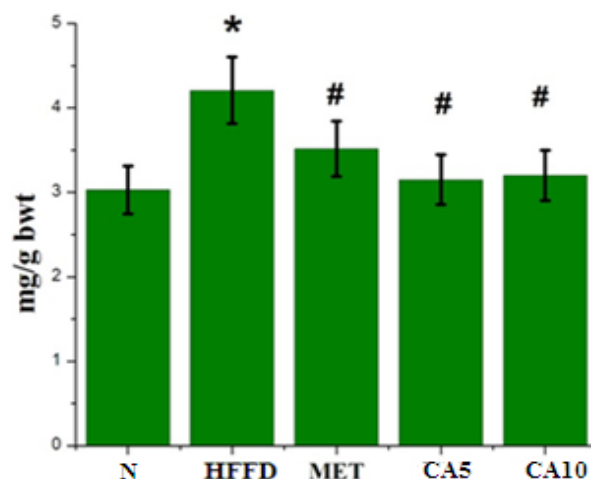
Figure. 5.5. **Action of CA on heart mass index during diabetes**. N - Control group (Normal diet) ; HFFD - High fat and fructose diet group/ STZ; MET - High fat and fructose diet group/ STZ with metformin 50 mg/kg bwt , CA5 - High fat and fructose diet group/ STZ with CA 5mg/kg bwt; CA10 - High fat and fructose diet group/ STZ with CA 10 mg/kg bwt. Results are expressed as mean ± SEM where n = 6. * p ≤ 0.05 significantly different from the control group. # p ≤ 0.05 significantly different from HFFD group

5.4.9. Estimation of concentration of ANP and BNP during diabetes

The natriuretic peptides ANP (1.3 fold; Figure.5.6a) and BNP (1.54 fold; Figure.5.6b) are significantly upregulated in the HFFD group compared to control rats, whereas CA treatment reduced the concentration of ANP (1.18 and 1.13 fold for CA5 and CA10) and BNP (1.15 and 1.31 fold for CA5 and CA10) in HFFD rats which shows the protective effect of CA against cardiac hypertrophy in rats. Metformin does not show any significant effect on ANP as well as BNP.

a

b
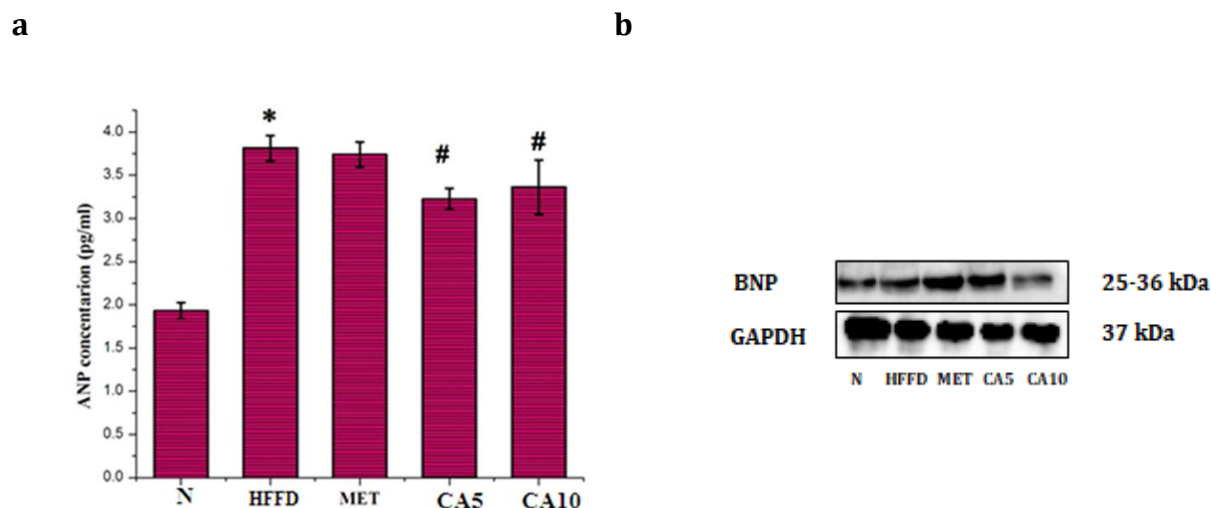
Figure.5.6. Effect of CA on cardiac injury markers. a) Concentration of ANP by ELISA kit. b) b) Expression of BNP with respect to GAPDH by western blot analysis. N - Control group (Normal diet) ; HFFD - High fat and fructose diet group/ STZ; MET - High fat and fructose diet group/ STZ with metformin 50 mg/kg bwt , CA5 - High fat and fructose diet group/ STZ with CA 5 mg/kg bwt; CA10 - High fat and fructose diet group/ STZ with CA 10 mg/kg bwt. Results are expressed as mean ± SEM where n = 6. * $p \leq 0.05$ significantly different from the control group. # $p \leq 0.05$ significantly different from HFFD group.

5.4.10. Assessment of proteins involved in DCM

The protein expressions of copeptin and fetuin A were increased by 1.45 and 1.78 fold respectively in HFFD rats with respect to control rats (Figure.5.7a). CA administration showed decreased levels of copeptin (1.02 and 1.89 fold for 5 and 10 mg/kg bwt respectively and fetuin A (2.74 and 6.32 fold for 5 and 10 mg/kg bwt respectively compared to diabetic group in a significant manner (p ≤0.05, Figure.5.7b). Metformin also resumed both the protein levels in a significant manner.

a
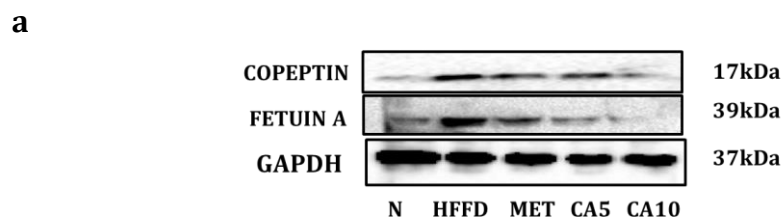
b
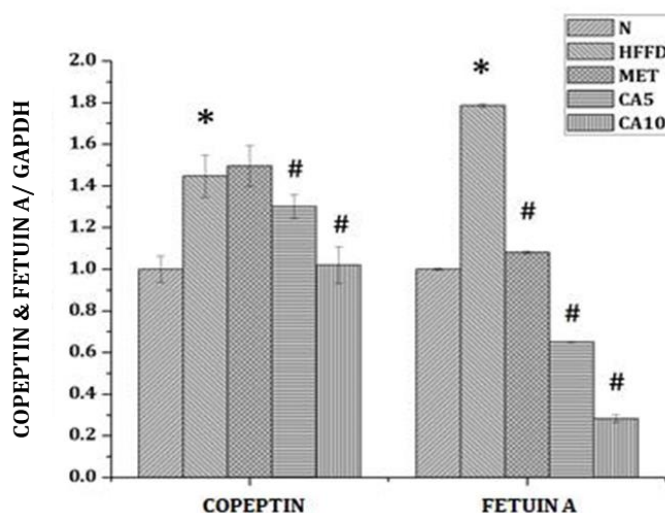
Figure.5.7. **Determination of markers relevant to DCM. a) Western blot analysis of copeptin, fetuin A, GAPDH. b) Densitometric analysis of copeptin and fetuin A with respect to GAPDH.** N - Control group (Normal diet) ; HFFD - High fat and fructose diet group/ STZ; MET - High fat and fructose diet group/ STZ with metformin 50 mg/kg bwt , CA5 - High fat and fructose diet group/ STZ with CA 5 mg/kg bwt; CA10 - High fat and fructose diet group/ STZ with CA 10 mg/kg bwt. Results are expressed as mean ± SEM where n = 3. * p ≤ 0.05 significantly different from the control group. # p ≤ 0.05 significantly different from the HFFD group.

5.4.11. Release of cardiac injury markers in diabetic rats

HFFD caused significant upregulation in the CVD marker proteins HFABP (2.63 fold), troponin (1.48 fold; Figure.5.8b). CA and metformin supplementation prevented the increased expression of troponin (1.86, 1.97 for CA5 and CA10 and 1.15 for metformin Figure.5.8b) and HFABP (1.2 and 1.41 fold for CA5 and CA10, 1.03 for metformin; Figure.5.8c).

a

b c
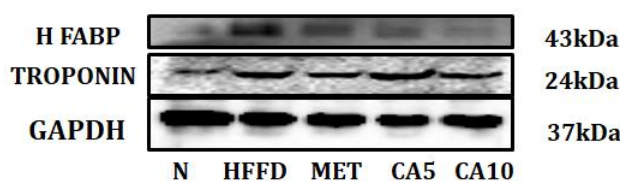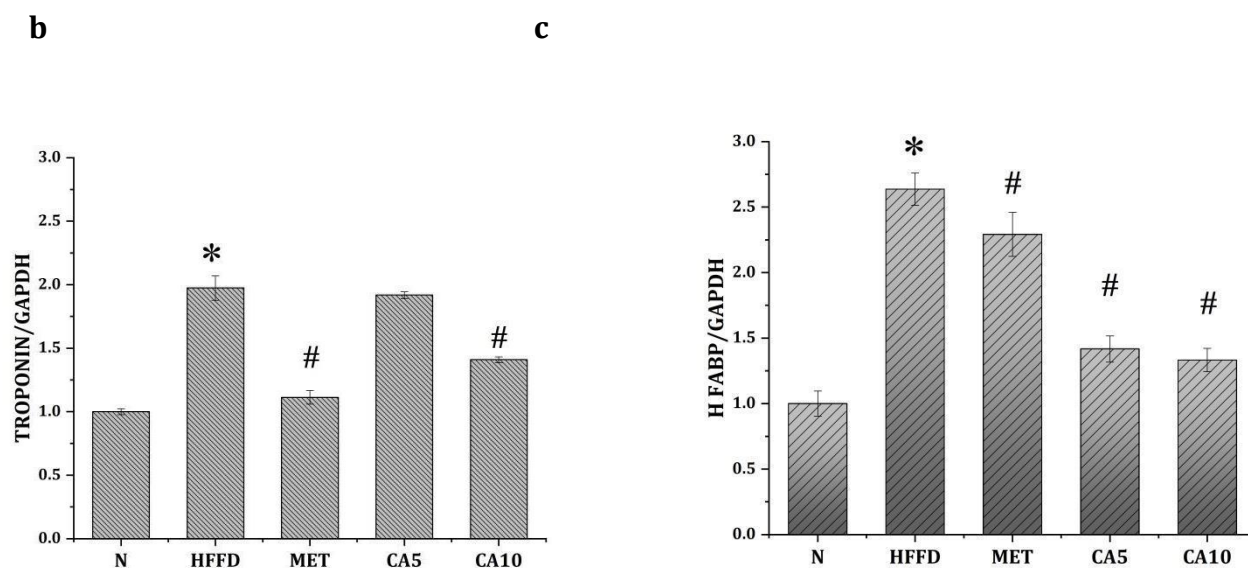
Figure.5.8. Expression of cardiovascular disease markers, troponin, HFABP and GAPDH. a) Immunoblot analysis of troponin, HFABP, GAPDH. b)Densitometric analysis of Troponin. C) Densitometric analysis of HFABP. GAPDH antibody served as an internal control. N - Control group (Normal diet) ; HFFD - High fat and fructose diet group/ STZ; MET - High fat and fructose diet group/ STZ with metformin 50 mg/kg bwt , CA5 - High fat and fructose diet group/ STZ with CA 5 mg/kg bwt; CA10 - High fat and fructose diet group/ STZ with CA 10 mg/kg bwt. Results are expressed as mean ± SEM where n = 3. * $p \leq 0.05$ significantly different from the control group. # $p \leq 0.05$ significantly different from the HFFD group.

5.4.12. ER stress upregulated in diabetic hearts

I further analysed important markers of ER stress in the diabetic hearts. Expression level of GRP78 (2.6 fold, $p \leq 0.05$; Figure.5.9a) and calnexin (2.14 fold,) was increased in diabetic hearts. Furthermore, in diabetic hearts, the expression of PERK (2.42 fold $p \leq 0.05$), IRE1α (1.74 fold $p \leq 0.05$ Figure 5.9) and ATF6α (2.1 fold, $p \leq 0.05$) were also increased in a significant manner compared to normal group (Figure.5.9c). I also measured the CHOP levels. It was also increased by 3.6 fold ($p \leq 0.05$) in diabetic hearts compared to control. CA (5 mg/kg.bwt) administration was found to reduce ER stress by downregulating GRP78 (1.62 fold), PERK (2.49 fold), IRE1α (1.06 fold), ATF6α (1.31 fold), calnexin (1.6 fold). Metformin also reduced the ER stress, GRP78 (1.3 fold), PERK (2.05 fold), ATF6α (1.96 fold), calnexin (3.4 fold) but not IRE1α and CHOP.

a
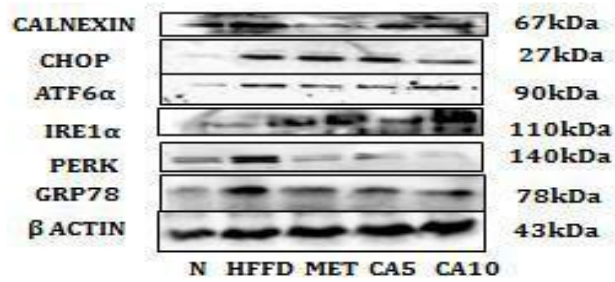
b
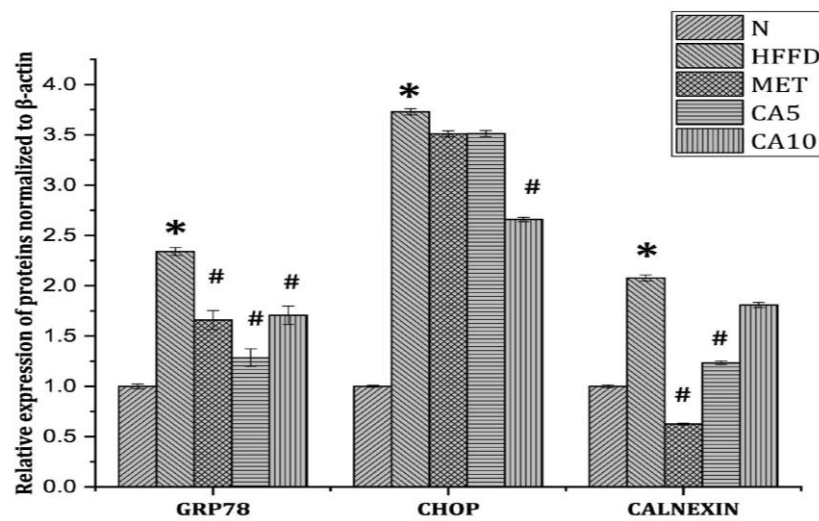
c
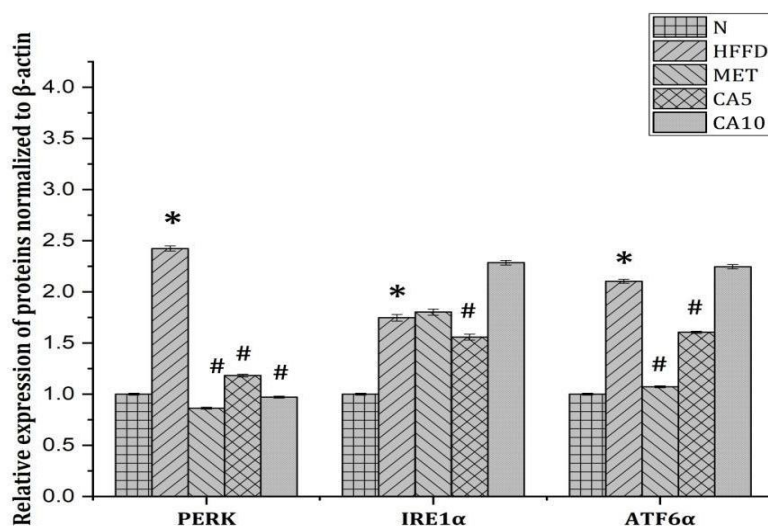
Figure. 5.9. Expressions of ER stress markers in diabetic animals. a) Western blot analysis of GRP78, PERK, IRE1α, ATF6α, CHOP, calnexin, β-actin. b) Densitometric analysis of

GRP78, CHOP, calnexin. c) Densitometric analysis of PERK, IRE1α, ATF6α. β-actin antibody served as an internal control. N - Control group (Normal diet) ; HFFD - High fat and fructose diet group/ STZ; MET - High fat and fructose diet group/ STZ with metformin 50 mg/kg bwt , CA5 - High fat and fructose diet group/ STZ with CA 5mg/kg bwt; CA10 - High fat and fructose diet group/ STZ with CA 10 mg/kg bwt. Values are expressed as mean ± SEM where n = 3. * p ≤ 0.05 significantly different from the control group. # p ≤ 0.05 significantly different from the HFFD treated group

5.4.13. ER-phagy during DCM

Expression of SEC62 was found increased (2.04 fold; p ≤ 0.05; Figures.5.10a & b) in the heart of the diabetic rats with respect to the normal rats. Administration of CA5 (1.24 fold) and metformin (1.81 fold) significantly reduced the expression of SEC62 (Figures.5.10a & b).
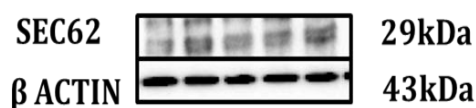
a   **b**
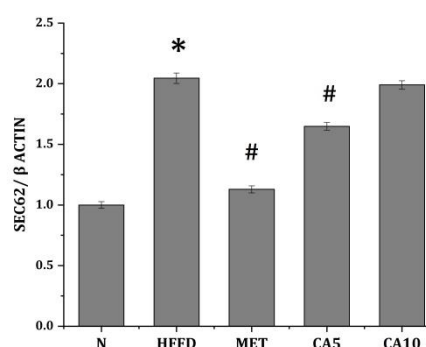
Figure. 5.10. Expressions of SEC62 in diabetic animals. a) Western blot analysis of SEC62 and β-actin. b) Densitometric analysis of SEC62 normalised to β-actin. N - Control group (Normal diet) ; HFFD - High fat and fructose diet group/ STZ; MET - High fat and fructose diet group/ STZ with metformin 50 mg/kg bwt , CA5 - High fat and fructose diet group/ STZ with CA 5mg/kg bwt; CA10 - High fat and fructose diet group/ STZ with CA 10 mg/kg bwt. Values are expressed as mean ± SEM where n = 3. * p ≤ 0.05 significantly different from the control group. # p ≤ 0.05 significantly different from HFFD group

### 5.4.14. Effects of CA on histopathological changes in heart induced by diabetes in rats

Hematoxylin and eosin (H & E) staining of the heart tissue (Figure. 5.11 a (a)) showed that the myocardial fibers arranged regularly and the cardiac myocytes showed

normal morphology with distinct cell borders and homogeneous oval nuclei in control group rats. However, in diabetic model group, the arrangement of cardiac fibers was disrupted, loss of nucleus existed in some of cardiomyocytes and the intercellular border was obscure (Figure.5.11a (b)). CA treatment ameliorated the structural abnormalities in the hearts of diabetic rats (Figure.5.11a (d & e)). Metformin also reduced the structural abnormalities in diabetic rats (Figure.5.11a (c)).

Van Geison staining of heart tissue revealed severe fibrosis in HFFD rats compared with normal rats (Figure.5.11b (b)). CA treatment was found to be effective in attenuating cardiac fibrosis in HFFD induced DCM (Figure.5.11b (d & e)). Metformin also reduced fibrosis (Figure.5.11b (c)).

a
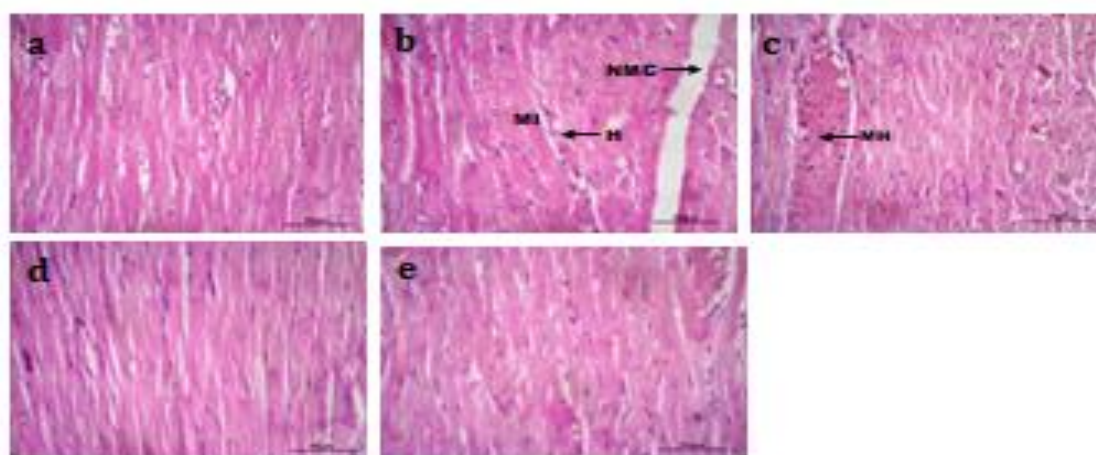
b
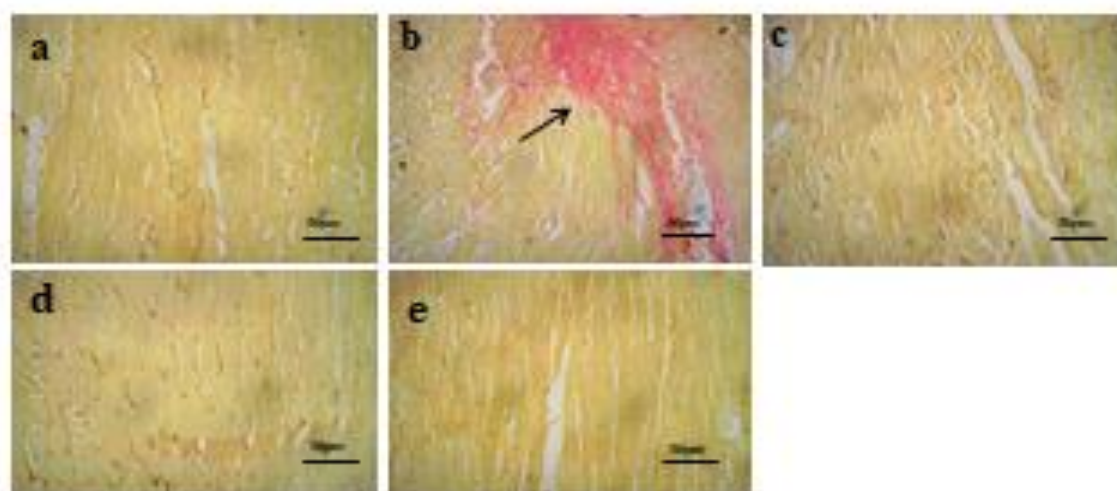
Figure. 5.11. Representative image showing pathology of heart tissue. a) Hematoxylin

Eosin (H&E) stain of the heart tissue. b) Van Geison stain of the heart tissue. a- control group (normal diet); b-HFFD- high fat and fructose diet group/ STZ; c- high fat and fructose diet group/ STZ with metformin 50 mg/kg bwt , d- high fat and fructose diet group/ STZ with CA 5 mg/kg bwt; e- high fat and fructose diet group/ STZ with CA 10 mg/kg bwt.

Discussion

While DCM is progressively perceived, the underlying mechanisms remain unclear. The majority of the understanding of disease mechanisms has come from studies in animal models that mimic human pathophysiological pathways. However the rodents are considered as a good model organism for studying DCM (Bugger and Abel, 2009). In recent years, rats have been the preferred rodent model in cardiac research. Therefore here I evaluated the ER stress and cardiac injury in the animal model and also explore the protective effect of CA on DCM. For the study I used male wistar rats of 6-8 weeks old. For the induction of diabetes associated cardiac complications, I selected a high fructose high fat diet and a low dose of STZ. Because, currently a number of animal studies validates that a low dose STZ combined with a high fat diet, sucrose or fructose can reiterate several features of diet induced type 2 diabetes in humans (Barrière et al., 2018).

Fasting blood glucose is the typical parameter used for the diagnosis of diabetes. Blood glucose of the rats in the diabetic group markedly increased and the rats also manifested classical symptoms of diabetes, including polyuria, polydipsia, hyperglycemia which could be due to deficiency in insulin secretion/action (Ramesh and Pugalendi, 2006). CA is found to reduce blood glucose level of the diabetic rats. Also there was a marked reduction in the extent and severity of classical symptoms like polyuria, polydipsia after administration of CA; which indicates improved glycemic control and insulin sensitivity.

HbA1c levels are recognized biomarker in medical practice (Nathan et al., 2007; Lyons and Basu, 2012). Also, it is directly proportional to fasting blood glucose levels over extended periods of time (Nathan et al., 2008). It is a glycated product. Most of the studies have revealed that elevated HbA1c levels are a risk factor of CVD and mortality (Selvin, 2010; Liu et al., 2011; Olofsso et al., 2010). However, the association between HbA1c level and the CVD in the general population remains unclear. Here I found a significant elevation of HbA1c in the diabetic group. This was reduced with the administration of CA

and metformin. Thus, CA successfully prevented hyperglycemia induced elevated HbA1c. The key drawback of HbA1c is that it does not represent long-term exposure to hyperglycemia and does not include details about glycemic variability.

Moreover, I also measured AGE levels in diabetic rats. The development and accumulation of AGE products is one of the major pathogenetic mechanisms of diabetic complications (Hartog et al., 2007). In diabetes and heart failure the levels of AGEs rise causing myocardial stiffness (Nożyński et al., 2009). AGEs levels in the blood have been related with the growth and severity of heart failure. AGEs may conceivably stimulate CVD through inflammation, endothelial dysfunction and lipid aberrations (Meerwaldt et al., 2008). Furthermore recent research suggests that therapies targeting AGEs may have a therapeutic potential in heart failure patients (Hegab, 2012). Here also I found an elevated AGEs level in the HFFD group compared to normal rats. CA was found to be reducing AGE levels. The same result was observed in *in vitro* conditions too.

One of the major symptoms of diabetes is a marked reduction in plasma insulin level (Frode and Medeiros, 2008). Here also I found a decreased level of insulin in HFFD rats with respect to normal ones. Insulin resistance is mainly regarded as hyperglycemia, hyperlipidemia, elevated HbA1c levels, increased plasma inflammatory markers (Ye, 2013). HOMA IR, a tool for measuring insulin resistance and beta-cell activity was found higher in diabetic control rats compared to normal. This suggests that diabetic animals experience insulin resistance. This may be due to the high dose of fructose which causes insulin sensitivity. At the same time CA treatment resulted in significant decrease in plasma glucose with an improvement in insulin level and HOMA-IR.

Another main risk factor in diabetes is dyslipidemia which plays a significant role in the development of CVDs (Mathe, 1995). The pathogenesis of diabetic dyslipidemia has been linked to insulin resistance (Jialal and Singh, 2019). Diabetic dyslipidemia mainly consists of elevated triglycerides (TG), low density lipoprotein (LDL), total cholesterol and a small dense of high density lipoprotein (HDL) (Mazzone et al., 2008; Vergès, 2015; Lorenzo et al., 2013). Evidence from various clinical trials has shown that lipid lowering therapy has beneficial effects on cardiovascular outcomes in diabetic conditions. An elevated level of LDL is accompanied with higher risk of CVDs. Recent research has found a cross relation between TG rich lipoprotein and heart diseases caused by mutations in the apolipoproetin C3 (Do et al., 2013). Triglycerides have a

positive relationship with cholesterol and glucose tolerance while having a negative relationship with HDL cholesterol (Schofield,et al., 2016). Low HDL cholesterol appears to be more important in patients with high cardiometabolic risk. It is one of the factors that favour further LDL cholesterol reduction (Chapman et al., 2011). Elevated TG, cholesterol and LDL levels were observed in the HFFD group. There was also a notable reduction in the HDL level in the diabetic animals but the treatment with CA and metformin improved dyslipidemia.

Meanwhile cardiac risk markers like CK-MB, CRP, SGOT and LDH in the serum were also measured in diabetic rats. The activity of the enzyme serum glutamic oxaloacetic transaminase (SGOT) increased and remained elevated for several days after a heart attack, which was the first blood test to help in the diagnosis of a heart attack (Ladue et al., 1954). Since SGOT activity can be elevated in conditions other than a heart attack, researchers began looking for new, more accurate laboratory diagnostic markers of myocardial injury. As a result of this search, several other cytoplasmic enzymes that could be used to detect a cardiac injury were discovered. Lactate dehydrogenase (LDH) and creatine kinase (CK) were two of the several candidates that gained widespread clinical acceptance (Bodor, 2016). The CK enzyme is a dimer composed of two polypeptide chains that are encoded by two genes and translated independently. The dimer of CK-MB is formed by the CK-M and CK-B monomers, and since heart muscle expresses the B gene at a higher rate than other skeletal muscle, the CK-MB isoenzyme has greater cardiac specificity than total CK. The measurement of CK-MB isoenzyme had a stronger track record. I found that a significant rise in the levels of LDH, CK-MB and SGOT in the serum of diabetic rats is an indication of the damage to the myocardial membrane. Besides, I measured CRP levels. C-reactive protein (CRP), a nonspecific inflammatory marker, is thought to play a direct role in coronary plaque atherogenesis. At both the primary and secondary prevention stages, an elevated CRP level independently predicted adverse cardiac events (Anand et al.,2005). Elevated levels of CRP were also found in the serum of diabetic rats. While treatment with CA and metformin reduces the cardiac risk markers. Thus a reduction in the risk markers represents a decrease in the degree of myocardial injury.

Oxidative stress plays a significant role in the development of various CVDs such as heart failure, myocardial ischemia, cardiomyopathy, atherosclerosis etc (Yang et al.,

2015). Proteins and lipids are the foremost targets of oxidative stress and the oxidative products of lipids and proteins are elevated in the diabetic patients (Ramakrishna and Jailkhani, 2008). The lipid peroxidation bioassay can be used as a predictor of cardiovascular risk (Zhang et al., 2014). Lipid peroxidation products like MDA were significantly elevated in the heart of the diabetic rats compared to normal rats. Treatment with CA significantly reduced the MDA levels compared to the diabetic control. This effect was comparable to metformin treatment.

Several health conditions such as diabetes, atherosclerosis, cardiovascular diseases and other chronic conditions have been linked to free radicals or reactive species as a result of oxidative stress (Giustarini et al., 2009). The role and effectiveness of the first line defence antioxidants primarily include superoxide dismutase; catalase and GPx are critical in overall defence strategy, particularly in relation to superoxide anion radical which is constantly produced in normal body through a variety of process (Ighodaro and Akinloye, 2018). SOD plays an important role in protecting cellular and histological damages produced by ROS. In diabetic rats, there is a decreased activity of SOD. The administration of CA and metformin to diabetic rats increased the SOD activity and thereby it may ameliorate the diabetic complications.

In addition, I also calculated cardiac mass index. The cardiac mass index was used as a key factor to estimate the development of cardiac hypertrophy (Yang et al., 2017). In diabetic rats, cardiac mass index was found to be higher than normal rats. This indicates hypertrophy in diabetic rats. Another important marker for cardiac injury is natriuretic peptides like ANP and BNP. These two markers were elevated in accordance with severity of the heart failure (Yoshimura et al., 2001). In the present study, ANP and BNP are found to be released more in diabetic rats than control. Also I have shown that CA significantly reduced cardiac injury by improving cardiac mass index as well as reducing ANP and BNP levels. Besides, here I proposed that in diabetic patients with high BNP levels, HbA1c and fasting plasma glucose should be tested for cardiac failure. Because one of the studies reported that high BNP levels can be caused by poor glycemic control, leading to an overdiagnosis of chronic heart failure (Dal et al., 2014).

Another biomarker for cardiac dysfunction is the troponin level. Here I quantified troponin. Troponin is currently the most essential protein used in the diagnosis of CVDs

(Aydin et al., 2019). It is released from the cytosolic pool of the myocytes. Besides it can also be used to estimate the infarct size (Chia et al., 2008). Cardiac troponin regulates the calcium dependent interaction of actin and myosin which causes myocardial contraction. A significant increase of troponin was found in the diabetic rats. It indicates the abnormal regulation of calcium level. Moreover, a similar pattern of results was observed in in *vitro* study too. This may be due to the chronic ER stress. Administration of CA and metformin was found to be reducing the troponin level and thereby trying to control the calcium imbalance in diabetic group.

In addition to routinely analysing cardiac biomarkers like ANP, BNP, troponin, I also evaluated novel biomarkers, copeptin. Copeptin, C terminal pro-vasopressin found in serum and plasma and is a stable convenient biomarker. In recent days, it was found to predict heart disease and death in diabetic conditions implying that copeptin and vasopressin system could be used as a prognostic marker and therapeutic target for the diabetic induced heart diseases (Enhörning et al., 2015). Besides, researchers reported that there is an association between copeptin, insulin resistance and other cardiometabolic risks such as hyperlipidemia, hypertension and abdominal obesity (Goya et al., 2015). Here I found an elevated copeptin level in diabetic rats. CA treatment could considerably decrease the copeptin levels in diabetic rats.

I also analysed an important cardiac specific marker HFABP. It has been considered as a biomarker for the myocardial injury (Rezar et al., 2020). Unlike cardiac troponins bound to myocyte structural apparatus,it is a soluble protein in the cytoplasm. As a result the release into the systemic circulation could be detected sooner even after slight myocardial injury (Iida et al., 2007). In decompensated heart failure, the HFABP troponin ratio may be useful in separating acute ischemia from chronic myocardial injury (Rezar et al., 2020). I observed a high level of HFABP in high fat high fructose diet rats compared to control. Treatment with CA and metformin significantly reduced the HFABP level indicating reduction in the myocardial damage. Furthermore, I quantified fetuin A. Fetuin A, a 64KD glycoprotein generated in the liver and secreted into circulation is considered as a biomarker for various metabolic diseases such as diabetes, obesity, cardiovascular diseases and NASH (Bourebaba and Marycz, 2019). In this study I found a significant elevation in the fetuin A levels in the serum of the diabetic rats. CA administration could considerably reduce the level of fetuin A in diabetic rats.

In order to interpret *in vitro* results, I also analysed ER stress in the heart of high fat high fructose diet group by scrutinizing major ER stress marker proteins like GRP78, PERK, and IRE1α, ATF6, CHOP and calnexin. ER stress is a stress relieving process that is triggered in response to various pathophysiological conditions. PERK, IRE1α and ATF6α are the three signaling branches that make up the UPR. These three proteins are found in the ER membrane and embedded with a protein GRP78 and in normal conditions these proteins are found in inactive form. Under stress conditions, GRP78 detaches from these proteins and activates UPR pathways. Here I observed a similar pattern that was found in *in vitro* study. High fat high fructose diet rats induced ER stress in the heart which was evident from the elevated level of GRP78. In addition, GRP78 levels are higher in the adipose tissue of diabetic and obese patients (Fang et al., 2015; Khadir, 2016). High fat high fructose diet fed rats also triggers three UPR pathway which is confirmed by the increased expression of PERK, IRE1α and ATF6α. The treatment with CA is found to attenuate three UPR pathways. Besides I also measured another two important ER stress proteins, CHOP and calnexin. CHOP is mainly involved in ER stress mediated apoptosis (Nishitoh, 2012). In diabetic rats, CHOP was found to be upregulated. On the other hand, the administration of CA reduced the expression of CHOP. I also evaluated calnexin, which has a significant role in the translocation of newly synthesised polypeptides and their folding. It is also involved in apoptosis that is aggravated by ER stress (Guérin et al., 2018). Heart of diabetic rats shows a significant level of calnexin. Here also CA reduced the expression of calnexin. Metformin also reduced ER stress proteins but not all. Besides I also analysed ER-phagy protein, SEC62. SEC62 protein expression was found upregulated in the diabetic hearts. This result was in consistent with *in vitro* study too. CA administration decreased ER-phagy by regulating SEC62.

Finally, I also analysed histopathological alterations of heart tissue. Fibrosis is a well-known cause of disease and death. Hypertensive heart diseases, diabetic hypertrophic cardiomyopathy, dilated cardiomyopathy all promote cardiac fibrosis (Disertori et al., 2017; Jellis et al., 2010). After a myocardial infraction, fibrotic scars of the cardiac muscle are common. Cardiac fibrosis is a condition in which extracellular matrix undergoes pathological remodelling resulting in irregular matrix organization and quality, as well as weakened functioning of heart muscle (Kania et al., 2009). In this study diabetic heart shows severe fibrosis. This may be due to high glucose level which makes

AGE accumulation more likely. This AGE causes the modification of endothelial cells extracellular matrix proteins such as collagen and laminin. It affects the normal structure and function of blood vessels and cardiac fibrosis is accelerated. CA administration reduced the severity of fibrosis by regulating blood glucose level, AGE accumulation and oxidative stress induced ER stress.

In conclusion, *in vivo* study reveals that CA was found to have beneficial effects against diabetes induced cardiac complications. The protective property of CA appears to be mediated by the inhibition of ER stress. CA is also found to reduce HbA1c levels, AGE levels and improves insulin resistance also. Besides, CA regulates dyslipidemia. CA abridged cardiac dysfunction as evident from decreased levels of ANP, BNP, copeptin and HFABP. Similarly, calcium homeostasis is also maintained by regulating troponin levels. CA treatment inhibits oxidative stress and improves the activity of antioxidant enzymes. I also found that three UPR pathways were also downregulated by CA which was evident from decreasing the protein expression of PERK, IRE1α, ATF6α. CA reduced ER stress mediated apoptosis and ER-phagy by decreasing levels of CHOP, calnexin and SEC62. CA reduces fibrosis which indicates that CA affords cardioprotection. Overall results show that CA exhibits cardioprotection during hyperglycemia *via* downregulating a series of pathways which leads to oxidative stress, AGEs, calcium homeostasis, ER stress and ER-phagy.

References

1. Anand IS, Latini R, Florea VG, et al. C-reactive protein in heart failure: prognostic value and the effect of valsartan. *Circulation*. 2005; 112(10):1428-1434. doi:10.11 61/CIRCULATIONAHA.104.508465.

2. Aydin S, Ugur K, Aydin S, Sahin İ, Yardim M. Biomarkers in acute myocardial infarction: current perspectives. *Vasc Health Risk Manag*. 2019; 15:1-10. doi:10.2147/VHRM.S166157.

3. Barrière DA, Noll C, Roussy G, et al. Combination of high-fat/high-fructose diet and low-dose streptozotocin to model long-term type-2 diabetes complications. *Sci Rep*. 2018;8(1):424. doi:10.1038/s41598-017-18896-5.

4. Bodor GS. Biochemical Markers of Myocardial Damage. *EJIFCC*. 2016;27(2):95-111.

5. Bourebaba L, Marycz K. Pathophysiological Implication of Fetuin-A Glycoprotein in the Development of Metabolic Disorders: A Concise Review. *J Clin Med*. 2019;8(12):2033. doi:10.3390/jcm8122033.

6. Chapman MJ, Ginsberg HN, Amarenco P, et al. Triglyceride-rich lipoproteins and high-density lipoprotein cholesterol in patients at high risk of cardiovascular disease: evidence and guidance for management. *Eur Heart J*. 2011;32(11):1345-1361. doi:10.1093/eurheartj/ehr112.

7. Chia S, Senatore F, Raffel OC, Lee H, Wackers FJ, Jang IK. Utility of cardiac biomarkers in predicting infarct size, left ventricular function, and clinical outcome after primary percutaneous coronary intervention for ST-segment elevation myocardial infarction. *JACC Cardiovasc Interv*. 2008; 1(4):415-423. doi:10.1016/j.jcin.2008.04.010.

8. Dal K, Ata N, Yavuz B, et al. The relationship between glycemic control and BNP levels in diabetic patients. *Cardiol J*. 2014; 21(3):252-256. doi:10.5603/CJ.a2013.0109.

9. Disertori M, Masè M, Ravelli F. Myocardial fibrosis predicts ventricular tachyarrhythmias. *Trends Cardiovasc Med*. 2017; 27(5):363-372. doi:10.1016/j.tcm.2017.01.011.

10. Do R, Willer CJ, Schmidt EM, et al. Common variants associated with plasma triglycerides and risk for coronary artery disease. *Nat Genet*. 2013;45(11):1345-1352. doi:10.1038/ng.2795.

11. Eeg-Olofsson K, Cederholm J, Nilsson PM, et al. New aspects of HbA1c as a risk factor for cardiovascular diseases in type 2 diabetes: an observational study from the Swedish National Diabetes Register (NDR). *J Intern Med*. 2010; 268(5):471-482. doi:10.1111/j.1365-2796.2010.02265.x.

12. Enhörning S, Hedblad B, Nilsson PM, Engström G, Melander O. Copeptin is an independent predictor of diabetic heart disease and death. *Am Heart J*. 2015; 169(4):549-556. doi:10.1016/j.ahj.2014.11.020.

13. Fang L, Kojima K, Zhou L, Crossman DK, Mobley JA, Grams J. Analysis of the Human Proteome in Subcutaneous and Visceral Fat Depots in Diabetic and Non-diabetic

Patients with Morbid Obesity. *J Proteomics Bioinform*. 2015;8(6):133-141. doi:10.4172/jpb.1000361.

14. Fröde TS, Medeiros YS. Animal models to test drugs with potential antidiabetic activity. *J Ethnopharmacol*. 2008; 115(2):173-183. doi:10.1016/j.jep.2007.10.038.

15. Giustarini D, Dalle-Donne I, Tsikas D, Rossi R. Oxidative stress and human diseases: Origin, link, measurement, mechanisms, and biomarkers. *Crit Rev Clin Lab Sci*. 2009;46(5-6):241-281. doi:10.3109/10408360903142326.

16. Guérin R, Arseneault G, Dumont S, Rokeach LA. Calnexin is involved in apoptosis induced by endoplasmic reticulum stress in the fission yeast. *Mol Biol Cell*. 2008;19(10):4404-4420. doi:10.1091/mbc.e08-02-0188.

17. Hartog JW, Voors AA, Schalkwijk CG, et al. Clinical and prognostic value of advanced glycation end-products in chronic heart failure. *Eur Heart J*. 2007;28(23):2879-2885. doi:10.1093/eurheartj/ehm486.

18. Hegab Z, Gibbons S, Neyses L, Mamas MA. Role of advanced glycation end products in cardiovascular disease. *World J Cardiol*. 2012;4(4):90-102. doi:10.4330/wjc.v4.i4.90.

19. Ighodaro OM, Akinloye OA. First line defence antioxidants-superoxide dismutase (SOD), catalase (CAT) and glutathione peroxidase (GPX): Their fundamental role in the entire antioxidant defence grid. *Alexandria J. Med*. 2018. 54(4), 287-293. doi.org/10.1016/j.ajme.2017.09.001.

20. Iida M, Yamazaki M, Honjo H, Kodama I, Kamiya K. Predictive value of heart-type fatty acid-binding protein for left ventricular remodelling and clinical outcome of hypertensive patients with mild-to-moderate aortic valve diseases. *J. Hum. Hypertens*. 2007;21:551–557. doi: 10.1038/sj.jhh.1002195.

21. Jellis C, Martin J, Narula J, Marwick TH. Assessment of nonischemic myocardial fibrosis. *J Am Coll Cardiol*. 2010;56(2):89-97. doi:10.1016/j.jacc.2010.02.047.

22. Jialal I, Singh G. Management of diabetic dyslipidemia: An update. *World J Diabetes*. 2019;10(5):280-290. doi:10.4239/wjd.v10.i5.280.

23. Kania G, Blyszczuk P, Eriksson U. Mechanisms of cardiac fibrosis in inflammatory heart disease. *Trends Cardiovasc Med*. 2009;19(8):247-252. doi:10.1016/j.tcm.2010.02.005.

24. Khadir A, Kavalakatt S, Abubaker J, et al. Physical exercise alleviates ER stress in obese humans through reduction in the expression and release of GRP78

chaperone. *Metabolism.* 2016; 65(9):1409-1420. doi:10.1016/j.metabol.2016. 06.004.

25. Ladue Js, Wroblewski F, Karmen A. Serum glutamic oxaloacetic transaminase activity in human acute transmural myocardial infarction. *Science.* 1954;120 (3117):497-499. doi:10.1126/science.120.3117.497.

26. Liu Y, Yang YM, Zhu J, Tan HQ, Liang Y, Li JD. Prognostic significance of hemoglobin A1c level in patients hospitalized with coronary artery disease. A systematic review and meta-analysis. *Cardiovasc Diabetol.* 2011; 10:98. doi:10.1186/1475-2840-10-98.

27. Lorenzo C, Hartnett S, Hanley AJ, et al. Impaired fasting glucose and impaired glucose tolerance have distinct lipoprotein and apolipoprotein changes: the insulin resistance atherosclerosis study. *J Clin Endocrinol Metab.* 2013; 98(4):1622-1630. doi:10.1210/jc.2012-3185.

28. Lyons TJ, Basu A. Biomarkers in diabetes: hemoglobin A1C, vascular and tissue markers. *Transl Res.* 2012; 159(4):303-312. doi:10.1016/j.trsl.2012.01.009.

29. Mathé D. Dyslipidemia and diabetes: animal models. *Diabete Metab.* 1995;21(2):106-111.

30. Mazzone T, Chait A, Plutzky J. Cardiovascular disease risk in type 2 diabetes mellitus: insights from mechanistic studies. *Lancet.* 2008; 371(9626):1800-1809. doi:10.1016/S0140-6736(08)60768-0.

31. Meerwaldt R, Links T, Zeebregts C, Tio R, Hillebrands JL, Smit A. The clinical relevance of assessing advanced glycation endproducts accumulation in diabetes. *Cardiovasc Diabetol.* 2008; 7:29. doi:10.1186/1475-2840-7-29.

32. Nathan DM, Kuenen J, Borg R, et al. Translating the A1C assay into estimated average glucose values (published correction appears in Diabetes Care. 2009 Jan;32(1):207). *Diabetes Care.* 2008;31(8):1473-1478. doi:10.2337/dc08-0545.

33. Nathan DM, Turgeon H, Regan S. Relationship between glycated haemoglobin levels and mean glucose levels over time. *Diabetologia.* 2007;50(11):2239-2244. doi:10.1007/s00125-007-0803-0.

34. Nishitoh H. CHOP is a multifunctional transcription factor in the ER stress response. *J Biochem.* 2012; 151(3):217-219. doi:10.1093/jb/mvr143.

35. Nozyński J, Zakliczyński M, Konecka-Mrówka D, Nikiel B, Mlynarczyk-Liszka J, Zembala-Nozyńska E, Lange D, Maruszewski M, Zembala M. Advanced glycation

end products in the development of ischemic and dilated cardiomyopathy in patients with diabetes mellitus type 2. Transplant Proc. 2009;41(1):99-104. doi: 10.1016/j.transproceed.2008.09.065.

36. Ramakrishna V, Jailkhani R. Oxidative stress in non-insulin-dependent diabetes mellitus (NIDDM) patients. *Acta Diabetol*. 2008;45(1):41-46. doi:10.1007/s 00592-007-0018-3.

37. Ramesh B, Pugalendi KV. Antihyperglycemic effect of umbelliferone in streptozotocin-diabetic rats. *J Med Food*. 2006;9(4):562-566. doi:10.1089/j mf.2006.9.562.

38. Rezar R, Jirak P, Gschwandtner M, et al. Heart-Type Fatty Acid-Binding Protein (H-FABP) and its Role as a Biomarker in Heart Failure: What Do We Know So Far?. *J Clin Med*. 2020; 9(1):164. doi:10.3390/jcm9010164.

39. Schofield JD, Liu Y, Rao-Balakrishna P, Malik RA, Soran H. Diabetes Dyslipidemia. *Diabetes Ther*. 2016; 7(2):203-219. doi:10.1007/s13300-016-0167-x.

40. Selvin E, Steffes MW, Zhu H, et al. Glycated hemoglobin, diabetes, and cardiovascular risk in non-diabetic adults. *N Engl J Med*. 2010; 362(9):800-811. doi:10.1056/NEJMoa0908359.

41. Vergès B. Pathophysiology of diabetic dyslipidaemia: where are we?. *Diabetologia*. 2015;58(5):886-899. doi:10.1007/s00125-015-3525-8.

42. Wannamethee SG, Welsh P, Papacosta O, Lennon L, Whincup PH, Sattar N. Copeptin, Insulin Resistance, and Risk of Incident Diabetes in Older Men. *J Clin Endocrinol Metab*. 2015;100(9):3332-3339. doi:10.1210/JC.2015-2362.

43. Yang X, Li Y, Li Y, et al. Oxidative Stress-Mediated Atherosclerosis: Mechanisms and Therapies. *Front Physiol*. 2017; 8:600. doi:10.3389/fphys.2017.00600.

44. Ye J. Mechanisms of insulin resistance in obesity. *Front Med*. 2013;7(1):14-24. doi:10.1007/s11684-013-0262-6.

45. Yoshimura M, Yasue H, Ogawa H. Pathophysiological significance and clinical application of ANP and BNP in patients with heart failure. *Can J Physiol Pharmacol*. 2001;79(8):730-735.

46. Zhang PY, Xu X, Li XC. Cardiovascular diseases: oxidative damage and antioxidant protection. *Eur Rev Med Pharmacol Sci*. 2014; 18(20):3091-3096.

Summary and conclusion

Diabetic heart disease has been one of the leading causes of death and disability among diabetics in recent decades. DCM has been identified in approximately 55% of diabetics with no evidence of heart disease caused by other reasons. A variety of metabolic abnormalities that may lead to the development of DCM. Among these hyperglycemia is the principal contributor. However, prolonged hyperglycemia causes a variety of molecular as well as metabolic changes in the myocyte resulting in cellular injury. Oxidative stress, inflammation, mitochondrial dysfunction, ER stress and apoptosis have all been suggested and researched as molecular mechanisms that may lead to cellular injury. Other pathways like ER-phagy, ER stress induced impaired calcium homeostasis are still understudied and need further study. Therefore, there is much attention given to the in-depth understanding of mechanisms, primarily emphasizing ER stress and associated pathways that are attributed to the progression of DCM. The treatment of DCM is still based on drug therapy. Till now there is no drug found to be effective for the treatment and management of DCM. So there is an urgent need for discovering or finding a therapeutic approach that would be effective for the DCM. In this scenario, the aim of the present study was to see the effect of CA on biochemical pathways that are significant to the DCM and explain the molecular mechanism mainly focusing on ER stress and associated pathways responsible for its cardioprotective property against hyperglycemia induced complications using both in *vitro* and *in vivo* models.

The current study showed the importance of ER stress in the progression of DCM. ER stress is considered as the important pathological mechanism for the development of various cardiovascular diseases. In this background, I designed studies to explore the molecular mechanism of ER stress during hyperglycemia by analyzing UPR pathway. The results showed that hyperglycemia induced ER stress, which was clear from the overexpression of GRP78. Besides high glucose treated H9c2 cells enhanced UPR response by activating three UPR pathways namely PERK, ATF6 and IRE1. It also increased the expression of ERO1 as well as PDI, two important enzymes that play a major role in maintaining the oxidation of ER. Besides, several transcription factors that

are crucial in the ER stress pathways also found to be upregulated. From these results I demonstrated that ER stress plays a major role in the induction of hyperglycemia.

Several studies have recently discovered connections between ER stress pathways and oxidative stress. A significant increase in lactate dehydrogenase (LDH) release into the medium, as well as a decrease in cell viability, confirmed the development of cardiac dysfunction during hyperglycemia. Hyperglycemia increased reactive oxygen species production. This might be because of the increased activity of NADPH oxidase, a non-mitochondrial source of ROS and prooxidant enzymes and also increased the expression of p47phox and Rac1. Hyperglycemia also impaired innate antioxidant system by decreasing SOD activity and expression, particularly of CuZnSOD (SOD1) and MnSOD (SOD2). Furthermore, high glucose disturbs the intracellular redox scavenger system which was visible with the decreased activity of GPx and GSH. In particular I found that high glucose treatment was associated with elevated oxidative stress. This was evident from the increased production of lipid peroxides as well as protein carbonyls. In addition, high levels of AGE RAGE interaction and decreased AGER1 was also found in high glucose condition. Furthermore, during hyperglycemia, PKCα dependent ERK signaling pathway was found to be activated. This might be due to upregulation of AGE RAGE axis as well as increased oxidative stress.

In order to evaluate whether ER stress impairs calcium homeostasis during DCM, I analyzed various calcium channels. I found that treatment with high glucose induced intracellular calcium overload. In addition, phosphorylation of RYR2 was found altered with high glucose. This might be due to the hperactivation of CaMKII, a key regulator of Ca^{2+} homeostasis in cardiac myocytes. Besides, NCX1, another important membrane protein for maintaining calcium homeostasis also found upregulated in hyperglycemic conditions. Furthermore, downregulation of SERCA2a expression was found with high glucose resulting in impaired Ca^{2+} uptake and reduced ER Ca^{2+} load and impairs contractility of the cardiomyocyte. I then investigated mitochondria ER dynamics in response to high glucose stimulation. As a result, I found altered mitochondrial transition pore as well as decreased activity of aconitase. This might be in association with altered calcium homeostasis because of hyperglycemia induced ER stress.

I further investigated the role of ER-phagy in DCM, which is not yet to be revealed. By analysing various ER-phagy receptors I concluded that high glucose treatment triggered ER-phagy. This was marked with the increased expression of RTN3, SEC62 and FAMB134. Moreover, prolonged ER stress leads to apoptosis. Here also high glucose induced apoptosis *via* increased levels of CHOP, caspase 12, calnexin and caspase 3 activity.

In order to validate the role of ER stress in DCM, I conducted an *in vivo* experiment in rats fed with a high fat, high fructose diet and a low dose of streptozotocin as a diabetic model. Besides ER stress markers, various parameters that are relevant to DCM like concentration of ANP, BNP, troponin, copeptin HFABP, serum AGE levels, activity of antioxidant enzymes, and histopathology of heart tissue are also evaluated. In diabetic rat model, there was an increased cardiac mass index, indication of hypertrophy. In addition, various enzymes like CK-MB, SGOT, CRP and LDH were found to be activated more in the diabetic rats. Furthermore, elevated HbA1c and serum AGE was found in the diabetic group. Diabetic rats also exhibited insulin resistance and dyslipidemia. Insulin resistance was again confirmed by the overexpression of fetuin A, indicator of insulin resistance. Diabetic rats showed oxidative damage which was evident from the decreased activity of SOD and increased lipid peroxidation product. Heart section stained with Van Geison showed severe fibrosis in the diabetic rats. Besides, ER stress marker GRP78 was found overexpressed in diabetic rats. Three UPR sensors PERK, IRE1, ATF6 was also found increased in diabetic group. ER-phagy was also found to be overexpressed in diabetic rats. Likewise, troponin level was found to be upregulated in diabetic animals. In addition, CHOP, the key indicator of ER stress mediated apoptosis was also found upregulated. These results were consistent with or *in vitro* results.

I also evaluated the cardioprotective property of CA during hyperglycemia. CA is an abundant polyphenol compound, bioavailable and possesses various biological activities. My research demonstrated that CA was found to be effective in controlling ER stress by regulating UPR pathways, namely PERK, IRE1α, and ATF6α. I found that CA administration inhibits ROS generation and restores redox status by activating innate antioxidant systems. CA is found to improve the activity of SOD, GPx and GSH. CA also moderates oxidative stress by reducing the oxidation of lipids and proteins. AGE RAGE interaction as well as PKC activity was found reduced upon treatment with CA. CA is also

found to be effective in reducing dyslipidemia as well as insulin resistance. Moreover, I also found that CA not only regulates UPR pathway and oxidative stress but also maintains Ca^{2+} homeostasis by regulating different Ca^{2+} channels like RYR2, NCX1, SERCA2a. Meanwhile CA protects mitochondria from hyperglycemia induced ER stress shock by improving aconitase activity and pore opening. In addition, it also reversed ER-phagy and eventually suppressed ER stress induced apoptosis. Finally CA was found to reduce cardiac injury markers like copeptin, ANP, BNP, HFABP and also reduced fibrosis of the heart. All these ensure protection against DCM.

Overall results showed the importance of ER stress and associated pathways in the progression of DCM. This study emphasizes the importance of ER stress as a drug target. Besides CA reveals its cardioprotective potential against DCM.
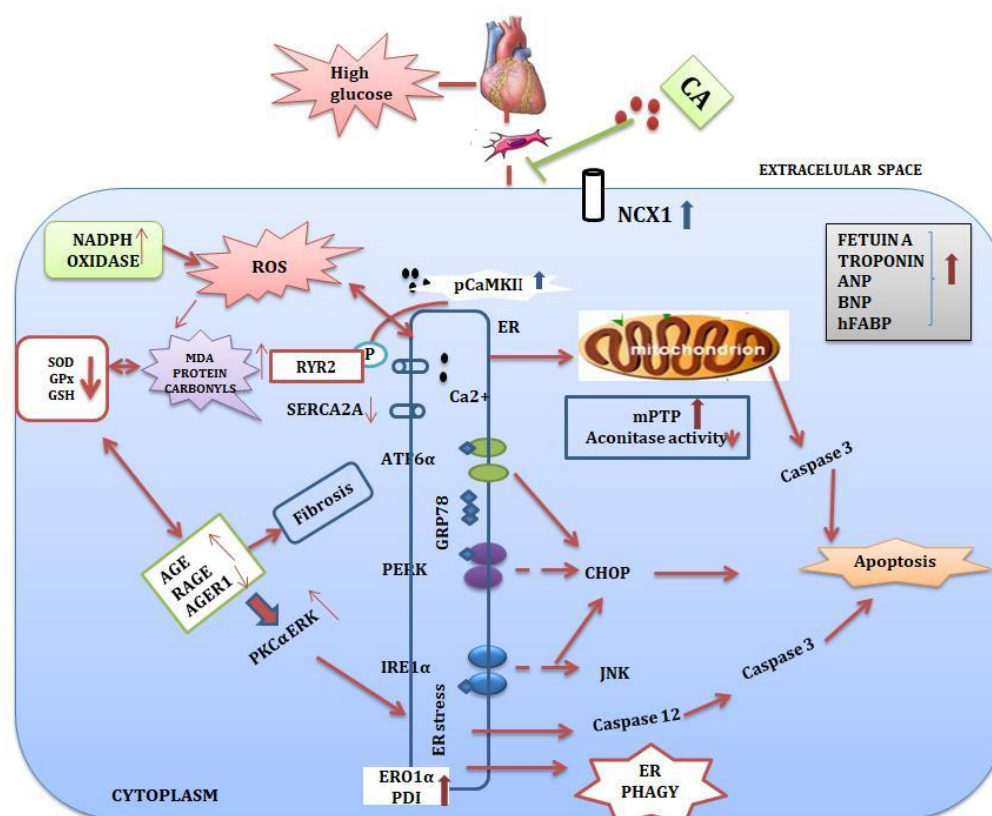

Figure. 6.1. Schematic representation of ER stress and associated pathways during DCM and possible amelioration with CA

ABSTRACT

Title of the thesis: Exploration of ER stress and associated complications in the genesis of hyperglycemia induced cardiomyopathy and possible amelioration with chlorogenic acid

A series of cardiovascular complications associated with hyperglycemia is a critical threat to the diabetic population. Here I elucidate the link between hyperglycemia and cardiovascular diseases onset, focusing on the role of ER stress and associated pathways such as oxidative stress, calcium homeostasis, ER-phagy, apoptosis and their underlying mechanisms using appropriate models. H9c2 cells were incubated with 33 mM glucose for 48 h to mimic the diabetic condition in *in vitro* system. Male wistar rats fed with a high fat high fructose diet (HFFD) with a single dose of streptozotocin (25 mg/kg bwt) induced diabetic model was used as *in vivo* model. I have observed significant increase of lactate dehydrogenase release to the medium and associated decrease in cell viability during high glucose insult. This confirms the development of cardiac dysfunction. Various parameters like free radical generation, innate antioxidant system, lipid peroxidation, AGE production and PKC α ERK signaling pathways were investigated during hyperglycemia and with chlorogenic acid treatment. Hyperglycemia has significantly enhanced ROS generation, depleted SOD activity and expression of particularly CuZnSOD (SOD1) and MnSOD (SOD2), increased production of AGE. Besides, PKC α dependent ERK signaling pathway during hyperglycemia was found activated leading to cardiac dysfunction. Further we investigated endoplasmic reticulum (ER) stress and associated signaling pathways. H9c2 cells incubated with high glucose showed significant activation of ER stress response proteins (GRP78, PERK, IRE1α, ATF6α) and altered its regulatory proteins (PDI, ERO1α). This was confirmed in *vivo* study too. Calcium homeostasis was found altered with calcium overload and increased pCaMKII activity. pCaMKII mediated RYR2 hyperactivity and reduction of SERCA2a were also found *in vitro* model. Also it enhanced ER-phagy through upregulation of SEC62, RTN3 and FAM134B. Moreover high glucose caused apoptosis via increased levels of CHOP, caspase 12 and calnexin. All these proteins (PERK, IRE1α, ATF6 α, pCaMKII, RYR2, NCX1, SERCA2a, RTN3, SEC62, FAM134B) have been found to have a significant role in the functioning of heart such as excitation contraction coupling and we expect these alterations to induce cardiomyopathy. Diabetic rat exhibited an increased expression of BNP, troponin, ANP and copeptin revealing cardiac injury. Besides, enhanced expression of fetuin A observed in HFFD rats shows insulin resistance as well. Results from the present study clearly reveal the significant role of ER stress in the genesis of DCM. We found chlorogenic acid is effective up to certain extend against hyperglycemia induced pathological alterations both *in vitro* and *in vivo* models.

Publications

From thesis

1. **Preetha Rani MR**, Anupama N, Sreelekshmi M, Raghu KG. Chlorogenic acid attenuates glucotoxicity in H9c2 cells via inhibition of glycation and PKC α upregulation and safeguarding innate antioxidant status. *Biomed Pharmacother*. 2018; 100:467-477. doi:10.1016/j.biopha.2018.02.027

Submitted to journal

2. **Preetha Rani M R**, Salin Raj P, Anupama Nair, Ranjith S, Rajankutty K, Raghu K G. Involvement of ER stress in the genesis of diabetic cardiomyopathy through multiple mechanisms and beneficial effect of chlorogenic acid.

Other than thesis

1. Anupama N, **Preetha Rani MR**, Shyni GL, Raghu KG. Corrigendum to < "Glucotoxicity results in apoptosis in H9c2 cells via alteration in redox homeostasis linked mitochondrial dynamics and polyol pathway and possible reversal with cinnamic acid"*Toxicol In Vitro*. 2021;72:105020. doi:10.1016/j.tiv.2020.105020

2. Mohan S, **R PRM,** Brown L, Ayyappan P, G RK. Endoplasmic reticulum stress: A master regulator of metabolic syndrome. *Eur J Pharmacol*. 2019;860:172553. doi:10.1016/j.ejphar.2019.172553

3. Anusree SS, Sindhu G, **Preetha Rani MR**, Raghu KG. Insulin resistance in 3T3-L1 adipocytes by TNF-α is improved by punicic acid through upregulation of insulin signalling pathway and endocrine function, and downregulation of proinflammatory cytokines. *Biochimie*. 2018;146:79-86. doi:10.1016/j.biochi. 2017.11.014

4. Priyanka A, Sindhu G, Shyni GL, **Preetha Rani MR**, Nisha VM, Raghu KG. Bilobalide abates inflammation, insulin resistance and secretion of angiogenic factors induced by hypoxia in 3T3-L1 adipocytes by controlling NF-κB and JNK

activation. *Int Immunopharmacol.* 2017;42:209-217. doi:10.1016/j.intimp.2016.11.019

5. Ajish KR, Antu KA, Riya MP, **M. R. Preetharani,** et al. Studies on α-glucosidase, aldose reductase and glycation inhibitory properties of sesquiterpenes and flavonoids of Zingiber zerumbet Smith. *Nat Prod Res.* 2015; 29 (10):947-952. doi:10.1080/14786419.2014.956741

6. Raj PS, Prathapan A, Sebastian J, **MR Preetha Rani,** et al. Parmotrema tinctorum exhibits antioxidant, antiglycation and inhibitory activities against aldose reductase and carbohydrate digestive enzymes: an in vitro study. *Nat Prod Res.* 2014; 28(18):1480-1484. doi:10.1080/14786419.2014.909420

7. Swapna Alex, **Preetha Rani.M.R**, Soni. K. B, et al. Biosynthesis of silver nanoparticles with antibacterial activity using leaf extract of *Michelia champaca*. *Jour Pl Sci Res.* 2012; 28 (1) :121-126.

Scientific Conferences

Oral presentations

- **Preetha Rani.M.R & Raghu.K.G.** Chlorogenic acid (CA) ameliorates hyperglycemia induced oxidative stress in H9c2 cells through mitochondria mediated pathway at International Conference on Nutraceuticals & Chronic Diseases held at Cochin, Kerala from September 9-11 2016 **(Best oral presentation award).**

- **Preetha Rani.M.R & Raghu.K.G.** Chlorogenic acid (CA) a common bioactive from coffee and fruits ameliorates hyperglycemia mediated redox status through involvement of PKC α –ERK signaling pathway at International Conference on Nutraceuticals & Chronic Diseases held at Goa, from September 1-3 2017 **(Best oral presentation award).**

- **Preetha Rani.M.R & Raghu.K.G.** Chlorogenic acid protects H9c2 cells from high glucose induced Endoplasmic Reticulum (ER)stress At National Virtual Conference On Recent Breakthroughs In Biotechnology (NCRBB-2021) & Annual Meet of Society for Biotechnologists (India) Organized by Department of Human Genetics and Molecular Biology Bharathiar University, Coimbatore, from January 22 – 23 2021.

Poster presentations

- **PreethaRani.M.R,** AnupamaNair & Raghu.K.G. Modulation of estradiol induced electrophysiological alterations on cardiac action potential by ionic imbalance, gender difference, pacing frequency, ischemia reperfusion insult at Indo Canadian Symposium on Heart Failure: Progress & Prospects, held at RGCB, Trivandrum on 12-14 March 2015.

- **Preetha Rani.M.R** & Raghu.K.G. Chlorogenic acid (CA) ameliorates hyperglycemia mediated redox status through involvement of PKC α –ERK signaling pathway in H9c2 at International Seminar on Phyochemistry 2018 held at JNTBGRI, Thiruvananthapuram, from March 26-27 2018.

- **Preetha Rani.M.R** & Raghu.K.G**.** Chlorogenic acid (CA) mitigates glucotoxicity mediated oxidative stress through protection of PKC α –ERK cascade at International Congress on Obesity and Metabolic Syndrome co-hosted by the KSSO
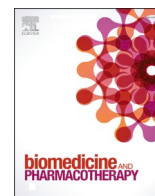
and KSMBS held at Seoul, South Korea, from September 6-9 2018 (**Travel grant award**).

Corrigendum

Corrigendum to "Chlorogenic acid attenuates glucotoxicity in H9c2 cells via inhibition of glycation and PKC α upregulation and safeguarding innate antioxidant status" [Biomed. Pharmacother. 100 (2018) 467–477]

Preetha Rani M.R [a,b], Anupama Nair [a,b], Sreelekshmi Mohan [a,b], Raghu K.G [a,b,*]

[a] Biochemistry and Molecular Mechanism Laboratory, Agro-Processing and Technology Division, CSIR- National Institute for Interdisciplinary Science and Technology, Thiruvananthapuram, 695019, Kerala, India
[b] Academy of Scientific and Innovative Research (AcSIR), CSIR-HRDC Campus, Ghaziabad, Uttar Pradesh, 201 002, India

The authors regret [b]Academy of Scientific and Innovative Research (AcSIR), CSIR-HRDC Campus, Ghaziabad, Uttar Pradesh, 201 002, India.

The authors would like to apologise for any inconvenience caused.

Chlorogenic acid attenuates glucotoxicity in H9c2 cells via inhibition of glycation and PKC α upregulation and safeguarding innate antioxidant status

Preetha Rani M.R., Anupama Nair, Sreelekshmi Mohan, Raghu K.G.*

Biochemistry and Molecular Mechanism Laboratory, Agroprocessing and Technology Division, CSIR-National Institute for Interdisciplinary Science and Technology, Thiruvananthapuram, 695019, Kerala, India

A R T I C L E   I N F O

A B S T R A C T

A series of cardiovascular complications associated with hyperglycemia is a critical threat to the diabetic population. Here we elucidate the link between hyperglycemia and cardiovascular diseases onset, focusing on oxidative stress and associated cardiac dysfunctions. The contribution of advanced glycation end products (AGE) and protein kinase C (PKC) signaling is extensively studied. For induction of hyperglycemia, H9c2 cells were incubated with 33 mM glucose for 48 h to simulate the diabetic condition in *in vitro* system. Development of cardiac dysfunction was confirmed with the significant increase of lactate dehydrogenase (LDH) release to the medium and associated decrease in cell viability. Various parameters like free radical generation, alteration in innate antioxidant system, lipid peroxidation, AGE production and PKC α -ERK axis were investigated during hyperglycemia and with chlorogenic acid. Hyperglycemia has significantly enhanced reactive oxygen species (ROS- 4 fold) generation, depleted SOD activity (1.3 fold) and expression of enzymes particularly CuZnSOD (SOD1) and MnSOD (SOD2), increased production of AGE (2.18 fold). Besides, PKC α dependent ERK signaling pathway was found activated (1.43 fold) leading to cardiac dysfunction during hyperglycemia. Chlorogenic acid (CA) was found beneficial against hyperglycemia most probably through its antioxidant mediated activity. The outcome of this preliminary study reveals the importance of integrated approach emphasizing redox status, glycation and signaling pathways like PKC α - ERK axis for control and management of diabetic cardiomyopathy (DCM) and potential of bioactives like CA.

1. Introduction

The prevalence of diabetes is steadily increasing worldwide [1]. Diabetes can lead to complications of multiorgan dysfunction and increase the chance of dying prematurely. But more than 60% of deaths in diabetic patients are due to CVD and associated problems [2]. Diabetic cardiomyopathy (DCM) constitutes structural and functional abnormalities of the myocardium without coronary artery disease or hypertension [3]. Relationships between glucose levels and CVD are remarkably inconsistent [4]. The complexity of the problem is so great that we have not yet unraveled the knot. However, there is much evidence of the occurrence of oxidative stress during hyperglycemia [5,6]. Oxidative stress results when the rate of oxidant production exceeds the rate of oxidant scavenging. Increased glucose flux enhances both

oxidant production and impairs antioxidant defenses via multiple interacting pathways [7]. Some of these changes are in the activity of protein kinase C (PKC) [8], advanced glycation end products (AGEs) production [9], and enhanced sorbitol pathway [10,11]. PKC has received special attention in the pathogenesis of cardiomyopathy due to its important role in the intracellular signaling pathway for regulating cardiac myocyte development, inotropic function and cellular growth [12]. Previous studies have also indicated that PKC α, the major isozyme is a necessary mediator of cardiomyocyte hypertrophic growth through an ERK1/2-dependent signaling pathway [13]. Some studies have made a putative hypothesis regarding the connection between ROS and ERK1/2 activation [14]. There is no report on the functional hazards of cross talk between AGE, PKC, ERK and weakened antioxidant defense system during hyperglycemia. This is very much

required for target identification for therapeutic intervention. Based on this, efforts are made in this study to understand precisely the contribution of these pathways in the genesis of diabetic cardiomyopathy in *in vitro* model.

Extensive research has led to the discovery of various drugs for control and management of diabetes. Unfortunately, this is still an incurable disease, and the prevalence is increasing day by day. So the risk for development of other complication is also increased. This creates an urgent need for exclusive therapeutics for CVD as classical anti-diabetic drugs are not much effective to control and manage the heart issues [15]. Recently much heed has been given to bioactive from medicinal plant in search of therapeutics against hyperglycemic cardiomyopathy. There are ample examples of the natural product derived cardiovascular therapeutics such as reserpine, diltiazem, statins, etc. [16]. Affordability, minimum adverse effects and tolerability to prolonged use necessitates for better therapeutics to the general public. In this scenario chlorogenic acid (CA), an ester of caffeic acid and (−)-quinic acid, abundant in our daily beverage coffee [17] and common fruits [18–20] with plenty of medicinal properties is an ideal choice. It also shows blood pressure lowering property [21]. In addition antibacterial, antioxidant, and anticarcinogenic activities [22,23] also its beneficial role in glucose and lipid metabolism [24] are mentioned in literature. There is report of cardioprotective properties of the extract containing CA from our group [25] also. So we are curious to check beneficial properties of CA against hyperglycemia induced alterations in H9c2 cells.

So experiments are planned to investigate the alterations in H9c2 cells during hyperglycemia emphasizing the cross talk between oxidative stress, glycation, and PKC α - ERK axis for identification of probable biochemical targets for future drug development and protective effect of CA.

2. Materials and methods

D-glucose and metformin were purchased from SRL (India). Dulbecco's modified eagle's medium (DMEM), penicillin-streptomycin antibiotics and fetal bovine serum (FBS) were from Gibco (USA).3-(4,5-dimethyl-thiazol-2-yl)-2,5-diphenyl tetrazolium bromide (MTT), RIPA buffer and 2, 7-dichlorodihydrofluorescein diacetate (DCFH-DA) were from Sigma Aldrich (St Louis, MO, USA).CA (99% purity) was from Natural Remedies Pvt. Ltd. (Bangalore, India).All antibodies were from Santa Cruz (USA). All other chemicals used were of analytical grade.

2.1. Cell culture

H9c2 embryonic rat heart-derived cell line from American Type Culture Collection (ATCC), USA, were grown in low glucose DMEM supplemented with 10% FBS and antibiotics (100 U/mL of penicillin and 100 µg/mL of streptomycin) under a humidified atmosphere with 5% CO_2 at 37 °C. In order to rule out the effect of changes in osmolarity on vital parameters of cell function, mannitol containing group was included in the study. Parameters like cell viability, ROS generation and PKCα - ERK pathway were studied with mannitol group.

2.2. Induction of hyperglycemia and treatment with CA

After 50% confluence, H9c2 cells were incubated with 33 mM glucose for 48 h. All the parameters were studied after 48 h of incubation of cells with glucose (33 mM) in presence or absence of various concentrations of CA (10 µM or 30 µM) or metformin (1 mM).

Experimental group consists of control (5.5 mM glucose, C), high glucose (33 mM glucose, HG), high glucose + metformin 1 mM (Met), high glucose + CA 10 µM (CA1), high glucose + CA 30 µM (CA2).

2.3. Evaluation of cell viability

Cell viability was determined by MTT assay. Briefly, 100 µL of MTT solution (5 mg/mL) was added to each well and incubated for 4 h at 37 °C. Thus the formazan crystals formed were dissolved in DMSO. Then the plates were read after 20 min in a microplate reader (Biotek Synergy 4, USA) at 570 nm and percentage of cell viability were calculated [26].

2.4. Determination of LDH leakage

LDH release was measured using LDH cytotoxicity assay kit (Clontech, USA). Briefly, 100 µL of medium was collected from cultured cells and was added with 100 µL of LDH reaction solution containing NAD +, lactic acid, iodonitrotetrazolium (INT) and diaphorase. The mixture was then incubated with gentle shaking for 30 min at room temperature, and the absorbance was read at 490 nm.

2.5. Detection of intracellular ROS

Intracellular ROS levels were determined using DCFH-DA as probe [27]. DCFH-DA is cleaved intracellularly by nonspecific esterase and turn to high fluorescence upon oxidation by ROS. After respective treatments, cells were washed with phosphate buffer saline (PBS, pH 7.4) and then incubated with DCFH-DA (20 µM) for 20 min at 37 °C in a humidified atmosphere of 5% CO_2. After incubation, cells were washed with phosphate buffer (pH 7.4). Fluorescence imaging was done (Ex. 488 nm; Em. 525 nm) to visualize the ROS generation with a spinning disk fluorescent microscope.

2.6. Estimation of TBARS

Lipid peroxidation was estimated for all experimental groups with TBARS estimation kit (Himedia, India).After respective treatments, the cells were collected along with culture medium and sonicated for 5 s. 100 µL of sample and standard were added to labeled tubes. To that 100 µL of sodium dodecyl sulfate (SDS) and 4 mL of coloring reagent were added. Then tubes were boiled for 1 h and were placed in an ice bath for 10 min to stop the reaction. After incubation, it was centrifuged for 10 min at $1600 \times g$ at 4 °C and incubated at room temperature for 30 min. From this 150 µL of samples were transferred to plate and absorbance was read at 530 nm in a plate reader.

2.7. Estimation of protein carbonyl content

Protein carbonyl content was determined using assay kit (Cayman, USA). Briefly, after respective treatments, cells were collected and homogenized on ice in 1–2 mL of cold buffer (50 mM phosphate buffer, pH 6.7 containing 1 mM EDTA). After centrifugation at $10,000 \times g$ for 15 min at 4 °C, the supernatants were collected. 200 µL of the sample (supernatant) was transferred to 2 mL plastic tubes. 800 µL of DNPH was added to the sample tubes and 800 µL of 2.5 M HCl to the control tube. All the tubes were kept in the dark for 1 h. 1 mL of 20% TCA was added to each tube and vortexed. The samples were centrifuged at $10,000 \times g$ for 10 min at 4 °C, and the supernatant was removed. The pellet was resuspended in 1 mL of 60% TCA. Then it was incubated on ice for 5 min and then centrifuged at $10,000 \times g$ for 10 min at 4 °C. The supernatant was removed, and the pellet was resuspended in 1 mL of (1:1) ethyl acetate/ethanol mixture. It was then vortexed well and centrifuged at $10,000 \times g$ for 1 min at 4 °C. The protein pellet was resuspended in 500 µL of guanidine hydrochloride and vortexed. Again it was centrifuged at $10,000 \times g$ for 10 min at 4 °C to remove any leftover debris. 220 µL of supernatant was taken, and the absorbance was read at 370 nm using a multimode plate reader.

2.8. Activity of superoxide dismutase (SOD)

We evaluated the total SOD activity (cytosolic and mitochondrial components) as detailed in the instructions of a kit (Biovision, USA). The assay depends on utilizing a highly water soluble tetrazolium salt, WST-1 (2-(4-iodophenyl)-3-(4-nitrophenyl) - 5-(2, 4-disulfo-phenyl)-2H-tetrazolium, monosodium salt), which develops a water-soluble formazan dye by reduction with a superoxide anion. The absorbance was read at 450 nm.

2.9. Activity of glutathione peroxidase (GPx)

GPx activity was assayed spectrophotometrically using Cayman assay kit, which is based on reducing the oxidized glutathione coupled to the oxidation of NADPH. The disappearance of NADPH was determined at 340 nm. One unit of GPx activity was defined as the amount of enzyme that can cause the oxidation of NADPH to NADP + per min at 25 °C. The cells after respective treatments were collected by centrifugation ($2000 \times g$) for 10 min at 4 °C. The cell pellets were homogenized in cold buffer (50 mM tris-HCl, pH 7.5, 5 mM EDTA and 1 mM DTT) and centrifuged ($10,000 \times g$) for 15 min at 4 °C. 100 μL of assay buffer, 50 μL of a co-substrate mixture and 20 μL of supernatant were added to the subsequent wells. Then 20 μL of cumene hydroperoxide was added to all wells for initiating the reaction. The absorbance was read at 340 nm.

2.10. Total antioxidant assay

Total antioxidant activity of the samples was assayed as per Cayman protocol. This assay was based on the ability of antioxidants in the sample to inhibit the oxidation of 2, 2′-azino-bis(3-ethylbenzothiazoline-6-sulphonic acid (ABTS*) to reduced ABTS** + by metmyoglobin. The amount of ABTS** + produced was monitored by measuring the absorbance at 405 nm. For performing the assay cells were collected by centrifugation ($2000 \times g$) for 10 min at 4 °C. The pellets were sonicated and centrifuged at $10,000 \times g$ for 15 min at 4 °C. Then 10 μL of the sample (supernatant) and 10 μL of the standard were added in two different wells. 10 μL of metmyoglobin and 150 μL of chromogen were added to both wells. The reaction was initiated by adding hydrogen peroxide. The wells were incubated for 5 min at room temperature, and then absorbance was read at 405 nm.

2.11. Glutathione (GSH) determination

The GSH assay kit (Cayman, USA) utilizes glutathione reductase for the quantification of GSH. Briefly the cell pellets were homogenized in 2 mL of cold buffer and centrifuged at $10,000 \times g$ for 15 min at 4 °C. After that the supernatant was deproteinized. To that 50 μL of standard and sample were added to the designated wells and covered. The assay cocktail mixture containing MES buffer, reconstituted cofactor mixture, enzyme mixture, water and reconstituted DTNB was prepared, and 150 μL of assay cocktail mixture was added to each well containing sample and standard and incubated in the dark on a shaker for 30 min, and the absorbance was measured at 407 nm.

2.12. Quantification of advanced glycated end (AGE) products

The content of AGE protein adducts was determined by enzyme immunoassay kit (Cell Biolabs, Inc, USA). Samples and standard of 50 μL were added to the wells of the AGE conjugate coated plate. It was incubated at room temperature for 10 min on an orbital shaker. To that 50 μL of the diluted anti-AGE antibody was added, incubated at room temperature for 1 h. It was washed with 250 μL of 1X wash Buffer. 100 μL of the diluted secondary antibody-HRP conjugate was added to all wells and incubated for 1 h at room temperature. Then 100 μL of substrate solution was added to each well and incubated at room temperature for 2–20 min. The enzyme reaction was terminated by adding 100 μL of stop solution to each well. The colour development was measured at 450 nm.

2.13. Activity of protein kinase C (PKC)

PKC activity was determined spectrophotometrically by ELISA method (Enzo Lifesciences, USA). In this assay, the substrate was readily phosphorylated by PKC which is precoated on the wells. Briefly samples were added to these wells followed by addition of ATP to initiate the reaction. The plate was incubated for 90 min, and a phosphospecific substrate antibody was added to the wells. The phosphospecific antibody was subsequently bound by a peroxidase conjugated secondary antibody. The colour was developed with TMB in proportion to PKC phosphotransferase activity. The reaction was stopped with the acid solution, and the absorbance was measured at 450 nm.

2.14. Quantification of atrial natriuretic peptide(ANP)

ANP was quantified using the assay kit from Elabscience, USA. Briefly, the cells were washed with precooled PBS and trypsinized. The cells were centrifuged for 5 min. The pellet was washed with PBS and centrifuged for 10 min, and the supernatants were collected. 50 μL of samples were added to each well. To this, 50 μL of biotinylated detection antibody working solution was added. Then it was incubated for 45 min at 37 °C. After decanting, 350 μL of wash buffer was added. Then it was soaked for 1 min, and the solution was aspirated. 100 μL of HRP conjugate solution was added to each well and incubated for 30 min at 37 °C. The solution was aspirated again and 90 μL of substrate reagent was added to each well and incubated for about 15 min at 37 °C. Finally 50 μL of stop solution was added, and the absorbance was measured at 450 nm.

2.15. Western blotting

Immunoblotting was used to analyze the expression of SOD1, SOD2, PKC α, ERK1/2, pERK1/2 and β actin proteins. Cells were seeded in a T25 flask containing 5 mL of DMEM medium and treatments were carried out. At the end of the treatments, the cells were harvested and lysed with ice-cold RIPA buffer containing a protease inhibitor cocktail and the homogenate was centrifuged at $10,000 \times g$ for 15 min at 4 °C. Total protein in the supernatant was quantified using a BCA protein assay kit. Total protein (40 μg) from each sample was separated by 10% SDS-PAGE at 55 V. 25 μL of experimental samples was loaded into each wells. The protein in the gel was transferred into PVDF membrane using Trans-Blot Turbo™ (BioRad, USA). The membrane was blocked with BSA in Tris buffered saline-Tween 20 (TBST) for 1 h at room temperature, and then incubated with the specific primary antibodies (1:1000), and actin (1:1000) in 1% BSA in TBST with gentle agitation at 4 °C overnight. The incubation was followed by 3 times wash with TBST for 10 min in a shaker, followed by addition of HRP-conjugated secondary antibodies (1:1000) in 0.25% BSA in TBST for 60 min at room temperature with shaking. After three washes with TBST, the membranes were developed using Clarity ™ Western ECL substrate (BioRad, USA) and the relative intensity of bands was quantified using Bio-Rad Quantity One version 4.5 software in a Bio-Rad gel documentation system.

2.16. Statistical analysis

All experiments were performed in sextuplicates (n = 6). Data were reported as mean ± SD. The data were subjected to one-way analysis of variance (ANOVA) and the significance of differences between means was calculated by Duncan's multiple range tests using SPSS for windows, standard version 7.5.1, and the significance accepted at p ≤ 0.05
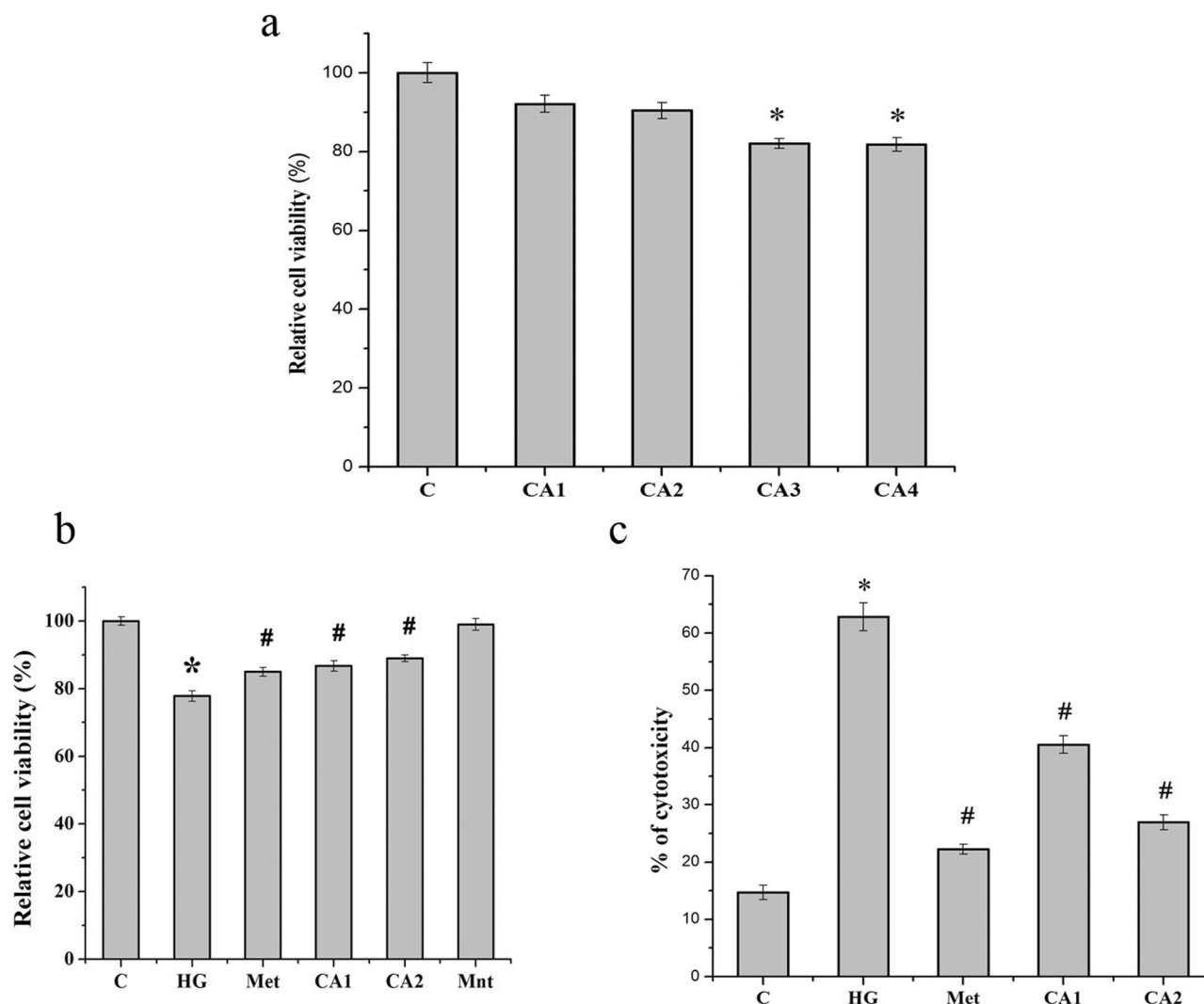
Fig. 1. MTT assay a) H9c2 cells were treated with different concentrations of chlorogenic acid (10 μM, 30 μM, 50 μM, 75 μM). C- Control (5.5 mM glucose), Control + CA1- chlorogenic acid (10 μM), CA2- Control + chlorogenic acid (30 μM), CA3- Control + chlorogenic acid (50 μM), CA4- Control + chlorogenic acid (75 μM) b) Cell death in H9c2 cells after treatment with 33 mM glucose (high glucose) C- Control (5.5mM glucose), HG-High glucose treated group (33 mM glucose), Met – High glucose treated cells + Metformin (1 mM), CA1 – High glucose treated cells + chlorogenic acid (10 μM), CA2 - High glucose treated cells + chlorogenic acid (30 μM), Mnt- mannitol treated group (33 mM mannitol). Values are expressed as mean ± SEM where n = 6. *p ≤ 0.05 significantly different from the control group. #p ≤ 0.05 significantly different from HG treated group. c) Lactate Dehydrogenase (LDH) release C- Control (5.5 mM glucose), HG-High glucose treated group(33 mM glucose), Met – High glucose treated cells + Metformin (1 mM), CA1 – High glucose treated cells + chlorogenic acid (10 μM), CA2 - High glucose treated cells + chlorogenic acid (30 μM). Values are expressed as mean ± SEM where n = 6. *p ≤ 0.05 significantly different from the control group. #p ≤ 0.05 significantly different from HG treated group.

3. Results

3.1. Cytoprotective effect of CA

In order to select an ideal dose of CA, cell viability was checked with 10 μM, 30 μM, 50 μM and 75 μM of the same. We selected 10 μM and 30 μM based on results (for data, please see Fig. 1a).

3.2. Effect of CA on HG induced cell death

Incubation of H9c2 cells with 33 mM glucose (HG) caused significant cell death (1.32 fold; p ≤ 0.05; Fig. 1b) for 48 h of incubation. Interestingly CA of 10 μM and 30 μM concentrations or metformin (1 mM) significantly (p ≤ 0.05) improved (1.2, 1.27 and 1.18 fold respectively) cell viability compared to HG group (Fig. 1b)

3.3. LDH release

LDH release to the medium is a significant marker of cardiac cell

death. There was a significant increase in LDH release in HG (4.27 fold ; Fig. 1c) compared to control while with CA, LDH release was reduced by 1.5 and 2.33 fold (p ≤ 0.05) for 10 μM and 30 μM respectively compared to HG treated cells, indicating the cytoprotective potential of CA (Fig. 1c). Metformin also reduced the release of LDH by 2.82 fold (p ≤ 0.05) compared to HG cells.

3.4. Intracellular ROS generation during hyperglycemia

To check the effect of hyperglycemia on redox status, the amount of ROS was quantified using DCFDA. There was a significant increase (p ≤ 0.05) in the ROS levels during hyperglycemia (4 fold; Fig. 2a). ROS was found reduced upon treatment with CA (1.63 and 1.88 for 10 μM and 30 μM) in a dose-dependent manner compared to HG and 2.105 fold for metformin respectively, (p ≤ 0.05; Fig. 2a and b)

3.5. Lipid peroxidation during hyperglycemia

High glucose treatment increased lipid peroxidation (MDA level) by

a

b
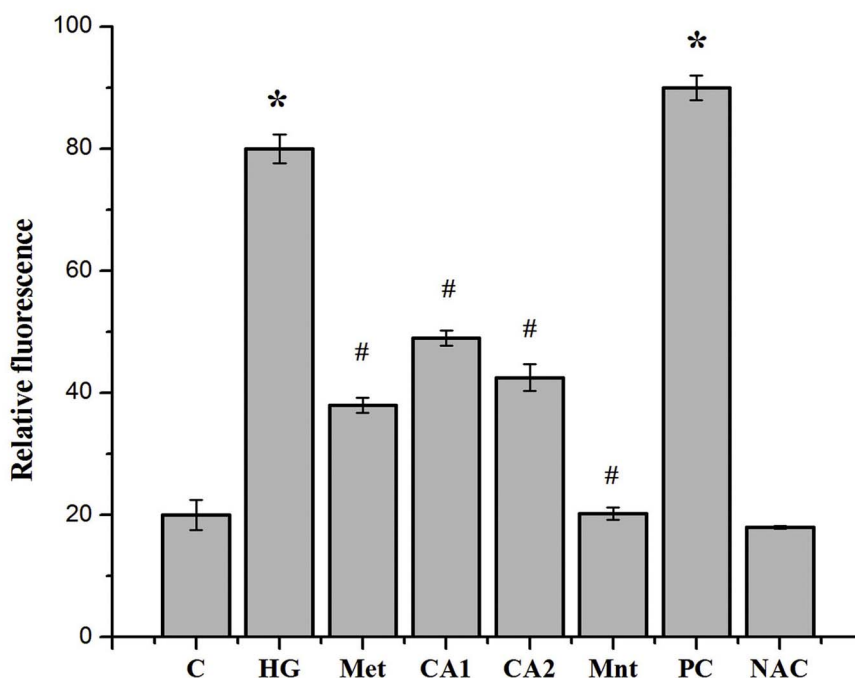
Fig. 2. Intracellular Reactive Oxygen Species generation determined using DCFDA (a) Reactive oxygen species generation in various groups (a) Control, (b) high glucose treated group, (c) HG + metformin, (d) HG + chlorogenic acid (10 μM), (e) HG + chlorogenic acid (30 μM), Scale bar corresponds to 100 μm. (b). Relative fluorescent intensity of the fluorescent images. C-Control (5.5 mM glucose), HG-High glucose treated group (33 mM glucose), Met – High glucose treated cells + Metformin (1 mM), CA1 – High glucose treated cells + chlorogenic acid (10μM), CA2 - High glucose treated cells + chlorogenic acid (30 μM), Mnt- mannitol treated group (33mM mannitol), PC (Control + 300 μM H_2O_2), NAC (Control + 1 mM n acetyl cysteine). Values are expressed as mean ± SEM where n = 6. *$p \leq 0.05$ significantly different from the control group. #$p \leq 0.05$ significantly different from HG treated group.

a

b

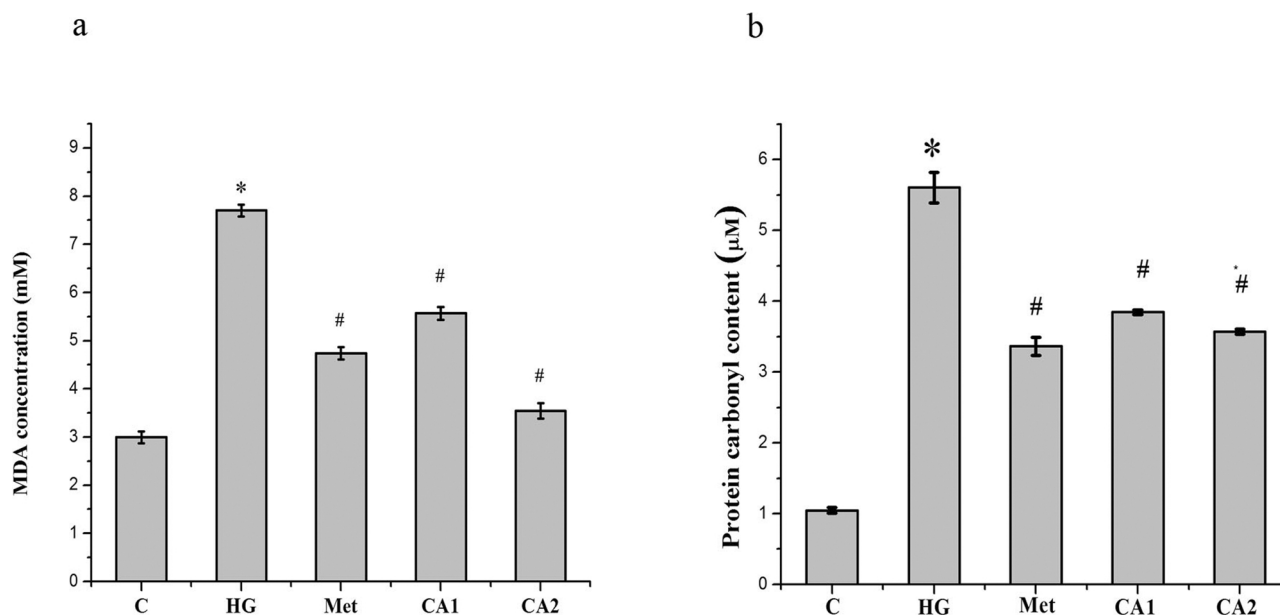**Fig. 3.** a) Level of malondialdehyde (MDA) generation in different groups C- Control (5.5 mM glucose), HG-High glucose treated group(33 mM glucose), Met – High glucose treated cells + Metformin (1 mM), CA1 – High glucose treated cells + chlorogenic acid (10 μM), CA2 - High glucose treated cells + chlorogenic acid (30 μM). Values are expressed as mean ± SEM where n = 6. * p ≤ 0.05 significantly different from the control group. #p ≤ 0.05 significantly different from HG treated group. b) Estimation of protein carbonyl content C- Control (5.5 mM glucose), HG-High glucose treated group (33 mM glucose), Met – High glucose treated cells + Metformin (1 mM), CA1 – High glucose treated cells + chlorogenic acid (10 μM), CA2 - High glucose treated cells + chlorogenic acid (30 μM). Values are expressed as mean ± SEM where n = 6. *p ≤ 0.05 significantly different from the control group. #p ≤ 0.05 significantly different from HG treated group.

2.5 fold compared to control (p ≤ 0.05, Fig. 3a). Treatment with CA significantly decreased MDA levels by 1.38 and 2.17 fold at 10 μM and 30 μM (p ≤ 0.05) respectively compared to HG indicating protection against oxidative stress during hyperglycemia. Metformin treatment also reduced MDA levels significantly by 1.6 fold (p ≤ 0.05) compared to HG (Fig. 3a).

3.6. Protein oxidation in high glucose treated cardiomyoblast

Oxidative stress is associated with protein oxidation and the concentration of protein carbonyls was also significantly higher (5.3 fold; p ≤ 0.05, Fig. 3b) with HG. CA co-treatment significantly reduced the concentration of protein carbonyls by 1.45 fold and 1.56 fold for 10 μM and 30 μM when compared to HG. Metformin treatment also decreased protein carbonyl level significantly (p ≤ 0.05; 1.6 fold reduction compared to HG treated cells; Fig. 3b).

3.7. Effect of hyperglycemia on endogenous antioxidant system

Alteration in innate antioxidant status (SOD, GPx, GSH, and total antioxidant activity) of the cell during hyperglycemia was studied. Activities of SOD and GPx were significantly (p ≤ 0.05) reduced by 1.3 fold and 1.79 fold respectively during hyperglycemia (Figs. 4a and 5a).CA co-treatment improved innate antioxidant enzymes activity in a significant manner. 10 μM and 30 μM of CA caused 1.3 and 1.4 fold increase of SOD, and for GPx, CA caused 1.8 and 1.92 fold increase respectively (Figs. 4a and 5a). SOD1 (Cu Zn SOD) and SOD2 (MnSOD) protein expression were also reduced significantly (p ≤ 0.05, Fig. 4b) in HG treated cells when compared with control (1.14 and 5.5 fold respectively). CA or metformin resumed the protein levels of SOD1 (1.15, 1.334 and 1.06 for 10 μM and 30 μM of CA and metformin respectively; p ≤ 0.05; Fig. 4b and c) and SOD2 (4.21, 4.9 and 3.38 for 10 μM and 30 μM of CA and metformin respectively; p ≤ 0.05; Fig. 4b and c) in a significant manner. We also evaluated total antioxidant capacity during hyperglycemia. There was significant (p ≤ 0.05) reduction in antioxidant capacity in HG treated cells (1.3 fold; Fig. 5b) compared to control while CA significantly improved total antioxidant capacity

(1.04 and 1.32 for 10 μM and 30 μM of CA; p ≤ 0.05; Fig. 5b). Depletion of GSH, a non-enzymatic antioxidant was also studied. In HG treated cells, there was significant depletion of GSH (8.27 fold; Fig. 5c) compared to control while treatment with CA prevented the reduction of GSH significantly relative to HG treated cells (5.9 and 6.8 for 10 μM and 30 μM of CA; p ≤ 0.05; Fig. 5c). Metformin also improved GSH significantly (7.52 fold; p ≤ 0.05; Fig. 5c).

3.8. Production of AGE during hyperglycemia

During hyperglycemia, there were elevated levels of AGE products (2.18 fold increase compared to control; p ≤ 0.05, Fig. 5d). While CA at 10 μM and 30 μM decreased the level of AGE by 1.34 and 1.54 fold (p ≤ 0.05) respectively compared to HG (Fig. 5d). Metformin also decreased the AGE content by 1.8 fold with respect to HG.

3.9. Activity of PKC during hyperglycemia

High glucose treated cells showed an enhanced activity of PKC by 2.6 fold (p ≤ 0.05; Fig. 6a) compared to control whereas CA ameliorated the activity of PKC significantly (1.99 and 2.16 fold for 10 μM and 30 μM CA; p ≤ 0.05) compared to HG treated cells. Metformin also reduced the activity of PKC by 2.33 fold as compared to hyperglycemia group (Fig. 6a).

3.10. PKCα and phosphorylation of ERK1/2

Western blot analysis performed for PKC α showed the expression of PKC α isoform in the lysate was increased by 1.31 fold (Fig. 6b and c) in the hyperglycemic groups compared with the control groups. CA treatment had a mitigatory effect and showed decreased levels of PKC α compared to HG cells in a significant manner (1.17 and 1.36 for 10 μM and 30 μM of CA compared to hyperglycemia group, p ≤ 0.05, Fig. 6b and c). The activation state of ERK1/2 was evaluated in different groups using the ratio of phosphorylated ERK1/2 to total ERK1/2. In HG treated cells, phosphorylated ERK1/2 to total ERK1/2 ratio was increased by 1. 43-fold (Fig. 6b and d) compared with those in control
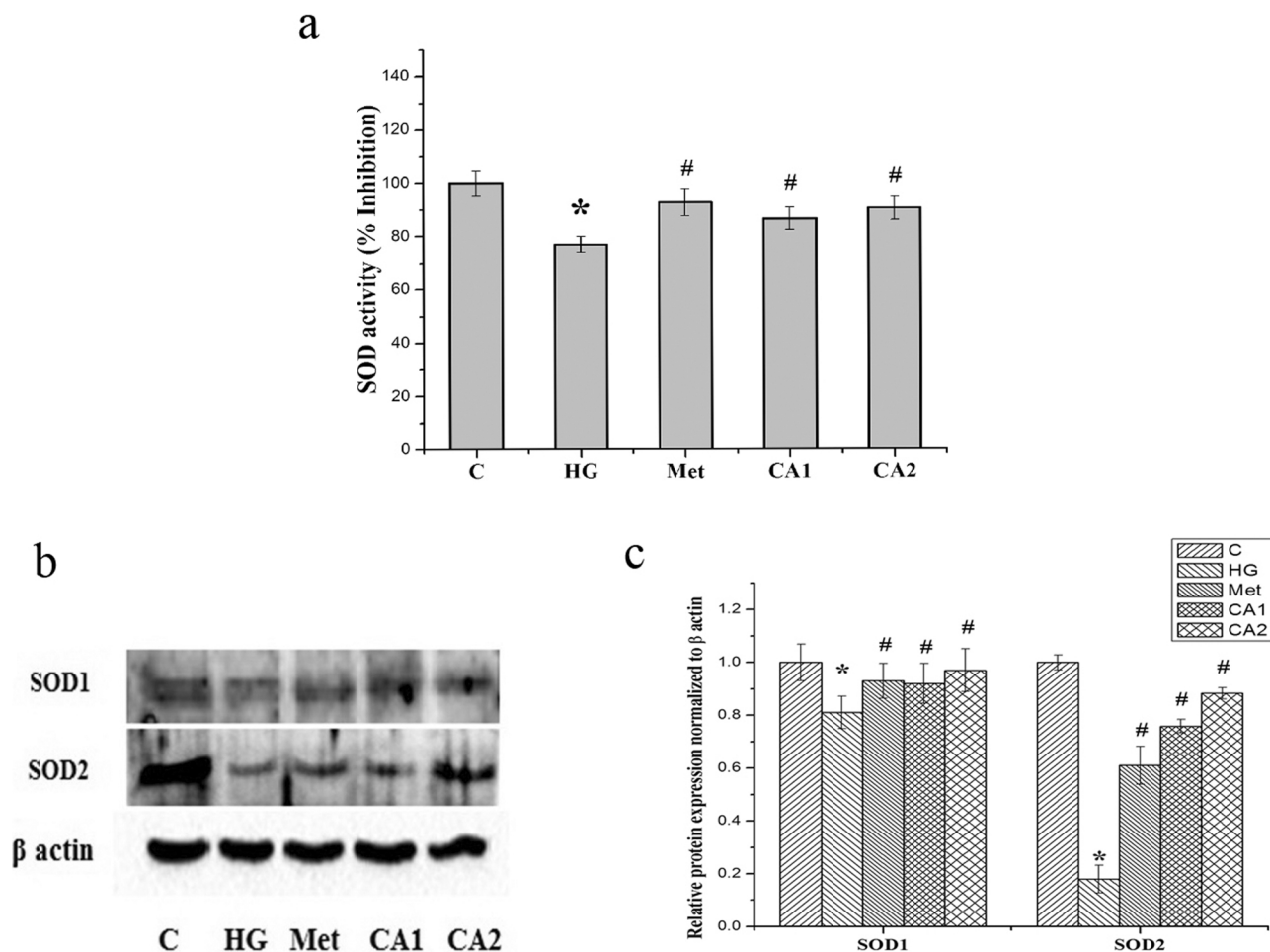
Fig. 4. (a) Activity of SOD during hyperglycemia (b) Immunoblot analysis of SOD1 and SOD2 (c) Densitometric analysis of SOD1 and SOD2C- Control (5.5 mM glucose), HG-High glucose treated group(33 mM glucose), Met – High glucose treated cells + Metformin (1 mM), CA1 – High glucose treated cells + chlorogenic acid (10 µM), CA2 - High glucose treated cells + chlorogenic acid (30 µM). Values are expressed as mean ± SEM where n = 6. *p ≤ 0.05 significantly different from the control group. #p ≤ 0.05 significantly different from HG treated group.

groups (p ≤ 0.05), whereas treatment with CA resulted in normalized activation states of pERK1/2 compared with HG treated groups (1.13 and 1.25 for 10 µM and 30 µM of CA compared to hyperglycemia group, p ≤ 0.05) ; Fig. 6b and d). Metformin resumed the protein levels in a significant manner relative to HG treated cells (1.11 for PKC α and 1.29 for pERK1/2 /ERK1/2, p ≤ 0.05; Fig. 6b–d)

3.11. Detection of ANP

There was a significant increase (p ≤ 0.05) in ANP levels in HG group (3.49 fold; Fig. 7). Co-treatment with CA at 10 µM and 30 µM reduced ANP levels significantly (p ≤ 0.05) by 2.14 and 2.35 fold respectively compared to HG. Treatment with metformin also significantly (p ≤ 0.05) reduced ANP levels by 2.53 fold compared to HG (Fig. 7).

4. Discussion

Diabetes mellitus is a developing public health issue that needs to be tackled at multiple levels. For this, prevention and management of associated comorbidities such as CVD, neuropathy and nephropathy is of paramount importance. CVD remains the prominent cause of mortality and morbidity with diabetes [1]. The role of hyperglycemic oxidative stress in the development of DCM is a fact and is under extensive investigation for prevention and management of diabetic CVD [28,29]. H9c2 cell line is our *in vitro* model which mimics almost all electrical

and biochemical features of adult cardiac myocytes [30]. Many effective interventions through antioxidant property of both natural and synthetic origin are recommended for attenuating oxidative stress associated cardiac complications [31], but it is still an unmet need. So this is a burning health issue and need to be researched from various corners for better therapeutic outcome due to the involvement of pleiotropic pathways in the genesis of oxidative stress in cardiovascular system [32]. The emerging importance of AGE in cardiac health during diabetes has attracted the attention of basic scientists and cardiologists recently [33]. The exact role of AGE in inducing cardiac dysfunction has not been studied yet in detail for therapeutic intervention. In the present investigation, studies were conducted in an integrated way with special emphasis on innate antioxidant status, glycation, signaling pathways like PKC and ERK and to reveal their cumulative contribution to cardiac injury. This approach is expected to generate data for identification of a novel druggable target for DCM.

The initial observation revealed the surplus generation of ROS with hyperglycemia. So in order to identify the various factors associated with ROS in evoking cardiac pathology detailed investigation was done on the innate antioxidant status of H9c2 cells. Maintenance of adequate antioxidant levels is crucial to prevent or even manage a significant number of diseases of stress. Total antioxidant capacity reflects as a biomarker of disease in biochemistry, medicine, food and nutritional sciences [34]. The major enzymatic innate antioxidants include SOD and GPx. As a major antioxidant enzyme family, superoxide dismutases (SODs), including copper-zinc superoxide dismutase (SOD1, Cu/
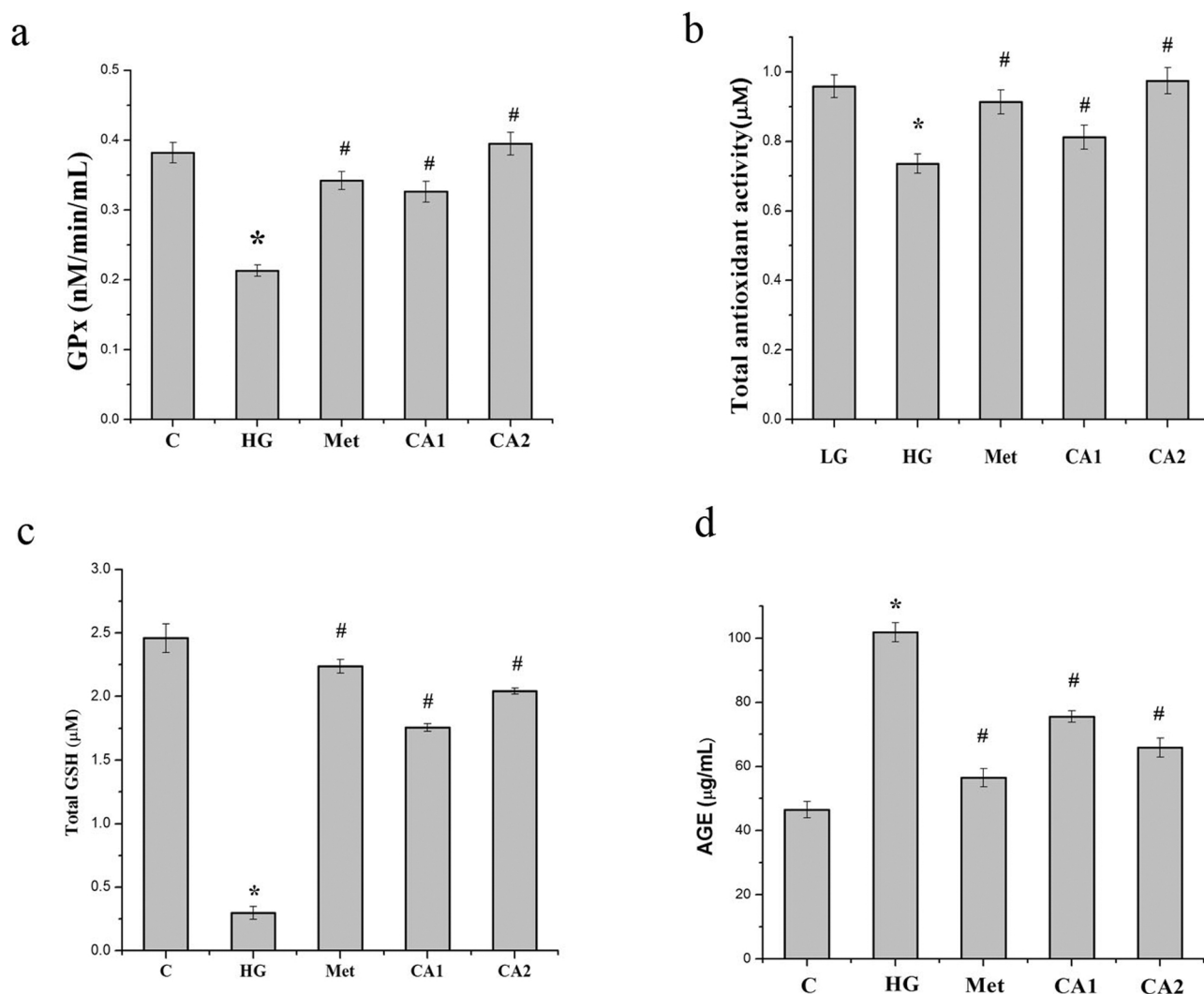
Fig. 5. a) Glutathione peroxidase (GPx) activity C- Control (5.5 mM glucose), HG-High glucose treated group (33 mM glucose), Met – High glucose treated cells + Metformin (1 mM), CA1 – High glucose treated cells chlorogenic acid (10 μM), CA2 - High glucose treated cells + chlorogenic acid (30 μM). Values are expressed as mean ± SEM where n = 6. *p ≤ 0.05 significantly different from the control group. #p ≤ 0.05 significantly different from HG treated group. b) Total antioxidant activity during hyperglycemia C- Control (5.5mM glucose), HG-High glucose treated group (33 mM glucose), Met – High glucose treated cells + Metformin (1 mM), CA1 – High glucose treated cells + chlorogenic acid (10 μM), CA2 - High glucose treated cells + chlorogenic acid (30 μM). Values are expressed as mean ± SEM where n = 6. *p ≤ 0.05 significantly different from the control group. #p ≤ 0.05 significantly different from HG treated group. c) Determination of total glutathione (GSH) levels C- Control (5.5 mM glucose), HG-High glucose treated group (33 mM glucose), Met – High glucose treated cells + Metformin (1 mM), CA1 – High glucose treated cells + chlorogenic acid (10 μM), CA2 - High glucose treated cells + chlorogenic acid (30 μM). Values are expressed as mean ± SEM where n = 6. *p ≤ 0.05 significantly different from the control group. #p ≤ 0.05 significantly different from HG treated group. d) Estimation of advanced glycated end (AGE) content C- Control (5.5mM glucose), HG-High glucose treated group (33 mM glucose), Met – High glucose treated cells + Metformin (1 mM), CA1 – High glucose treated cells + chlorogenic acid (10 μM), CA2 - High glucose treated cells + chlorogenic acid (30 μM). Values are expressed as mean ± SEM where n = 6. *p ≤ 0.05 significantly different from the control group. #p ≤ 0.05 significantly different from HG treated group.

ZnSOD) and manganese superoxide dismutase (SOD2, MnSOD) play a pivotal role in scavenging free radicals. SOD catalyzes the conversion of superoxide anion radicals produced in the body to hydrogen peroxide, thereby reducing the feasibility of interaction of superoxide anion with nitric oxide to form reactive peroxynitrite [35]. The mechanism of conversion of $O_2 \cdot -$ to H_2O_2 by SOD consists alternate oxidation and reduction of a redox active transition metal, such as copper (Cu) and manganese (Mn) at the active site of the enzyme [36]. Because of the sectional localization of each SOD, proposals to target their site-specific expression will be very important and could be used in the development of novel SOD-dependent therapeutics [37]. It is worth to note that over expression of MnSOD ultimately prevented an increase in polyol pathway flux, increased intracellular AGE formation, increased PKC activation and an increase in hexosamine pathway activity in endothelial cells [38]. This reveals the significant role of SOD during stress. This report was our inspiration to see in detail the alteration of MnSOD & CuSOD in H9c2 cells during hyperglycemia, and our finding

in H9c2 cells are in accordance with Michael Brownlee, 2001 [38] and we found significant down regulation of protein and activity level with hyperglycemia. GPx/GSH system is important in oxidative stress [39]. GPx is located in the cytoplasm, mitochondria, and nucleus. It metabolizes hydrogen peroxide to water by using reduced glutathione as a hydrogen donor [40,41]. It is a major intracellular redox scavenger system. GSH acts as a substrate for other detoxifying enzymes against oxidative stress, such as GSH transferases [42]. The impact of oxidative stress is clearly visible with depletion of GSH in the present study with HG.

Lipids are reported as one of the vital targets of ROS. ROS oxidize the lipids to generate peroxides and aldehydes. Lipid peroxidation products are tangled in the transcriptional regulation of innate antioxidant systems [39]. Lipid peroxidation products have been observed in many inflammatory complications including cardiovascular disorders [43] and can serve as a marker for the risk of CVD [44]. Lipid peroxidation was found increased with hyperglycemia. This is expected
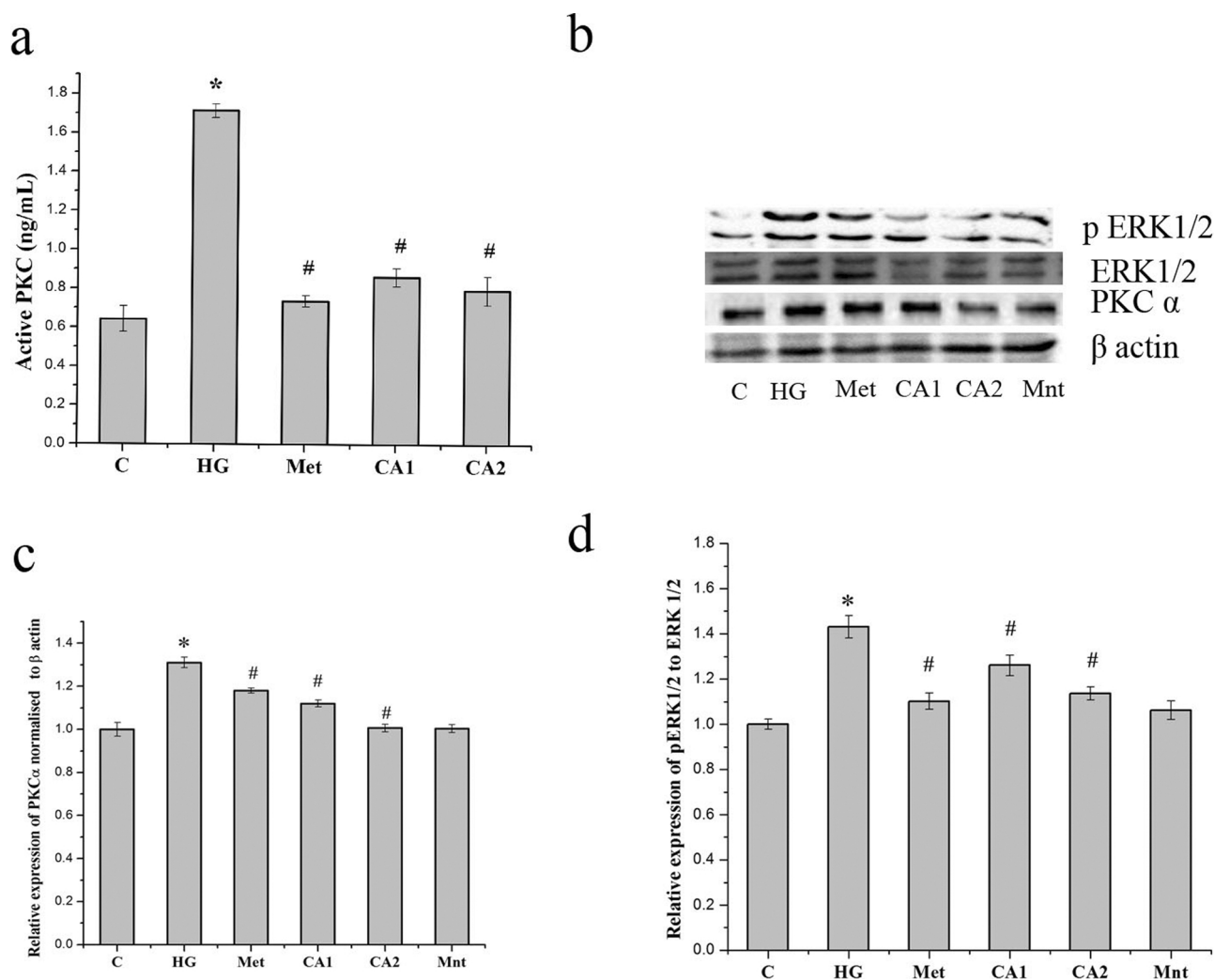
Fig. 6. Studies on protein kinase C (PKC) activation in various experimental groups(a) PKC Activity; (b) Immunoblot analysis of PKC α, ERK, pERK, β actin; (c) Densitometric analysis of protein expression of PKC α with respect to β-actin (d) Densitometric analysis of relative expression of pERK1/2 to ERK1/2 C- Control (5.5 mM glucose), HG-High glucose treated group (33 mM glucose), Met – High glucose treated cells + Metformin (1 mM), CA1 – High glucose treated cells + chlorogenic acid (10 μM), CA2 - High glucose treated cells + chlorogenic acid (30 μM), Mnt- mannitol treated group (33 mM mannitol). Values are expressed as mean ± SEM where n = 6. *p ≤ 0.05 significantly different from the control group. #p ≤ 0.05 significantly different from HG treated group.

to amplify the severity of complications of oxidative stress in myoblast and contribute significantly to the pathogenesis of DCM most probably through activation of various signaling pathways like PKC α and ERK axis [45].

AGE content has been shown to be a biomarker for the DCM [46] individualistic from other well-known risk factors such as hyperlipidemia, hypertension, and smoking. AGEs are reported to cause serious complications on the myocardium via cross linking of extracellular cardiac proteins and actions mediated by AGE receptors expressed on the myocardium [47–49]. They have been linked to systolic and diastolic cardiac dysfunction in diabetics. There are now emerging evidences that glycation induces oxidative stress and vice versa [50]. Physiologically sustained exposure of proteins to glucose for a long time causes them to undergo a series of non-enzymatic reaction and forms AGEs. It may change the structure and function of cardiac antioxidant enzymes such that they are unable to detoxify free radicals, exacerbating oxidative stress [35]. We found a significant increase in AGE content in cell lysate revealing hyperglycemia induced AGE formation in H9c2 cells. This result gives an idea to explore the possibilities of development of antiglycation agents as therapeutics for hyperglycemia induced cardiac complications. For a better scientific basis for this idea, the details of cross talk between glycation and other pathways relevant

to cardiac function are very important. So efforts were made to study alterations in PKC α -ERK axis which has strong link with AGE formation and associated complications [51] in the myocardium.

PKC represents a family of more than 11 phospholipid-dependent ser/thr kinases that are entangled in a variety of pathways that regulate cell death, growth, and stress responsiveness [52]. Some isoforms of PKC family that are particularly influencing redox stress are incriminated in CVD [53]. In the heart, PKC activation leads to rapid changes in contractility performance [54]. During hyperglycemia, there is preferential activation of PKC α and PKC βI/2 isoforms in the heart and aorta [55]. We found a significant increase in activity of PKC during hyperglycemia. In addition, we also found the overexpression of isoform of PKC (PKC α) and phosphorylated ERK1/2 with hyperglycemia. Activation of PKC-ERK axis during hyperglycemia has been reported by various researchers too. There are reports to connect that oxidative stress and AGE cause overexpression of PKC [56]. Based on this information and our own result there is a possibility of cross talk between oxidative stress, AGE and PKC which together contribute to cardiac dysfunction. In order to check injury relevant to human cardiac diagnosis, we analyzed ANP. ANP is a 28-amino acid peptide that is synthesized and released by cardiac cells during any stress for protective adaptation. It is also an important diagnostic serum marker for
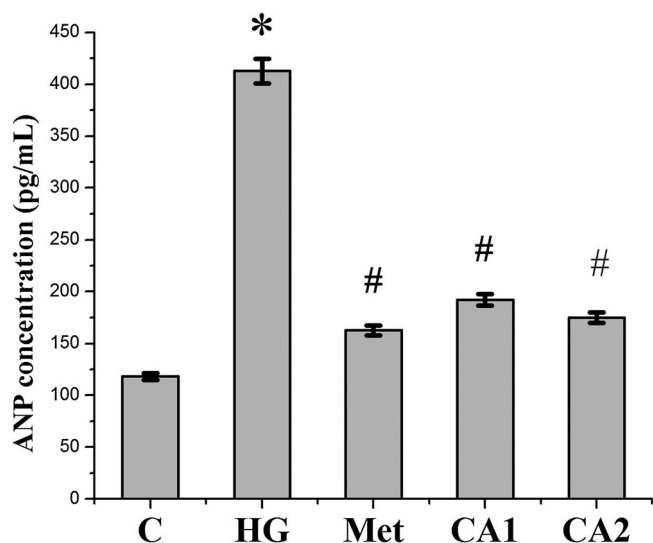
Fig. 7. Quantification of atrial natriuretic peptide (ANP) during hyperglycemia C- Control (5.5 mM glucose), HG-High glucose treated group (33 mM glucose), Met – High glucose treated cells + Metformin (1 mM), CA1 – High glucose treated cells + chlorogenic acid (10 μM), CA2 - High glucose treated cells + chlorogenic acid (30 μM). Values are expressed as mean ± SEM where n = 6. *p ≤ 0.05 significantly different from the control group. #p ≤ 0.05 significantly different from HG treated group.

cardiac injury and health. ANP secretion is a calcium dependent process, initiated by intracellular calcium overload [57]. This cardiac peptide induces cardioprotection by modulating the mPTP opening at reperfusion [58]. Currently the studies based on the correlation between ANP and ROS generation during the development of cardiovascular diseases is limited [59]. During acute hyperglycemia there is a rapid increase of ANP levels in response to sodium and fluid retention [60–62].With hyperglycemia, there was a significant increase in ANP for protective (physiological) adaptation in H9c2 cells revealing the genesis of cardiac stress through various pathway.

CA is one of the most abundant polyphenols found in the human diet. There are not many reports on the beneficial property of CA against any type of cardiac disorder, and so this study is very significant one. We are sure that the potential antioxidant activity of CA contributes significantly to its beneficial activity against hyperglycemia in H9c2 cells. It is reported to have antidiabetic activity through inhibition of glucose-6-phosphate translocase 1 and reduction of the sodium gradient-driven apical glucose transport [62]. These additional properties may be contributing partially to the beneficial activity of CA in this study.

From our findings, we conclude that during hyperglycemia there is an alteration in redox machinery of the cells through cross talk between oxidative stress, glycation, PKC α- ERK axis and CA was found beneficial to cardiac cells against hyperglycemia. The result of this study opens new avenues for research on "glycation -PKC α -ERK axis " for cardiac health during diabetes.

Conflict of interest

The authors declare no conflict of interest.

Acknowledgement

References

[1] Global Reports on Diabetes, WHO, 2016.
[2] B.M. Leon, T.M. Maddox, Diabetes and cardiovascular disease: epidemiology, biological mechanisms, treatment recommendations and future research, World J. Diabetes 6 (13) (2015) 1246–1258.
[3] A. Aneja, W.H. Tang, S. Bansilal, M.J. Garcia, M.E. Farkouh, Diabetic cardiomyopathy: insights into pathogenesis, diagnostic challenges, and therapeutic options, Am. J. Med. 121 (9) (2008) 748–757.
[4] C. Park, E. Guallar, J.A. Linton, et al., Fasting glucose level and the risk of incident atherosclerotic cardiovascular diseases, Diabetes Care 36 (7) (2013) 1988–1993.
[5] A.I. Vinik, T.S. Park, K.B. Stansberry, G.L. Pittenger, Diabetic neuropathies, Diabetologia 43 (2000) 957–973.
[6] R.A. Kowluru, A. Kennedy, Therapeutic potential of anti-oxidants and diabetic retinopathy, Expert Opin. Investig. Drugs 10 (9) (2001) 1665–1676.
[7] B. Turan, N.S. Dhalla, Diabetic Cardiomyopathy Biochemical and Molecular Mechanisms. Advances in Biochemistry in Health and Disease, Springer, New York, 2014.
[8] D. Koya, G. King, Protein kinase C activation and the development of diabetic complications, Diabetes 47 (6) (1998) 859–866.
[9] M.A. Queisser, D. Yao, S. Geisler, et al., Hyperglycemia impairs proteasome function by methylglyoxal, Diabetes 59 (3) (2010) 670–678.
[10] W.C. Duckworth, Hyperglycemia and cardiovascular disease, Curr. Atheroscler. Rep. 3 (5) (2001) 383–391.
[11] F. Giacco, M. Brownlee, Oxidative stress and diabetic complications, Circ. Res. 107 (9) (2010) 1058–1070.
[12] M. Meier, G.L. King, Protein kinase C activation and its pharmacological inhibition in vascular disease, Vasc. Med. 5 (3) (2000) 173–185.
[13] H.S. Hahn, Y. Marreez, A. Odley, et al., Protein kinase C α negatively regulates systolic and diastolic function in pathological hypertrophy, Circ. Res. 93 (11) (2003) 1111–1119.
[14] Z. Xu, J. Sun, Q. Tong, et al., The role of ERK1/2 in the development of diabetic cardiomyopathy, Int. J. Mol. Sci. 17 (12) (2016) 2001.
[15] C.R. Triggle, H. Ding, Cardiovascular impact of drugs used in the treatment of diabetes, Ther. Adv. Chronic Dis. 5 (6) (2014) 245–268.
[16] S. Suroowan, F. Mahomoodally, Common phyto-remedies used against cardiovascular diseases and their potential to induce adverse events in cardiovascular patients, Clin. Phytosci. 1 (1) (2015) 1–13.
[17] A. Farah, C.M. Donangelo, Phenolic compounds in coffee, Braz. J. Plant Physiol. 18 (1) (2006) 23–36.
[18] M.N. Clifford, Chlorogenic acids and other cinnamates—nature, occurrence and dietary burden, J. Sci. Food Agric. 79 (3) (1999) 362–372.
[19] M.P. Gonthier, M.A. Verny, C. Besson, C. Rémésy, A. Scalbert, Chlorogenic acid bioavailability largely depends on its metabolism by the gut microflora in rats, J. Nutr. 133 (6) (2003) 1853–1859.
[20] T. Mahmood, F. Anwar, M. Abbas, N. Saari, Effect of maturity on phenolics (phenolic acids and flavonoids) profile of strawberry cultivars and mulberry species from Pakistan, Int. J. Mol. Sci. 13 (4) (2012) 4591–4607.
[21] T. Watanabe, Y. Arai, Y. Mitsui, et al., The blood pressure-lowering effect and safety of chlorogenic acid from green coffee bean extract in essential hypertension, Clin. Exp. Hypertens. 28 (5) (2006) 439–449.
[22] H. Kasai, S. Fukada, Z. Yamaizumi, S. Sugie, H. Mori, Action of chlorogenic acid in vegetables and fruits as an inhibitor of 8-hydroxydeoxyguanosine formation in vitro and in a rat carcinogenesis model, Food Chem. Toxicol. 38 (5) (2000) 467–471.
[23] Y. Kono, K. Kobayashi, S. Tagawa, et al., Antioxidant activity of polyphenolics in diets rate constants of reactions of chlorogenic acid and caffeic acid with reactive species of oxygen and nitrogen, Biochim. Biophys. Acta 1335 (3) (1997) 335–342.
[24] S. Meng, J. Cao, Q. Feng, J. Peng, Y. Hu, Roles of chlorogenic acid on regulating glucose and lipids metabolism: a review, Evid. Based Complement. Alternat. Med. 2013 (2013) 801457.
[25] P.L. Reshma, V.S. Lekshmi, V. Sankar, K.G. Raghu, Tribulus terrestris (Linn.) attenuates cellular alterations induced by ischemia in H9c2 cells via antioxidant potential, Phytother. Res. 29 (6) (2015) 933–943.
[26] A.P. Wilson, Cytotoxicity and viability assays, in: J.R.W. Masters (Ed.), Animal Cell Culture, Oxford University, Oxford, 2000, pp. 175–219.
[27] S.W. Choi, I.F. Benzie, S.W. Ma, et al., Acute hyperglycemia and oxidative stress: direct cause and effect, Free Radic. Biol. Med. 44 (7) (2008) 1217–1231.
[28] H. Kaneto, N. Katakami, M. Matsuhisa, T.A. Matsuoka, Role of reactive oxygen species in the progression of type 2 diabetes and atherosclerosis, Mediators Inflamm. 2010 (2010) 453892.
[29] H. Tsutsui, S. Kinugawa, S. Matsushima, Oxidative stress and heart failure, Am. J. Physiol. Heart Circ. Physiol. 301 (6) (2011) H2181–H2190.
[30] A.V. Kuznetsov, S. Javadov, S. Sickinger, et al., H9c2 and HL-1 cells demonstrate distinct features of energy metabolism, mitochondrial function, and sensitivity to hypoxia-reoxygenation, Biochim. Biophys Acta 1853 (2) (2015) 276–284.
[31] M.F. Hill, Emerging role for antioxidant therapy in protection against diabetic cardiac complications: experimental and clinical evidence for utilization of classic and new antioxidants, Curr. Cardiol. Rev. 4 (4) (2008) 259–268.
[32] R.F. Mapanga, M.F. Essop, Damaging effects of hyperglycemia on cardiovascular function: spotlight on glucose metabolic pathways, Am. J. Physiol. Heart Circ. Physiol. 310 (2016) H153–H173.
[33] E. Baye, M.P. de Courten, K. Walker, et al., Effect of dietary advanced glycation end products on inflammation and cardiovascular risks in healthy overweight adults: a randomized crossover trial, Sci. Rep. 7 (2017) 4123.
[34] C. Kusano, B. Ferrari, Total antioxidant capacity: a biomarker in biomedical and nutritional studies, J. Cell. Mol. Biol. 7 (1) (2008) 1–15.
[35] A.C. Maritim, A. Sanders, J.B. Watkins III, Diabetes, oxidative stress, and antioxidants: a review, J. Biochem. Mol. Toxicol. 17 (1) (2003) 24–38.
[36] T. Fukai, M. Ushio-Fukai, Superoxide Dismutases: role in redox signaling, vascular function, and diseases, Antioxid. Redox Signal. 15 (6) (2011) 1583–1606.

[37] I.N. Zelko, T.J. Mariani, R.J. Folz, Superoxide dismutase multigene family: a comparison of the CuZn-SOD (SOD1), Mn-SOD (SOD2), and EC-SOD (SOD3) gene structures, evolution, and expression, Free Radic. Biol. Med. 33 (3) (2002) 337–349.

[38] M. Brownlee, Biochemistry and molecular cell biology of diabetic complications, Nature 414 (2001) 813–820.

[39] C. Espinosa-Diez, V. Miguel, D. Mennerich, T. Kietzmann, P. Sánchez-Pérez, S. Cadenas, S. Lamas, Antioxidant responses and cellular adjustments to oxidative stress, Redox Biol. 6 (2015) 183–197.

[40] H. Sies, Glutathione and its role in cellular functions, Free Radic. Biol. Med. 27 (9) (1999) 916–921.

[41] S.A. Santini, G. Marra, B. Giardina, et al., Defective plasma antioxidant defenses and enhanced susceptibility to lipid peroxidation in uncomplicated IDDM, Diabetes 46 (11) (1997) 1853–1858.

[42] S. Jurkovič, J. Osredkar, J. Marc, Molecular impact of glutathione peroxidases in antioxidant processes, Biochem. Med. 18 (2) (2008) 162–174.

[43] K.V. Ramana, S. Srivastava, S.S. Singhal, Lipid peroxidation products in human health and disease, Oxid. Med. Cell. Longev. 2013 (2013) 583438.

[44] A. Trpkovic, I. Resanovic, J. Stanimirovic, et al., Oxidized low-density lipoprotein as a biomarker of cardiovascular diseases, Crit. Rev. Clin. Lab Sci. 52 (2) (2015) 70–85.

[45] A.A. Von Ruecker, B.G. Han-Jeon, M. Wild, F. Bidlingmaier, Protein kinase C involvement in lipid peroxidation and cell membrane damage induced by oxygen-based radicals in hepatocytes, Biochem. Biophys. Res. Commun. 163 (2) (1989) 836–842.

[46] F.K. Yeboah, I. Alli, V.A. Yaylayan, et al., Effect of limited solid-state glycation on the conformation of lysozyme by ESI-MSMS peptide mapping and molecular modeling, Bioconjug. Chem. 15 (2004) 27–34.

[47] K.R. Bidasee, K. Nallani, Y. Yu, et al., Chronic diabetes increases advanced glycation end products on cardiac ryanodine receptors/calcium-release channels, Diabetes 52 (7) (2003) 1825–1836.

[48] K.R. Bidasee, Y. Zhang, C.H. Shao, et al., Diabetes increases the formation of advanced glycation end products on Sarco(endo)plasmic reticulum Ca2 + -ATPase, Diabetes 53 (2) (2004) 463–473.

[49] S.J. Zieman, D.A. Kass, Advanced glycation end product crosslinking in the cardiovascular system: potential therapeutic target for cardiovascular disease, Drugs 64 (3) (2004) 459–470.

[50] E. Schleicher, U. Friess, Oxidative stress, AGE, and atherosclerosis, Kidney Int. Suppl. 106 (2007) S17–S26.

[51] V. Thallas-Bonke, S.R. Thorpe, M.T. Coughlan, et al., Inhibition of NADPH oxidase prevents advanced glycation end product-mediated damage in diabetic nephropathy through a protein kinase C-dependent pathway, Diabetes 57 (2) (2008) 460–469.

[52] R.Q. Ding, J. Tsao, H. Chai, et al., Therapeutic potential for protein kinase C inhibitor in vascular restenosis, J. Cardiovasc. Pharmacol. Ther. 16 (2) (2011) 160–167.

[53] C. Giorgi, C. Agnoletto, C. Baldini, et al., Redox control of protein kinase C: cell-and disease-specific aspects, Antioxid. Redox Signal. 13 (7) (2010) 1051–1085.

[54] G.W. Dorn, D. Mochly-Rosen, Intracellular transport mechanisms of signal transducers, Annu. Rev. Physiol. 64 (1) (2002) 407–429.

[55] T. Inoguchi, R. Battan, E. Handler, et al., Preferential elevation of PKC isoform II and DAG levels in the aorta and heart of diabetic rats: differential reversibility to glycemic control by islet cell transplantation, Proc. Natl. Acad. Sci. 89 (22) (1992) 11059–11063.

[56] V. Scivittaro, M.B. Ganz, M.F. Weiss, AGEs induce oxidative stress and activate protein kinase C-beta(II) in neonatal mesangial cells, Am. J. Physiol. Renal Physiol. 278 (4) (2000) F676–F683.

[57] H. Ruskoaho, R.E. Lang, M. Toth, et al., Release and regulation of atrial natriuretic peptide (ANP), Eur. Heart J. 8 (Suppl. B) (1987) 99–109.

[58] L. Hong, J. Xi, Y. Zhang, et al., Atrial natriuretic peptide prevents the mitochondrial permeability transition pore opening by inactivating glycogen synthase kinase 3β via PKG and PI3K in cardiac H9c2 cells, Eur. J. Pharmacol. 695 (1) (2012) 13–19.

[59] B.A. Clark, A. Sclater, F.H. Epstein, et al., Effect of glucose, insulin, and hypertonicity on atrial natriuretic peptide levels in man, Metabolism 42 (2) (1993) 224–228.

[60] L. Böhlen, P. Ferrari, M. Papiri, et al., Atrial natriuretic factor increases in response to an acute glucose load, J. Hypertens. 12 (7) (1994) 803–807.

[61] K. McKenna, D. Smith, W. Tormey, et al., Acute hyperglycaemia causes elevation in plasma atrial natriuretic peptide concentrations in type 1 diabetes mellitus, Diabet. Med. 17 (7) (2000) 512–517.

[62] M.F. McCarty, A chlorogenic acid-induced increase in GLP-1 production may mediate the impact of heavy coffee consumption on diabetes risk, Med. Hypotheses 64 (4) (2005) 848–853.